Water Waves Over a Muddy Seabed

by

Mikhael Krotov

Submitted to the Department of Aeronautics and Astronautics
in partial fulfillment of the requirements for the degree of

Master of Science in Aeronautics and Astronautics

at the

MASSACHUSETTS INSTITUTE OF TECHNOLOGY
[June 2008]
May 2008

Author .....
Department of Aeronautics and Astronautics
May 18, 2008

Certified by .....
Chiang C. Mei
Ford Professor of Engineering,
Department of Civil and Environmental Engineering
Thesis Supervisor

Accepted by .....
Prof. David L. Darmofal
Associate Department Head Chair, Committee on Graduate Students

Water Waves Over a Muddy Seabed

by

Mikhael Krotov

Submitted to the Department of Aeronautics and Astronautics
on May 18, 2008, in partial fulfillment of the
requirements for the degree of
Master of Science in Aeronautics and Astronautics

Abstract

A generalized viscoelastic model is used to describe the rheological properties of mud and is fitted to the available experimental data, so that its constitutive coefficients are just material properties independent of the frequency of the external forcing. We integrate this model into a perturbation analysis to solve the interaction between a thin layer of viscoelastic mud and sinusoidal waves propagating on top of a water layer of intermediate depth. In contrast with the previous studies the analysis is done for decaying water waves and a rheological model with frequency independent coefficients. The leading order motion and the mean second order motion inside the mud layer is determined analytically together with the first two orders motion in water. The analysis is done in a fixed Eulerian frame and it is shown that both a mean horizontal displacement and a Eulerian mean horizontal velocity exists inside the mud layer at the second order. The effect of elasticity and viscosity on the damping of water waves and on the mean motion of the mud is studied. It is shown that a light mud with a high proportion of elasticity will significantly modify the leading order movement through damping. The results are applied to solve analytically the problem of the evolution of the narrow-banded waves propagating on top of a semi-infinite mud layer. It is shown that the presence of the mud layer gives rise to a negative mean current in water layer and to free waves generated at the edge of the mud layer and propagating at the dimensional velocity $\sqrt{gh}$.

Thesis Supervisor: Chiang C. Mei
Title: Ford Professor of Engineering,
Department of Civil and Environmental Engineering

Acknowledgments

The research has been funded by the US office of Naval Research as a part of the MURI (Mechanisms of Fluid-Mud Interactions Under Waves) program under grant number N00014-06-1-0718.

I would like to thank my thesis supervisor Professor Chiang C. Mei for guiding and supporting me during the two years and for being always available to discuss and help me with the research.

This work could not be completed without the moral support of my family and friends, to whom I am very grateful.

Contents

List of Figures

List of Tables

Introduction

The behavior of the cohesive sediments under ocean waves is a vast topic that has long been studied by various authors. The major goals of such studies are the understanding of the transport by the water waves toward the beaches of the potentially contaminated sediments and the modeling of a significant water waves' damping that occurs when the waves propagate over coastal seabeds loaded with cohesive sediments. The major difficulties arise in these studies because of a highly complex rheological behavior of cohesive sediments that renders their modeling challenging. Moreover, any analytical work is possible only for simple rheological models of the mud. This is why the mud was often modeled as a Newtonian viscous fluid (e.g., [10] and [7]). The results of such modeling do not predict large values of damping for shallow mud layers and hence are inconsistent with the experimental data. The mud was also modeled as a linear elastic solid (e.g., [11]) and as a poro-elastic medium (e.g., [12]). A more accurate way is to model the mud as a viscoelastic material, that combines at the same time the properties of a fluid and of a solid. This approach was taken by a number of authors: MacPherson [13] in 1980, Maa and Mehta [14] in 1990, Ng and Zhang [6], [5] in 2006 and 2007 and by others. It was shown that the the elastic properties of the mud can produce resonant motion of the layer and significantly enhance the energy dissipation.

In all the previous studies the models used were similar to the Voigt body:

$$\bar{\underline{\underline{\tau}}} = \bar{G}\bar{\underline{\underline{\gamma}}} + \bar{\mu}\dot{\bar{\underline{\underline{\gamma}}}} \tag{0.0.1}$$

where $\bar{\underline{\underline{\tau}}}$ is the dimensional stress tensor, $\bar{\underline{\underline{\gamma}}}$ is the dimensional strain tensor and $\dot{\bar{\underline{\underline{\gamma}}}}$ is the dimensional rate of strain tensor. However, as the experimental data suggests (see next chapter),the coefficients $\bar{G}$ and $\bar{\mu}$ depend strongly on frequency. This suggests that the models used are not appropriate to represent the mud, as they not only depend on the mud properties but also on the frequency of the external forcing. We will present a generalized viscoelastic model that will have all the coefficients independent of frequency and will be valid for any sinusoidal forcing.

In the most recent paper on oscillatory motion of a viscoelastic mud [6] Zhang and Ng solved the equations of motion in Lagrangian for the problem of a viscoelastic mud layer put into motion by harmonic pressure applied on the surface of the layer. In our analysis the mud layer will be put into motion by the waves propagating on the overlying water column. We allow the water waves to decay due to energy dissipation inside the viscoelastic mud and we solve the equations of motion in the Eulerian form allowing a nonzero mean horizontal velocity inside the mud layer. Zhang and Ng applied the perturbation analysis to obtain first and second order equations of motion inside the mud layer and then solved them numerically. In our approach we solved the equations of motion analytically, in particular for the mean displacement inside the mud layer, and compared to the numerical results of Zhang and Ng. The profiles' shapes of the mean horizontal displacement are the same but the quantitative results differ because Zhang and Ng considered that there is no shear stress on the top of the mud layer even at the second order. However, as it will be shown later, due to the second order movement of the interface between mud and water layers the shear stress at the interface is non zero at the second order.

The plan of this thesis is the following. First, we introduce a generalized viscoelastic model and fit it to the experimental data available, so that its coefficients depend only on the properties of the mud and not on the external forcing. Second, we use the perturbation analysis to analytically solve the interaction of a thin mud layer with sinusoidal waves propagating on top of a water layer of intermediate depth. Finally we apply the obtained results to analytically solve the propagation of narrow-banded waves on top of a thin semi-infinite layer of viscoelastic mud.

Chapter 1

General viscoelastic model of fluid mud

1.1 Experimental Background

In a technical report from Institute of Mechanics, Beijing China, Huhe and Huang (1993) describe experiments on the rheology of fluid mud in Hangchow Bay. Using a RMS-605 rotating drum viscometer they recorded stress/strain relations in both steady and time harmonic tests for a wide range of fluid-mud densities and clay concentrations. For steady flows the relation is essentially Bingham plastic in accord with nearly all past experiments. For time-periodic tests within the frequency range of $0.2 < \omega < 70$ rad/sec, the relation is much more complex, suggesting that the rheology of mud under waves differs considerably from that of steady flows. Their results are reported in the form of a simple viscoelastic material,

$$\bar{\tau} = G_m \bar{\gamma} + \mu_m \dot{\bar{\gamma}} \tag{1.1.1}$$

where

$$\bar{\gamma} = \frac{\partial \bar{U}}{\partial \bar{y}}, \quad \dot{\bar{\gamma}} = \frac{\partial \bar{u}}{\partial \bar{y}}, \quad \text{with} \quad \bar{u} \equiv \frac{\partial \bar{U}}{\partial \bar{t}} \tag{1.1.2}$$

and where the symbol $\bar{u}$ represents the velocity and the symbol $\bar{U}$ represents the displacement. Note that in this thesis the dimensional variables will be marked by a bar ($\bar{u}$, $\bar{U}$, ...) and the dimensionless without.

The data show however that both G_m and μ_m measured depend not only on mud properties (chemistry, salinity density and sediment concentration, etc.), but also strongly on the frequency. Specifically, G_m increases while the viscosity coefficient μ_m decreases sharply with frequency. This dependence on frequency implies that the simple model (1.1.1) is inadequate.

In a more recent study Jiang and Mehta (1998) reported extensive time-periodic tests for fluid mud from the south coast of India for circular frequencies in the range of $0.02 < f < 4$ hertz, or $0.12 < \omega < 24$ rad/sec. They fitted their data to a three-parameter viscoelastic model. These parameters however are also dependent on the frequency.

Since in both known experiments the frequency dependences are similar and the frequencies tested coincide with the common range of wind-induced sea waves. Both sets of data are of direct relevance to coastal/ocean engineering.

In the following of the present chapter we treat the available data to obtain the experimental complex viscosity μ_d as function of ω, then we propose a generalized visco-elastic model based on all the experimental data. The frequency dependence is taken into account by the proposed model rather than by frequency dependent coefficients of the simpler models used by Jiang & Mehta (1998) and Huhe & Huang (1993). Meaning that the coefficients of the proposed model are independent of frequency. In the next chapter the resulting rheological law is applied to a simple problem of wave attenuation and the wave induced mass transport inside the mud layer. In the last chapter we will treat the nonlinear evolution of the narrow-banded waves over a semi-infinite and finite length mud layer.

1.2 Data by Huhe & Huang, 1993

In this section we deduce the experimental values of the complex viscosity $\mu_d(\omega)$ characterizing the mud from the data supplied by Huhe & Huang.
For harmonic motion

$$\bar{\tau} = \tilde{\bar{\tau}} e^{-i\omega t}, \quad \bar{\gamma} = \tilde{\bar{\gamma}} e^{-i\omega t}, \quad \dot{\bar{\gamma}} = \tilde{\dot{\bar{\gamma}}} e^{-i\omega t} \tag{1.2.1}$$

and

$$\tilde{\bar{\gamma}} = \frac{i}{\omega} \tilde{\dot{\bar{\gamma}}} \tag{1.2.2}$$

In the simple Maxwell model used by Huhe & Huang (1993), one gets

$$\tilde{\bar{\tau}} = (G_m - i\omega\mu_m)\tilde{\bar{\gamma}} = \left(\frac{iG_m}{\omega} + \mu_m\right)\tilde{\dot{\bar{\gamma}}} \tag{1.2.3}$$

Defining the complex viscosity μ_d relating stress and strain by

$$\tilde{\bar{\tau}} = \mu_d(\omega)\tilde{\dot{\bar{\gamma}}}, \quad \text{where} \quad \mu_d = \mu_d^r + i\mu_d^i, \tag{1.2.4}$$

it is evident that

$$\mu_d^r(\omega) = \mu_m(\omega), \quad \mu_d^i(\omega) = \frac{G_m(\omega)}{\omega} \tag{1.2.5}$$

With these relations the frequency dependence of the real and imaginary parts of μ_d can be inferred from the data of Huhe & Huang.

The data from Huhe & Huang is available from two different flume tests noted A and B. The values of μ_m and G_m provided by Huhe & Huang are listed in the Appendix A.2 in tables A.4 and A.5 for the flume A and in tables A.6 and A.7 for the flume B. The deduced values of μ_d^r and μ_d^i are plotted in figure (1-1) for the flume A and in figure (1-2) for the flume B. In both figures the log-log scale was used instead of the normal scale. The reason for this is that the complex viscosity varies sharply with the frequency and the data cannot be clearly visualized using the normal scale.

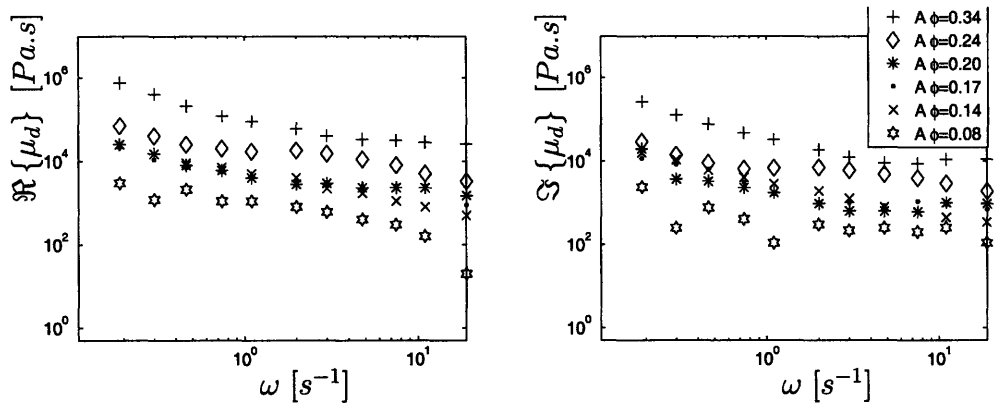

(a) Real part of viscosity μ_d

(b) Imaginary part of viscosity μ_d

Figure 1-1: Experimental data by Huhe & Huang (1993), data set A. Real and imaginary parts of the complex viscosity μ_d in log-log scale.

As the viscosity μ_d is complex we can define its modulus $|\mu_d|$ and phase $\theta \in [0, \pi/2]$ such that

$$\mu_d = |\mu_d| e^{i\theta} \tag{1.2.6}$$

The parameter has to be necessarily confined into the interval $[0, \pi/2]$ because the experimental values of real and imaginary parts of the complex viscosity μ_d are both positive.

$$\theta \in [0, \pi/2]$$

It is clear that the parameter θ indicates whether the mud is more or less elastic. In the extreme case when θ is equal to zero the mud is a simple Newtonian fluid. At the other extreme the mud behaves as an elastic solid when the parameter θ is equal to $\pi/2$. Because of the importance that the parameter θ has on the mud properties it is plotted in figure (1-3) for the data set A, and in figure (1-4) for the data set B.

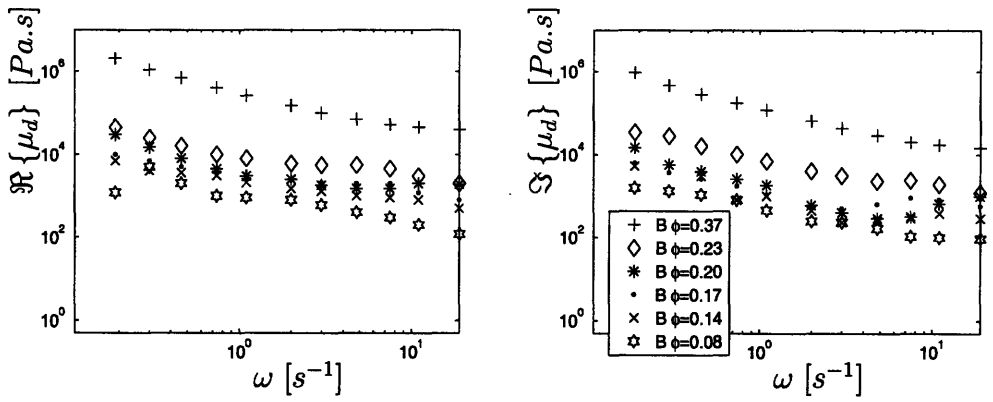

(a) Real part of viscosity μ_d

(b) Imaginary part of viscosity μ_d

Figure 1-2: Experimental data by Huhe & Huang (1993), data set B. Real and imaginary parts of the complex viscosity μ_d in log-log scale.

1.3 Data by Jiang and Mehta, 1998

In this section we deduce the experimental values of the complex viscosity $\mu_d(\omega)$ from the data supplied by Jiang & Mehta.

Jiang & Mehta chose the three-parameter viscoelastic model to model the rheology of the mud:

$$\bar{\tau} + \alpha_1 \dot{\bar{\tau}} = \beta_0 \bar{\gamma} + \beta_1 \dot{\bar{\gamma}} \tag{1.3.1}$$

The mechanical analogy of this model is represented in figure (1-5). It consists of a spring $2G_1$ in series with a Maxwell unit, which is a spring $2G_2$ and a dashpot $2\mu_m$ in parallel. The parameters α_1, β_0 and β_1 will be deduced as functions of G_1, G_2 and μ_m later in this section. Jiang and Mehta plotted their recorded values of G_1, G_2 and μ_m for eight frequencies in the range of $0.02\ Hz < \omega < 4\ Hz$ for Attapulgite and Kaolinate (AK) mud and summarized similar results for other mud samples in an empirical formula (eq. 1.3.2) with two parameters ϵ and Δ depending on the frequency, mud type and the solid fraction ϕ

$$\mu_d,\ G_1,\ G_2,\ = exp(\epsilon) f^{\Delta} \tag{1.3.2}$$

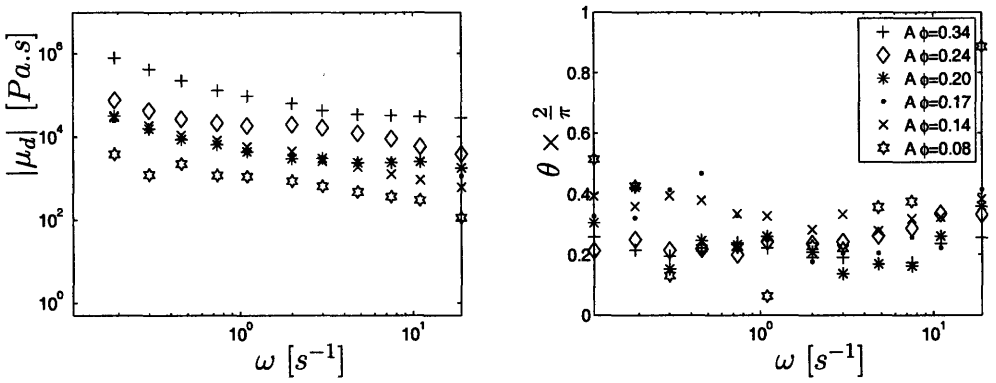

(a) Modulus of viscosity μ_d

(b) Phase of viscosity μ_d

Figure 1-3: Experimental data by Huhe & Huang (1993), data set A. Modulus and phase of the complex viscosity μ_d in log-log scale.

The data provided by Jiang & Mehta is presented in the appendix A.1. The physical characteristics of the mud samples considered by Jiang & Mehta are summarized in the table A.1, and the values of the parameters ϵ and Δ for each mud sample are listed in table A.2.

Unfortunately the raw data is no longer available and Jiang & Mehta report only the parameters ϵ and Δ which represent the fit of the data on the entire range of experimental frequencies $0.12 < \omega < 24$ rad/sec. In the following section we will present a generalized viscoelastic model and will describe a method to obtain the coefficients of this model based on a finite number of the experimental points. Therefore we will base our computation as if Jiang and Mehta measured the viscosity for all mud samples at the same eight frequencies ω= [.12 .24 .54 1.2 2.4 5.4 12 24] rad/s as they did for AK mud sample. The values of the parameters G_1, G_2 and μ_m will be evaluated at these eight frequencies using the data for ϵ and Δ and the empirical formula (eq. 1.3.2).

By applying force balance on the mechanical analogy, the coefficients α_1, β_0 and β_1 can be related to G_1, G_2 and μ_m as follows

$$\alpha_1 = \frac{\mu_m}{G_1 + G_2}, \quad \beta_0 = \frac{2G_1G_2}{G_1 + G_2}, \quad \beta_1 = \frac{2\mu_m G_1}{G_1 + G_2} \tag{1.3.3}$$

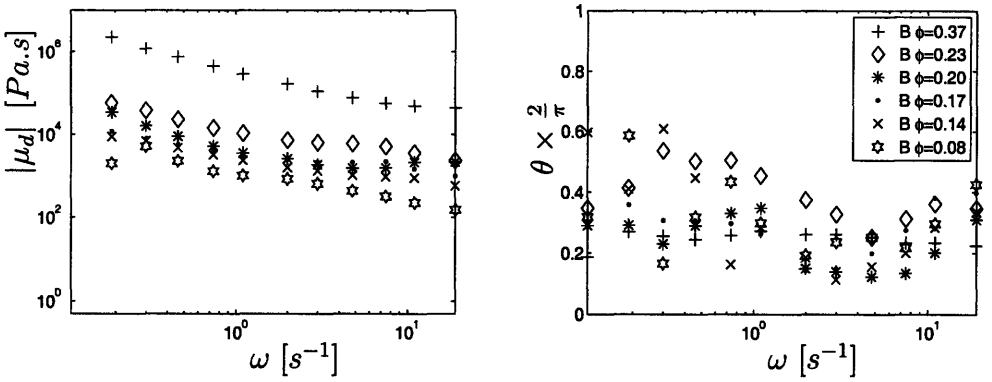

(a) Modulus of viscosity μ_d (b) Phase of viscosity μ_d

Figure 1-4: Experimental data by Huhe & Huang (1993), data set B. Modulus and phase of the complex viscosity μ_d in log-log scale.

Using the three-parameter model (eq. 1.3.1) and considering the case of a simple harmonic motion, the complex viscosity becomes

$$\mu_d = \frac{\beta_1 + i\frac{\beta_0}{\omega}}{1 - i\omega\alpha_1} \tag{1.3.4}$$

hence its real and imaginary parts are

$$\mu_d^r = \frac{\beta_1 - \alpha_1\beta_0}{1 + \omega^2\alpha_1^2} \tag{1.3.5}$$

$$\mu_d^i = \frac{\frac{\beta_0}{\omega} + \omega\alpha_1\beta_1}{1 + \omega^2\alpha_1^2} \tag{1.3.6}$$

$$\tag{1.3.7}$$

Thus knowing for each mud sample the parameters ϵ and Δ we can evaluate the parameters G_1, G_2 and μ_m at any frequency and in particular at the 8 frequencies considered. From these we can deduce the parameters α_1, β_0 and β_1 and finally the experimental complex viscosity μ_d. The real and imaginary parts of the complex viscosity are plotted in figure (1-6) using the log-log scale. The modulus and phase of the complex viscosity μ_d are plotted in figure (1-8). The values of the phase θ are close to $\pi/2$, which indicates that the mud samples considered by Jiang & Mehta have an important component of elasticity.

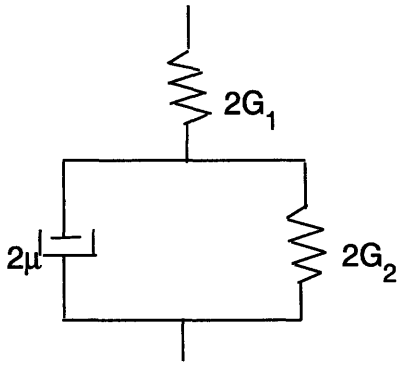

Figure 1-5: The three-parameter viscoelastic model of Jiang & Mehta, 1998.

In figure (1-7) only the data for the mud samples MB (Mobile Bay mud) was plotted. All three samples plotted have the same composition but different solid volume fractions ϕ (0.07, 0.11, 0.17). As one can expect the real part of the viscosity increases with the solid volume fraction ϕ. It is interesting to note that the imaginary part of the complex viscosity also increases with the solid volume fraction ϕ, keeping the ratio of elasticity to viscosity approximately unchanged for different values of ϕ (see the right-hand side plot in figure (1-8)). In the same figure we observe that the mud samples studied by Jiang & Mehta have a much greater elasticity to viscosity ratio compared to mud samples studied by Huhe & Huang.

1.4 Generalized viscoelastic model

Let us introduce the generalized viscoelastic model, relating the components of the stress and the strain tensors by a differential equation:

$$\left(1+\sum_{n=1}^{N}\bar{a}_n(\partial_{\bar{t}})^n\right)\bar{\tau}^{ij}=\left(\sum_{n=0}^{N-1}\bar{b}_n(\partial_{\bar{t}})^n\right)\bar{\gamma}^{ij} \tag{1.4.1}$$

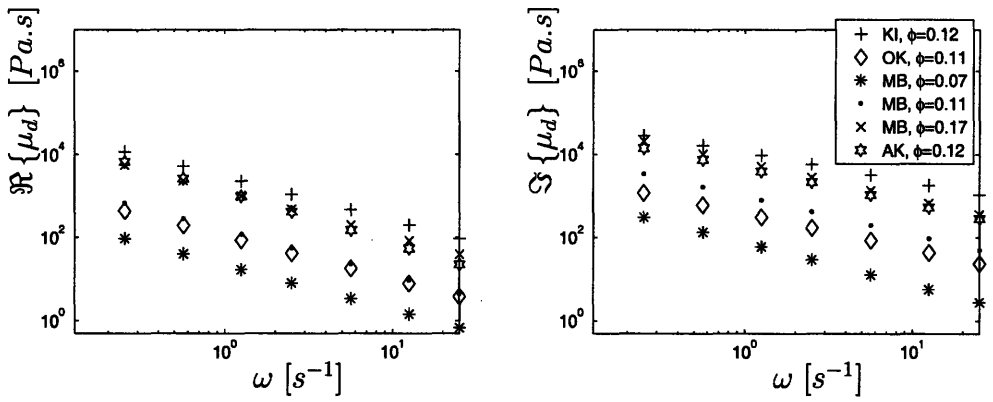

(a) Real part of viscosity μ_d

(b) Imaginary part of viscosity μ_d

Figure 1-6: Experimental data by Jiang & Mehta (1995). Real and imaginary parts of the complex viscosity μ_d in log-log scale.

with the symbols $\partial_{\bar{t}}$ representing the partial derivative with respect to time $\bar{t}$. A similar form of a viscoelastic model was introduced by Bird et al. [2]. The only difference with the last one is the fact that we introduced the coefficient $\bar{b}_0$ responsible for the elastic behavior at zero frequency. In our model (eq. 1.4.1) the material behaves as purely elastic solid at zero frequency, with the elasticity coefficient being $\bar{b}_0$ ($\bar{\tau}^{ij} = \bar{b}_0 \bar{\gamma}^{ij}$). Note that the linear cases of a purely viscous fluid is captured by the proposed model (eq. 1.4.1) when all the coefficients $\bar{a}_n$ and $\bar{b}_n$, except $\bar{b}_1$ are equal to zero. In this case the model reduces to

$$\bar{\tau}^{ij} = \bar{b}_1 \left(\partial_{\bar{t}} \bar{\gamma}^{ij}\right) = \bar{b}_1 \dot{\bar{\gamma}}^{ij} \tag{1.4.2}$$

Indeed the dimensional coefficients $\bar{a}_n$ (in s^n) and $\bar{b}_n$ (in $Pa.s^n$), which should depend only on the properties of mud, can be found from the experimental data of the complex viscosity μ_d. It should be pointed out that, in a linear problem and simple harmonic motion, empirical information on the frequency dependence of the complex viscosity μ_d is sufficient for modeling purposes as long as the shear motion is dominated by one component, as in the case of long waves over a shallow layer of fluid mud. The generalized viscoelastic law (1.4.1) can however be used for more complex problems where convective nonlinearity may introduce higher harmonics.

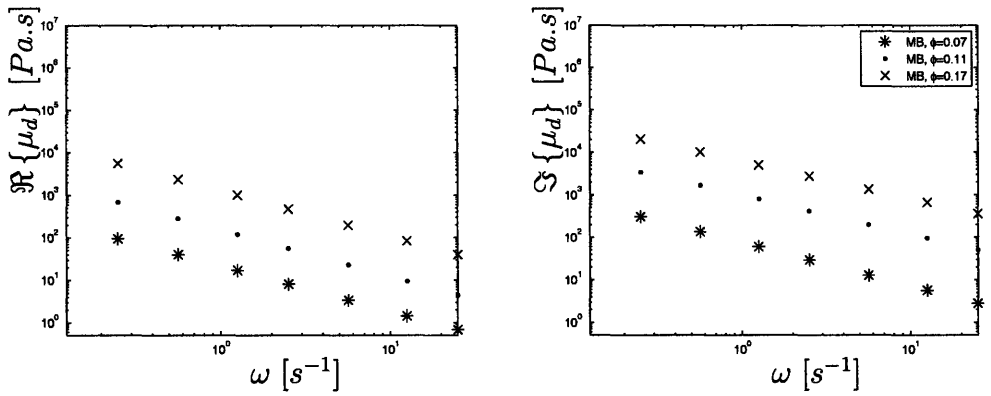

(a) Real part of viscosity μ_d (b) Imaginary part of viscosity μ_d

Figure 1-7: Experimental data by Jiang & Mehta (1995), MB mud samples only. Real and imaginary parts of the complex viscosity μ_d in log-log scale.

This situation is similar to the nonlinear Navier-Stokes equations in which the linear Newtonian viscosity is determined empirically from steady shearing experiments in concentric rotating cylinders.

For the special case of a purely sinusoidal motion in time

$$\bar{\bar{\tau}} = \bar{\bar{\tau}} e^{-i\omega \bar{t}}, \quad \bar{\dot{\gamma}} = \bar{\bar{\dot{\gamma}}} e^{-i\omega \bar{t}} \tag{1.4.3}$$

we have from (1.4.1)

$$\bar{\bar{\tau}} = \mu \bar{\bar{\dot{\gamma}}}, \tag{1.4.4}$$

where μ is complex

$$\mu = |\mu| e^{i\theta} = \frac{i}{\omega} \frac{\bar{b}_0 + \sum_{n=1}^{N-1} \bar{b}_n (-i\omega)^n}{1 + \sum_{n=1}^{N} \bar{a}_n (-i\omega)^n} \tag{1.4.5}$$

The constant $\bar{a}_0$ was taken to be equal to one without modifying the generality of the model. In fact if the constant $\bar{a}_0$ is not equal to one and is different from zero, it is enough to divide the numerator and the denominator by the value of $\bar{a}_0$ simultaneously to get the equation (1.4.5). Note that in the numerator the highest index of summation is $N-1$ as opposed to the one in the denominator which is N. This is done to keep the same number of unknown coefficients in the numerator and denominator - N.

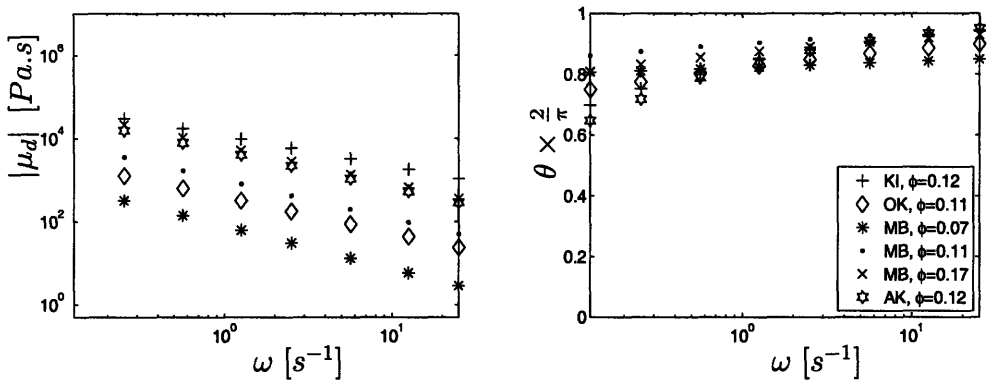

(a) Modulus of viscosity μ_d (b) Phase of viscosity μ_d

Figure 1-8: Experimental data by Jiang & Mehta (1995). Modulus and phase of the complex viscosity μ_d in log-log scale.

Note that using the expression (1.4.5) the limit of complex viscosity at zero frequency can be evaluated. In fact when $\omega \to 0$ the viscosity tends to a finite real value and an infinite complex value

$$\mu \to (\bar{b}_1 - \bar{a}_0\bar{a}_1) + i\frac{\bar{b}_0}{\omega} \tag{1.4.6}$$

1.4.1 General method for finding the coefficients $\bar{a}_n$ and $\bar{b}_n$

There are $2N$ unknowns to be determined $\bar{a}_n, \bar{b}_{n-1},\ n = 1, 2, 3, \ldots N$. For this we need $2N$ real or N complex equations. Suppose that the experimental value of the complex viscosity μ_d is given at N frequencies $\omega_1,\ \omega_2,\ \ldots\omega_N$. By equating the values of $\mu_d(\omega_l)$ at N frequencies $\omega_l,\ l = 1, 2, 3, \ldots N$ to the complex viscosity μ given by the equation (1.4.5), one obtains N complex or $2N$ real linear algebraic equations for $2N$ unknowns $\bar{a}_n, \bar{b}_{n-1},\ n = 1, 2, 3, \ldots N$

$$\mu_d(\omega_l) = \mu(\omega_l), \quad l = 1, 2, 3, \ldots N; \tag{1.4.7}$$

The equation 1.4.7 can be rewritten more explicitly in terms of coefficients $\bar{a}_n$ and $\bar{b}_n$

$$A_d^r(\omega_l) + iA_d^i(\omega_l) = \frac{\bar{b}_0 + \sum_{n=1}^{N-1} \bar{b}_n(-i\omega_l)^n}{1 + \sum_{n=1}^{N} \bar{a}_n(-i\omega_l)^n} \tag{1.4.8}$$

where $A_d^r = -i\omega\mu_d^r$ and $A_d^i = -i\omega\mu_d^i$ are known from the experimental data.

Separating the real and imaginary parts, one gets $2N$ real equations for $\bar{a}_n$ and $\bar{b}_n$.

Two cases are to be considered: N is even or N is odd.

In case when N is even, $N = 2M$ and the equations are:

$$\begin{aligned}
A_d^r(\omega_l)\sum_{p=1}^{M}(-1)^p\bar{a}_{2p}\omega_l^{2p} + A_d^i(\omega_l)\sum_{p=0}^{M-1}(-1)^p\bar{a}_{2p+1}\omega_l^{2p+1} - \sum_{p=0}^{M-1}(-1)^p\bar{b}_{2p}\omega_l^{2p} &= -A_d^r(\omega_l) \\
A_d^i(\omega_l)\sum_{p=1}^{M}(-1)^p\bar{a}_{2p}\omega_l^{2p} - A_d^r(\omega_l)\sum_{p=0}^{M-1}(-1)^p\bar{a}_{2p+1}\omega_l^{2p+1} + \sum_{p=0}^{M-1}(-1)^p\bar{b}_{2p+1}\omega_l^{2p+1} &= -A_d^i(\omega_l)
\end{aligned}$$

In case when N is odd, $N = 2M + 1$ and the equations become:

$$\begin{aligned}
A_d^r(\omega_l)\sum_{p=1}^{M}(-1)^p\bar{a}_{2p}\omega_l^{2p} + A_d^i(\omega_l)\sum_{p=0}^{M}(-1)^p\bar{a}_{2p+1}\omega_l^{2p+1} - \sum_{p=0}^{M-1}(-1)^p\bar{b}_{2p}\omega_l^{2p} &= -A_d^r(\omega_l) \\
A_d^i(\omega_l)\sum_{p=1}^{M}(-1)^p\bar{a}_{2p}\omega_l^{2p} - A_d^r(\omega_l)\sum_{p=0}^{M}(-1)^p\bar{a}_{2p+1}\omega_l^{2p+1} + \sum_{p=0}^{M-1}(-1)^p\bar{b}_{2p+1}\omega_l^{2p+1} &= -A_d^i(\omega_l)
\end{aligned}$$

The system of equations for $\bar{a}_n$ and $\bar{b}_n$ can be written as $\Delta.X = Y$ with the unknown $X = \left(\bar{a}_1, ...\bar{a}_N, \bar{b}_0, ...\bar{b}_{N-1}\right)^T$. Let us obtain explicit expressions for the matrices Y and Δ.

Let Y_l be the l-th component of the matrix Y. Than

$$\begin{aligned}
Y_l &= -A_d^r(\omega_l) \quad for \quad 1 \le l \le N \\
Y_l &= -A_d^i(\omega_l) \quad for \quad N+1 \le l \le 2N
\end{aligned}$$

To get the expression of the matrix Δ we consider two distinct cases. The case when N is even and the case when N is odd.

In case of an even N we can find an integer M such that $N = 2M$. The elements Δ_{lp} of the matrix Δ are for the first N lines ($1 \leq l \leq N$):

$$\begin{aligned}
\Delta_{l\ 2p} &= A_d^r(\omega_l)(-1)^p \bar{a}_{2p}\omega_l^{2p} \quad for \quad 1 \leq p \leq M \\
\Delta_{l\ 2p+1} &= A_d^i(\omega_l)(-1)^p \bar{a}_{2p+1}\omega_l^{2p+1} \quad for \quad 0 \leq p \leq M-1 \\
\Delta_{l\ N+1+2p} &= -(-1)^p \bar{b}_{2p}\omega_l^{2p} \quad for \quad 0 \leq p \leq M-1
\end{aligned}$$

for the next N lines ($N+1 \leq l \leq 2N$):

$$\begin{aligned}
\Delta_{l\ 2p} &= A_d^i(\omega_l)(-1)^p \bar{a}_{2p}\omega_l^{2p} \quad for \quad 1 \leq p \leq M \\
\Delta_{l\ 2p+1} &= -A_d^r(\omega_l)(-1)^p \bar{a}_{2p+1}\omega_l^{2p+1} \quad for \quad 0 \leq p \leq M-1 \\
\Delta_{l\ N+2+2p} &= (-1)^p \bar{b}_{2p+1}\omega_l^{2p+1} \quad for \quad 0 \leq p \leq M-1
\end{aligned}$$

In case of an odd N we can find an integer M such that $N = 2M+1$. The elements Δ_{lp} of the matrix Δ are for the first N lines ($1 \leq l \leq N$):

$$\begin{aligned}
\Delta_{l\ 2p} &= A_d^r(\omega_l)(-1)^p \bar{a}_{2p}\omega_l^{2p} \quad for \quad 1 \leq p \leq M \\
\Delta_{l\ 2p+1} &= A_d^i(\omega_l)(-1)^p \bar{a}_{2p+1}\omega_l^{2p+1} \quad for \quad 0 \leq p \leq M \\
\Delta_{l\ N+1+2p} &= -(-1)^p \bar{b}_{2p}\omega_l^{2p} \quad for \quad 0 \leq p \leq M-1
\end{aligned}$$

for the next N lines ($N+1 \leq l \leq 2N$):

$$\begin{aligned}
\Delta_{l\ 2p} &= A_d^i(\omega_l)(-1)^p \bar{a}_{2p}\omega_l^{2p} \quad for \quad 1 \leq p \leq M \\
\Delta_{l\ 2p+1} &= -A_d^r(\omega_l)(-1)^p \bar{a}_{2p+1}\omega_l^{2p+1} \quad for \quad 0 \leq p \leq M \\
\Delta_{l\ N+2+2p} &= (-1)^p \bar{b}_{2p+1}\omega_l^{2p+1} \quad for \quad 0 \leq p \leq M-1
\end{aligned}$$

The unknown matrix X is obtained by inverting the matrix Δ

$$X = \Delta^{-1} Y \tag{1.4.9}$$

Note that in the viscoelastic model (1.4.1) the order N of the highest derivative is equal to the number of used data points. Thus the order of differentiation increases with the number of data points within a given range of frequencies.

1.4.2 Generalized model for Huhe & Huang, data set A

At this point the values of the complex viscosity was deduced from the experimental data of Huhe & Huang and a method was presented to compute the coefficient $\bar{a}_n$ and $\bar{b}_n$ of the generalized viscoelastic model. For the data set A Huhe & Huang presented the results for 12 different frequencies. Using the method described above we could compute 12 coefficients $\bar{a}_n$ and 12 coefficients $\bar{b}_n$, such that the resulting complex viscosity μ would match exactly all the data points. However as the data is highly scattered but possess clear trends there is no need in to exactly match all the twelve data points available. Instead we chose four points (N=4) inside the data range which capture the trends given by the data but avoid the irregularities. The number of the coefficients is the reduced from 12×2 to $N \times 2$. The resulting complex viscosity is plotted together with the experimental data in figure (1-9) for different volume fractions in log-log scale. The data points used for the evaluation of the coefficients $\bar{a}_n$ and $\bar{b}_n$ are marked by squares.

The corresponding values of the coefficients $\bar{a}_n$ and $\bar{b}_n$ are plotted in figure (1-10). The values of the computed coefficients $\bar{a}_n$ and $\bar{b}_n$ are listed in table (1.1).

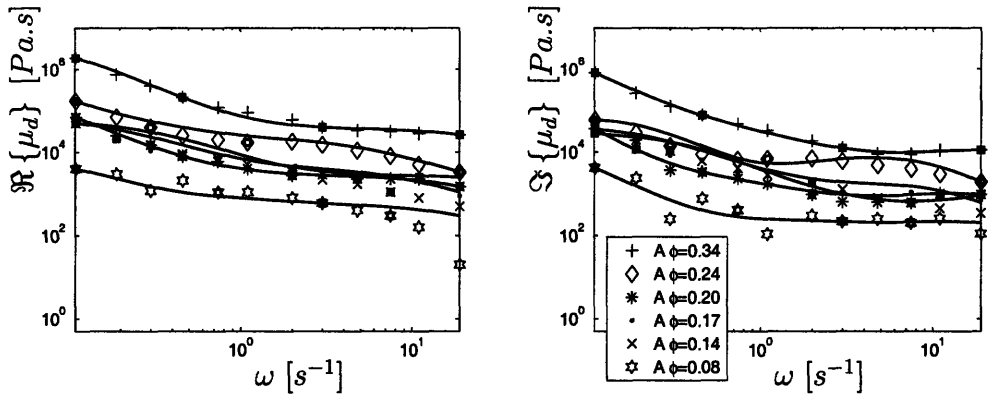

(a) Real part of viscosity μ_d

(b) Imaginary part of viscosity μ_d

Figure 1-9: Experimental data by Huhe & Huang (1993), data set A and fitted real and imaginary parts of the complex viscosity $\mu(\omega)$ (continuous lines) using selected data points (marked by squares). Log-log scale.

ϕ	0.37	0.23	0.20	0.17	0.14	0.08
$\bar{a}_1$	-0.12218	-41.9780	-15.1629	108.529	-375.600	-175.717
$\bar{a}_2$	-118.133	-67.9081	-69.241	-1753.64	628.434	163.232
$\bar{a}_3$	-2.88248	-5.93441	-2.65462	-62.8995	212.318	30.4877
$\bar{a}_4$	0.07374	0.42527	0.04753	3.34052	-34.6822	-2.02384
$\bar{b}_0$	180159	85454.7	18467.0	24831.1	179539	6240.70
$\bar{b}_1$	4555330	25932.1	65989.3	1376920	-1759440	-83303.4
$\bar{b}_2$	-3346770	-1040300	-140502	-2280260	-1940330	-151503
$\bar{b}_3$	-4356320	-940117	-176451	-6021200	3791420	132053
$\bar{b}_1 - \bar{b}_0\bar{a}_1$	4577350	3613150	346004	4071810	65675300	1013290

Table 1.1: Coefficients $\bar{a}_n$ (in s^n) and $\bar{b}_n$ (in $Pa.s^n$) - Data by Huhe & Huang, data set A

1.4.3 Generalized model for Huhe & Huang, data set B

For the data set B provided by Huhe & Huang the coefficients $\bar{a}_n$ and $\bar{b}_n$ as well as the resulting complex viscosity μ were computed using four data points ($N = 4$). The resulting complex viscosity μ is plotted as function of frequency in figure 1-11

The corresponding values of the coefficients $\bar{a}_n$ and $\bar{b}_n$ are plotted in figure 1-12.

The values of the computed coefficients $\bar{a}_n$ (in s^n) and $\bar{b}_n$ (in $Pa.s^n$) are listed in table A.6.

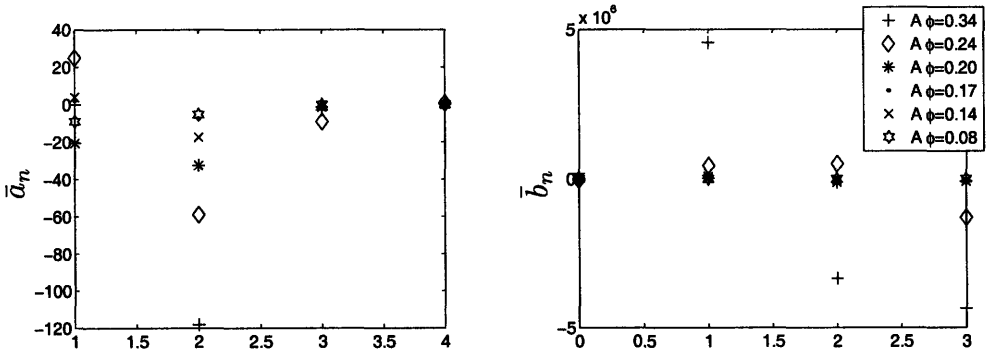

(a) $\bar{a}_n$ (b) $\bar{b}_n$

Figure 1-10: Dimensional coefficients $\bar{a}_n$ and $\bar{b}_n$ for mud samples provided by Huhe & Huang (1993), data set A

1.4.4 Generalized model for Jiang & Mehta

The data provided by Jiang & Mehta was treated in the same way as the one provided by Huhe & Huang using four data points ($N = 4$) from the available frequency range. Four coefficients $\bar{a}_n$, four coefficients $\bar{b}_n$ as well as the resulting complex viscosity μ were computed.

The resulting complex viscosity μ is plotted as function of frequency in figure (1-13). The corresponding values of the coefficients $\bar{a}_n$ (in s^n) and $\bar{b}_n$ (in $Pa.s^n$) are plotted in figure (1-14).

The values of the computed coefficients $\bar{a}_n$ and $\bar{b}_n$ are listed in table (1.2).

ϕ	0.37	0.23	0.20	0.17	0.14	0.08
$\bar{a}_1$	3.39210	15.6591	-155.898	15.4006	11.1584	9.58842
$\bar{a}_2$	0.19550	13.0727	4.11920	12.8004	6.85566	5.41669
$\bar{a}_3$	-0.05810	0.91256	28.5325	0.88478	0.32268	0.14459
$\bar{a}_4$	0.00021	-0.00111	-0.20689	-0.00039	0.00038	0.00095
$\bar{b}_0$	4294.43	90.3429	505.357	516.287	2964.15	1008.04
$\bar{b}_1$	40368.6	4765.02	-11906.4	13458.3	62655.7	40132.4
$\bar{b}_2$	5422.86	6102.73	-2813.15	14077.0	51952.7	33268.5
$\bar{b}_3$	-1641.19	589.746	2097.43	1165.82	3104.06	1114.9
$\bar{b}_1 - \bar{b}_0\bar{a}_1$	25801.5	3350.32	66877.8	5507.14	29580.6	30466.9

Table 1.2: Coefficients $\bar{a}_n$ (in s^n) and $\bar{b}_n$ (in $Pa.s^n$) - Data by Jiang & Mehta

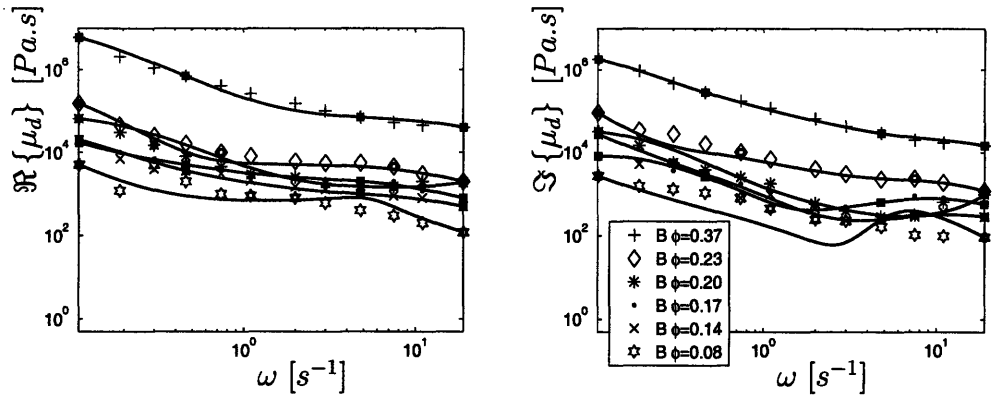

(a) Real part of viscosity μ_d

(b) Imaginary part of viscosity μ_d

Figure 1-11: Experimental data by Huhe & Huang (1993), data set B and fitted real and imaginary parts of the complex viscosity $\mu(\omega)$ (continuous lines) using selected data points (marked by squares). Log-log scale.

1.4.5 Conclusion

A viscoelastic model with frequency-independent coefficients was fitted to the available experimental data. The number of the time derivatives present in the model and the values of its coefficients depend on the number of the data points considered. For the available experimental results it was shown that a fair agreement with experiments can be obtained using 4 data points and 3 time derivatives.

It was noticed that the real part of the complex viscosity should tend to a finite value even when the frequency tends to 0. To prove it experiments should be done at low frequency (lower than $f = 0.02Hz$).

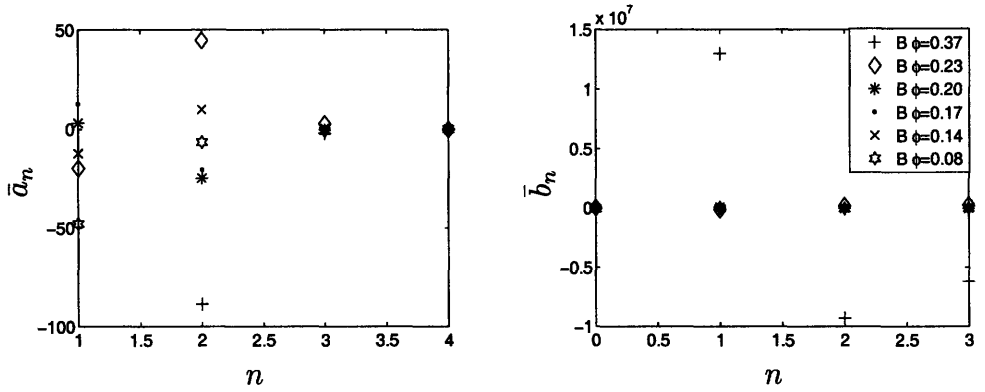

(a) $\bar{a}_n$ (b) $\bar{b}_n$

Figure 1-12: Dimensional coefficients $\bar{a}_n$ and $\bar{b}_n$ for mud samples provided by Huhe & Huang (1993), data set B

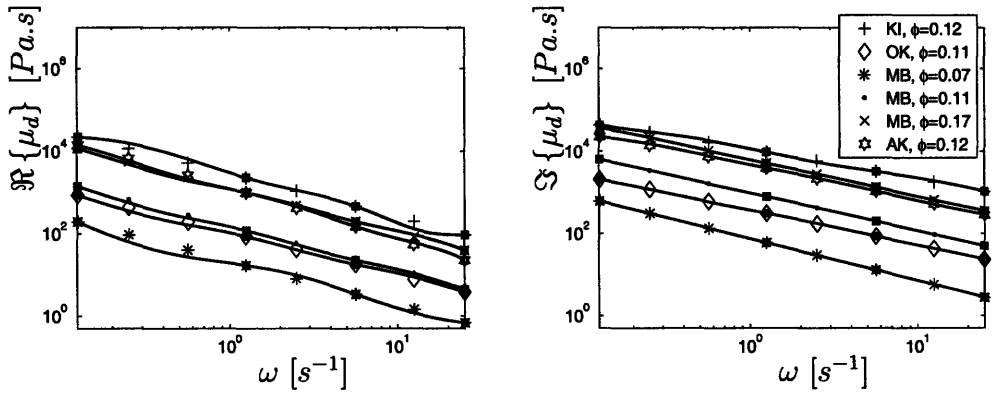

(a) Real part of viscosity μ_d (b) Imaginary part of viscosity μ_d

Figure 1-13: Experimental data by Jiang & Mehta (1995), and fitted real and imaginary parts of the complex viscosity $\mu(\omega)$ (continuous lines) using selected data points (marked by squares). Log-log scale.

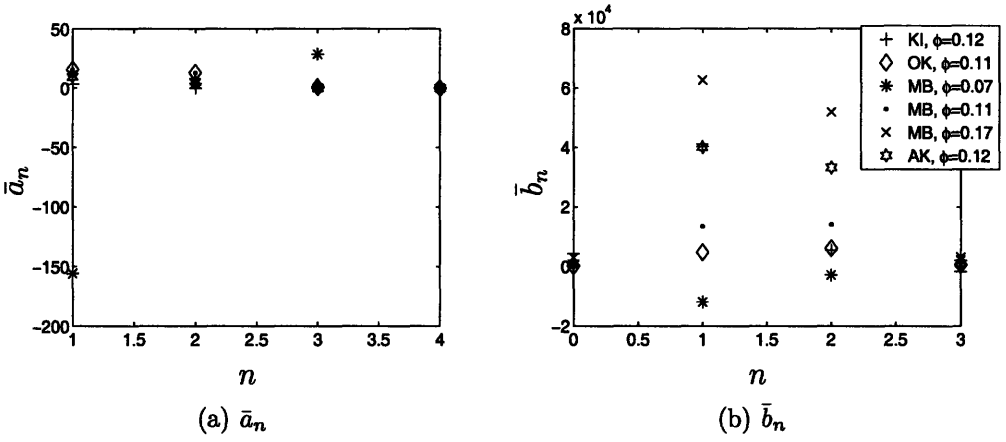

(a) $\bar{a}_n$ (b) $\bar{b}_n$

Figure 1-14: Dimensional coefficients $\bar{a}_n$ and $\bar{b}_n$ for mud samples provided by Jiang & Mehta (1995)

Chapter 2

Multiple-scale analysis of water waves interacting with a muddy seabed

The problem of the small amplitude water waves riding over a thin layer of mud inherently possesses small parameters which are the wave steepness and ratio of the mud layer to the water layer depths. Thanks to the existence of these small parameters the problem of the evolution of water waves over a thin layer of mud can be linearized by expanding the unknowns into the perturbation series. This also give us the possibility to introduce slow scales characterizing the time and the distance at which the waves are damped.

The solution at the leading order will give the rate of damping of water waves and the wavenumber shift that arise through the interaction with the mud layer. The second order solution will provide the mean displacement inside the mud layer, the higher order corrections to the leading order movement and the analytical expressions of the long waves generated by the slow modulations of the envelope of the free surface waves. The analysis will be conducted for the case of a single frequency characterizing the sinusoidal oscillations of the free surface waves.

The studied problem is the propagation of waves on a layer of water of depth h over a thin layer of mud of depth d. The forcing water waves are harmonic of frequency ω

and have a wavenumber $\bar{k}_0$ that will be determined using the dispersion relationship. The forced free surface displacement is $\bar{\eta}(\bar{x}, \bar{t})$, where $\bar{x}$ is the horizontal coordinate and $\bar{t}$ represents the time. The displacement of the interface of the mud layer is $\bar{\zeta}(\bar{x}, \bar{t})$. The viscosity and density of the mud are μ and $\rho^{(m)}$, and the viscosity of water is $\rho^{(w)}$. The mud will be modeled as a linear viscoelastic material as described in the first chapter of the present thesis. The local erosion and deposition rates are neglected as they are too small to affect the wave-induced motion of the mud layer to the leading order (Liu and Mei 1989).

Given the experimental data, a reasonable assumption will be that the water layer

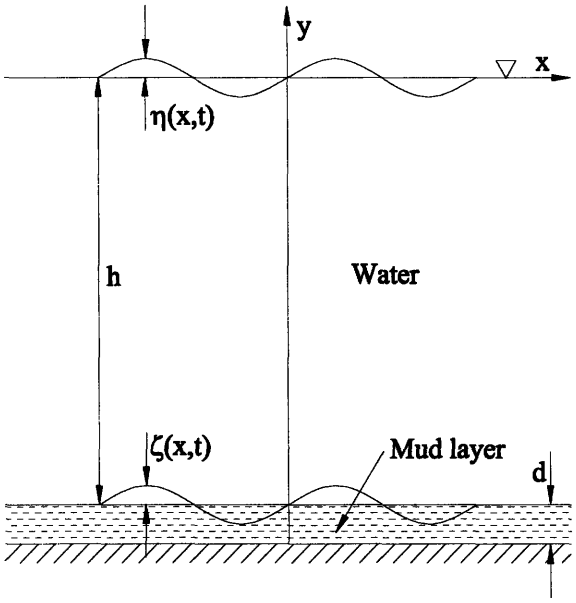

Figure 2-1: Studied problem

can be treated as inviscid. That is to say that the mud is much more viscous than the water. In fact the experimental data suggests that the viscosity of water is smaller than that of the mud by a factor 10^{-5} on average for the mud samples considered. As a consequence the water layer can be treated as inviscid to a very good approximation. The water layer is also assumed to be homogeneous, incompressible, initially irrotational and of intermediate depth (i.e. $\bar{k}h = O(1)$).

2.1 Scaling

The dimensional quantities will be marked by a bar, and the dimensionless without. The obvious common scale to both water and mud layers is the time scale ω^{-1}.

2.1.1 Water layer

It is natural to scale the free surface displacement by its amplitude that will be noted a. It is expected that the movement of a thin and dense mud layer does not affect the water motion at the leading order. Therefore it is reasonable to expect that the scale of the wave number is $\frac{\omega^2}{g}$ and that the horizontal length scale inside the water layer is given by $\frac{g}{\omega^2}$ that neglects the effect of the mud layer. The scale of the water horizontal velocity is $a\omega$. The scale of the velocity potential is then given by $\frac{ag}{\omega}$. In water of intermediate depth it is expected that the horizontal and vertical length scales are comparable and therefore the mass conservation equation requires the horizontal and vertical velocity scales to be equal. The dimensionless height of the water layer is defined as $H = \frac{h\omega^2}{g}$. Finally the dynamic pressure scale is $\rho^{(w)}ga$.
The scales for the water layer are summarized in the table (2.1) below.

$$\begin{array}{lllll} \bar{x} = \frac{g}{\omega^2}x & \bar{U} = a\omega U & \bar{t} = \omega^{-1}t & \bar{\Phi} = \frac{ag}{\omega}\Phi & \bar{k} = \frac{\omega^2}{g}k \\ \bar{y} = \frac{g}{\omega^2}y & \bar{V} = a\omega V & \bar{p}^{(w)} = \rho^{(w)}gap^{(w)} & \bar{\eta} = a\eta & h = \frac{gH}{\omega^2} \end{array}$$

Table 2.1: Scaled quantities inside the water layer

2.1.2 Mud layer

The horizontal length scale and the wave number inside the mud layer are the same as the ones inside the water layer. However, as the mud layer is thin compared to the wavelength, it is natural to chose the mud layer depth d as the mud layer's vertical length scale $\bar{y}'$. Note that $\bar{y}' = \bar{y} + h + d$ is the vertical coordinate inside the mud layer and $\bar{y}$ is the vertical coordinate inside the water layer. The horizontal velocity has the same scale as the one inside the water layer $a\omega$. The scale of the vertical velocity however is given by the balance of the terms in the conservation of mass equation

and is equal to $\epsilon\omega d$, with the small parameter ϵ defined as:

$$\epsilon \equiv \frac{\omega^2 a}{g} << 1 \tag{2.1.1}$$

The mud viscosity is scaled by its real value at constant shear (zero frequency) which was obtained by interpolation of the experimental data using the method described in previous section:

$$\mu_0 \equiv \bar{b}_1 - \bar{b}_0 \bar{a}_1 \tag{2.1.2}$$

The components of the rate of strain tensor scale as $\frac{a\omega}{d}$ and the components of the stress tensor scale as $\frac{\mu_0 a\omega}{d}$. The pressure scale is the same as the one inside the water layer. The components of the stress tensor scale as their larger term which is expected to be the pressure term. The displacement inside the mud layer is scales as velocity times ω which gives a for the displacement in the horizontal direction and ϵd for the scale of the displacement in the vertical direction.The strain tensor is then naturally scaled as $\frac{a}{d}$, and the rate of strain tensor as $\frac{a\omega}{d}$. The scale of the interface displacement can be estimated using the fact that the ratios of the upper surface displacement to the height of the underlying layer are expected to be the same in both water and mud layers, i.e. $\frac{b}{d} \sim \frac{a}{h}$ (Liu and Mei 1989). The water/mud interface displacement scales then as ϵa because of the assumption that $d \sim a$.

The scales inside the mud layer are summarized in the table (2.2) below.

$\bar{x} = \frac{g}{\omega^2}x$	$\bar{u} = a\omega u$	$\bar{\gamma}^{ij} = \frac{a}{d}\gamma^{ij}$	$\bar{p}^{(m)} = \gamma\rho^{(m)}gap^{(m)}$	$\bar{X} = aX$
$\bar{y}' = dy'$	$\bar{v} = \epsilon a\omega\frac{d}{a}v$	$\bar{\tau}^{ij} = \frac{\mu_0 a\omega}{d}\tau^{ij}$	$\bar{\sigma}^{ij} = \gamma\rho^{(m)}ga\sigma^{ij}$	$\bar{Y} = \epsilon dY$
$\bar{t} = \omega^{-1}t$	$\bar{k} = \frac{\omega^2}{g}k$	$\bar{\zeta} = \epsilon a\zeta$	$\bar{\gamma}^{ij} = \frac{a}{d}\gamma^{ij}$	$\bar{\dot{\gamma}}^{ij} = \frac{a\omega}{d}\dot{\gamma}^{ij}$

Table 2.2: Scaled quantities inside the mud layer

where the parameter γ represents the densities ratio:

$$\gamma = \frac{\rho^{(w)}}{\rho^{(m)}}$$

The depth of the mud layer is assumed to be comparable to the amplitude of the free surface waves:

$$\frac{d}{a} = O(1)$$

The symbols σ^{ij} and τ^{ij} represent respectively the components of the total stress tensor $\underline{\underline{\sigma}}$ and the viscous stress tensor $\underline{\underline{\tau}}$. Each of the dimensionless components of the two tensors are related by

$$\sigma^{ij} = -p^{(m)}\delta_{ij} + \frac{\epsilon}{\gamma Re}\tau^{ij}$$

where δ_{ij} is the Kronecker delta and where the Reynolds' number Re is defined as

$$Re \equiv \frac{\rho^{(m)} a\omega d}{\mu_0} \tag{2.1.3}$$

The magnitude of the Reynolds number for the mud samples available is of order $O(10^{-2})$ for the case $a = d = 0.1m$ and of order $O(1)$ for the case of $a = d = 1m$.
In all that follows all the equations will be written in terms of dimensionless quantities, unless otherwise specified.

2.2 Exact governing equations and boundary conditions

2.2.1 Exact governing equations

In this section the exact equations governing water and mud motions are stated. It is assumed that water and mud layers are separated by a clearly defined interface and the erosion and deposition are neglected. In all that follows the partial derivatives with respect to a variable x of a function f will be denoted by f_x, and the derivative with respect to x as an operator will be denoted as ∂_x.

Water layer

The governing equation for the inviscid water is the Laplace equation

$$\Phi_{yy} + \Phi_{xx} = 0 \qquad -H \leq y \leq \epsilon\eta \tag{2.2.1}$$

The pressure inside the water $p^{(w)}$ layer can be deduced from the velocity potential Φ by using the Bernoulli equation which is

$$p^{(w)} = -\Phi_t - \frac{\epsilon}{2}\left[(\Phi_x)^2 + (\Phi_y)^2\right] \tag{2.2.2}$$

Mud layer

The governing equations for the mud layer are the Navier-Stokes equations for an incompressible fluid. They are the mass conservation equation

$$u_x + v_{y'} = 0 \tag{2.2.3}$$

the x-momentum conservation equation

$$u_t + \epsilon(uu_x + vu_{y'}) \;=\; -\gamma p_x^{(m)} + \frac{1}{Re}\frac{a}{d}\left(\tau_{y'}^{xy} + \epsilon\frac{d}{a}\tau_x^{xx}\right) \tag{2.2.4}$$

and y-momentum conservation

$$\left(\epsilon\frac{d}{a}\right)^2\left[v_t + \epsilon(uv_x + vv_{y'})\right] = -\gamma p_{y'}^{(m)} + \frac{\epsilon}{Re}\left(\tau_{y'}^{yy} + \epsilon\frac{d}{a}\tau_x^{xy}\right) \tag{2.2.5}$$

2.2.2 Exact boundary conditions

Free surface

The kinematic boundary condition on the free surface is

$$\eta_t = \Phi_y - \epsilon\eta_x\Phi_x, \quad y = \epsilon\eta \tag{2.2.6}$$

The dynamic boundary condition is

$$-\eta = \Phi_t + \frac{\epsilon}{2}\left(\Phi_x^2 + \Phi_y^2\right), \quad y = \epsilon\eta \tag{2.2.7}$$

The kinematic and dynamic boundary conditions (equations (2.2.6) and (2.2.7)) can be combined by taking the Lagrangian derivative of the dynamic boundary condition (2.2.7) with respect to time. The combined boundary condition becomes:

$$\Phi_{tt} + \Phi_y + \epsilon\left[\partial_t + \frac{\epsilon}{2}\left(\Phi_x\partial_x + \Phi_y\partial_y\right)\right]\left(\Phi_x^2 + \Phi_y^2\right) = 0, \quad y = \epsilon\eta \tag{2.2.8}$$

Water/Mud interface

The kinematic boundary condition on the water/mud interface is in terms of the water quantities:

$$\Phi_y = \epsilon\zeta_t + \epsilon^2\zeta_x\Phi_x, \quad y = -H + \epsilon^2\zeta \tag{2.2.9}$$

and in terms of the mud quantities:

$$\zeta_t = \frac{d}{a}v - \epsilon\zeta_x u, \quad y' = 1 + \epsilon\frac{a}{d}\zeta \tag{2.2.10}$$

The dynamic boundary condition on the water/mud interface requires the continuity of stresses through the interface ($\underline{\underline{\sigma}}.\vec{n} = -p^{(w)}\vec{n}$) with $\vec{n} = (n^{(x)}, n^{(y)})$ being the unit vector normal to the interface and pointing inside the water layer. In component form the continuity of stresses through the interface reads:

$$\begin{cases} \sigma^{xx}n^{(x)} + \sigma^{xy}n^{(y)} = & -p^{(w)}n^{(x)}, \\ \sigma^{yx}n^{(x)} + \sigma^{yy}n^{(y)} = & -p^{(w)}n^{(y)}, \end{cases} \qquad y' = 1 + \epsilon\tfrac{a}{d}\zeta, \quad (y = -H + \epsilon^2\zeta) \tag{2.2.11}$$

Bottom of the mud layer

Finally the no slip boundary condition on the bottom of the mud layer reads in terms of the velocity field:

$$u = 0, \quad y' = 0 \tag{2.2.12}$$

$$v = 0, \quad y' = 0 \tag{2.2.13}$$

In terms of the displacement the no slip boundary condition is:

$$X = 0, \quad y' = 0 \tag{2.2.14}$$

$$Y = 0, \quad y' = 0 \tag{2.2.15}$$

2.3 Approximate governing equations and boundary conditions

In this section the exact governing equations will be approximated using the fact that the parameter ϵ governing the nonlinearities of the problem is small. At first the slow variables will be introduced and the physical quantities will be developed into perturbation series. Secondly the approximate equations up to the third order $O(\epsilon^2)$ in water and up to the second order $O(\epsilon)$ in mud will be obtained and the approximation of the sinusoidal forcing will be introduced. Finally the approximate equations will be deduced for each order.

2.3.1 Slow variables

Given the fact that the mud layer is thin compared to the water wavelength and because its dimensionless depth $\frac{d\omega^2}{g} = O(\epsilon)$ is of order ϵ, we expect the leading order equations to be unchanged by the presence of the mud layer. The mud layer will influence the order $O(\epsilon)$ equations and the length and time corresponding to the damping of waves will be of order $O(1/\epsilon)$. It is therefore natural to introduce new

time variables t, t_1, t_2,... and space variables x and x_1 such that $t^n = O(1/\epsilon^n)$ and $x_1 = O(1/\epsilon)$ represent the slow scales. They new time and space variables are defined as follows:

$$t \equiv t, \qquad t_1 \equiv \epsilon t, \qquad t_2 \equiv \epsilon^2 t, \quad \ldots \tag{2.3.1}$$

$$x \equiv x, \qquad x_1 \equiv \epsilon x. \tag{2.3.2}$$

Note that the slowest horizontal length scale is x_1. This is due to the fact that after the distance x_1 waves will be significantly damped and there will be no more point in studying their evolution afterward.

The derivatives with respect to t and x should be replaced with the derivatives with respect to the slow variables:

$$\begin{aligned}
\partial_t &\rightarrow \partial_t + \epsilon\partial_{t_1} + \epsilon^2\partial_{t_2} + O(\epsilon^3) \\
\partial_x &\rightarrow \partial_x + \epsilon\partial_{x_1} + \epsilon^2\partial_{x_2} + O(\epsilon^3) \\
\partial_{tt} &\rightarrow \partial_{tt} + 2\epsilon\partial_{tt_1} + \epsilon^2\partial_{t_1t_1} + \epsilon^2\partial_{tt_2} + O(\epsilon^3) \\
\partial_{xx} &\rightarrow \partial_{xx} + 2\epsilon\partial_{xx_1} + \epsilon^2\partial_{x_1x_1} + O(\epsilon^3)
\end{aligned}$$

2.3.2 Perturbation series

Using the fact that the nonlinearities of the problem are governed by a small parameter ϵ, the unknowns of the problem can be developed into the perturbation series:

$$\begin{aligned}
\eta(x,t,x_1,t_1,t_2,...) &= \eta_0(x,t,x_1,t_1,t_2,...) + \epsilon\eta_1(x,t,x_1,t_1,t_2,...) + \dots \\
\zeta(x,t,x_1,t_1,t_2,...) &= \zeta_0(x,t,x_1,t_1,t_2,...) + \epsilon\zeta_1(x,t,x_1,t_1,t_2,...) + \dots \\
\Phi(x,y,t,x_1,t_1,t_2,...) &= \Phi_0(x,y,t,x_1,t_1,t_2,...) + \epsilon\Phi_1(x,y,t,x_1,t_1,t_2,...) + \dots \\
p^{(w)}(x,y,t,x_1,t_1,t_2,...) &= p_0^{(w)}(x,y,t,x_1,t_1,t_2,...) + \epsilon p_1^{(w)}(x,y,t,x_1,t_1,t_2,...) + \dots \\
u(x,y,t,x_1,t_1,t_2,...) &= u_0(x,y,t,x_1,t_1,t_2,...) + \epsilon u_1(x,y,t,x_1,t_1,t_2,...) + \dots \\
v(x,y,t,x_1,t_1,t_2,...) &= v_0(x,y,t,x_1,t_1,t_2,...) + \epsilon v_1(x,y,t,x_1,t_1,t_2,...) + \dots \\
p^{(m)}(x,y,t,x_1,t_1,t_2,...) &= p_0^{(m)}(x,y,t,x_1,t_1,t_2,...) + \epsilon p_1^{(m)}(x,y,t,x_1,t_1,t_2,...) + \dots \\
\tau^{ij}(x,y,t,x_1,t_1,t_2,...) &= \tau_0^{ij}(x,y,t,x_1,t_1,t_2,...) + \epsilon\tau_1^{ij}(x,y,t,x_1,t_1,t_2,...) + \dots \\
\gamma^{ij}(x,y,t,x_1,t_1,t_2,...) &= \gamma_0^{ij}(x,y,t,x_1,t_1,t_2,...) + \epsilon\gamma_1^{ij}(x,y,t,x_1,t_1,t_2,...) + \dots \\
\dot{\gamma}^{ij}(x,y,t,x_1,t_1,t_2,...) &= \dot{\gamma}_0^{ij}(x,y,t,x_1,t_1,t_2,...) + \epsilon\dot{\gamma}_1^{ij}(x,y,t,x_1,t_1,t_2,...) + \dots
\end{aligned}$$

where for $n = 0, 1, 2, \dots$ the unknowns Φ_n, η_n, $p_n^{(w)}$, ζ_n, u_n, v_n, $p_n^{(m)}$, τ_n^{ij}, γ_n^{ij} and $\dot{\gamma}_n^{ij}$ are of order O(1).

2.3.3 Governing perturbation equations

Using the perturbation series expansions stated in previous section, the governing equations can be approximated to the wanted precision. The purpose of the present chapter is to compute the damping rate, the wavenumber shift and the mean displacement inside the mud layer. In the water layer we also want to determine the characteristics of the generated long waves due to the modulation of the short waves. To get these properties, we need to write the governing equations for the first three orders (up to the order $O(\epsilon^2)$) inside the water layer and for the first two orders (up to the order $O(\epsilon)$) inside the mud layer.

Water layer - Laplace equation

Let us first deal with the Laplace equation (2.2.1). Introducing the slow scales we get:

$$\Phi_{xx} + 2\epsilon\Phi_{xx_1} + \epsilon^2\Phi_{x_1x_1} + \Phi_{yy} = 0$$

Now using the perturbation series expansion and keeping the terms up to the order $O(\epsilon^2)$, the approximate Laplace equation becomes

$$\begin{aligned} O(\epsilon^3) &= \Phi_{0,yy} + \Phi_{0,xx} + \epsilon\left(\Phi_{1,yy} + \Phi_{1,xx} + 2\Phi_{0,xx_1}\right) \\ &\quad +\epsilon^2\left(\Phi_{2,yy} + \Phi_{2,xx} + 2\Phi_{1,xx_1} + \Phi_{0,x_1x_1}\right) \end{aligned}$$

Summarizing the equations order by order we get the final expressions of the approximate Laplace equation

$$O(\epsilon^0): \quad \Phi_{0,yy} + \Phi_{0,xx} = F_0 \tag{2.3.3}$$

$$O(\epsilon^1): \quad \Phi_{1,yy} + \Phi_{1,xx} = F_1 \tag{2.3.4}$$

$$O(\epsilon^2): \quad \Phi_{2,yy} + \Phi_{2,xx} = F_2 \tag{2.3.5}$$

where the functions F_0, F_1 and F_2 were defined as:

$$F_0 = 0 \tag{2.3.6}$$

$$F_1 = -2\Phi_{0,xx_1} \tag{2.3.7}$$

$$F_2 = -2\Phi_{1,xx_1} - \Phi_{0,x_1x_1} \tag{2.3.8}$$

Water layer - Bernoulli equation

Using the slow scales the Bernoulli equation (2.2.2) becomes:

$$p^{(w)} = -\Phi_t - \epsilon\Phi_{t_1} - \epsilon^2\Phi_{t_2} - \frac{\epsilon}{2}\left(\Phi_x^2 + \Phi_y^2 + 2\epsilon\Phi_x\Phi_{x_1}\right) + O(\epsilon^3)$$

Introducing the perturbation series expansion

$$\begin{aligned} p_0^{(w)} + \epsilon p_1^{(w)} + \epsilon^2 p_2^{(w)} &= -\Phi_{0,t} - \epsilon\Phi_{1,t} - \epsilon^2\Phi_{2,t} - \epsilon\Phi_{0,t_1} - \epsilon^2\Phi_{1,t_1} - \epsilon^2\Phi_{0,t_2} \\ &\quad -\frac{\epsilon}{2}\left(\Phi_{0,x}^2 + 2\epsilon\Phi_{0,x}\Phi_{1,x} + \Phi_{0,y}^2 + 2\epsilon\Phi_{0,y}\Phi_{1,y} + 2\epsilon\Phi_{0,x}\Phi_{0,x_1}\right) + O(\epsilon^3) \end{aligned}$$

Regrouping the equations order by order we get

$$O(\epsilon^0): \quad p_0^{(w)} = -\Phi_{0,t} \tag{2.3.9}$$

$$O(\epsilon^1): \quad p_1^{(w)} = -\left[\Phi_{1,t} + \Phi_{0,t_1} + \frac{1}{2}\left(\Phi_{0,x}^2 + \Phi_{0,y}^2\right)\right] \tag{2.3.10}$$

$$\begin{aligned} O(\epsilon^2): \quad p_2^{(w)} &= -[\Phi_{2,t} + \Phi_{1,t_1} + \Phi_{0,t_2} \\ &\quad +\Phi_{0,x}\Phi_{1,x} + \Phi_{0,y}\Phi_{1,y} + \Phi_{0,x}\Phi_{0,x_1}] \end{aligned} \tag{2.3.11}$$

Mud layer - Mass Conservation equation

Introducing the slow scales the conservation of mass equation (2.2.3) becomes

$$u_x + \epsilon u_{x_1} + v_{y'} = 0 \tag{2.3.12}$$

Introducing the perturbation series

$$u_{0,x} + \epsilon u_{1,x} + \epsilon u_{0,x_1} + v_{0,y'} + \epsilon v_{1,y'} = O(\epsilon^2) \tag{2.3.13}$$

For the first two orders the mass conservation equation is

$$O(\epsilon^0): \quad u_{0,x} + v_{0,y'} = 0 \tag{2.3.14}$$

$$O(\epsilon^1): \quad u_{1,x} + v_{1,y'} = -u_{0,x_1} \tag{2.3.15}$$

Mud layer - Horizontal Momentum Conservation equation

Using the slow variables the x-momentum conservation equation (2.2.4) becomes

$$u_t + \epsilon u_{t_1} + \epsilon(uu_x + vu_{y'}) = -\gamma p_x^{(m)} - \epsilon\gamma p_{x_1}^{(m)} + \frac{1}{Re}\frac{a}{d}\left(\tau_{y'}^{xy} + \epsilon\frac{d}{a}\tau_x^{xx}\right) + O(\epsilon^2)$$

Introducing the perturbation series we get

$$\begin{aligned} u_{0,t} + \epsilon u_{1,t} + \epsilon u_{0,t_1} + \epsilon(u_0 u_{0,x} + v_0 u_{0,y'}) &= -\gamma p^{(m)}_{0,x} - \epsilon\gamma p^{(m)}_{1,x} - \epsilon\gamma p^{(m)}_{0,x_1} \\ &\quad + \frac{1}{Re}\frac{a}{d}\left(\tau^{xy}_{0,y'} + \epsilon\tau^{xy}_{1,y'} + \epsilon\frac{d}{a}\tau^{xx}_{0,x}\right) + O(\epsilon^2) \end{aligned}$$

Collecting the terms order by order, we obtain the final expressions of the approximate equations for the horizontal momentum conservation:

$$O(\epsilon^0): \quad u_{0,t} = -\gamma p^{(m)}_{0,x} + \frac{1}{Re}\frac{a}{d}\tau^{xy}_{0,y'} \tag{2.3.16}$$

$$O(\epsilon^1): \quad u_{1,t} + u_{0,t_1} + u_0 u_{0,x} + v_0 u_{0,y'} = -\gamma p^{(m)}_{1,x} - \gamma p^{(m)}_{0,x_1} + \frac{1}{Re}\frac{a}{d}\tau^{xy}_{1,y'} + \frac{1}{Re}\tau^{xx}_{0,x} \tag{2.3.17}$$

Mud layer - Vertical Momentum Conservation equation

The introduction of the slow scales do not modify the vertical momentum conservation equation (2.2.5) to order $O(\epsilon)$. The introduction of the perturbation series expansions gives:

$$O(\epsilon^2) = -\gamma p^{(m)}_{0,y'} - \epsilon\gamma p^{(m)}_{1,y'} + \frac{\epsilon}{Re}\tau^{yy}_{0,y'} \tag{2.3.18}$$

The final expressions order by order are:

$$O(\epsilon^0): \quad p^{(m)}_{0,y'} = 0 \tag{2.3.19}$$

$$O(\epsilon^1): \quad p^{(m)}_{1,y'} = \frac{1}{\gamma Re}\tau^{yy}_{0,y'} \tag{2.3.20}$$

2.3.4 Boundary conditions in terms of the perturbation series

Free Surface - Combined Kinematic and Dynamic Boundary Condition

Let us first introduce the slow scales. The combined kinematic and dynamic boundary condition on the free surface (2.2.8) becomes:

$$\begin{aligned} O(\epsilon^3) &= \Phi_{tt} + 2\epsilon\Phi_{tt_1} + \epsilon^2\left[\Phi_{t_1t_1} + 2\Phi_{tt_2}\right] + \Phi_y \\ &\quad +\epsilon\left[\partial_t + \epsilon\partial_{t_1} + \frac{\epsilon}{2}\left(\Phi_x\partial_x + \Phi_y\partial_y\right)\right]\left(\Phi_x^2 + \Phi_y^2 + 2\epsilon\Phi_x\Phi_{x_1}\right), \quad y = \epsilon\eta \end{aligned}$$

By expanding the last parenthesis we obtain on the free surface ($y = \epsilon\eta$):

$$\begin{aligned} O(\epsilon^3) &= \Phi_{tt} + \Phi_y + 2\epsilon\Phi_{tt_1} + \epsilon^2\left[\Phi_{t_1t_1} + 2\Phi_{tt_2}\right] \\ &\quad +\epsilon\left[\left(\Phi_x^2 + \Phi_y^2\right)_t + \epsilon\left(\Phi_x^2 + \Phi_y^2\right)_{t_1} + 2\epsilon\left(\Phi_x\Phi_{x_1}\right)_t + \frac{\epsilon}{2}\left(\Phi_x\partial_x + \Phi_y\partial_y\right)\left(\Phi_x^2 + \Phi_y^2\right)\right] \end{aligned}$$

Grouping the terms order by order and introducing the differential operator $\Gamma \equiv \partial_{tt} + \partial_y$ the boundary condition on $y = \epsilon\eta$ becomes:

$$\begin{aligned} O(\epsilon^3) &= \Gamma\Phi + \epsilon\left[2\Phi_{tt_1} + \left(\Phi_x^2 + \Phi_y^2\right)_t\right] \\ &\quad +\epsilon^2\left[\Phi_{t_1t_1} + 2\Phi_{tt_2} + 2\left(\Phi_x\Phi_{x_1}\right)_t + \left(\Phi_x^2 + \Phi_y^2\right)_{t_1} + \frac{1}{2}\left(\Phi_x\partial_x + \Phi_y\partial_y\right)\left(\Phi_x^2 + \Phi_y^2\right)\right] \end{aligned}$$

Now expanding the unknowns dependent on y around the average position of the free surface ($y = 0$) we get:

$$\begin{aligned} O(\epsilon^3) &= (\Gamma\Phi)|_0 + \epsilon\eta(\Gamma_y\Phi)|_0 + \frac{\epsilon^2}{2}\eta^2(\Gamma_{yy}\Phi)|_0 \\ &\quad +\epsilon\left[2(\Phi_{tt_1})|_0 + 2\epsilon\eta(\Phi_{ytt_1})|_0 + \left(\Phi_x^2 + \Phi_y^2\right)_t|_0 + \epsilon\eta\left(\Phi_x^2 + \Phi_y^2\right)_{ty}|_0 +\right] \\ &\quad +\epsilon^2\Bigg[(\Phi_{t_1t_1})|_0 + 2(\Phi_{tt_2})|_0 + 2\left(\Phi_x\Phi_{x_1}\right)_t|_0 + \left(\Phi_x^2 + \Phi_y^2\right)_{t_1}|_0 \\ &\qquad + \frac{1}{2}\left[\left(\Phi_x\partial_x + \Phi_y\partial_y\right)\left(\Phi_x^2 + \Phi_y^2\right)\right]\Big|_0\Bigg] \end{aligned}$$

Grouping the terms order by order:

$$
\begin{aligned}
O(\epsilon^3) \;=\; & (\Gamma\Phi)|_0 + \epsilon\left[\eta(\Gamma_y\Phi)|_0 + 2(\Phi_{tt_1})|_0 + \left(\Phi_x^2+\Phi_y^2\right)_t|_0\right] \\
& +\epsilon^2\Bigg[\frac{\eta^2}{2}(\Gamma_{yy}\Phi)|_0 + 2\eta(\Phi_{ytt_1})|_0 + \eta\left(\Phi_x^2+\Phi_y^2\right)_{ty}|_0 + (\Phi_{t_1t_1})|_0 + 2(\Phi_{tt_2})|_0 \\
& \quad + 2\left(\Phi_x\Phi_{x_1}\right)_t|_0 + \left(\Phi_x^2+\Phi_y^2\right)_{t_1}|_0 + \frac{1}{2}\left[\left(\Phi_x\partial_x+\Phi_y\partial_y\right)\left(\Phi_x^2+\Phi_y^2\right)\right]\Big|_0\Bigg]
\end{aligned}
$$

Expanding the unknown functions into perturbation series the boundary condition becomes:

$$
\begin{aligned}
O(\epsilon^3) \;=\; & (\Gamma\Phi_0)|_0 + \epsilon(\Gamma\Phi_1)|_0 + \epsilon^2(\Gamma\Phi_2)|_0 \\
& +\epsilon\Bigg[\eta_0(\Gamma_y\Phi_0)|_0 + \epsilon\eta_1(\Gamma_y\Phi_0)|_0 + \epsilon\eta_0(\Gamma_y\Phi_1)|_0 + 2(\Phi_{0,tt_1})|_0 + 2\epsilon(\Phi_{1,tt_1})|_0 \\
& \quad + \left(\Phi_{0,x}^2+\Phi_{0,y}^2+2\epsilon(\Phi_{0,x}\Phi_{1,x}+\Phi_{0,y}\Phi_{1,y})\right)_t\Big|_0\Bigg] \\
& +\epsilon^2\Bigg[\frac{\eta_0^2}{2}(\Gamma_{yy}\Phi_0)|_0 + 2\eta_0\left(\Phi_{0,ytt_1}\right)|_0 + \eta_0\left(\Phi_{0,x}^2+\Phi_{0,y}^2\right)_{ty}\Big|_0 + (\Phi_{0,t_1t_1})|_0 + 2(\Phi_{0,tt_2})|_0 \\
& \quad + 2\left(\Phi_{0,x}\Phi_{0,x_1}\right)_t\Big|_0 + \left(\Phi_{0,x}^2+\Phi_{0,y}^2\right)_{t_1}\Big|_0 + \frac{1}{2}\left[\left(\Phi_{0,x}\partial_x+\Phi_{0,y}\partial_y\right)\left(\Phi_{0,x}^2+\Phi_{0,y}^2\right)\right]\Big|_0\Bigg]
\end{aligned}
$$

Grouping the terms order by order we get:

$$
\begin{aligned}
O(\epsilon^3) \;=\; & (\Gamma\Phi_0)|_0 \\
& +\epsilon\Bigg[(\Gamma\Phi_1)|_0 + \eta_0(\Gamma_y\Phi_0)|_0 + 2(\Phi_{0,tt_1})|_0 + \left(\Phi_{0,x}^2+\Phi_{0,y}^2\right)_t\Big|_0\Bigg] \\
& +\epsilon^2\Bigg[(\Gamma\Phi_2)|_0 + \eta_1(\Gamma_y\Phi_0)|_0 + 2(\Phi_{0,x}\Phi_{1,x}+\Phi_{0,y}\Phi_{1,y})_t + \frac{\eta_0^2}{2}(\Gamma_{yy}\Phi_0)|_0 + 2\eta_0(\Phi_{0,ytt_1})|_0 \\
& \quad + \eta_0\left(\Phi_{0,x}^2+\Phi_{0,y}^2\right)_{ty}\Big|_0 + \eta_0(\Gamma_y\Phi_1)|_0 + (\Phi_{0,t_1t_1})|_0 + 2(\Phi_{0,tt_2})|_0 + 2\left(\Phi_{0,x}\Phi_{0,x_1}\right)_t\Big|_0 \\
& \quad + 2(\Phi_{1,tt_1})|_0 + \left(\Phi_{0,x}^2+\Phi_{0,y}^2\right)_{t_1}\Big|_0 + \frac{1}{2}\left[\left(\Phi_{0,x}\partial_x+\Phi_{0,y}\partial_y\right)\left(\Phi_{0,x}^2+\Phi_{0,y}^2\right)\right]\Big|_0\Bigg]
\end{aligned}
$$

The combined kinematic and dynamic boundary condition can now be written for the first three orders:

$$O(\epsilon^0): \quad (\Gamma\Phi_0)|_0 = G_0 \tag{2.3.21}$$

$$O(\epsilon^1): \quad (\Gamma\Phi_1)|_0 = G_1 \tag{2.3.22}$$

$$O(\epsilon^2): \quad (\Gamma\Phi_2)|_0 = G_2 \tag{2.3.23}$$

with the constants G_0, G_1 and G_2 defined by:

$$G_0 = 0 \tag{2.3.24}$$

$$G_1 = -\left[\eta_0(\Gamma_y\Phi_0)|_0 + 2(\Phi_{0,tt_1})|_0 + \left(\Phi_{0,x}^2 + \Phi_{0,y}^2\right)_t\Big|_0\right] \tag{2.3.25}$$

$$\begin{aligned} G_2 = -\Big[&\eta_1(\Gamma_y\Phi_0)|_0 + \eta_0(\Gamma_y\Phi_1)|_0 + 2(\Phi_{0,x}\Phi_{1,x} + \Phi_{0,y}\Phi_{1,y})_t + \frac{\eta_0^2}{2}(\Gamma_{yy}\Phi_0)|_0 + 2\eta_0(\Phi_{0,ytt_1})|_0 \\ &+ 2(\Phi_{1,tt_1})|_0 + \eta_0\left(\Phi_{0,x}^2 + \Phi_{0,y}^2\right)_{ty}\Big|_0 + (\Phi_{0,t_1t_1})|_0 + 2(\Phi_{0,tt_2})|_0 + 2\left(\Phi_{0,x}\Phi_{0,x_1}\right)_t\Big|_0 \\ &+ \left(\Phi_{0,x}^2 + \Phi_{0,y}^2\right)_{t_1}\Big|_0 + \frac{1}{2}\left[(\Phi_{0,x}\partial_x + \Phi_{0,y}\partial_y)\left(\Phi_{0,x}^2 + \Phi_{0,y}^2\right)\right]\Big|_0\Big] \end{aligned} \tag{2.3.26}$$

Free Surface - Dynamic Boundary Condition

Let us first introduce the slow scales. The dynamic boundary condition on the free surface (2.2.7) becomes:

$$-\eta = \Phi_t + \epsilon\Phi_{t_1} + \epsilon^2\Phi_{t_2} + \frac{\epsilon}{2}\left(\Phi_x^2 + \Phi_y^2 + 2\epsilon\Phi_x\Phi_{x_1}\right) = 0, \quad y = \epsilon\eta$$

Due to the small amplitude of the free surface waves the terms that depend on the vertical position of the interface can be developed into Taylor series around the average interface ($y = 0$):

$$\begin{aligned} -\eta = &(\Phi_t)|_0 + \epsilon\eta(\Phi_{yt})|_0 + \frac{\epsilon^2}{2}\eta^2(\Phi_{yyt})|_0 + \epsilon(\Phi_{t_1})|_0 + \epsilon^2\eta(\Phi_{t_1y})|_0 + \epsilon^2(\Phi_{t_2})|_0 \\ &+\frac{\epsilon}{2}\left\{(\Phi_x^2 + \Phi_y^2)|_0 + \epsilon\eta\left[(\Phi_x^2 + \Phi_y^2)_y\right]|_0 + 2\epsilon(\Phi_x)|_0(\Phi_{x_1})|_0\right\} + O(\epsilon^3) \end{aligned}$$

Grouping the terms of the respective orders, we get:

$$\begin{aligned}
-\eta &= (\Phi_t)|_0 + \epsilon\left[\eta(\Phi_{yt})|_0 + (\Phi_{t_1})|_0 + \frac{1}{2}(\Phi_x^2+\Phi_y^2)|_0\right] + O(\epsilon^3) \\
&\quad +\epsilon^2\left[\frac{1}{2}\eta^2(\Phi_{yyt})|_0 + \eta(\Phi_{t_1y})|_0 + (\Phi_{t_2})|_0 + \frac{1}{2}\eta\left[(\Phi_x^2+\Phi_y^2)_y\right]\big|_0 + (\Phi_x)|_0(\Phi_{x_1})|_0\right]
\end{aligned}$$

Expanding the unknown functions into perturbation series we obtain:

$$\begin{aligned}
-\eta_0 - \epsilon\eta_1 - \epsilon^2\eta_2 &= (\Phi_{0,t})|_0 + \epsilon(\Phi_{1,t})|_0 + \epsilon^2(\Phi_{2,t})|_0 \\
&\quad +\epsilon\Big\{\eta_0(\Phi_{0,yt})|_0 + \epsilon\eta_1(\Phi_{0,yt})|_0 + \epsilon\eta_0(\Phi_{1,yt})|_0 + (\Phi_{0,t_1})|_0 + \epsilon(\Phi_{1,t_1})|_0 \\
&\qquad + \frac{1}{2}(\Phi_{0,x}^2+\Phi_{0,y}^2)|_0 + \epsilon\left[(\Phi_{0,x}\Phi_{1,x})|_0 + (\Phi_{0,y}\Phi_{1,y})|_0\right]\Big\} \\
&\quad +\epsilon^2\Big\{\frac{1}{2}\eta_0^2(\Phi_{0,yyt})|_0 + \eta_0(\Phi_{0,t_1y})|_0 + (\Phi_{0,t_2})|_0 \\
&\qquad + \frac{1}{2}\eta_0\left[(\Phi_{0,x}^2+\Phi_{0,y}^2)_y + \Phi_{0,x}\Phi_{0,x_1}\right]|_0\Big\} + O(\epsilon^3)
\end{aligned}$$

Grouping the terms by order we get:

$$\begin{aligned}
-\eta_0 - \epsilon\eta_1 - \epsilon^2\eta_2 &= (\Phi_{0,t})|_0 + \epsilon\Big\{(\Phi_{1,t})|_0 + \eta_0(\Phi_{0,yt})|_0 + (\Phi_{0,t_1})|_0 + \frac{1}{2}(\Phi_{0,x}^2+\Phi_{0,y}^2)|_0\Big\} \\
&\quad +\epsilon^2\Big\{(\Phi_{2,t})|_0 + \eta_1(\Phi_{0,yt})|_0 + \eta_0(\Phi_{1,yt})|_0 + (\Phi_{1,t_1})|_0 + \frac{1}{2}\eta_0^2(\Phi_{0,yyt})|_0 \\
&\qquad + \eta_0(\Phi_{0,t_1y})|_0 + (\Phi_{0,t_2})|_0 + \left[(\Phi_{0,x}\Phi_{1,x})|_0 + (\Phi_{0,y}\Phi_{1,y})|_0\right] \\
&\qquad + \frac{1}{2}\eta_0\left[(\Phi_{0,x}^2+\Phi_{0,y}^2)_y + \Phi_{0,x}\Phi_{0,x_1}\right]\big|_0\Big\} + O(\epsilon^3)
\end{aligned}$$

The dynamic boundary condition on the free surface can now be written for the first three orders:

$$O(\epsilon^0): \quad -\eta_0 = H_0 \tag{2.3.27}$$

$$O(\epsilon^1): \quad -\eta_1 = H_1 \tag{2.3.28}$$

$$O(\epsilon^2): \quad -\eta_2 = H_2 \tag{2.3.29}$$

with the constants H_0, H_1 and H_2 defined by:

$$H_0 = (\Phi_{0,t})|_0 \tag{2.3.30}$$

$$H_1 = (\Phi_{1,t})|_0 + \eta_0(\Phi_{0,yt})|_0 + (\Phi_{0,t_1})|_0 + \frac{1}{2}\left(\Phi_{0,x}^2 + \Phi_{0,y}^2\right)\Big|_0 \tag{2.3.31}$$

$$\begin{aligned} H_2 = {} & (\Phi_{2,t})|_0 + \eta_1(\Phi_{0,yt})|_0 + \eta_0(\Phi_{1,yt})|_0 + (\Phi_{1,t_1})|_0 + \frac{1}{2}\eta_0^2(\Phi_{0,yyt})|_0 \\ & + \eta_0(\Phi_{0,t_1y})|_0 + (\Phi_{0,t_2})|_0 + (\Phi_{0,x}\Phi_{1,x})|_0 + (\Phi_{0,y}\Phi_{1,y})|_0 \\ & + \frac{1}{2}\eta_0\left[(\Phi_{0,x}^2 + \Phi_{0,y}^2)_y + \Phi_{0,x}\Phi_{0,x_1}\right]\Big|_0 \end{aligned} \tag{2.3.32}$$

Interface - Kinematic Boundary Condition in terms of water quantities

After the introduction of the slow scales the dynamic boundary condition on the interface in terms of the water quantities (2.2.9) becomes:

$$\Phi_y = \epsilon\zeta_t + \epsilon^2\zeta_{t_1} + \epsilon^2\zeta_x\Phi_x + O(\epsilon^3) \qquad y = -H + \epsilon^2\zeta$$

Expanding into the Taylor series around the average interface ($y = -H$):

$$(\Phi_y)|_{-H} + \epsilon^2\zeta(\Phi_{yy})|_{-H} = \epsilon\zeta_t + \epsilon^2\zeta_{t_1} + \epsilon^2\zeta_x(\Phi_x)_{-H} + O(\epsilon^3)$$

Expanding into the perturbation series we get:

$$(\Phi_{0,y})|_{-H}+\epsilon(\Phi_{1,y})|_{-H}+\epsilon^2(\Phi_{2,y})|_{-H}+\epsilon^2\zeta_0(\Phi_{0,yy})|_{-H} = \epsilon\zeta_{0,t}+\epsilon^2\zeta_{1,t}+\epsilon^2\zeta_{0,t_1}+\epsilon^2\zeta_{0,x}(\Phi_{0,x})_{-H}+O(\epsilon^3)$$

Grouping the terms of the last equation order by order we get:

$$O(\epsilon^0): \quad (\Phi_{0,y})|_{-H} = L_0 \tag{2.3.33}$$

$$O(\epsilon^1): \quad (\Phi_{1,y})|_{-H} = L_1 \tag{2.3.34}$$

$$O(\epsilon^2): \quad (\Phi_{2,y})|_{-H} = L_2 \tag{2.3.35}$$

with the constants L_0, L_1 and L_2 equal to

$$L_0 = 0 \tag{2.3.36}$$

$$L_1 = \zeta_{0,t} \tag{2.3.37}$$

$$L_2 = \zeta_{1,t} + \zeta_{0,t_1} + [(\zeta_0 \Phi_{0,x})_x]|_{-H} \tag{2.3.38}$$

To compute the expression of L_2 the fact was used that $\Phi_{0,yy} = -\Phi_{0,xx}$. This identity comes from the Laplace equation at the leading order (equations (2.3.3) and (2.3.6)).

Interface - Kinematic Boundary Condition in terms of mud quantities

After the introduction of the slow scales, the dynamic boundary condition in terms of the mud quantities (2.2.10) becomes

$$\zeta_t + \epsilon\zeta_{t_1} = \frac{d}{a}v - \epsilon\zeta_x u + O(\epsilon^2), \quad y' = 1 + \epsilon\frac{a}{d}\zeta$$

Expanding into Taylor series around the average interface position ($y' = 1$) we get:

$$\zeta_t + \epsilon\zeta_{t_1} = \frac{d}{a}(v)|_1 + \epsilon\zeta(v_{y'})|_1 - \epsilon\zeta_x(u)|_1 + O(\epsilon^2)$$

Expanding the unknowns into the perturbation series we get:

$$\zeta_{0,t} + \epsilon\zeta_{1,t} + \epsilon\zeta_{0,t_1} = \frac{d}{a}(v_0)|_1 + \epsilon\frac{d}{a}(v_1)|_1 + \epsilon\zeta_0(v_{0,y'})|_1 - \epsilon\zeta_{0,x}(u_0)|_1 + O(\epsilon^2)$$

The dynamic boundary condition at the interface in terms of the mud quantities can now be written for the first two orders:

$$O(\epsilon^0): \quad \zeta_{0,t} = \frac{d}{a}(v_0)|_1 \tag{2.3.39}$$

$$O(\epsilon^1): \quad \zeta_{1,t} = \frac{d}{a}(v_1)|_1 - \zeta_{0,t_1} - [(\zeta_0 u_0)_x]|_1 \tag{2.3.40}$$

where we made use of the fact that $v_{0,y'} = -u_{0,x}$. This identity comes from the mass conservation equation to the leading order (2.3.14).

Interface - Dynamic Boundary Condition

The dynamic boundary condition on the interface (2.2.11) can be simplified by using the fact that due to the shallowness of the mud layer the interface stays relatively flat. Let us estimate the orders of magnitude of the components of the vector $\vec{n} = (n_x, n_y)$ normal to the interface. In terms of the dimensional variables these components are equal to

$$\begin{aligned} n^{(x)} &= \frac{d\bar{\zeta}}{\sqrt{(d\bar{x})^2 + (d\bar{\zeta})^2}} = \frac{\frac{d\bar{\zeta}}{d\bar{x}}}{\sqrt{(1 + (\frac{d\bar{\zeta}}{d\bar{x}})^2}} \\ n^{(y)} &= \frac{d\bar{x}}{\sqrt{(d\bar{x})^2 + (d\bar{\zeta})^2}} = \frac{1}{\sqrt{(1 + (\frac{d\bar{\zeta}}{d\bar{x}})^2}} \end{aligned}$$

In terms of the dimensionless variables the components of the normal vector are

$$\begin{aligned} n^{(x)} &= \frac{\epsilon^2 \frac{d}{a} \frac{d\zeta}{dx}}{\sqrt{(1 + \epsilon^4 (\frac{d\zeta}{dx})^2}} = O(\epsilon^2) \\ n^{(y)} &= \frac{1}{\sqrt{(1 + \epsilon^4 \left(\frac{d}{a}\right)^2 (\frac{d\bar{\zeta}}{d\bar{x}})^2}} = 1 + O(\epsilon^4) \end{aligned}$$

Therefore the dimensionless components of the tangential stress are to order $O(\epsilon^2)$

$$\begin{aligned} (\underline{\underline{\sigma}}.\vec{n}).\vec{e}^{(x)} &= \sigma^{xx} n_x + \sigma^{xy} n_y = \sigma^{xy} + O(\epsilon^3) = \frac{\epsilon}{\gamma Re} \tau^{xy} + O(\epsilon^3) \\ (\underline{\underline{\sigma}}.\vec{n}).\vec{e}^{(y)} &= \sigma^{xy} n_x + \sigma^{yy} n_y = \sigma^{yy} + O(\epsilon^2) = -p^{(m)} + \frac{\epsilon}{\gamma Re} \tau^{yy} + O(\epsilon^2) \end{aligned}$$

The dynamic boundary condition on the interface (2.2.11) can now be rewritten as

$$\begin{aligned} O(\epsilon^3) &= \tau^{xy} \\ -p^{(w)} &= -p^{(m)} + \frac{\epsilon}{\gamma Re} \tau^{yy} + O(\epsilon^2) \end{aligned}$$

By using the Taylor expansion around the average position of the interface ($y' = 0$) the approximate dynamic boundary condition on the interface becomes

$$\begin{aligned} O(\epsilon^2) &= \tau^{xy}|_{y'=1} + \epsilon\frac{a}{d}\zeta\left(\tau^{xy}_{y'}\right)\Big|_{y'=1} \\ -p^{(w)}|_{y=-H} &= -p^{(m)}\Big|_{y'=1} - \epsilon\frac{a}{d}\zeta\left(p^{(m)}_{y'}\right)\Big|_{y'=1} + \frac{\epsilon}{\gamma Re}(\tau^{yy})|_{y'=1} + O(\epsilon^2) \end{aligned}$$

Expanding the unknowns into perturbation series, the conditions expressing the continuity of the stresses through the interface become

$$\begin{aligned} O(\epsilon^2) &= \tau_0^{xy}|_{y'=1} + \epsilon\tau_1^{xy}|_{y'=1} + \epsilon\frac{a}{d}\zeta_0\left(\tau^{xy}_{0,y'}\right)\Big|_{y'=1} \\ -p_0^{(w)}\Big|_{y=-H} - \epsilon\, p_1^{(w)}\Big|_{y=-H} &= -p_0^{(m)}\Big|_{y'=1} - \epsilon\, p_1^{(m)}\Big|_{y'=1} \\ &\quad -\epsilon\frac{a}{d}\zeta_0\left(p^{(m)}_{0,y'}\right)\Big|_{y'=1} + \frac{\epsilon}{\gamma Re}(\tau_0^{yy})|_{y'=1} + O(\epsilon^2) \end{aligned}$$

The dynamic boundary conditions - tangential and normal stress continuity - on the interface can now be written for the first two orders.

Tangential stress continuity:

$$O(\epsilon^0): \quad \tau_0^{xy}|_{y'=1} = 0 \tag{2.3.41}$$

$$O(\epsilon^1): \quad \tau_1^{xy}|_{y'=1} = -\frac{a}{d}\zeta_0\left(\tau^{xy}_{0,y'}\right)\Big|_{y'=1} \tag{2.3.42}$$

Normal stress continuity:

$$O(\epsilon^0): \quad p_0^{(m)}|_{y'=1} = p_0^{(w)}|_{y=-H} \tag{2.3.43}$$

$$O(\epsilon^1): \quad p_1^{(m)}|_{y'=1} = p_1^{(w)}|_{y=-H} - \frac{a}{d}\zeta_0\left(p^{(m)}_{0,y'}\right)\Big|_{y'=1} + \frac{1}{\gamma Re}\tau_0^{yy}|_{y'=1} \tag{2.3.44}$$

Bottom - Horizontal Velocity

It is straightforward to see that the no slip condition for the horizontal velocity (2.2.12) for the first two orders is

$$O(\epsilon^0): \quad (u_0)|_0 = 0 \tag{2.3.45}$$

$$O(\epsilon^1): \quad (u_1)|_0 = 0 \tag{2.3.46}$$

Bottom - Vertical Velocity

The no slip condition for the vertical velocity (2.2.13) becomes

$$O(\epsilon^0): \quad (v_0)|_0 = 0 \tag{2.3.47}$$

$$O(\epsilon^1): \quad (v_1)|_0 = 0 \tag{2.3.48}$$

Bottom - Horizontal Displacement

The no slip boundary condition in terms of the horizontal displacement (2.2.14) is

$$O(\epsilon^0): \quad (X_0)|_0 = 0 \tag{2.3.49}$$

$$O(\epsilon^1): \quad (X_1)|_0 = 0 \tag{2.3.50}$$

Bottom - Vertical Displacement

The no slip boundary condition in terms of the vertical displacement (2.2.15) is

$$O(\epsilon^0): \quad (Y_0)|_0 = 0 \tag{2.3.51}$$

$$O(\epsilon^1): \quad (Y_1)|_0 = 0 \tag{2.3.52}$$

2.3.5 Sinusoidal waves

We will assume the waves to be sinusoidal with respect to the fast scales x and t at the leading order. The amplitude of the sinusoidal waves is allowed to vary with the slow scales. Note also that as viscoelastic model of the mud involves derivatives with

respect to time t, the assumption of sinusoidal wavetrain will simplify the computations of the stress strain relationship.

In fact we will assume that at the leading order the free surface displacement is a slowly varying in time and space sinusoidal wave train of the form:

$$\eta_0(x,t,x_1,t_1,t_2,...) = \frac{1}{2}\left[A(x_1,t_1,t_2,...)e^{i\psi(x,t)} + c.c.\right] \tag{2.3.53}$$

with $A = A(x_1,t_1,t_2,...)$ being a function slowly varying with time and with the real function $\psi(x,t)$ given by

$$\psi = \psi(x,t) \equiv k_0 x - t \tag{2.3.54}$$

In that case the dependence on time t and on short length scale x is known at the leading order. In fact, under this assumption, any leading order F_0 quantity will be of the form

$$F_0(x,y,t,x_1,t_1,t_2,...) = F_{00} + \left(F_{01}e^{i\psi} + c.c.\right)$$

with $F_{00} = F_{00}(y,x_1,t_1,t_2,...)$ and $F_{01} = F_{01}(y,x_1,t_1,t_2,...)$ being slowly varying functions with time and horizontal coordinate.

For the next order $O(\epsilon)$ the governing equations indicate that the second order solutions will not only be composed of zeroth and first harmonics, but also will include second harmonic. Therefore any second order quantity F_1 will be of the form

$$F_1(x,y,t,x_1,t_1,t_2,...) = F_{10} + \left(F_{11}e^{i\psi} + c.c.\right) + \left(F_{12}e^{2i\psi} + c.c.\right)$$

with $F_{10} = F_{10}(y,x_1,t_1,t_2,...)$, $F_{11} = F_{11}(y,x_1,t_1,t_2,...)$ and $F_{12} = F_{12}(y,x_1,t_1,t_2,...)$ being slowly varying functions of time.

Finally for the third order $O(\epsilon^2)$ the governing equations indicate that the solutions will also include third harmonics. Therefore any second order quantity F_2 will be of the form

$$F_2(x,t,x_1,t_1,t_2,...) = F_{20} + \left(F_{21}e^{i\psi} + c.c.\right) + \left(F_{22}e^{2i\psi} + c.c.\right) + \left(F_{23}e^{3i\psi} + c.c.\right)$$

with $F_{20} = F_{20}(y, x_1, t_1, t_2, ...)$, $F_{21} = F_{21}(y, x_1, t_1, t_2, ...)$, $F_{22} = F_{22}(y, x_1, t_1, t_2, ...)$ and $F_{23} = F_{23}(y, x_1, t_1, t_2, ...)$ being slowly varying functions of time of order $O(1)$. Using the assumption of the sinusoidal forcing we will now obtain explicit relationships between the stress and strain tensors for the first two orders.

2.3.6 Relationship between stress tensor and the velocity and displacement fields

In this section the relationship between the stress tensor $\underline{\underline{\tau}}$, the velocity (u, v) and the displacement field (X, Y) will be obtained for the first two orders. To do it we first express the stress tensor in terms of the strain tensor, then we express the strain tensor in terms of the displacement field and link the displacement field to the velocity field.

Dimensionless Stress-Strain Relationship

The mud is modeled as a viscoelastic fluid using the model (1.4.1). As opposed to the case of a purely viscous fluid, the stress tensor is not simply proportional to the rate of strain tensor, but is related to the strain tensor by the differential equation (1.4.1), which in dimensionless terms is:

$$\left(1 + \sum_{n=1}^{N} a_n (\partial_t)^n\right) \underline{\underline{\tau}} = \left(\sum_{n=0}^{N-1} b_n (\partial_t)^n\right) \underline{\underline{\gamma}} \tag{2.3.55}$$

with the dimensionless coefficients a_n and b_n defined as

$$a_n = \bar{a}_n \omega^n \tag{2.3.56}$$

$$b_n = \frac{\bar{b}_n}{\mu_0 \omega} \omega^n \tag{2.3.57}$$

Note that the dimensional values of $\bar{a}_n$ and $\bar{b}_n$ were computed in chapter 1 and listed in tables (1.1) and (1.2).

Our objective is to express in terms of the displacement and the velocity field the components of the stress tensor appearing in the governing equations of the mud layer movement (2.3.16), (2.3.17) and (2.3.20), which are: τ_0^{xy}, τ_0^{yy}, τ_0^{xx} and τ_1^{xy}. Before we can do this we first need to compute explicitly the strain components in terms of the perturbation series.

Explicit expressions of the components of the strain tensor

Now the strain tensor will be expressed in terms of the displacement field.
The strain is defined as:

$$\underline{\underline{\gamma}} = \begin{pmatrix} \gamma^{xx} & \gamma^{xy} \\ \gamma^{yx} & \gamma^{yy} \end{pmatrix} = \begin{pmatrix} 2\epsilon\frac{d}{a}X_x & X_{y'} + \left(\epsilon\frac{d}{a}\right)^2 Y_x \\ X_{y'} + \left(\epsilon\frac{d}{a}\right)^2 Y_x & 2\epsilon\frac{d}{a}Y_{y'} \end{pmatrix} = \begin{pmatrix} 2\epsilon\frac{d}{a}X_x & X_{y'} \\ X_{y'} & 2\epsilon\frac{d}{a}Y_{y'} \end{pmatrix} + O(\epsilon^2)$$

Note that the introduction of the slow scales does not modify the last expression to the studied order $O(\epsilon^2)$. Expanding the unknown displacement (X, Y) into perturbation series we get

$$\underline{\underline{\gamma}} = \begin{pmatrix} 2\epsilon\frac{d}{a}X_{0,x} & X_{0,y'} + \epsilon X_{1,y'} \\ X_{0,y'} + \epsilon X_{1,y'} & 2\epsilon\frac{d}{a}Y_{0,y'} \end{pmatrix} + O(\epsilon^2)$$

Grouping the terms order by order we get

$$O(\epsilon^0): \begin{cases} \gamma_0^{xx} = 0, \\ \gamma_0^{xy} = X_{0,y'}, \\ \gamma_0^{yy} = 0 \end{cases} \qquad O(\epsilon): \begin{cases} \gamma_1^{xx} = 2\frac{d}{a}X_{0,x}, \\ \gamma_1^{xy} = X_{1,y'}, \\ \gamma_1^{yy} = 2\frac{d}{a}Y_{0,y'} \end{cases}$$

Note that as the strain tensor is symmetric its components γ_1^{xy} and γ_1^{yx} are equal. The expression of the strain tensor can now be deduced straightforwardly for each harmonic. We assume that the mean displacement inside the mud layer is of the second order $O(\epsilon)$, therefore the terms X_{00} and Y_{00} are equal to zero.

At the leading order $O(\epsilon^0)$ we have:

$$\begin{cases} \gamma_{00}^{xx} = 0, \\ \gamma_{00}^{xy} = X_{00,y'} = 0, \\ \gamma_{00}^{yy} = 0 \end{cases} \qquad \begin{cases} \gamma_{01}^{xx} = 0, \\ \gamma_{01}^{xy} = X_{01,y'}, \\ \gamma_{01}^{yy} = 0 \end{cases} \tag{2.3.58}$$

At the second order $O(\epsilon)$ we have:

$$\begin{cases} \gamma_{10}^{xx} = 0, \\ \gamma_{10}^{xy} = X_{10,y'}, \\ \gamma_{10}^{yy} = 2\frac{d}{a}Y_{00,y'} = 0 \end{cases} \qquad \begin{cases} \gamma_{11}^{xx} = 2ik_0\frac{d}{a}X_{01}, \\ \gamma_{11}^{xy} = X_{11,y'}, \\ \gamma_{11}^{yy} = 2\frac{d}{a}Y_{01,y'} \end{cases} \qquad \begin{cases} \gamma_{12}^{xx} = 0, \\ \gamma_{12}^{xy} = X_{12,y'}, \\ \gamma_{12}^{yy} = 0 \end{cases} \tag{2.3.59}$$

Approximation of the generalized visco-elastic model

Introducing the slow time scales the differential operators appearing in the generalized visco-elastic model (2.3.55) become:

$$1 + \sum_{n=1}^{N} a_n(\partial_t)^n \;\rightarrow\; 1 + \sum_{n=1}^{N} a_n(\partial_t)^n + \epsilon \sum_{n=1}^{N} n a_n(\partial_{t_1})(\partial_t)^{(n-1)} + O(\epsilon^2) \tag{2.3.60}$$

$$\sum_{n=0}^{N-1} b_n(\partial_t)^n \;\rightarrow\; \sum_{n=0}^{N-1} b_n(\partial_t)^n + \epsilon \sum_{n=0}^{N-1} n b_n(\partial_{t_1})(\partial_t)^{(n-1)} + O(\epsilon^2) \tag{2.3.61}$$

Introducing the perturbation series expansions the viscoelastic model (2.3.55) becomes:

$$\left(1 + \sum_{n=1}^{N} a_n(\partial_t)^n\right) \underline{\underline{\tau_0}} + \epsilon \left[\left(1 + \sum_{n=1}^{N} a_n(\partial_t)^n\right) \underline{\underline{\tau_1}} + \left(\sum_{n=1}^{N} n a_n(\partial_{t_1})(\partial_t)^{(n-1)}\right) \underline{\underline{\tau_0}} \right]$$
$$= \left(\sum_{n=0}^{N-1} b_n(\partial_t)^n\right) \underline{\underline{\gamma_0}}$$
$$+ \epsilon \left[\left(\sum_{n=0}^{N-1} b_n(\partial_t)^n\right) \underline{\underline{\gamma_1}} + \left(\sum_{n=0}^{N-1} n b_n(\partial_{t_1})(\partial_t)^{(n-1)}\right) \underline{\underline{\gamma_0}} \right] + O(\epsilon^2)$$

Combining the terms of the last equation order by order we get the stress-strain relationship for the first two orders:

$$O(\epsilon^0): \qquad \left(1+\sum_{n=1}^{N} a_n(\partial_t)^n\right)\underline{\underline{\tau_0}} = \left(\sum_{n=0}^{N-1} b_n(\partial_t)^n\right)\underline{\underline{\gamma_0}} \tag{2.3.62}$$

$$\begin{aligned} O(\epsilon^1): \qquad & \left(1+\sum_{n=1}^{N} a_n(\partial_t)^n\right)\underline{\underline{\tau_1}} + \left(\sum_{n=1}^{N} n a_n(\partial_t)^{(n-1)}\right)\underline{\underline{\tau_{0,t_1}}} \\ & = \left(\sum_{n=0}^{N-1} b_n(\partial_t)^n\right)\underline{\underline{\gamma_1}} + \left(\sum_{n=0}^{N-1} n b_n(\partial_t)^{(n-1)}\right)\underline{\underline{\gamma_{0,t_1}}} \end{aligned} \tag{2.3.63}$$

Introducing the sinusoidal movement approximation we get to decompose the unknown stress, strain and rate of strain tensors into different harmonics.
At the leading order $O(\epsilon^0)$, the stress-strain relationship (2.3.62) becomes:

$$\begin{aligned} O(\epsilon^0): \qquad & \underline{\underline{\tau_{00}}} + \left[\left(1+\sum_{n=1}^{N} a_n(-i)^n\right)\underline{\underline{\tau_{01}}} e^{i\psi} + c.c.\right] \\ & = b_0\underline{\underline{\gamma_{00}}} + \left[\left(\sum_{n=0}^{N-1} b_n(-i)^n\right)\underline{\underline{\gamma_{01}}} e^{i\psi} + c.c.\right] \end{aligned}$$

Equating the terms of the last equation harmonic by harmonic we get

$$\underline{\underline{\tau_{00}}} = b_0\underline{\underline{\gamma_{00}}} = 0 \tag{2.3.64}$$

$$\left(1+\sum_{n=1}^{N} a_n(-i)^n\right)\underline{\underline{\tau_{01}}} = \left(\sum_{n=0}^{N-1} b_n(-i)^n\right)\underline{\underline{\gamma_{01}}} \tag{2.3.65}$$

Where in the equation (2.3.64) the fact was used that there is no mean displacement at the leading order $O(1)$ and thus $\underline{\underline{\gamma_{00}}} = 0$.
We can now determine the leading order components of the stress τ_0^{xy}, τ_0^{yy}, τ_0^{xx} needed for the governing equations (2.3.16), (2.3.17) and (2.3.20). In fact from the equation

(2.3.64) we get for the zeroth harmonic

$$\tau_{00}^{xx} = 0 \tag{2.3.66}$$

$$\tau_{00}^{xy} = 0 \tag{2.3.67}$$

$$\tau_{00}^{yy} = 0 \tag{2.3.68}$$

From the equation (2.3.65) we get for the first harmonic:

$$\left(1+\sum_{n=1}^{N} a_n(-i)^n\right)\tau_{01}^{xx} = \left(\sum_{n=0}^{N-1} b_n(-i)^{(n}\right)\gamma_{01}^{xx} = 0 \tag{2.3.69}$$

$$\begin{aligned}\left(1+\sum_{n=1}^{N} a_n(-i)^n\right)\tau_{01}^{xy} &= \left(\sum_{n=0}^{N-1} b_n(-i)^n\right)\gamma_{01}^{xy} \\ &= \left(\sum_{n=0}^{N-1} b_n(-i)^n\right)X_{01,y'}\end{aligned} \tag{2.3.70}$$

$$\left(1+\sum_{n=1}^{N} a_n(-i)^n\right)\tau_{01}^{yy} = \left(\sum_{n=0}^{N-1} b_n(-i)^n\right)\gamma_{01}^{yy} = 0 \tag{2.3.71}$$

Note that in the equation (2.3.70) the shear stress is related to the displacement X_{01}. A more compact and usual form can be obtained as the displacement can be expressed in terms of the velocity. In fact the velocity is simply the Lagrangian derivative of the displacement:

$$u = D_t X = \left[\partial_t + \epsilon\left(u\partial_x + v\partial_{y'}\right)\right]X$$

Introducing the slow scales we get

$$u = \left[\partial_t + \epsilon\left(\partial_{t_1} + u\partial_x + v\partial_{y'}\right)\right]X + O(\epsilon^2)$$

Introducing the perturbation series:

$$u_0 + \epsilon u_1 = X_{0,t} + \epsilon\left(X_{1,t} + X_{0,t_1} + u_0 X_{0,x} + v_0 X_{0,y'}\right) + O(\epsilon^2)$$

Separating the orders we get:

$$u_0 = X_{0,t} \tag{2.3.72}$$

$$u_1 = X_{0,t_1} + X_{1,t} + u_0 X_{0,x} + v_0 X_{0,y'} \tag{2.3.73}$$

Introducing harmonics we get for the equation (2.3.72):

$$u_{00} + \left(u_{01} e^{i\psi} + c.c.\right) = -iX_{01} e^{i\psi} + c.c. \tag{2.3.74}$$

which gives the following relationships between the leading order velocity and displacement:

$$u_{00} = 0 \tag{2.3.75}$$

$$u_{01} = -iX_{01} \tag{2.3.76}$$

For the second order $O(\epsilon)$ the equation (2.3.73) gives:

$$\begin{aligned} u_{10} + \left(u_{11} e^{i\psi} + c.c.\right) + \left(u_{12} e^{2i\psi} + c.c.\right) = {} & X_{00,t_1} + \left(ik_0 X_{01} u_{01}^* + X_{01,y'} v_{01}^* + c.c\right) \\ & + \left[\left(X_{01,t_1} - iX_{11} + ik_0 u_{00} X_{01} + v_{00} X_{01,y'}\right) e^{i\psi} + c.c.\right] \\ & + \left[\left(-2iX_{12} + ik_0 u_{01} X_{01} + v_{01} X_{01,y'}\right) e^{2i\psi} + c.c.\right] \end{aligned}$$

remembering that there is no leading order displacement $X_{00} = 0$ and using the equation (2.3.75) saying that $u_{00} = 0$ we get:

$$u_{10} = 2\Re\left\{ik_0 X_{01} u_{01}^* + X_{01,y'} v_{01}^*\right\} \tag{2.3.77}$$

$$u_{11} = -iX_{11} + X_{01,t_1} + v_{00} X_{01,y'} = -iX_{11} + X_{01,t_1} \tag{2.3.78}$$

$$u_{12} = -2iX_{12} + ik_0 u_{01} X_{01} + v_{01} X_{01,y'} \tag{2.3.79}$$

where in the equation (2.3.78) we used the equation (2.3.80) to say that $v_{00} = 0$.
The relationship between the vertical velocity v and the vertical displacement Y is in all ways similar ($v = D_t Y$) and can be written immediately in terms of the different

harmonics of the perturbation series. At the leading order $O(\epsilon^0)$ we get:

$$v_{00} = 0 \tag{2.3.80}$$

$$v_{01} = -iY_{01} \tag{2.3.81}$$

At the second order $O(\epsilon)$ we get:

$$v_{10} = 2\Re\left\{ik_0 Y_{01} u_{01}^* + Y_{01,y'} v_{01}^*\right\} \tag{2.3.82}$$

$$v_{11} = -iY_{11} + Y_{01,t_1} + v_{00} Y_{01,y'} = -iY_{11} + Y_{01,t_1} \tag{2.3.83}$$

$$v_{12} = -2iY_{12} + ik_0 u_{01} Y_{01} + v_{01} Y_{01,y'} \tag{2.3.84}$$

where in (2.3.83) we again used the equation (2.3.80) to say that $v_{00} = 0$.
Noticing that at the leading order the first harmonic of the velocity u_{01} and of the displacement X_{01} are related simply by equation (2.3.76) we deduce that $X_{01} = iu_{01}$. Now using this fact we can rewrite the equation (2.3.70) in terms of stress and velocity only:

$$\left(1 + \sum_{n=1}^{N} a_n (-i)^n\right) \tau_{01}^{xy} = i \left(\sum_{n=0}^{N-1} b_n (-i)^n\right) u_{01,y'} \tag{2.3.85}$$

Defining the dimensionless viscosity μ

$$\mu \equiv i \frac{\sum_{n=0}^{N-1} b_n (-i)^n}{1 + \sum_{n=1}^{N} a_n (-i)^n} \tag{2.3.86}$$

we can rewrite the leading order components of the stress tensor (equations (2.3.66)-(2.3.68) and (2.3.69)-(2.3.71)) in a compact form. For the zeroth harmonic components we have:

$$\tau_{00}^{xx} = 0 \tag{2.3.87}$$

$$\tau_{00}^{xy} = 0 \tag{2.3.88}$$

$$\tau_{00}^{yy} = 0 \tag{2.3.89}$$

For the first harmonic components we get:

$$\tau_{01}^{xx} = 0 \tag{2.3.90}$$

$$\tau_{01}^{xy} = \mu u_{01,y'} \tag{2.3.91}$$

$$\tau_{01}^{yy} = 0 \tag{2.3.92}$$

Let us now express the second order $O(\epsilon)$ shear component of the stress in terms of the velocity and the displacement. The second order $O(\epsilon)$ relationship between stress, strain and the rate of strain is given by the equation (2.3.63) and is rewritten below for easier reference:

$$O(\epsilon^1): \quad \left(1+\sum_{n=1}^{N} a_n(\partial_t)^n\right)\underline{\underline{\tau_1}} + \left(\sum_{n=1}^{N} n a_n(\partial_t)^{(n-1)}\right)\underline{\underline{\tau_{0,t_1}}} \tag{2.3.93}$$
$$= \left(\sum_{n=0}^{N-1} b_n(\partial_t)^n\right)\underline{\underline{\gamma_1}} + \left(\sum_{n=0}^{N-1} n b_n(\partial_t)^{(n-1)}\right)\underline{\underline{\gamma_{0,t_1}}}$$

The left-hand side of the equation (2.3.93) is:

$$\underline{\underline{\tau_{10}}} + \left[\left(1+\sum_{n=1}^{N} a_n(-i)^n\right)\underline{\underline{\tau_{11}}}e^{i\psi} + c.c.\right] + \left[\left(1+\sum_{n=1}^{N} a_n(-2i)^n\right)\underline{\underline{\tau_{12}}}e^{2i\psi} + c.c.\right]$$
$$+ a_1\underline{\underline{\tau_{00,t_1}}} + \left[\left(\sum_{n=1}^{N} n a_n(-i)^{(n-1)}\right)\underline{\underline{\tau_{01,t_1}}}e^{i\psi} + c.c.\right]$$

The right-hand side of the equation (2.3.93) is:

$$b_0\underline{\underline{\gamma_{10}}} + \left[\left(\sum_{n=0}^{N-1} b_n(-i)^n\right)\underline{\underline{\gamma_{11}}}e^{i\psi} + c.c.\right] + \left[\left(\sum_{n=0}^{N-1} b_n(-2i)^n\right)\underline{\underline{\gamma_{12}}}e^{2i\psi} + c.c.\right]$$
$$+ b_1\underline{\underline{\gamma_{00,t_1}}} + \left[\left(\sum_{n=1}^{N-1} n b_n(-i)^{(n-1)}\right)\underline{\underline{\gamma_{01,t_1}}}e^{i\psi} + c.c.\right]$$

Equating the zeroth harmonic of the left-hand side and the right-hand side:

$$\underline{\underline{\tau_{10}}} + a_1\underline{\underline{\tau_{00,t_1}}} = b_0\underline{\underline{\gamma_{10}}} + b_1\underline{\underline{\gamma_{00,t_1}}}$$

Using the fact that there is no mean displacement at the leading order ($\underline{\underline{\gamma_{00}}} = 0$), the relationship (2.3.64) between $\underline{\underline{\tau_{00}}}$ and $\underline{\underline{\gamma_{00}}}$ $\left(\underline{\underline{\tau_{00}}} = b_0\underline{\underline{\gamma_{00}}} = 0\right)$ the last equation is rewritten as

$$\underline{\underline{\tau_{10}}} = b_0\underline{\underline{\gamma_{10}}}$$

Finally the shear component is:

$$\tau_{10}^{xy} = b_0\gamma_{10}^{xy}$$

Or in terms of the velocity and the displacement field:

$$\tau_{10}^{xy} = b_0 X_{10,y'} \tag{2.3.94}$$

Now let us evaluate the second order $O(\epsilon)$ first harmonic of the stress, equating the first harmonic of the left-hand side and the right-hand side:

$$\begin{aligned}&\left(1+\sum_{n=1}^{N} a_n(-i)^n\right)\underline{\underline{\tau_{11}}} + \left(\sum_{n=1}^{N} n a_n(-i)^{(n-1)}\right)\underline{\underline{\tau_{01,t_1}}} \\ &= \left(\sum_{n=0}^{N-1} b_n(-i)^n\right)\underline{\underline{\gamma_{11}}} + \left(\sum_{n=0}^{N-1} n b_n(-i)^{(n-1)}\right)\underline{\underline{\gamma_{01,t_1}}}\end{aligned}$$

Dividing both left- and right-hand sides by $\left(1+\sum_{n=1}^{N} a_n(-i)^n\right)$ and using the definition (2.3.86) of the complex viscosity μ we get for the shear component τ_{11}^{xy}:

$$\tau_{11}^{xy} + \frac{\left(\sum_{n=1}^{N} n a_n(-i)^{(n-1)}\right)}{\left(1+\sum_{n=1}^{N} a_n(-i)^n\right)}\tau_{01,t_1}^{xy} = -i\mu\gamma_{11}^{xy} + \frac{\left(\sum_{n=0}^{N-1} n b_n(-i)^{(n-1)}\right)}{\left(1+\sum_{n=1}^{N} a_n(-i)^n\right)}\gamma_{01,t_1}^{xy}$$

From the system of equations (2.3.59) we have that $\gamma_{11}^{xy} = X_{11,y'}$, from the system of equations (2.3.58) and from the equation (2.3.76) we get that $\gamma_{01}^{xy} = X_{01,y'} = iu_{01,y'}$

and the equation (2.3.91) says that $\tau_{01}^{xy} = \mu u_{01,y'}$. The expression of τ_{11}^{xy} becomes:

$$\tau_{11}^{xy} = -i\mu X_{11,y'} + \left(i\frac{\sum_{n=0}^{N-1} n b_n (-i)^{(n-1)}}{1 + \sum_{n=1}^{N} a_n (-i)^n} - \mu \frac{\sum_{n=1}^{N} n a_n (-i)^{(n-1)}}{1 + \sum_{n=1}^{N} a_n (-i)^n} \right) u_{01,y't_1}$$

Multiplying and dividing the first term in the parenthesis by $\sum_{n=1}^{N-1} b_n (-i)^{(n)}$ and using again the definition (2.3.86) of the complex viscosity μ the last equation can be rewritten:

$$\tau_{11}^{xy} = -i\mu X_{11,y'} + \mu \left(\frac{\sum_{n=0}^{N-1} n b_n (-i)^{(n-1)}}{\sum_{n=0}^{N-1} b_n (-i)^{(n)}} - \frac{\sum_{n=1}^{N} n a_n (-i)^{(n-1)}}{1 + \sum_{n=1}^{N} a_n (-i)^n} \right) u_{01,y't_1}$$

Equating the second harmonic of the left-hand side and the right-hand side of the equation (2.3.93) we get:

$$\left(1 + \sum_{n=1}^{N} a_n (-2i)^n \right) \underline{\underline{\tau_{12}}} = \left(\sum_{n=0}^{N-1} b_n (-2i)^n \right) \underline{\underline{\gamma_{12}}}$$

Dividing by $1 + \sum_{n=1}^{N} a_n (-2i)^n$ both left- and right-hand sides of the last equation we get for the shear component of the stress τ^{xy}:

$$\tau_{12}^{xy} = \frac{\sum_{n=0}^{N-1} b_n (-2i)^n}{1 + \sum_{n=0}^{N} a_n (-2i)^n} \gamma_{12}^{xy}$$

From the system of equations (2.3.59) we have $\gamma_{12}^{xy} = X_{12,y'}$, and the last equation in terms of the displacement field becomes:

$$\tau_{12}^{xy} = \frac{\sum_{n=0}^{N-1} b_n(-2i)^n}{1+\sum_{n=1}^{N} a_n(-2i)^n} X_{12,y'}$$

Summarizing the above analysis the second order $O(\epsilon)$ shear stress is:

$$\tau_{10}^{xy} = b_0 X_{10,y'} \tag{2.3.95}$$

$$\tau_{11}^{xy} = -i\mu X_{11,y'} + \mu \left(\frac{\sum_{n=0}^{N-1} n b_n(-i)^{(n-1)}}{\sum_{n=0}^{N-1} b_n(-i)^{(n)}} - \frac{\sum_{n=1}^{N} n a_n(-i)^{(n-1)}}{1+\sum_{n=1}^{N} a_n(-i)^n} \right) u_{01,y't_1} \tag{2.3.96}$$

$$\tau_{12}^{xy} = \frac{\sum_{n=0}^{N-1} b_n(-2i)^n}{1+\sum_{n=1}^{N} a_n(-2i)^n} X_{12,y'} \tag{2.3.97}$$

2.3.7 Approximate governing equations under the assumption of sinusoidal waves

Using the assumption of sinusoidal waves the governing equations can be simplified by being separated into different harmonics. Let us rewrite the governing equations in terms of different harmonics for the water and mud layers.

Water Layer - Laplace Equation

The Laplace equation for the first three orders and for each harmonic will now be written.

At the leading order $O(\epsilon^0)$ the Laplace equation (2.3.3) becomes, after using sinusoidal

wavesn:

$$\Phi_{00,yy} + (\Phi_{01,yy}e^{i\psi} + c.c.) + (-k_0^2\Phi_{01}e^{i\psi} + c.c.) \;=\; F_{00} + (F_{01}e^{i\psi} + c.c.)$$

With the right-hand side (2.3.6) being:

$$F_0 = F_{00} + (F_{01}e^{i\psi} + c.c.) = 0$$

Grouping the terms of the last two equations harmonic by harmonic we get:

$$\begin{cases} \Phi_{00,yy} = F_{00} = 0, \\ \Phi_{01,yy} - k_0^2\Phi_{01} = F_{01} = 0 \end{cases} \tag{2.3.98}$$

At the second order $O(\epsilon)$ the Laplace equation (2.3.4) becomes for sinusoidal waves:

$$\Phi_{10,yy} + (\Phi_{11,yy}e^{i\psi} + c.c.) + (-k_0^2\Phi_{11}e^{i\psi} + c.c.) + (\Phi_{12,yy}e^{2i\psi} + c.c.) + (-4k_0^2\Phi_{12}e^{i\psi} + c.c.)$$
$$= F_{10} + (F_{11}e^{i\psi} + c.c.) + (F_{12}e^{2i\psi} + c.c.)$$

The right-hand side (2.3.4) is equal to

$$\begin{aligned} F_{10} + (F_{11}e^{i\psi} + c.c.) + (F_{11}e^{2i\psi} + c.c.) &= -2\Phi_{0,xx_1} \\ &= -2ik_0\Phi_{01,x_1}e^{i\psi} + c.c. \end{aligned}$$

Grouping the terms of the last two equations harmonic by harmonic we get:

$$\begin{cases} \Phi_{10,yy} = F_{10} = 0, \\ \Phi_{11,yy} - k_0^2\Phi_{11} = F_{11} = -2ik_0\Phi_{01,x_1}, \\ \Phi_{12,yy} - 4k_0^2\Phi_{12} = F_{12} = 0 \end{cases} \tag{2.3.99}$$

Finally at the third order $O(\epsilon^2)$ the Laplace equation (2.3.5) becomes for sinusoidal waves:

$$\begin{aligned}
& \Phi_{20,yy} + (\Phi_{21,yy}e^{i\psi} + c.c.) + (-k_0^2\Phi_{21}e^{i\psi} + c.c.) + (\Phi_{22,yy}e^{2i\psi} + c.c.) + (-4k_0^2\Phi_{22}e^{2i\psi} + c.c.) \\
+ \; & (\Phi_{23,yy}e^{3i\psi} + c.c.) + (-9k_0^2\Phi_{23}e^{3i\psi} + c.c.) \\
= \; & F_{20} + (F_{21}e^{i\psi} + c.c.) + (F_{22}e^{2i\psi} + c.c.) + \left(F_{23}e^{3i\psi} + c.c.\right)
\end{aligned}$$

with the right-hand side (2.3.8) being equal to

$$\begin{aligned}
F_2 &= F_{20} + \left(F_{21}e^{i\psi} + c.c.\right) + \left(F_{22}e^{2i\psi} + c.c.\right) + \left(F_{23}e^{3i\psi} + c.c.\right) \\
&= -2\Phi_{1,xx_1} - \Phi_{0,x_1x_1} \\
&= (-2ik_0\Phi_{11,x_1}e^{i\psi} + c.c.) + (-4ik_0\Phi_{12,x_1}e^{2i\psi} + c.c.) - \Phi_{00,x_1x_1} + (-\Phi_{01,x_1x_1}e^{i\psi} + c.c.)
\end{aligned}$$

Grouping the terms of the last two equations harmonic by harmonic we get:

$$\begin{cases}
\Phi_{20,yy} = F_{20} = -\Phi_{00,x_1x_1}, \\
\Phi_{21,yy} - k_0^2\Phi_{21} = F_{21} = -(2ik_0\Phi_{11,x_1} + \Phi_{01,x_1x_1}), \\
\Phi_{22,yy} - 4k_0^2\Phi_{22} = F_{22} = -4ik_0\Phi_{12,x_2}, \\
\Phi_{23,yy} - 9k_0^2\Phi_{23} = F_{23} = 0
\end{cases} \tag{2.3.100}$$

Water Layer - Bernoulli Equation

The Bernoulli equation relates the pressure to the velocity potential of the same order. As it will be observed later we do not need to determine third order pressure relation. Therefore we only need to write expression of pressure for the first two orders.
At the leading order $O(\epsilon^0)$ the Bernoulli equation (2.3.9) is:

$$p_{00}^{(w)} + (p_{01}^{(w)}e^{i\psi} + c.c.) = -\Phi_{0,t} = i\Phi_{01}e^{i\psi} + c.c.$$

Grouping the terms of the last equation harmonic by harmonic we get:

$$\begin{cases} p_{00}^{(w)} = 0, \\ p_{01}^{(w)} = i\Phi_{01} \end{cases} \tag{2.3.101}$$

At the second order $O(\epsilon)$ the Bernoulli equation (2.3.10) is:

$$\begin{aligned} & p_{10}^{(w)} + (p_{11}^{(w)} e^{i\psi} + c.c.) + (p_{12}^{(w)} e^{2i\psi} + c.c.) = -\left[\Phi_{1,t} + \Phi_{0,t_1} + \frac{1}{2}\left(\Phi_{0,x}^2 + \Phi_{0,y}^2\right)\right] \\ = & -\Big\{(-i\Phi_{11}e^{i\psi} + c.c.) + (-2i\Phi_{12}e^{2i\psi} + c.c.) + \Phi_{00,t_1} + (\Phi_{01,t_1}e^{i\psi} + c.c.) \\ & + \frac{1}{2}\left[2k_0^2|\Phi_{01}|^2 + (-k_0^2\Phi_{01}^2 e^{2i\psi} + c.c.) + 2|\Phi_{01,y}|^2 + (\Phi_{01,y}^2 e^{2i\psi} + c.c.)\right]\Big\} \end{aligned}$$

Grouping the terms of the last equation harmonic by harmonic we get:

$$\begin{cases} p_{10}^{(w)} = -\left(\Phi_{00,t_1} + k_0^2|\Phi_{01}|^2 + |\Phi_{01,y}|^2\right), \\ p_{11}^{(w)} = i\Phi_{11} - \Phi_{01,t_1}, \\ p_{12}^{(w)} = 2i\Phi_{12} + \frac{1}{2}k_0^2\Phi_{01}^2 - \frac{1}{2}\Phi_{01,y}^2 \end{cases} \tag{2.3.102}$$

Mud Layer - Mass Conservation Equation

The mass conservation of the mud layer (equations (2.3.14) and (2.3.15)) will now be written harmonic by harmonic for the first two orders.
At the leading order $O(\epsilon^0)$ the mass conservation equation (2.3.14) is:

$$(ik_0u_{01}e^{i\psi} + c.c.) + v_{00,y'} + (v_{01,y'}e^{i\psi} + c.c.) = 0$$

Grouping the terms of the last equation harmonic by harmonic we get:

$$\begin{cases} v_{00,y'} = 0 \\ v_{01,y'} + ik_0u_{01} = 0 \end{cases} \tag{2.3.103}$$

As it was stated previously by the equation (2.3.80) the zeroth harmonic of the vertical velocity is zero $v_{00} = 0$ and the first equation of the system (2.3.103) is

trivially satisfied.

At the second order $O(\epsilon)$ the mass conservation equation (2.3.15) is:

$$\begin{aligned}(ik_0u_{11}e^{i\psi}+c.c.)+(2ik_0u_{12}e^{2i\psi}+c.c.)\\ +v_{10,y'}+(v_{11,y'}e^{i\psi}+c.c.)+(v_{12,y'}e^{2i\psi}+c.c.)\\ =-u_{00,x_1}+(-u_{01,x_1}e^{i\psi}+c.c.)\end{aligned}$$

Grouping the terms of the last equation harmonic by harmonic we get:

$$\begin{cases} v_{10,y'}=-u_{00,x_1}=0 \\ v_{11,y'}+ik_0u_{11}=-u_{01,x_1} \\ v_{12,y'}+2ik_0u_{12}=0 \end{cases} \tag{2.3.104}$$

Where the fact was used that there is no leading order mean velocity inside mud layer (equation (2.3.75)). Note that the first equation of the last system is consistent with the previously found result (2.3.82) which says that:

$$v_{10} \;=\; 2\Re\left\{ik_0Y_{01}u_{01}^*+Y_{01,y'}v_{01}^*\right\}$$

In fact the second equation of the system (2.3.103) says that $ik_0u_{01}^*=v_{01,y'}^*$ and the equation (2.3.81) dictates that $Y_{01}=iv_{01}$. Therefore we can write:

$$v_{10} \;=\; 2\Re\left\{Y_{01}v_{01,y'}^*+Y_{01,y'}v_{01}^*\right\}=2\Re\left\{\left(Y_{01}v_{01}^*\right)_{y'}\right\}=2\Re\left\{i\left(|v_{01}|^2\right)_{y'}\right\}=0$$

Mud Layer - Horizontal Momentum Conservation

The horizontal momentum conservation inside the mud layer (equations (2.3.16) and (2.3.17)) will now be written harmonic by harmonic for the first two orders.

At the leading order $O(\epsilon^0)$ the horizontal momentum conservation equation (2.3.16) is:

$$(-iu_{01}e^{i\psi}+c.c.)=-\gamma(ik_0p_{01}^{(m)}e^{i\psi}+c.c.)+\frac{1}{Re}\frac{a}{d}\left[\tau_{00,y'}^{xy}+(\tau_{01,y'}^{xy}e^{i\psi}+c.c.)\right]$$

Grouping the terms of the last equation harmonic by harmonic we get:

$$\begin{cases} \tau^{xy}_{00,y'} = 0 \\ -iu_{01} = -ik_0\gamma p^{(m)}_{01} + \frac{1}{Re}\frac{a}{d}\tau^{xy}_{01,y'} \end{cases}$$

Using the leading order expressions of the shear stress (2.3.88) and (2.3.91) the last system of equations becomes:

$$\begin{cases} 0 = 0 \\ -iu_{01} = -ik_0\gamma p^{(m)}_{01} + \frac{1}{Re}\mu\frac{a}{d}u_{01,y'y'} \end{cases} \tag{2.3.105}$$

At the second order $O(\epsilon)$ the horizontal momentum conservation equation (2.3.17) is:

$$\begin{aligned} &(-iu_{11}e^{i\psi} + c.c.) + (-2iu_{12}e^{2i\psi} + c.c.) + u_{00,t_1} + (u_{01,t_1}e^{i\psi} + c.c.) \\ &+\big[u_{00} + (u_{01}e^{i\psi} + c.c.)\big](ik_0u_{01}e^{i\psi} + c.c.) + \big[v_{00} + (v_{01}e^{i\psi} + c.c.)\big](u_{01,y'}e^{i\psi} + c.c.) \\ &= -\gamma\big[(ik_0p^{(m)}_{11}e^{i\psi} + c.c.) + (2ik_0p^{(m)}_{12}e^{2i\psi} + c.c.) + p^{(m)}_{00,x_1} + (p^{(m)}_{01,x_1}e^{i\psi} + c.c.)\big] \\ &+\frac{1}{Re}\frac{a}{d}\big[\tau^{xy}_{10,y'} + (\tau^{xy}_{11,y'}e^{i\psi} + c.c.) + (\tau^{xy}_{12,y'}e^{2i\psi} + c.c.)\big] + \frac{1}{Re}\big[\tau^{xy}_{00,y'} + (ik_0\tau^{xx}_{01}e^{i\psi} + c.c.)\big] \end{aligned}$$

Opening the parenthesis we get:

$$\begin{aligned} &(-iu_{11}e^{i\psi} + c.c.) + (-2iu_{12}e^{2i\psi} + c.c.) + u_{00,t_1} + (u_{01,t_1}e^{i\psi} + c.c.) \\ &+u_{00}(ik_0u_{01}e^{i\psi} + c.c.) + (ik_0u^2_{01}e^{2i\psi} + c.c.) \\ &+2\Re\left\{v_{01}u^*_{01,y'}\right\} + v_{00}u_{00,y'} + (u_{00,y'}v_{01}e^{i\psi} + c.c.) + v_{00}(u_{01,y'}e^{i\psi} + c.c.) + (v_{01}u_{01,y'}e^{2i\psi} + c.c.) \\ &= -\gamma\big[(ik_0p^{(m)}_{11}e^{i\psi} + c.c.) + (2ik_0p^{(m)}_{12}e^{2i\psi} + c.c.) + p^{(m)}_{00,x_1} + (p^{(m)}_{01,x_1}e^{i\psi} + c.c.)\big] \\ &+\frac{1}{Re}\frac{a}{d}\big[\tau^{xy}_{10,y'} + (\tau^{xy}_{11,y'}e^{i\psi} + c.c.) + (\tau^{xy}_{12,y'}e^{2i\psi} + c.c.)\big] + \frac{1}{Re}(ik_0\tau^{xx}_{01}e^{i\psi} + c.c.) \end{aligned}$$

Grouping the terms of the last equation harmonic by harmonic we get:

$$\begin{cases} u_{00,t_1} + v_{00}u_{00,y'} + 2\Re\left\{v_{01}u^*_{01,y'}\right\} = -\gamma p^{(m)}_{00,x_1} + \frac{1}{Re}\frac{a}{d}\tau^{xy}_{10,y'} \\ -iu_{11} + u_{01,t_1} + ik_0u_{00}u_{01} + u_{00,y'}v_{01} + v_{00}u_{01,y'} = -\gamma\big[ik_0p^{(m)}_{11} + p^{(m)}_{01,x_1}\big] + \frac{1}{Re}\frac{a}{d}\tau^{xy}_{11,y'} + ik_0\frac{1}{Re}\tau^{xx}_{01} \\ -2iu_{12} + ik_0u^2_{01} + v_{01}u_{01,y'} = -2i\gamma k_0p^{(m)}_{12} + \frac{1}{Re}\frac{a}{d}\tau^{xy}_{12,y'} \end{cases}$$

Using the expression (2.3.95) of the zeroth harmonic of the shear stress τ_{10}^{xy}, the equation (2.3.90) saying that $\tau_{01}^{xx} = 0$, and the equations (2.3.75) and (2.3.80) saying that $u_{00} = v_{00} = 0$, the last system of equations becomes:

$$\begin{cases} 2\Re\left\{v_{01}u_{01,y'}^{*}\right\} = -\gamma p_{00,x_1}^{(m)} + \frac{1}{Re}\frac{a}{d}\left(b_0 X_{10,y'y'}\right) \\ -iu_{11} + u_{01,t_1} = -\gamma\left[ik_0 p_{11}^{(m)} + p_{01,x_1}^{(m)}\right] + \frac{1}{Re}\frac{a}{d}\tau_{11,y'}^{xy} \\ -2iu_{12} + ik_0 u_{01}^2 + v_{01}u_{01,y'} = -2i\gamma k_0 p_{12}^{(m)} + \frac{1}{Re}\frac{a}{d}\tau_{12,y'}^{xy} \end{cases} \tag{2.3.106}$$

With τ_{11}^{xy} and τ_{12}^{xy} given by equations (2.3.96) and (2.3.97) respectively.

Mud Layer - Vertical Momentum Conservation

The vertical momentum conservation inside the mud layer (equations (2.3.19) and (2.3.20)) will now be written harmonic by harmonic for the first two orders.
At the leading order $O(\epsilon^0)$ the vertical momentum conservation equation (2.3.19) is:

$$p_{00,y'}^{(m)} + \left(p_{01,y'}^{(m)}e^{i\psi} + c.c.\right) = 0$$

Grouping the terms of the last equation harmonic by harmonic we get:

$$\begin{cases} p_{00,y'}^{(m)} = 0 \\ p_{01,y'}^{(m)} = 0 \end{cases} \tag{2.3.107}$$

At the second order $O(\epsilon)$ the vertical momentum conservation equation (2.3.20) is:

$$p_{10,y'}^{(m)} + \left(p_{11,y'}^{(m)}e^{i\psi} + c.c.\right) + \left(p_{12,y'}^{(m)}e^{2i\psi} + c.c.\right) = \frac{1}{\gamma Re}\left[\tau_{00,y'}^{yy} + \left(\tau_{01,y'}^{yy}e^{i\psi} + c.c.\right)\right]$$

Grouping the terms of the last equation harmonic by harmonic we get:

$$\begin{cases} p_{10,y'}^{(m)} = \frac{1}{\gamma Re}\tau_{00,y'}^{yy} \\ p_{11,y'}^{(m)} = \tau_{01,y'}^{yy} \\ p_{12,y'}^{(m)} = 0 \end{cases}$$

Using the leading order expressions of $\tau_{00}^{yy} = 0$ (equation 2.3.68), the last system of equations becomes:

$$\begin{cases} p_{10,y'}^{(m)} = 0 \\ p_{11,y'}^{(m)} = 0 \\ p_{12,y'}^{(m)} = 0 \end{cases} \tag{2.3.108}$$

2.3.8 Approximate boundary conditions under the assumption of sinusoidal wave

In this section the approximate boundary conditions will be obtained explicitly for each order and each harmonic.

Free Surface - Combined Kinematic and Dynamic Boundary Condition

At the leading order $O(\epsilon^0)$ the combined kinematic and dynamic boundary condition (2.3.21) with the use of the equation (2.3.24) becomes:

$$\begin{cases} (\Phi_{00,y})|_0 = G_{00} = 0, \\ (\Phi_{01,y})|_0 - (\Phi_{01})|_0 = G_{01} = 0 \end{cases} \tag{2.3.109}$$

At the second order $O(\epsilon)$ the combined kinematic and dynamic boundary condition (2.3.22) with the use of the equation (2.3.25) can also be computed explicitly. But first we need to compute the different harmonic components of $G_1 = G_{10} + (G_{11}e^{i\psi} + c.c.) + (G_{12}e^{2i\psi} + c.c.)$. As a reminder the expression (2.3.25) is rewritten here:

$$G_1 = -\left[\eta_0(\Gamma_y\Phi_0)|_0 + 2(\Phi_{0,tt_1})|_0 + \left(\Phi_{0,x}^2 + \Phi_{0,y}^2\right)_t\Big|_0\right]$$

Term by term we obtain:

$$
\begin{aligned}
\Gamma_y\Phi_0 &= (\partial_{yy}+\partial_{tty})\left[\Phi_{00}+(\Phi_{01}e^{i\psi}+c.c.)\right]=\Phi_{00,yy}+\left[(\Phi_{01,yy}-\Phi_{01,y})e^{i\psi}+c.c.\right]\\
\eta_0\left(\Gamma_y\Phi_0\right) &= (\frac{A}{2}e^{i\psi}+c.c.)\left\{\Phi_{00,yy}+\left[(\Phi_{01,yy}-\Phi_{01,y})e^{i\psi}+c.c.\right]\right\}\\
&= 2\Re\left\{\frac{A^*}{2}\left(\Phi_{01,yy}-\Phi_{01,y}\right)\right\}+(\frac{A}{2}(\Phi_{00,yy})e^{i\psi}+c.c.)+\left[\frac{A}{2}(\Phi_{01,yy}-\Phi_{01,y})e^{2i\psi}+c.c.\right]\\
2\Phi_{0,tt_1} &= (-2i\Phi_{01,t_1}e^{i\psi}+c.c.)\\
\left(\Phi_{0,x}^2\right)_t &= \left[\left(ik_0\Phi_{01}e^{i\psi}+c.c.\right)^2\right]_t=\left[2k_0^2|\Phi_{01}|^2+(-k_0^2\Phi_{01}^2e^{2i\psi}+c.c.)\right]_t\\
&= (2ik_0^2\Phi_{01}^2e^{2i\psi}+c.c.)\\
\left(\Phi_{0,y}^2\right)_t &= \left[\Phi_{00,y}+\left(\Phi_{01,y}e^{i\psi}+c.c.\right)^2\right]_t\\
&= \left[2|\Phi_{01,y}|^2+\Phi_{00,y}^2+(2\Phi_{00,y}\Phi_{01,y}e^{i\psi}+c.c.)+(\Phi_{01,y}^2e^{2i\psi}+c.c.)\right]_t\\
&= (-2i\Phi_{00,y}\Phi_{01,y}e^{i\psi}+c.c.)+(-2i\Phi_{01,y}^2e^{2i\psi}+c.c.)
\end{aligned}
$$

where the assumed expression (2.3.53) for η_0 was used. Now each harmonic of the constant G_1 can be deduced:

$$
\begin{cases}
G_{10}=-\Re\left\{A^*\left(\Phi_{01,yy}-\Phi_{01,y}\right)|_0\right\}\\
G_{11}=-\left[\frac{A}{2}\left(\Phi_{00,yy}\right)|_0-2i\left(\Phi_{01,t_1}\right)|_0-2i\left(\Phi_{00,y}\Phi_{01,y}\right)|_0\right]\\
G_{12}=-\left[\frac{A}{2}(\Phi_{01,yy}-\Phi_{01,y})+2ik_0^2\Phi_{01}^2-2i\Phi_{01,y}^2\right]|_0
\end{cases}
\tag{2.3.110}
$$

And the boundary condition at the second order $O(\epsilon)$ being:

$$
\begin{cases}
(\Phi_{10,y})|_0=G_{10}=-\Re\left\{A^*\left(\Phi_{01,yy}-\Phi_{01,y}\right)|_0\right\},\\
(\Phi_{11,y})|_0-(\Phi_{11})|_0=G_{11}=-\left[\frac{A}{2}(\Phi_{00,yy})-2i\left(\Phi_{01,t_1}\right)-2i\left(\Phi_{00,y}\Phi_{01,y}\right)\right]|_0,\\
(\Phi_{12,y})|_0-4(\Phi_{12})|_0=G_{12}=-\left[\frac{A}{2}(\Phi_{01,yy}-\Phi_{01,y})+2ik_0^2\Phi_{01}^2-2i\Phi_{01,y}^2\right]|_0
\end{cases}
\tag{2.3.111}
$$

Finally at the third order $O(\epsilon^2)$ the combined kinematic and dynamic boundary condition (2.3.23) for the zeroth harmonic become:

$$
(\Phi_{20,y'})|_0=G_{20} \tag{2.3.112}
$$

with the constant G_{20} that will now be deduced from the equation (2.3.26). In fact we need to compute the zeroth harmonic of the constant G_2 given by the equation (2.3.26) and reminded for easier reference here:

$$\begin{aligned} G_2 &= -\Big[\eta_1(\Gamma_y\Phi_0)|_0 + \eta_0(\Gamma_y\Phi_1)|_0 + 2(\Phi_{0,x}\Phi_{1,x} + \Phi_{0,y}\Phi_{1,y})_t + \frac{\eta_0^2}{2}(\Gamma_{yy}\Phi_0)|_0 + 2\eta_0(\Phi_{0,ytt_1})|_0 \\ &\quad + 2(\Phi_{1,tt_1})|_0 + \eta_0\left(\Phi_{0,x}^2 + \Phi_{0,y}^2\right)_{ty}\Big|_0 + (\Phi_{0,t_1t_1})|_0 + 2(\Phi_{0,tt_2})|_0 + 2\left(\Phi_{0,x}\Phi_{0,x_1}\right)_t\Big|_0 \\ &\quad + \left(\Phi_{0,x}^2 + \Phi_{0,y}^2\right)_{t_1}\Big|_0 + \frac{1}{2}\left[(\Phi_{0,x}\partial_x + \Phi_{0,y}\partial_y)\left(\Phi_{0,x}^2 + \Phi_{0,y}^2\right)\right]\Big|_0\Big] \end{aligned} \tag{2.3.113}$$

Let us compute each term of G_2 separately.

The term $\eta_1(\Gamma_y\Phi_0)|_0$

$$\begin{aligned} \Gamma_y\Phi_0 &= (\partial_{yy} + \partial_{ytt})[\Phi_{00} + (\Phi_{01}e^{i\psi} + c.c.)] = (\Phi_{01,yy} - \Phi_{01,y})e^{i\psi} + c.c. \\ \eta_1(\Gamma_y\Phi_0)|_0 &= [\eta_{10} + (\eta_{11}e^{i\psi} + c.c.) + (\eta_{12}e^{i\psi} + c.c.)][(\Phi_{01,yy} - \Phi_{01,y})|_0\, e^{i\psi} + c.c.] \\ &= 2\Re\left\{\eta_{11}^*\left(\Phi_{01,yy} - \Phi_{01,y}\right)|_0\right\} + h.h. \end{aligned}$$

where the abbreviation $h.h.$ stands for 'higher harmonics'.

The term $\eta_0(\Gamma_y\Phi_1)|_0$

$$\begin{aligned} (\Gamma_y\Phi_1) &= (\partial_{yy} + \partial_{ytt})[\Phi_{10} + (\Phi_{11}e^{i\psi} + c.c.) + (\Phi_{12}e^{2i\psi} + c.c.)] \\ &= [(\Phi_{11,yy} - \Phi_{11,y})e^{i\psi} + c.c.] + [(\Phi_{12,yy} - 4\Phi_{12,y})e^{i\psi} + c.c.] \\ \eta_0(\Gamma_y\Phi_1)|_0 &= \frac{1}{2}(Ae^{i\psi} + c.c.)\left[(\Phi_{11,yy} - \Phi_{11,y})e^{i\psi} + c.c.\right] + \left[(\Phi_{12,yy} - 4\Phi_{12,y})e^{i\psi} + c.c.\right]\Big|_0 \\ &= \Re\{A^*(\Phi_{11,yy} - \Phi_{11,y})|_0\} + h.h. \end{aligned} \tag{2.3.114}$$

The term $\eta_0^2(\Gamma_{yy}\Phi_0)|_0$

$$\begin{aligned} \Gamma_{yy}\Phi_0 &= (\partial_{yyy} + \partial_{yytt})[\Phi_{00} + (\Phi_{01}e^{i\psi} + c.c.)] = (\Phi_{01,yyy} - \Phi_{01,yy})e^{i\psi} + c.c. \\ \eta_0^2(\Gamma_{yy}\Phi_0)|_0 &= \frac{1}{4}[2|A|^2 + (A^2e^{i\psi} + c.c.)][(\Phi_{01,yyy} - \Phi_{01,yy})e^{i\psi} + c.c.]|_0 \\ &= 0 + h.h. \end{aligned} \tag{2.3.115}$$

The term $2\eta_0(\Phi_{0,ytt_1})|_0$

$$2\eta_0(\Phi_{0,ytt_1})|_0 = (Ae^{i\psi} + c.c.)(-i\Phi_{01,yt_1}e^{i\psi} + c.c.) = 2\Re\{(iA\Phi^*_{01,yt_1})|_0\} + h.h.$$

The term $(\Phi_{0,t_1t_1})|_0$

$$(\Phi_{0,t_1t_1})|_0 = (\Phi_{00,t_1t_1})|_0 + h.h.$$

The term $\left(\Phi^2_{0,x} + \Phi^2_{0,y}\right)_{t_1}\Big|_0$

$$\begin{aligned}\left(\Phi^2_{0,x} + \Phi^2_{0,y}\right)_{t_1}\Big|_0 &= \left[(ik_0\Phi_{01}e^{i\psi} + c.c.)^2 + (\Phi_{01,y}e^{i\psi} + c.c.)^2\right]_{t_1}\Big|_0 \\ &= 2k_0^2\left(|\Phi_{01}|^2\right)_{t_1}\Big|_0 + 2\left(|\Phi_{01,y}|^2\right)_{t_1}\Big|_0 + h.h.\end{aligned}$$

$$\begin{aligned}\left(\Phi^2_{0,x} + \Phi^2_{0,y}\right)_{t_1}\Big|_0 &= \left[(ik_0\Phi_{01}e^{i\psi} + c.c.)^2 + (\Phi_{01,y}e^{i\psi} + c.c.)^2\right]_{t_1} \\ &= 2k_0^2\left(|\Phi_{01}|^2\right)_{t_1}\Big|_0 + 2\left(|\Phi_{01,y}|^2\right)_{t_1}\Big|_0 + h.h.\end{aligned}$$

The terms $2(\Phi_{0,x}\Phi_{1,x}+\Phi_{0,y}\Phi_{1,y})_t$, $2(\Phi_{1,tt_1})|_0$, $\eta_0\left(\Phi^2_{0,x} + \Phi^2_{0,y}\right)_{ty}\Big|_0$, $2(\Phi_{0,tt_2})|_0$ and $2\left(\Phi_{0,x}\Phi_{0,x_1}\right)_t\Big|_0$ do not have zeroth harmonic because of the differentiation with respect to fast time t.
It can be shown that the term $\left[\left(\Phi_{0,x}\partial_x + \Phi_{0,y}\partial_y\right)\left(\Phi^2_{0,x} + \Phi^2_{0,y}\right)\right]\Big|_0$ also does not have zeroth harmonic, and the expression of G_{20} can be worked out so that:

$$\begin{aligned}(\Phi_{20,y'})|_0 &= G_{20} \\ &= -\Big\{\Re\left[A^*\left(\Phi_{11,yy} - \Phi_{11,y}\right)|_0\right] + \Re\left[2\eta^*_{11}\left(\Phi_{01,yy} - \Phi_{01,y}\right)|_0\right] + \Re\left[2iA\left(\Phi^*_{01,yt_1}\right)|_0\right] \\ &\quad + (\Phi_{00,t_1t_1})|_0 + 2k_0^2\left(\left[|\Phi_{01}|^2\right]_{t_1}\right)\Big|_0 + 2\left(\left[|\Phi_{01,y}|^2\right]_{t_1}\right)\Big|_0\Big\} \qquad (2.3.116)\end{aligned}$$

Free Surface - Dynamic Boundary Condition

The dynamic boundary condition (equations (2.3.27)-(2.3.32)) on the free surface will now written for each harmonic for the first two orders.
At the leading order $O(\epsilon^0)$ the boundary condition expressed by (2.3.27) and (2.3.30)

becomes:

$$\begin{cases} 0 = H_{00} = 0, \\ -\frac{A}{2} = H_{01} = -i\Phi_{01} \end{cases} \tag{2.3.117}$$

At the second order $O(\epsilon)$ the boundary condition (2.3.28) with the use of the equation (2.3.31) can also be computed explicitly. But first we need to compute the different harmonic components of $H_1 = H_{10} + (H_{11}e^{i\psi} + c.c.) + (H_{12}e^{2i\psi} + c.c.)$. As a reminder the expression (2.3.31) is rewritten here:

$$H_1 = (\Phi_{1,t})|_0 + \eta_0(\Phi_{0,yt})|_0 + (\Phi_{0,t_1})|_0 + \frac{1}{2}\left(\Phi_{0,x}^2 + \Phi_{0,y}^2\right)\Big|_0 \tag{2.3.118}$$

Term by term we obtain:

$$\begin{aligned}
\Phi_{1,t} &= (-i\Phi_{10}e^{i\psi} + c.c.) + (-2i\Phi_{10}e^{2i\psi} + c.c.) \\
\Phi_{0,yt} &= (-i\Phi_{01,y}e^{i\psi} + c.c.) \\
\eta_0\Phi_{0,yt} &= (\frac{A}{2}e^{i\psi} + c.c.)(-i\Phi_{01,y}e^{i\psi} + c.c.) = 2\Re\left\{i\frac{A}{2}\Phi_{01,y}^*\right\} + (-i\frac{A}{2}\Phi_{01,y}e^{2i\psi} + c.c.) \\
\Phi_{0,t_1} &= \Phi_{00,t_1} + (\Phi_{01,t_1}e^{i\psi} + c.c.) \\
\Phi_{0,x}^2 &= (ik_0\Phi_{01}e^{i\psi} + c.c.)^2 = 2k_0^2|\Phi_{01}|^2 + (-k_0^2\Phi_{01}^2e^{2i\psi} + c.c) \\
\Phi_{0,y}^2 &= (\Phi_{01,y}e^{i\psi} + c.c.)^2 = 2|\Phi_{01,y}|^2 + (\Phi_{01,y}^2e^{2i\psi} + c.c)
\end{aligned}$$

The harmonic components of the constant H_1 become:

$$\begin{cases} H_{10} = \Re\left\{iA\left(\Phi_{01,y}^*\right)\big|_0\right\} + (\Phi_{00,t_1})|_0 + k_0^2\left(|\Phi_{01}|^2\right)|_0 + \left(|\Phi_{01,y}|^2\right)|_0 \\ H_{11} = -i\left(\Phi_{11}\right)|_0 + (\Phi_{01,t_1})|_0 \\ H_{12} = -2i\left(\Phi_{12}\right)|_0 - i\frac{A}{2}\left(\Phi_{01,y}\right)|_0 - \frac{1}{2}k_0^2\left(\Phi_{01}^2\right)|_0 + \frac{1}{2}\left(\Phi_{01,y}^2\right)\big|_0 \end{cases} \tag{2.3.119}$$

and the dynamic boundary condition itself is written as

$$\begin{cases} -\eta_{10} = H_{10} = \Re\left\{iA\left(\Phi_{01,y}^*\right)\big|_0\right\} + (\Phi_{00,t_1})|_0 + k_0^2\left(|\Phi_{01}|^2\right)|_0 + \left(|\Phi_{01,y}|^2\right)|_0, \\ -\eta_{11} = H_{11} = -i\left(\Phi_{11}\right)|_0 + (\Phi_{01,t_1})|_0, \\ -\eta_{12} = H_{12} = -2i\left(\Phi_{12}\right)|_0 - i\frac{A}{2}\left(\Phi_{01,y}\right)|_0 - \frac{1}{2}k_0^2\left(\Phi_{01}^2\right)|_0 + \frac{1}{2}\left(\Phi_{01,y}^2\right)\big|_0 \end{cases} \tag{2.3.120}$$

Interface - Kinematic Boundary Condition in terms of water quantities

At the leading order $O(\epsilon^0)$ the boundary condition expressed by (2.3.33) and (2.3.36) is simply:

$$\begin{cases} (\Phi_{00,y})|_{-H} = L_{00} = 0, \\ (\Phi_{01,y})|_{-H} = L_{01} = 0 \end{cases} \tag{2.3.121}$$

At the second order $O(\epsilon)$ the boundary condition expressed by (2.3.34) and (2.3.37) becomes

$$\begin{cases} (\Phi_{10,y})|_{-H} = L_{10} = 0, \\ (\Phi_{11,y})|_{-H} = L_{11} = -i\zeta_{01}, \\ (\Phi_{12,y})|_{-H} = L_{12} = 0 \end{cases} \tag{2.3.122}$$

At the third order $O(\epsilon^2)$ we first estimate the constant L_2 term by term:

$$\begin{aligned} \zeta_{1,t} &= (-i\zeta_{11}e^{i\psi} + c.c.) + (-2i\zeta_{12}e^{2i\psi} + c.c.) \\ \zeta_{0,t_1} &= \zeta_{00,t_1} + (\zeta_{01,t_1}e^{i\psi} + c.c.) \\ \zeta_0\Phi_{0,x} &= (Ae^{i\psi} + c.c.).(ik_0\Phi_{01}e^{i\psi} + c.c.) = 2\Re\{ik_0A^*\Phi_{01}\} + \left(ik_0A\Phi_{01}e^{2i\psi} + c.c.\right) \\ (\zeta_0\Phi_{0,x})_x &= \left(-2k_0^2A\Phi_{01}e^{2i\psi} + c.c.\right) \end{aligned}$$

The boundary condition expressed by (2.3.35) and (2.3.38) becomes

$$\begin{cases} (\Phi_{20,y})|_{-H} = L_{20} = \zeta_{00,t_1}, \\ (\Phi_{21,y})|_{-H} = L_{21} = -i\zeta_{11} + \zeta_{01,t_1}, \\ (\Phi_{22,y})|_{-H} = L_{22} = -2i\zeta_{12} - 2k_0^2A\Phi_{01}, \\ (\Phi_{23,y})|_{-H} = L_{23} = 0 \end{cases} \tag{2.3.123}$$

Interface - Kinematic Boundary Condition in terms of mud quantities

The Kinematic boundary condition on the interface expressed in terms of the mud quantities (2.3.39) and (2.3.40) will now be obtained for each harmonic.

At the leading order $O(\epsilon^0)$ the boundary condition (2.3.39) becomes:

$$\begin{cases} 0 = (v_{00})|_1, \\ -i\zeta_{01} = \frac{d}{a}(v_{01})|_1 \end{cases} \tag{2.3.124}$$

At the second order $O(\epsilon)$ we first rewrite in terms of harmonics the right-hand side of the boundary condition (2.3.40) term by term:

$$\begin{aligned} \frac{d}{a}v_1 &= \frac{d}{a}\left[v_{10} + (v_{11}e^{i\psi} + c.c.) + (v_{12}e^{2i\psi} + c.c.)\right] \\ -\zeta_{0,t_1} &= -\zeta_{00,t_1} + (-\zeta_{01,t_1}e^{i\psi} + c.c.) \\ \zeta_0 u_0 &= \left[\zeta_{00} + (\zeta_{01}e^{i\psi} + c.c.)\right] . \left[u_{00} + (u_{01}e^{i\psi} + c.c.)\right] \\ &= \zeta_{00}u_{00} + 2\Re\left\{\zeta_0 u_{01}^*\right\} + \left[(\zeta_{00}u_{01} + \zeta_{01}u_{00})e^{i\psi} + c.c.\right] + (\zeta_{01}u_{01}e^{2i\psi} + c.c.) \\ (\zeta_0 u_0)_x &= \left[ik_0(\zeta_{00}u_{01} + \zeta_{01}u_{00})e^{i\psi} + c.c.\right] + (2ik_0\zeta_{01}u_{01}e^{2i\psi} + c.c.) \end{aligned}$$

Finally the second order boundary condition (2.3.40) can now be written for each harmonic

$$\begin{cases} 0 = \frac{d}{a}(v_{10})|_1 - \zeta_{00,t_1}, \\ -i\zeta_{11} = \frac{d}{a}(v_{11})|_1 - \zeta_{01,t_1} + ik_0(\zeta_{00}u_{01} + \zeta_{01}u_{00}), \\ -2i\zeta_{12} = \frac{d}{a}(v_{12})|_1 + 2ik_0\zeta_{01}u_{01} \end{cases} \tag{2.3.125}$$

Interface - Dynamic Boundary Condition

The dynamic boundary conditions on the interface (equations (2.3.41)-(2.3.44)) will now be rewritten for each harmonic. First we will obtain the expressions for the tangential stress continuity (equations (2.3.41)-(2.3.42)) and then we will get the expressions for the normal stress continuity (equations (2.3.43) - (2.3.42)).
At the leading order $O(\epsilon^0)$ the tangential stress continuity (2.3.41) is:

$$\begin{cases} \tau_{00}^{xy}|_{y'=1} = 0, \\ \tau_{01}^{xy}|_{y'=1} = 0 \end{cases}$$

Using the leading order expressions of the shear stress (equations (2.3.88) and (2.3.91)) we rewrite the last system of equations:

$$\begin{cases} 0 = 0, \\ \mu u_{01,y'}|_{y'=1} = 0 \end{cases} \tag{2.3.126}$$

At the second order $O(\epsilon)$ the right-hand side of the tangential stress continuity (2.3.42) is:

$$\begin{aligned} -\frac{a}{d}\zeta_0(\tau^{xy}_{0,y'}) &= -\frac{a}{d}\left[\zeta_{00} + (\zeta_{01}e^{i\psi} + c.c.)\right].\left[\tau^{xy}_{00,y'} + (\tau^{xy}_{01,y'}e^{i\psi} + c.c.)\right] \\ &= -\frac{a}{d}\Big\{\zeta_{00}\tau^{xy}_{00,y'} + 2\Re\left\{\zeta^*_{01}\tau^{xy}_{01,y'}\right\} + \left[(\zeta_{00}\tau^{xy}_{01,y'} + \zeta_{01}\tau^{xy}_{00,y'})e^{i\psi} + c.c.\right] \\ &\qquad + (\zeta_{01}\tau^{xy}_{01,y'}e^{2i\psi} + c.c.)\Big\} \end{aligned}$$

The second order tangential stress continuity condition becomes:

$$\begin{cases} \tau^{xy}_{10}|_{y'=1} = -\frac{a}{d}\left[\zeta_{00}\left(\tau^{xy}_{00,y'}\right)\big|_{y'=1} + 2\Re\left\{\zeta^*_{01}\left(\tau^{xy}_{01,y'}\right)\big|_{y'=1}\right\}\right], \\ \tau^{xy}_{11}|_{y'=1} = -\frac{a}{d}\left[\zeta_{00}\left(\tau^{xy}_{01,y'}\right)\big|_{y'=1} + \zeta_{01}\left(\tau^{xy}_{00,y'}\right)\big|_{y'=1}\right], \\ \tau^{xy}_{12}|_{y'=1} = -\frac{a}{d}\zeta_{01}\left(\tau^{xy}_{01,y'}\right)\big|_{y'=1} \end{cases}$$

The equation (2.3.88) says $\tau^{xy}_{00} = 0$ and the equation (2.3.91) says $\tau^{xy}_{01} = \mu u_{01,y'}$, and the equation (2.3.95) says $\tau^{xy}_{10} = b_0 X_{10,y'}$ therefore we rewrite the last system of equations as:

$$\begin{cases} b_0\left(X_{10,y'}\right)|_{y'=1} = -\frac{a}{d}\left[2\Re\left\{\mu\zeta^*_{01}\left(u_{01,y'y'}\right)|_{y'=1}\right\}\right], \\ \tau^{xy}_{11}|_{y'=1} = -\frac{a}{d}\left[\mu\zeta_{00}\left(u_{01,y'y'}\right)|_{y'=1}\right], \\ \tau^{xy}_{12}|_{y'=1} = -\frac{a}{d}\mu\zeta_{01}\left(u_{01,y'}\right)|_{y'=1} \end{cases} \tag{2.3.127}$$

With τ^{xy}_{11} and τ^{xy}_{12} given by equations (2.3.96) and (2.3.97) respectively.

Now let us obtain the normal stress continuity boundary conditions (2.3.43) and (2.3.44) for each harmonic.

At the leading order $O(\epsilon^0)$ the normal stress continuity boundary condition (2.3.43) for each harmonic is straightforward:

$$\begin{cases} \left(p_{00}^{(m)}\right)\Big|_{y'=1} = \left(p_{00}^{(w)}\right)\Big|_{y=-H}, \\ \left(p_{01}^{(m)}\right)\Big|_{y'=1} = \left(p_{01}^{(w)}\right)\Big|_{y=-H} \end{cases} \tag{2.3.128}$$

At the second order $O(\epsilon)$ the term $-\frac{a}{d}\zeta_0\left(p_{0,y'}^{(m)}\right)$ in the right-hand side of the normal stress continuity (2.3.44) is:

$$\begin{aligned} -\frac{a}{d}\zeta_0\left(p_{0,y'}^{(m)}\right) &= -\frac{a}{d}\left[\zeta_{00} + (\zeta_{01}e^{i\psi} + c.c.)\right].\left[p_{00,y'}^{(m)} + \left(p_{01,y'}^{(m)}e^{i\psi} + c.c.\right)\right] \\ &= -\frac{a}{d}\Big\{\zeta_{00}p_{00,y'}^{(m)} + 2\Re\left\{\zeta_{01}^{*}p_{01,y'}^{(m)}\right\} + \left[\left(\zeta_{00}p_{01,y'}^{(m)} + \zeta_{01}p_{00,y'}^{(m)}\right)e^{i\psi} + c.c.\right] \\ &\quad + \left(\zeta_{01}p_{01,y'}^{(m)}e^{2i\psi} + c.c.\right)\Big\} \end{aligned}$$

The second order normal stress continuity condition (2.3.44) for each harmonic becomes:

$$\begin{cases} \left(p_{10}^{(m)}\right)\Big|_{y'=1} = \left(p_{10}^{(w)}\right)\Big|_{y=-H} - \frac{a}{d}\left[\zeta_{00}\left(p_{00,y'}^{(m)}\right)\Big|_{y'=1} + 2\Re\left\{\zeta_{01}^{*}\left(p_{01,y'}^{(m)}\right)\Big|_{y'=1}\right\}\right], \\ \left(p_{11}^{(m)}\right)\Big|_{y'=1} = \left(p_{11}^{(w)}\right)\Big|_{y=-H} - \frac{a}{d}\left[\zeta_{00}\left(p_{01,y'}^{(m)}\right)\Big|_{y'=1} + \zeta_{01}\left(p_{00,y'}^{(m)}\right)\Big|_{y'=1}\right], \\ \left(p_{12}^{(m)}\right)\Big|_{y'=1} = \left(p_{12}^{(w)}\right)\Big|_{y=-H} - \frac{a}{d}\zeta_{01}\left(p_{01,y'}^{(m)}\right)\Big|_{y'=1} \end{cases} \tag{2.3.129}$$

Bottom - Horizontal Velocity

At the leading $O(\epsilon)$ and second order $O(\epsilon)$ the boundary conditions (2.3.45) and (2.3.46) are expressed for each harmonic as:

$$\begin{cases} u_{00}|_0 = 0, \\ u_{01}|_0 = 0 \end{cases} \tag{2.3.130}$$

$$\begin{cases} u_{10}|_0 = 0, \\ u_{11}|_0 = 0, \\ u_{12}|_0 = 0 \end{cases} \tag{2.3.131}$$

Bottom - Vertical Velocity

At the leading $O(\epsilon)$ and second order $O(\epsilon)$ the boundary conditions (2.3.47) and (2.3.48) are expressed for each harmonic as:

$$\begin{cases} v_{00}|_0 = 0, \\ v_{01}|_0 = 0 \end{cases} \tag{2.3.132}$$

$$\begin{cases} v_{10}|_0 = 0, \\ v_{11}|_0 = 0, \\ v_{12}|_0 = 0 \end{cases} \tag{2.3.133}$$

Bottom - Horizontal Displacement

At the leading $O(\epsilon)$ and second order $O(\epsilon)$ the boundary conditions (2.3.49) and (2.3.50) are expressed for each harmonic as:

$$\begin{cases} X_{00}|_0 = 0, \\ X_{01}|_0 = 0 \end{cases} \tag{2.3.134}$$

$$\begin{cases} X_{10}|_0 = 0, \\ X_{11}|_0 = 0, \\ X_{12}|_0 = 0 \end{cases} \tag{2.3.135}$$

Bottom - Vertical Displacement

At the leading $O(\epsilon)$ and second order $O(\epsilon)$ the boundary conditions (2.3.51) and (2.3.52) are expressed for each harmonic as:

$$\begin{cases} Y_{00}|_0 = 0, \\ Y_{01}|_0 = 0 \end{cases} \tag{2.3.136}$$

$$\begin{cases} Y_{10}|_0 = 0, \\ Y_{11}|_0 = 0, \\ Y_{12}|_0 = 0 \end{cases} \tag{2.3.137}$$

2.3.9 Solvability Conditions

The differential equation governing different orders (indexed by the integer n) and different harmonics (indexed by the integer m) of the velocity potential Φ_{nm} is

$$\Phi_{nm,yy} - m^2 k_0^2 \Phi_{nm} = F_{nm} \tag{2.3.138}$$

with the functions F_{nm} defined previously by equations (2.3.98)-(2.3.100). The corresponding boundary conditions are:

$$\left(\Phi_{nm,y} - m^2 \Phi_{nm}\right)\Big|_0 = G_{nm} \tag{2.3.139}$$

$$(\Phi_{nm,y})|_{-H} = L_{nm} \tag{2.3.140}$$

with the constants G_{nm} defined by equations (2.3.109), (2.3.110) and (2.3.116) and the constants L_{nm} defined by equations (2.3.121) and (2.3.122).

The governing equation is an inhomogeneous ordinary differential equation. As the corresponding homogeneous problems may have nontrivial solutions, for each couple (n, m) the function F_{nm} and the constant G_{nm} and L_{nm} should verify the solvability condition.

Zeroth harmonic ($m = 0$)

For the zeroth harmonic the boundary value problem at order $O(\epsilon^n)$ is

$$\begin{aligned} \Phi_{n0,yy} &= F_{n0} \\ (\Phi_{n0,y})|_0 &= G_{n0} \\ (\Phi_{n0,y})|_{-H} &= L_{n0} \end{aligned}$$

The homogeneous solution is constant in y and the solvability condition to be verified is:

$$\int_{-H}^{0} F_{n0} dy = G_{n0} - L_{n0} \tag{2.3.141}$$

First harmonic ($m = 1$)

For the first harmonic the boundary-value problem is at order $O(\epsilon^n)$ is

$$\begin{aligned} \Phi_{n1,yy} - k_0^2 \Phi_{n1} &= F_{n1} \\ \left(\Phi_{n1,y} - m^2 \Phi_{n1}\right)\big|_0 &= G_{n1} \\ (\Phi_{n1,y})|_{-H} &= L_{n1} \end{aligned}$$

As it will be verified in the next section, the homogenious solution for $m = 1$ is proportional to $\cosh Q$ with $Q = Q(y) = k_0(y + H)$. The solvability condition follows from the Green's formula:

$$\int_{-H}^{0} F_{n1} \frac{\cosh Q}{\cosh q} dy = G_{n1} - \frac{L_{n1}}{\cosh q} \tag{2.3.142}$$

with $q = Q(y = 0) = k_0 H$.

Higher harmonics ($m \geq 2$)

For harmonics higher than the second one $m \geq 2$ there cannot be any homogeneous solution (see C.C. Mei, 1989). As it will be seen very soon, if the homogeneous solution existed, it could not satisfy the dispersion relationship (2.4.5). Thus the

corresponding inhomogeneous problems for $m \geq 2$ are always solvable.

2.4 Solution to the approximate equations

In this section we will derive the solution to the approximate equations for each order and for each harmonic. We will proceed incrementally. The first step consists in solving the leading order water problem, which is not affected by the presence of the mud layer. The next step is to couple the obtained solution with the leading order mud layer solution. The two are coupled through the interface kinematic and dynamic boundary conditions. The so obtained leading order movement of the mud layer affects second order $O(\epsilon)$ movement in water which will be computed. Then, the second order $O(\epsilon)$ solution inside the mud layer, which is coupled to the second order solution of the water layer through the interface, will be obtained. In particular the mean displacement inside the mud layer will be deduced. Finally the use of the solvability conditions for the inhomogenious water problems for the first three orders will give the equation governing the slow evolution of the free surface wavetrain.

2.4.1 Leading order $O(1)$ solution - Water layer

Because the mud layer is thin, the leading order water problem is not affected by the presence of the mud layer. It is confirmed by the governing equations which are summarized and solved below. Now each harmonic of the leading order velocity potential $\Phi_0 = \Phi_{00} + \left(\Phi_{01}e^{i\psi} + c.c.\right)$ and leading order pressure $p_0 = p_{00} + \left(p_{01}e^{i\psi} + c.c.\right)$ will be determined.

Zeroth harmonic

The equations governing the zeroth harmonic of the velocity potential are the Laplace equation (first line of the system (2.3.98)) and the Bernoulli equation (first line of the

system (2.3.101)):

$$\begin{aligned} \Phi_{00,yy} &= 0, \\ p_{00}^{(w)} &= 0 \end{aligned}$$

The corresponding boundary conditions are the combined kinematic and dynamic boundary condition on the free surface (first line of the system (2.3.109)) and the kinematic boundary condition on the interface (first line of the system (2.3.121)):

$$\begin{aligned} (\Phi_{00,y})|_0 &= G_{00} = 0, \\ (\Phi_{00,y})|_{-H} &= L_{00} = 0 \end{aligned}$$

The boundary-value problem above imply that the function $\Phi_{00} = \Phi_{00}(y, x_1, t_1, t_2, \dots)$ is independent of the variable y. It depends only on slow space and time-scales.

$$\Phi_{00} = \Phi_{00}(x_1, t_1, t_2, \dots) \tag{2.4.1}$$

First harmonic

The equations governing the zeroth harmonic of the velocity potential are the Laplace equation (second line of the system (2.3.98)) and the Bernoulli equation (second line of the system (2.3.101)) are:

$$\begin{aligned} \Phi_{01,yy} - k_0^2 \Phi_{01} &= F_{01} = 0 \\ p_{01}^{(w)} &= i\Phi_{01} \end{aligned}$$

The corresponding boundary conditions are the combined kinematic and dynamic boundary condition on the free surface (first lines of the system (2.3.109)), the kinematic boundary condition on the interface (first line of the system (2.3.121)) and the

dynamic boundary condition on the free surface (second line of the systems (2.3.117)):

$$\begin{aligned}(\Phi_{01,y})|_0 - (\Phi_{01})|_0 &= G_{01} = 0\\ (\Phi_{01,y})|_{-H} &= L_{01} = 0\\ -\frac{A}{2} &= H_{01} = -i\,(\Phi_{01})|_0\end{aligned}$$

This boundary-value problem is governed by a homogeneous ordinary differential equation and thus there is no need to use the solvability condition.
The solution of the above written boundary-value problem is the classical water problem solution which is:

$$\Phi_{01} = -i\frac{\cosh Q}{2\cosh q}A(x_1, t_1, t_2, \dots) \tag{2.4.2}$$

$$p_{01}^{(w)} = \frac{\cosh Q}{2\cosh q}A(x_1, t_1, t_2, \dots) \tag{2.4.3}$$

$$\tag{2.4.4}$$

and the dispersion relation:

$$k_0 \tanh q = 1 \tag{2.4.5}$$

with the constant q and function $Q = Q(y)$ being defined as

$$q \equiv k_0 H \tag{2.4.6}$$

$$Q \equiv k_0(H + y) \tag{2.4.7}$$

To see if we recover the usual water dispersion relationship from the obtained one (2.4.5) we need to transform the dimensionless variables into dimensional. As it was introduced in the section on the nondimensionalization $k_0 = \bar{k}_0 \frac{g}{\omega^2}$ and $H = h\frac{\omega^2}{g}$.

$$\omega^2 = g\bar{k}_0 \tanh(\bar{k}_0 h)$$

Therefore the usual water dispersion relation is recovered.

2.4.2 Leading order $O(1)$ solution - Mud layer

The mud layer is put into the movement because of the pressure gradient created by the leading order water waves. The momentum is transfered to the mud layer through stresses on the interface separating water and mud layers. Let us now obtain the expressions of the leading order quantities describing the leading order of the mud layer (u_0, v_0, p_0).

Zeroth harmonic

At the leading order the problem is linear and we expect the leading order solution to contain the first harmonics only. Therefore we predict all the leading order zeroth harmonic terms to be equal to zero. Let us show it mathematically. The equations governing the zeroth harmonic of the unknown quantities are the mass conservation (first line of the system (2.3.103)), the x-momentum conservation equation (first line of the system (2.3.105)), the y-momentum conservation equation (first line of the system (2.3.107)) and the condition on the zeroth harmonic of the velocity (2.3.75) and (2.3.80):

$$\begin{aligned} v_{00,y'} &= 0 \\ 0 &= 0 \\ p^{(m)}_{00,y'} &= 0 \\ u_{00} &= 0 \\ v_{00} &= 0 \end{aligned}$$

The corresponding boundary conditions are the non slip boundary conditions in terms of the velocity field (first lines of the systems (2.3.130) and (2.3.132)), the kinematic boundary condition at the interface (first line of the system (2.3.124)), the tangential stress continuity through the interface (first line of the system (2.3.126)) and

the normal stress continuity through the interface (first line of the system (2.3.128)):

$$\begin{aligned}
(u_{00})|_0 &= 0 \\
(v_{00})|_0 &= 0 \\
(v_{00})|_1 &= 0 \\
b_0\,(X_{00,y'})|_1 &= 0 \\
\left(p_{00}^{(m)}\right)\Big|_{y'=1} &= \left(p_{00}^{(w)}\right)\Big|_{y=-H}
\end{aligned}$$

In case when $b_0 \neq 0$, the obvious solution of these equations is:

$$u_{00} = 0 \tag{2.4.8}$$

$$v_{00} = 0 \tag{2.4.9}$$

$$p_{00}^{(m)} = 0 \tag{2.4.10}$$

$$X_{00} = 0 \tag{2.4.11}$$

The last equation comes from our initial assumption that there is no mean displacement of the mud layer at the leading order.
The zeroth harmonic terms come from the nonlinearities of the equations, but as the mud layer is thin these terms affect only the second order $O(\epsilon)$ solution. This explains why all the zeroth harmonic quantities are zero at the leading order.

First harmonic

The equations governing the evolution of the first harmonic are the mass conservation (second line of the system (2.3.103)), the x-momentum conservation equation (second line of the system (2.3.105)) and the y-momentum conservation equation (second line

of the system (2.3.107)):

$$\begin{aligned} v_{01,y'} + ik_0 u_{01} &= 0 \\ -iu_{01} &= -ik_0\gamma p_{01}^{(m)} + \frac{1}{Re}\mu\frac{a}{d}u_{01,y'y'} \\ p_{01,y'}^{(m)} &= 0 \end{aligned}$$

The corresponding boundary conditions are the non slip boundary condition (second lines of the systems (2.3.130) and (2.3.132)), the kinematic boundary condition at the interface (second line of the system (2.3.124)), the tangential stress continuity through the interface (second line of the system (2.3.126)) and the normal stress continuity through the interface (second line of the system (2.3.128)):

$$\begin{aligned} (u_{01})|_0 &= 0 \\ (v_{01})|_0 &= 0 \\ -i\zeta_{01} &= \frac{d}{a}(v_{01})|_1 \\ \mu(u_{01,y'})|_{y'=1} &= 0 \\ \left(p_{01}^{(m)}\right)\Big|_{y'=1} &= \left(p_{01}^{(w)}\right)\Big|_{y=-H} \end{aligned}$$

First, let us solve the y-momentum equation. Because the mud layer is thin the pressure is constant through the entire layer and equals to the pressure in water by continuity of stresses through the interface:

$$p_{01}^{(m)} = \left(p_{01}^{(w)}\right)\Big|_{y=-H} = \frac{A}{2\cosh q}$$

Secondly, let us solve the x-momentum equation. It can be rewritten as:

$$u_{01,y'y'} + i\frac{Re\,d}{\mu\;a}u_{01} = ik_0\gamma\frac{Re\,d}{\mu\;a}p_{01}^{(m)}$$

Using the definition (1.4.5) of the phase of the complex viscosity ($\mu = |\mu|e^{i\theta}$) we define the dimensionless complex parameter λ as a positive root of $\lambda^2 = -i\frac{Re}{\mu}\frac{d}{a}$

$$\lambda \equiv e^{-i\left(\frac{\theta}{2}+\frac{\pi}{4}\right)}\sqrt{\frac{Re}{|\mu|}\frac{d}{a}} \tag{2.4.12}$$

Note that the expression under the square root may be rewritten in terms of the ratio of the mud layer depth d to the Stokes' boundary layer thickness $\delta_s \equiv \sqrt{\frac{2|\bar{\mu}|}{\rho^{(m)}\omega}}$

$$d_s \equiv \frac{d}{\delta_s} \tag{2.4.13}$$

The expression under the square root becomes

$$Re\frac{d|\mu_0|}{a|\mu|} = \frac{\rho^{(m)}d^2\omega}{|\bar{\mu}|} = 2\frac{d^2}{\delta_s^2} = 2d_s^2$$

Finally the simplified expression for λ is

$$\lambda = d_s\sqrt{2}e^{-i\left(\frac{\theta}{2}+\frac{\pi}{4}\right)}$$

The experimental values of the parameter θ are confined into the first quadrant, so that the phase of λ is also confined into $[0, \pi/2]$ interval. The amplitude of λ increases with the dimensionless depth d_s.

The equation of conservation of the x-momentum becomes

$$u_{01,y'y'} - \lambda^2 u_{01} = -\lambda^2 k_0\gamma p_{01}^{(m)}$$

The solution is the sum of the solutions of the corresponding homogeneous equation ($\cosh(\lambda y')$ and $\sinh(\lambda y')$) and the particular solution ($k_0\gamma p_{01}^{(m)}$):

$$\begin{aligned} u_{01} &= k_0\gamma p_{01}^{(m)}\left[1 + G_0\cosh(\lambda y') + H_0\sinh(\lambda y')\right] \\ &= \frac{\gamma k_0 A}{2\cosh q}\left[1 + G_0\cosh(\lambda y') + H_0\sinh(\lambda y')\right] \end{aligned}$$

Note that if the only other root $\lambda^- \equiv -\frac{d}{\delta_s}\sqrt{2}e^{-i\left(\frac{\theta}{2}+\frac{\pi}{4}\right)}$ was selected as the square root of $-i\frac{Re}{\mu}\frac{d}{a}$ then the solution will be unchanged. This is due to the fact that $\lambda^- = -\lambda$ and that the solution always involves both $e^{\lambda y'}$ and $e^{-\lambda y'}$.
Applying the boundary conditions the constants G_0 and H_0 are determined:

$$u_{01}|_0 = 0 \quad \Leftrightarrow \quad G_0 = -1$$
$$u_{01,y'}|_1 = 0 \quad \Leftrightarrow \quad H_0 = \tanh(\lambda)$$

Therefore the horizontal velocity inside the mud layer is completely found:

$$u_{01} = \frac{\gamma k_0 A}{2\cosh q}\left[1 - \cosh(\lambda y') + \tanh(\lambda)\sinh(\lambda y')\right]$$

Now, we can solve the mass conservation equation to obtain the expression of the vertical velocity v_{01}:

$$v_{01}(y, x_1, t_1, t_2, \dots) = v_{01}|_{y'=0} - ik_0 \int_0^{y'} u_{01}(y", x_1, t_1, t_2, \dots)dy"$$

using the no slip boundary condition $(v_{01})|_0 = 0$ we get:

$$v_{01} \;=\; -i\frac{\gamma k_0^2 A}{2\lambda\cosh q}\left[\lambda y' - \sinh\lambda y' + \tanh\lambda(\cosh\lambda y' - 1)\right]$$

or using the dispersion relation:

$$v_{01} = -i\frac{\gamma k_0 A}{2\lambda\sinh q}\left[\lambda y' - \sinh\lambda y' + \tanh\lambda(\cosh\lambda y' - 1)\right]$$

Finally, the amplitude of the interface displacement ζ_{01} can now be found from the approximate kinematic boundary condition on the interface $(\zeta_{01} = i\frac{d}{a}(v_{01})|_1)$:

$$\zeta_{01} = i\frac{d}{a}(v_{01})|_{y'=1} = \frac{\gamma k_0 A}{2\sinh q}\frac{d}{a}\left(1 - \frac{\tanh\lambda}{\lambda}\right)$$

Since $\lambda \propto \frac{d}{\delta_s}$, the amplitude of the interface movement goes to zero $\zeta_{01} \to 0$ as $\frac{d}{\delta_s} \to 0$. Meaning that when the mud layer is shallow compared to the Stokes' boundary layer

thickness there is no movement inside mud. As the experimental values of the viscosity, and therefore of the Stokes' boundary layer thickness, increase sharply when the frequency ω goes to zero, we expect to have no mud movement at low frequencies.

Let us summarize the leading order solution inside the mud layer for the first harmonic:

$$p_{01}^{(m)} = \frac{A}{2\cosh q} \tag{2.4.14}$$

$$u_{01} = \frac{\gamma k_0 A}{2\cosh q}\left[1-\cosh(\lambda y')+\tanh(\lambda)\sinh(\lambda y')\right] \tag{2.4.15}$$

$$v_{01} = -i\frac{\gamma k_0 A}{2\lambda\sinh q}\left[\lambda y'-\sinh\lambda y'+\tanh\lambda(\cosh\lambda y'-1)\right] \tag{2.4.16}$$

$$\zeta_{01} = \frac{\gamma k_0 A}{2\sinh q}\frac{d}{a}\left(1-\frac{\tanh\lambda}{\lambda}\right) \tag{2.4.17}$$

The study of the properties of these solutions will be conducted in the section (2.5).

2.4.3 Second order $O(\epsilon)$ solution - Water layer

Zeroth harmonic

The equations governing the second order zeroth harmonic of the water layer are the Laplace equation (first line of the system (2.3.99)) and the Bernoulli equation (first line of the system (2.3.102)):

$$\begin{aligned}\Phi_{10,yy} &= F_{10}=0,\\ p_{10}^{(w)} &= -\left(\Phi_{00,t_1}+k_0^2|\Phi_{01}|^2+|\Phi_{01,y}|^2\right)\end{aligned}$$

The corresponding boundary conditions are the combined kinematic and dynamic boundary condition on the free surface (first line of the system (2.3.111)), the kinematic boundary condition on the interface (first line of the systems (2.3.122)) and the

dynamic boundary condition on the free surface (first line of the system (2.3.120)):

$$\begin{aligned}
(\Phi_{10,y})|_0 &= G_{10} = -\Re\left\{A^*\left(\Phi_{01,yy} - \Phi_{01,y}\right)|_0\right\} \\
(\Phi_{10,y})|_{-H} &= L_{10} = 0 \\
-\eta_{10} &= H_{10} = \Re\left\{iA\left(\Phi^*_{01,y}\right)|_0\right\} + \left(\Phi_{00,t_1} + k_0^2|\Phi_{01}|^2 + |\Phi_{01,y}|^2\right)|_0
\end{aligned}$$

The mean pressure correction can immediately be determined by plugging in the expressions of the leading order solution Φ_{01} and Φ_{00}:

$$\begin{aligned}
k_0^2|\Phi_{01}|^2 + |\Phi_{01,y}|^2 &= k_0^2|A|^2\frac{\cosh^2 Q}{4\cosh^2 q} + k_0^2|A|^2\frac{\sinh^2 Q}{4\cosh^2 q} \\
&= \frac{|A|^2}{4\sinh^2 q}\left(\cosh^2 Q + \cosh^2 Q\right) = \frac{|A|^2}{4\sinh^2 q}\cosh(2Q) \\
p_{10}^{(w)} &= -\Phi_{00,t_1} - \frac{|A|^2}{4\sinh^2 q}\cosh(2Q)
\end{aligned}$$

By plugging in the leading order solution Φ_{01} and Φ_{00} we obtain the expressions of the constants H_{10} and G_{10}.

For the constant G_{10} we have:

$$\begin{aligned}
\left(\Phi_{01,yy} - \Phi_{01,y}\right)|_0 &= \left(-ik_0^2 A\frac{\cosh Q}{2\cosh q} + ik_0 A\frac{\sinh Q}{2\cosh q}\right)\Bigg|_0 \\
&= -ik_0^2 A\frac{1}{2} + iA\frac{1}{2} = iA\frac{1}{2}\left(1 - k_0^2\right) \\
G_{10} &= -\Re\left[i|A|^2\frac{1}{2}\left(1 - k_0^2\right)\right] = 0
\end{aligned}$$

The solvability condition

$$\int_{-H}^{0} F_{10}dy = G_{10} - L_{10}$$

is trivially satisfied as all its terms are equal to zero.

The equations and the boundary conditions for Φ_{10} imply that the function $\Phi_{10} = \Phi_{10}(y, x_1, t_1, t_2, \dots)$ is independent of the variable y. It depends only on slow space and time-scales.

$$\Phi_{10} = \Phi_{10}(x_1, t_1, t_2, \dots)$$

For the constant H_{10} we have:

$$\begin{aligned}
\Re\left[iA\left(\Phi^*_{01,y}\right)\big|_0\right] &= \Re\left[iA\left(ik_0A^*\frac{\sinh Q}{2\cosh q}\right)\Big|_0\right] \\
&= \Re\left[iA\left(iA^*\frac{1}{2}\right)\right] = -\frac{1}{2}|A|^2 \\
\left(k_0^2|\Phi_{01}|^2 + |\Phi_{01,y}|^2\right)\big|_0 &= \left(k_0^2|A|^2\frac{\cosh^2 Q}{4\cosh^2 q} + k_0^2|A|^2\frac{\sinh^2 Q}{4\cosh^2 q}\right)\Big|_0 \\
&= \frac{|A|^2}{4}(k_0^2-1) \\
H_{10} &= -\frac{1}{2}|A|^2 + \Phi_{00,t_1} + \frac{|A|^2}{4}(k_0^2+1) \\
&= \Phi_{00,t_1} + \frac{|A|^2}{4}(k_0^2-1) = \Phi_{00,t_1} + \frac{|A|^2}{4\sinh^2 q}
\end{aligned}$$

Then the second order solution for the zeroth harmonic is

$$\Phi_{10} = \Phi_{10}(x_1, t_1, t_2, \dots) \tag{2.4.18}$$

$$p_{10}^{(w)} = -\Phi_{00,t_1} - \frac{|A|^2}{4\sinh^2 q}\cosh(2Q) \tag{2.4.19}$$

$$\eta_{10} = -\Phi_{00,t_1} - \frac{|A|^2}{4\sinh^2 q} \tag{2.4.20}$$

Note that in case of purely sinusoidal waves, there is no slow time modulation and all the derivatives with respect to t_1 vanish. In such case the usual nonlinear correction is found: the mean free surface is lowered ($\eta_{10} \leq 0$) and the mean pressure is negative $p_{10} \leq 0$. In case of narrow-banded waves, the slow time variation appears and the terms η_{10} and p_{10} depend on the time variation of the long waves (Φ_{00,t_1}).

First harmonic

The equations governing the second order first harmonic of the water layer are the Laplace equation (second line of the system (2.3.99)) and the Bernoulli equation

(second line of the system (2.3.102)):

$$\begin{aligned} \Phi_{11,yy} - k_0^2 \Phi_{11} &= F_{11}, \qquad & F_{11} &= -2ik_0 \Phi_{01,x_1}, \\ p_{11}^{(w)} &= i\Phi_{11} - \Phi_{01,t_1} \end{aligned}$$

The corresponding boundary conditions are the combined kinematic and dynamic boundary condition on the free surface (second line of the system (2.3.111)), the kinematic boundary condition on the interface (second line of the systems (2.3.122)) and the dynamic boundary condition on the free surface (second line of the system (2.3.120)):

$$\begin{aligned} (\Phi_{11,y})|_0 - (\Phi_{11})|_0 &= G_{11}, \\ (\Phi_{11,y})|_{-H} &= L_{11}, \\ -\eta_{11} &= H_{11} \end{aligned}$$

with the constants G_{11}, L_{11} and H_{11} given by the second line of the systems of equations (2.3.110), (2.3.122) and (2.3.119):

$$\begin{aligned} G_{11} &= -\left[\frac{A}{2}\left(\Phi_{00,yy}\right)|_0 - 2i\left(\Phi_{01,t_1}\right)|_0 - 2i\left(\Phi_{00,y}\Phi_{01,y}\right)|_0\right] \\ L_{11} &= -i\zeta_{01} \\ H_{11} &= -i\left(\Phi_{11}\right)|_0 + \left(\Phi_{01,t_1}\right)|_0 \end{aligned}$$

Let us first express the constant G_{11} in terms of the free surface amplitude A. As the function Φ_{00} is independent of the variable y its derivatives with respect to y vanish and we get

$$G_{11} = 2i\left(\Phi_{01,t_1}\right)|_0 = 2i\left(-i\frac{\cosh Q}{2\cosh q}A\right)_{t_1}\Bigg|_0 = A_{t_1}$$

Now let us compute the expression of the function F_{11} in terms of the free surface amplitude:

$$F_{11} = -2ik_0\Phi_{01,x_1} = -2ik_0\left(-i\frac{\cosh Q}{2\cosh q}A\right)_{x_1} = -k_0\frac{\cosh Q}{\cosh q}A_{x_1}$$

The solvability condition (2.3.142) can now be written explicitly in terms of terms of the free surface wave amplitude A:

$$\begin{aligned} A_{t_1} + i\frac{\zeta_{01}}{\cosh q} &= -k_0\frac{1}{\cosh q}A_{x_1}\int_{-H}^{0}\cosh Q\frac{\cosh Q}{\cosh q}dy \\ &= -\frac{k_0A_{x_1}}{2\cosh^2 q}\int_{-H}^{0}(1+\cosh 2Q)\,dy = -\frac{A_{x_1}}{\sinh 2q}\left(H + \left[\frac{1}{2k_0}\sinh 2Q\right]_{-H}^{0}\right) \\ &= -\frac{A_{x_1}}{\sinh 2q}\left(H + \frac{\sinh 2q}{2k_0}\right) = -\frac{A_{x_1}}{2k_0}\left(\frac{2q}{\sinh 2q} + 1\right) \end{aligned}$$

Note that the factor in the parenthesis of the last equation is equal to the group velocity C_g given by the dispersion relation (2.4.5). That is

$$C_g = \frac{1}{2k_0}\left(1 + \frac{2q}{\sinh 2q}\right) \tag{2.4.21}$$

Thus the solvability condition can be written in a compact form:

$$A_{t_1} + C_gA_{x_1} = -i\frac{\zeta_{01}}{\cosh q}$$

Replacing the expression of ζ_{01} by its expression (2.4.17) in terms of the free surface wave amplitude we get:

$$A_{t_1} + C_gA_{x_1} = ik_1C_gA \tag{2.4.22}$$

where the complex parameter k_1 was defined as:

$$k_1 = -\gamma\frac{d}{a}\left(\frac{2k_0^2}{2q + \sinh 2q}\right)\left(1 - \frac{\tanh\lambda}{\lambda}\right) \tag{2.4.23}$$

The newly defined parameter k_1 characterizes the rate of decay of the free surface wave amplitude due to the energy dissipation inside the mud layer.

The equation 2.4.22 describes the evolution of the free surface wave amplitude with the slow time- and space-scales. In case of a purely sinusoidal wave the slow time derivate ∂_{t_1} vanishes and the equation governing the slow evolution of the wave amplitude reduces to

$$A_{x_1} = ik_1 A$$

Its solution is an exponentially decaying function:

$$A(x_1) = A_0 e^{ik_1 x_1} = A_0 e^{-k_1^i x_1} e^{ik_1^r}$$

Note that the in terms of fast space-scale we have $k_1 x_1 = \epsilon k_1 x$. In the following by change in the wavenumber it will be meant ϵk_1 unless otherwise specified. We have:

$$\frac{\epsilon k_1}{k_0} = -\gamma \frac{d}{h}\left(1 - \frac{\tanh\lambda}{\lambda}\right)\frac{2q}{2q + \sinh(2q)} \tag{2.4.24}$$

The damping and the induced wavenumber shift can be computed respectively from the real and the imaginary parts of the expression (2.4.24)

$$D_0 = \Im\left(\frac{\epsilon k_1}{k_0}\right), \qquad \Delta k = \Re\left(\frac{\epsilon k_1}{k_0}\right) \tag{2.4.25}$$

Note that when $\frac{d}{h} \to 0$ then

$$\frac{\epsilon k_1}{k_0} \to 0$$

On the other hand if $d >> \delta_s$ ($d_s >> 1$) then $\frac{\tanh\lambda}{\lambda} \propto \frac{1}{d_s} \approx 0$ and

$$\frac{\epsilon k_1}{k_0} \approx -\gamma \frac{d}{h}\left(\frac{2q}{2\bar{q} + \sinh 2q}\right)$$

which is real and negative. In other words for a large values of d_s the damping is negligible and the waves become longer.

The influence of the water layer depth is the following. For very short waves or deep water, $q = k_0 H \gg 1$,

$$\frac{\epsilon k_1}{k_0} \approx 0. \tag{2.4.26}$$

and for long waves in shallow water,

$$\frac{\epsilon k_1}{k_0} \approx -\frac{\gamma}{2}\frac{d}{h} \tag{2.4.27}$$

Now let us obtain the solution for the first harmonic Φ_{11}. Φ_{11} is the solution of an inhomogeneous equation at the second order. It consist of a sum of the solution to the homogeneous equation and a particular solution Φ_{11}^p. The solutions of the corresponding homogeneous equation are $\sinh Q$ and $\cosh Q$. The part of the solution proportional to the $\cosh Q$ is already included into the leading order solution. We expect the solution to be of the form:

$$\Phi_{11} = C\sinh Q + \Phi_{11}^p$$

Note that there is only one constant to be determined, but two boundary conditions. This is not a problem, as the application of both boundary conditions produces equivalent results. This is due to the fact that the boundary conditions are linked by the solvability condition.

To find the particular solution the method of the variation of the constants is employed. Let us look for a particular solution in a form $\Phi_{11} = C(y)\sinh Q$, with $C(y)$ being a function of y. Then

$$\Phi_{11,yy} - k_0^2\Phi_{11} = C''(y)\sinh Q + 2C'(y)k_0\cosh Q = F_{11} = -k_0\frac{\cosh Q}{\cosh q}A_{x_1}$$

The equation above holds if

$$\begin{cases} C''(y) &= 0 \\ 2k_0C'(y) &= -\frac{A_{x_1}}{2\cosh q} \end{cases}$$

which is equivalent to

$$C(y) = -\frac{A_{x_1}y}{2\cosh q} + C_0$$

A particular solution is then

$$\Phi_{11}^{p} = -\frac{A_{x_1} y}{2\cosh q}\sinh Q + C_0 \sinh Q$$

This solution should satisfy the boundary conditions on the free surface and on the bottom. As the two boundary conditions are linked by the solvability condition we need only to impose one boundary condition and the second boundary condition will automatically be satisfied. For the ease of the computations the bottom boundary condition will be applied:

$$\begin{aligned}(\Phi_{11,y})|_{-H} &= \left(C_0 k_0 \cosh Q - \frac{A_{x_1}}{2\cosh q}\sinh Q - \frac{k_0 A_{x_1} y}{2\cosh q}\cosh Q\right)\Bigg|_{-H} \\ &= C_0 k_0 + \frac{q A_{x_1}}{2\cosh q} = -i\zeta_{01} = i k_1 C_g A \cosh q\end{aligned}$$

The constant C_0 is then

$$C_0 = i\frac{k_1}{k_0} C_g A \cosh q - \frac{q}{2k_0 \cosh q} A_{x_1} = i k_1 C_g A \sinh q - \frac{q}{2k_0 \cosh q} A_{x_1}$$

The total solution for the first harmonic of the second order velocity potential Φ_{11} is:

$$\begin{aligned}\Phi_{11} &= i k_1 C_g A \sinh q \sinh Q - \frac{q}{2k_0 \cosh q} A_{x_1} \sinh Q - \frac{A_{x_1} y}{2\cosh q}\sinh Q \\ &= i k_1 C_g A \sinh q \sinh Q - \frac{Q \sinh Q}{2k_0 \cosh q} A_{x_1}\end{aligned}$$

The pressure correction inside the water layer can be deduced straightforwardly

$$p_{11}^{(w)} = \frac{i}{2k_0 \cosh q}\left(k_0 A_{t_1} \cosh Q - A_{x_1} Q \sinh Q\right) - k_1 C_g A \sinh q \sinh Q$$

The first harmonic free surface movement correction is

$$\begin{aligned}\eta_{11} &= -H_{11} = i\left(\Phi_{11}\right)|_0 - \left(\Phi_{01,t_1}\right)|_0 = i\left(i k_1 C_g A \sinh^2 q - \frac{q \sinh q}{2k_0 \cosh q} A_{x_1} + \frac{1}{2} A_{t_1}\right) \\ &= \frac{i}{2} A_{t_1} - k_1 C_g A \sinh^2 q - i\frac{q \sinh q}{2k_0 \cosh q} A_{x_1}\end{aligned}$$

Note that in absence of the mud layer ($k_1 = 0$) the solutions are the known water layer solution (see C.C.Mei 1989).

Let us finally summarize the obtained solution for the second order first harmonic:

$$\Phi_{11} = ik_1 C_g A \sinh q \sinh Q - \frac{Q \sinh Q}{2k_0 \cosh q} A_{x_1} \tag{2.4.28}$$

$$p_{11}^{(w)} = \frac{i}{2k_0 \cosh q} (k_0 A_{t_1} \cosh Q - A_{x_1} Q \sinh Q) - k_1 C_g A \sinh q \sinh Q \tag{2.4.29}$$

$$\eta_{11} = \frac{i}{2} A_{t_1} - k_1 C_g A \sinh^2 q - i \frac{q \sinh q}{2k_0 \cosh q} A_{x_1} \tag{2.4.30}$$

Note that in the absence of the mud layer $k_1 = 0$ and we recover the solutions for inviscid water waves propagating over a solid bottom (C.C. Mei, 1989).

Second harmonic

The governing equations for the second harmonic are the Laplace equation (third line of the system (2.3.99)) and the Bernoulli equation (third line of the system (2.3.102))::

$$\Phi_{12,yy} - 4k_0^2 \Phi_{12} = F_{12}, \qquad F_{12} = 0$$

$$p_{12}^{(w)} = 2i\Phi_{12} + \frac{1}{2} k_0^2 \Phi_{01}^2 - \frac{1}{2} \Phi_{01,y}^2$$

The corresponding boundary conditions are the combined kinematic and dynamic boundary condition on the free surface (third line of the system (2.3.111)), the kinematic boundary condition on the interface (third line of the systems (2.3.122)) and the dynamic boundary condition on the free surface (third line of the system (2.3.120)):

$$(\Phi_{12,y})|_{-H} = L_{12}$$

$$(\Phi_{12,y})|_0 - 4(\Phi_{12})|_0 = G_{12}$$

$$-\eta_{12} = H_{12}$$

with the constants G_{12}, L_{12} and H_{12} given by the third line of the systems of equations (2.3.110), (2.3.122) and (2.3.119):

$$\begin{aligned} L_{12} &= 0 \\ G_{12} &= -\left[\frac{A}{2}(\Phi_{01,yy} - \Phi_{01,y}) + 2ik_0^2\Phi_{01}^2 - 2i\Phi_{01,y}^2\right]\Big|_0 \\ H_{12} &= -2i\,(\Phi_{12})|_0 - i\frac{A}{2}\,(\Phi_{01,y})|_0 - \frac{1}{2}k_0^2\,(\Phi_{01}^2)|_0 + \frac{1}{2}\,(\Phi_{01,y}^2)|_0 \end{aligned}$$

Let us first compute the constant G_{12}.

$$\begin{aligned} G_{12} &= -\left[\frac{A}{2}\left(-ik_0^2\frac{\cosh Q}{2\cosh q}A\right) - A\left(-i\frac{\sinh Q}{2\sinh q}A\right) + 2ik_0^2\left(-\frac{\cosh^2 Q}{4\cosh^2 q}A^2\right) - 2i\left(-\frac{\sinh^2 Q}{4\sinh^2 q}A^2\right)\right]\Big| \\ &= -\left[-A^2\frac{i}{4}k_0^2 + \frac{i}{4}A^2 - k_0^2\frac{i}{2}A^2 + \frac{i}{2}A^2\right]\Big|_0 = \frac{3}{4}iA^2(k_0^2 - 1) = \frac{3i}{4}\frac{A^2}{\sinh^2 q} \end{aligned}$$

Now the boundary-value problem for the velocity potential can be solved. In fact the corresponding governing differential equation is a homogeneous ordinary differential equation. Its solution is:

$$\Phi_{12} = C_1\cosh 2Q + C_2\sinh 2Q$$

Applying the boundary condition on the bottom we get:

$$0 = (\Phi_{12})|_{-H} = (2k_0C_1\sinh 2Q + 2k_0C_2\cosh 2Q)|_{-H} = 2k_0C_2$$

This implies

$$C_2 = 0$$

To determine the constant C_1 the boundary condition on the free surface is applied:

$$\begin{aligned} \frac{3i}{4}\frac{A^2}{\sinh^2 q} &= (\Phi_{12,y})|_0 - 4\,(\Phi_{12})|_0 = (2k_0C_1\sinh 2Q + 2k_0C_2\cosh Q)|_0 - 4\,(C_1\cosh 2Q)|_0 \\ &= 4C_1(k_0\sinh q\cosh q - \cosh 2q) = 4C_1(\cosh^2 q - \cosh^2 q + \sinh^2 q) \end{aligned}$$

This implies

$$C_1 = \frac{3i}{16}\frac{A^2}{\sinh^4 q}$$

And the second harmonic of the second order velocity potential is:

$$\Phi_{12} = \frac{3i}{16}\frac{A^2}{\sinh^4 q}\cosh 2Q$$

The pressure component $p_{12}^{(w)}$ can now be determined:

$$\begin{aligned}
p_{12}^{(w)} &= -\frac{3}{8}\frac{A^2}{\sinh^4 q}\cosh 2Q + \frac{1}{2}k_0^2\left(-\frac{\cosh^2 Q}{4\cosh^2 q}A^2\right) - \frac{1}{2}\left(-\frac{k_0^2\sinh^2 Q}{4\cosh^2 q}A^2\right) \\
&= -\frac{3}{8}\frac{A^2}{\sinh^4 q}\cosh 2Q - \frac{1}{8}\left(\frac{\cosh^2 Q}{\sinh^2 q}A^2\right) + \frac{1}{8}\left(\frac{\sinh^2 Q}{\sinh^2 q}A^2\right) \\
&= \frac{1}{8}\frac{1}{\sinh^2 q}A^2\left(\sinh^2 Q - \cosh^2 Q - 3\frac{\cosh 2Q}{\sinh^2 q}\right) \\
&= -\frac{1}{8}\frac{1}{\sinh^2 q}A^2\left(1 + 3\frac{\cosh 2Q}{\sinh^2 q}\right)
\end{aligned}$$

Finally the second harmonic of the free surface displacement can be determined:

$$\begin{aligned}
\eta_{12} &= 2i\left(\Phi_{12}\right)|_0 + i\frac{A}{2}\left(\Phi_{01,y}\right)|_0 + \frac{1}{2}k_0^2\left(\Phi_{01}^2\right)|_0 - \frac{1}{2}\left(\Phi_{01,y}^2\right)|_0 \\
&= 2i\left(\frac{3i}{16}\frac{A^2}{\sinh^4 q}\cosh 2Q\right)\Big|_0 + i\frac{A}{2}\left(-i\frac{k_0\sinh Q}{2\cosh q}A\right)\Big|_0 \\
&\quad + \frac{1}{2}k_0^2\left(-\frac{\cosh^2 Q}{4\cosh^2 q}A^2\right)\Big|_0 - \frac{1}{2}\left(-\frac{k_0^2\sinh^2 Q}{4\cosh^2 q}A^2\right)\Big|_0 \\
&= -\frac{3i}{8}\frac{A^2}{\sinh^4 q}\cosh 2q + \frac{A^2}{4}\frac{k_0\sinh q}{\cosh q} - \frac{A^2}{8}k_0^2\frac{\cosh^2 q}{\cosh^2 q} + \frac{A^2}{8}\frac{k_0^2\sinh^2 q}{\cosh^2 q} \\
&= -\frac{3i}{8}\frac{A^2}{\sinh^4 q}\cosh 2q + \frac{A^2}{4} - \frac{A^2}{8}k_0^2 + \frac{A^2}{8} \\
&= -\frac{3i}{8}\frac{A^2}{\sinh^4 q}\cosh 2q + \frac{A^2}{4} - \frac{A^2}{8}\frac{1}{\sinh^2 q} \\
&= \frac{A^2}{8}\frac{1}{\sinh^2 q}\left(2\sinh^2 q - 1 - \frac{3i}{\sinh^2 q}\right)
\end{aligned}$$

Summarizing the solution for the second order and second harmonic:

$$\begin{aligned}
\Phi_{12} &= \frac{3i}{16}\frac{A^2}{\sinh^4 q}\cosh 2Q \\
p_{12}^{(w)} &= -\frac{1}{8}\frac{1}{\sinh^2 q}A^2\left(1+3\frac{\cosh 2Q}{\sinh^2 q}\right) \\
\eta_{12} &= \frac{A^2}{8}\frac{1}{\sinh^2 q}\left(2\sinh^2 q - 1 - \frac{3i}{\sinh^2 q}\right)
\end{aligned}$$

The last expressions provide second order second harmonic correction to the leading order movement and they are unchanged by the presence or the absence of the mud layer.

2.4.4 Second order $O(\epsilon)$ solution - Mud layer

The second order solution for the mud layer provides the second order correction to the leading order movement. In particular the zeroth harmonic solution gives the mean displacement inside the mud layer, meaning the average displacement around which the mud layer oscillates. In the present section we will compute the average displacement of the mud layer. The first and second harmonic corrections to the leading order movement will not be computed here as they do not carry interesting physical significance.

Zeroth harmonic

The presence of the viscous component in the viscoelastic model makes it possible for the mud layer to dissipate the energy. Due to the nonlinearity introduced by the inertia terms, the displacement inside the mud layer has a non zero steady component - mean displacement. In the approximation of small amplitude waves, this steady correction is of second order $O(\epsilon)$ and will be computed in this section.

The governing equations for the zeroth harmonic mud quantities are the mass conservation (first line of the system (2.3.104)), the x-momentum conservation (first line of the system (2.3.106)) and y-momentum conservation equation (first line of the

equation (2.3.108)):

$$\begin{aligned} v_{10,y'} &= 0 \\ 2\Re\left\{v_{01}u^*_{01,y'}\right\} &= -\gamma p^{(m)}_{00,x_1} + \frac{1}{Re}\frac{a}{d}\left(b_0 X_{10,y'y'}\right) \\ p^{(m)}_{10,y'} &= 0 \end{aligned}$$

we also have the relationship (2.3.77) relating the velocity u_{10} to the previously obtained leading order displacement X_{01} and velocity u_{10}:

$$u_{10} = 2\Re\left\{ik_0 X_{01}u^*_{01} + X_{01,y'}v^*_{01}\right\}$$

This expression can be rewritten using the mass conservation equation (second line of the system 2.3.103) saying that $ik_0u^*_{01} = v^*_{01,y'}$ and using the equation (2.3.76) which implies $X_{01} = iu_{01}$:

$$\begin{aligned} u_{10} &= 2\Re\left\{X_{01}v^*_{01,y'} + X_{01,y'}v^*_{01}\right\} = 2\Re\left\{\left(X_{01}v^*_{01}\right)_{y'}\right\} = 2\Re\left\{i\left(u_{01}v^*_{01}\right)_{y'}\right\} \\ &= -2\Re\left\{i\left(u^*_{01}v_{01}\right)_{y'}\right\} = 2\Im\left\{\left(u^*_{01}v_{01}\right)_{y'}\right\} \end{aligned}$$

These equations can be simplified using the previously obtained solution for the zeroth harmonic of the leading order $O(1)$ (equations (2.4.8)-(2.4.11)). In fact, as the equations (2.4.8) to (2.4.11) state, all the zeroth harmonic mud-related quantities are identically zero at the leading order and we get for the second order zeroth harmonic governing equations:

$$v_{10,y'} = 0, \tag{2.4.31}$$

$$X_{10,y'y'} = 2\frac{Re\,d}{b_0\,a}\Re\left\{v_{01}u^*_{01,y'}\right\}, \tag{2.4.32}$$

$$p^{(m)}_{10,y'} = 0, \tag{2.4.33}$$

$$u_{10} = 2\Im\left\{\left(u^*_{01}v_{01}\right)_{y'}\right\} \tag{2.4.34}$$

Note that these equations are valid only in case when $b_0 \neq 0$. In particular in case of a purely Newtonian fluid these equations will not hold, and the assumption of having the zeroth harmonic displacement X_{10} will be not valid anymore.

The corresponding boundary conditions are the non slip boundary conditions in terms of the velocity field (first line of the systems (2.3.131) and (2.3.133)) and in terms of the displacement field (first line of the systems (2.3.135)), the kinematic boundary condition at the interface (first line of the system (2.3.125)), the tangential stress continuity through the interface (first line of the system (2.3.127)) and the normal stress continuity through the interface (first line of the system (2.3.129)):

$$\begin{aligned}
u_{10}|_0 &= 0 \\
v_{10}|_0 &= 0 \\
X_{10}|_0 &= 0 \\
0 &= \frac{d}{a}(v_{10})|_1 - \zeta_{00,t_1}, \\
b_0 \left(X_{10,y'}\right)\big|_{y'=1} &= -\frac{a}{d}\left[b_0\zeta_{00}\left(X_{00,y'y'}\right)\big|_{y'=1} + 2\Re\left\{\mu\zeta_{01}^*\left(u_{01,y'y'}\right)\big|_{y'=1}\right\}\right], \\
\left(p_{10}^{(m)}\right)\Big|_{y'=1} &= \left(p_{10}^{(w)}\right)\Big|_{y=-H} - \frac{a}{d}\left[\zeta_{00}\left(p_{00,y'}^{(m)}\right)\Big|_{y'=1} + 2\Re\left\{\zeta_{01}^*\left(p_{01,y'}^{(m)}\right)\Big|_{y'=1}\right\}\right],
\end{aligned}$$

Again using the previously computed leading order $O(1)$ solution (equations (2.4.8)-(2.4.11)) the boundary conditions are simplified:

$$\begin{aligned}
v_{10}|_1 &= 0, \\
\left(X_{10,y'}\right)\big|_{y'=1} &= -2\frac{a}{d}\frac{1}{b_0}\Re\left[\mu\zeta_{01}^*\left(u_{01,y'y'}\right)\big|_{y'=1}\right], \\
\left(p_{10}^{(m)}\right)\Big|_{y'=1} &= \left(p_{10}^{(w)}\right)\Big|_{y=-H} - 2\frac{a}{d}\left[\Re\left\{\zeta_{01}^*\left(p_{01,y'}^{(m)}\right)\Big|_{y'=1}\right\}\right], \\
u_{10}|_0 &= 0 \\
v_{10}|_0 &= 0 \\
X_{10}|_0 &= 0
\end{aligned}$$

The zeroth harmonic of the vertical velocity can be deduced straightforwardly from the governing equations and the boundary conditions. One can immediately see that:

$$v_{10} = v_{10}(y, x_1, t_1, t_2, \dots) \;=\; 0 \tag{2.4.35}$$

The pressure and the mean horizontal displacement require a little more work.
Let us first compute the mean pressure correction. From the equation (2.4.33) one can see that the zeroth harmonic of the pressure is constant through the layer and equal to its value on the interface plus a nonlinear correction which is due to the curvature of the interface. We have

$$p_{10}^{(m)} = \left(p_{10}^{(w)}\right)\Big|_{y=-H} - 2\frac{a}{d}\left[\Re\left\{\zeta_{01}^{*}\left(p_{01,y'}^{(m)}\right)\Big|_{y'=1}\right\}\right]$$

From the second order solution inside the water layer we obtain the first term of the right-hand side:

$$\left(p_{10}^{(w)}\right)\Big|_{y=-H} = -\Phi_{00,t_1} - \frac{|A|^2}{4\sinh^2 q}$$

The leading order solution for the mud layer tells us that the leading order pressure $p_{01}^{(m)}$ stays uniform inside the mud layer. As a consequence the term $p_{01,y'}^{(m)}$ is zero. The zeroth harmonic of the second order pressure inside the mud layer finally is:

$$p_{10}^{(m)} = -\Phi_{00,t_1} - \frac{|A|^2}{4\sinh^2 q} \tag{2.4.36}$$

Let us now compute the mean velocity u_{10} given by the equation (2.4.34). The nonlinear term $(v_{01}u_{01}^{*})_{y'}$ appearing in the equation (2.4.34) can be estimated. First

let us estimate $v_{01}u_{01}^*$:

$$\begin{aligned}
v_{01}u_{01}^* &= \left(-i\frac{\gamma k_0 A}{2\lambda\sinh q}\right)\left[\lambda y' - \sinh(\lambda y') + \tanh(\lambda)(\cosh(\lambda y') - 1)\right] \times \\
&\quad \times \left(\frac{\gamma A^*}{2\sinh q}\right)\left[1 - \cosh(\lambda^* y') + \tanh(\lambda^*)\sinh(\lambda^* y')\right] \\
&= -i\gamma^2 k_0 \frac{|A|^2}{4\sinh^2 q}\frac{1}{\lambda}\Big[\lambda y' - \lambda y'\cosh(\lambda^* y') + \tanh(\lambda^*)(\lambda y')\sinh(\lambda^* y') \\
&\quad - \sinh(\lambda y') + \sinh(\lambda y')\cosh(\lambda^* y') - \tanh(\lambda^*)\left|\sinh(\lambda y')\right|^2 \\
&\quad + \tanh(\lambda)\cosh(\lambda y') - \tanh(\lambda) - \tanh(\lambda)\left|\cosh(\lambda y')\right|^2 + \tanh(\lambda)\cosh(\lambda^* y') \\
&\quad + \left|\tanh(\lambda)\right|^2\cosh(\lambda y')\sinh(\lambda^* y') - \left|\tanh(\lambda)\right|^2\sinh(\lambda^* y')\Big]
\end{aligned}$$

The derivative of the last expression gives:

$$\begin{aligned}
(v_{01}u_{01}^*)_{y'} &= -i\gamma^2 k_0 \frac{|A|^2}{4\sinh^2 q}\frac{1}{\lambda}\Big[\lambda - \lambda\cosh(\lambda^* y') - |\lambda|^2 y'\sinh(\lambda^* y') + \lambda\tanh(\lambda^*)\sinh(\lambda^* y') \\
&\quad + \lambda^*\tanh(\lambda^*)(\lambda y')\cosh(\lambda^* y') - \lambda\cosh(\lambda y') + \lambda|\cosh(\lambda^* y')|^2 + \lambda^*|\sinh(\lambda^* y')|^2 \\
&\quad - 2\tanh(\lambda^*)\Re\{\lambda\cosh(\lambda y')\sinh(\lambda^* y')\} + \lambda\tanh(\lambda)\sinh(\lambda y') \\
&\quad - 2\tanh(\lambda)\Re\{\lambda\sinh(\lambda y')\cosh(\lambda^* y')\} + \lambda^*\tanh(\lambda)\sinh(\lambda^* y') \\
&\quad + \lambda\left|\tanh(\lambda)\right|^2|\sinh(\lambda y')|^2 + \lambda^*\left|\tanh(\lambda)\right|^2|\cosh(\lambda^* y')|^2 \\
&\quad - \lambda^*\left|\tanh(\lambda)\right|^2\cosh(\lambda^* y')\Big]
\end{aligned}$$

The expression of the mean velocity u_{10} given by the equation (2.4.34) is

$$u_{10} = 2\Im\left\{(u_{01}^* v_{01})_{y'}\right\}$$

Therefore

$$
\begin{aligned}
u_{10} = & -\gamma^2 k_0 \frac{|A|^2}{2\sinh^2 q} \Re\Big\{ 1 - \cosh(\lambda^* y') - \lambda^* y' \sinh(\lambda^* y') + \tanh(\lambda^*)\sinh(\lambda^* y') \\
& + \tanh(\lambda^*)(\lambda^* y')\cosh(\lambda^* y') - \cosh(\lambda y') + |\cosh(\lambda^* y')|^2 + \frac{\lambda^*}{\lambda}|\sinh(\lambda^* y')|^2 \\
& - 2\frac{\tanh(\lambda^*)}{\lambda}\Re\{\lambda\cosh(\lambda y')\sinh(\lambda^* y')\} + \tanh(\lambda)\sinh(\lambda y') \\
& - 2\frac{\tanh(\lambda)}{\lambda}\Re\{\lambda\sinh(\lambda y')\cosh(\lambda^* y')\} + \frac{\lambda^*}{\lambda}\tanh(\lambda)\sinh(\lambda^* y') \\
& + |\tanh(\lambda)|^2 |\sinh(\lambda y')|^2 + \frac{\lambda^*}{\lambda}|\tanh(\lambda)|^2 |\cosh(\lambda^* y')|^2 \\
& - \frac{\lambda^*}{\lambda}|\tanh(\lambda)|^2 \cosh(\lambda^* y') \Big\} \qquad (2.4.37)
\end{aligned}
$$

The last unknown to be computed is the horizontal displacement X_{10} governed by the equation

$$
X_{10,y'y'} = 2\frac{Re}{b_0}\frac{d}{a}\Re\left\{v_{01}u^*_{01,y'}\right\} \qquad (2.4.38)
$$

The corresponding boundary conditions are:

$$
(X_{10,y'})|_{y'=1} = -2\frac{a}{d}\frac{1}{b_0}\Re\left[\mu\zeta^*_{01}\left(u_{01,y'y'}\right)|_{y'=1}\right], \qquad (2.4.39)
$$

$$
X_{10}|_{y'=0} = 0 \qquad (2.4.40)
$$

The nonlinear term $v_{01}u^*_{01}$ appearing in the equation (2.4.38) can also be estimated

$$\begin{aligned}
v_{01}u^*_{01,y'} &= \left(-i\frac{\gamma k_0 A}{2\lambda\sinh q}\right)\left[\lambda y' - \sinh(\lambda y') + \tanh(\lambda)(\cosh(\lambda y') - 1)\right]\times \\
&\quad \times\left(\frac{\gamma A^*}{2\sinh q}\lambda^*\right)\left[-\sinh(\lambda^* y') + \tanh(\lambda^*)\cosh(\lambda^* y')\right] \\
&= -i\gamma^2 k_0\frac{|A|^2}{4\sinh^2 q}\frac{\lambda^*}{\lambda}\left[\lambda y' - \sinh(\lambda y') + \tanh(\lambda)(\cosh(\lambda y') - 1)\right]\times \\
&\quad \times\left[-\sinh(\lambda^* y') + \tanh(\lambda^*)\cosh(\lambda^* y')\right] \\
&= -i\gamma^2 k_0\frac{|A|^2}{4\sinh^2 q}\frac{\lambda^*}{\lambda}\Big\{\lambda y'\left[-\sinh(\lambda^* y') + \tanh(\lambda^*)\cosh(\lambda^* y')\right] + |\sinh(\lambda y')|^2 \\
&\quad - \tanh(\lambda^*)\sinh(\lambda y')\cosh(\lambda^* y') - \tanh(\lambda)\sinh(\lambda^* y')\cosh(\lambda y') \\
&\quad + |\tanh(\lambda)|^2|\cosh(\lambda y')|^2 + \tanh(\lambda)\sinh(\lambda^* y') - |\tanh(\lambda)|^2\cosh(\lambda^* y')\Big\} \\
&= -i\gamma^2 k_0\frac{|A|^2}{4\sinh^2 q}\Big\{\lambda^* y'\left[-\sinh(\lambda^* y') + \tanh(\lambda^*)\cosh(\lambda^* y')\right] \\
&\quad + \frac{\lambda^*}{\lambda}\Big[|\sinh(\lambda y')|^2 - 2\Re\big(\tanh(\lambda)\sinh(\lambda^* y')\cosh(\lambda y')\big) \\
&\quad + |\tanh(\lambda)|^2|\cosh(\lambda y')|^2 + \tanh(\lambda)\sinh(\lambda^* y') - |\tanh(\lambda)|^2\cosh(\lambda^* y')\Big]\Big\}
\end{aligned}$$

Adding the complex conjugate to obtain the real part we get

$$\begin{aligned}
2\Re\left(v_{01}u^*_{01,y'}\right) &= v_0 u^*_{01,y'} + v^*_{01}u_{01,y'} \\
&= -i\gamma^2 k_0\frac{|A|^2}{4\sinh^2 q}\Big\{\lambda^* y'\left[-\sinh(\lambda^* y') + \tanh(\lambda^*)\cosh(\lambda^* y')\right] \\
&\quad -\lambda y'\left[-\sinh(\lambda y') + \tanh(\lambda)\cosh(\lambda y')\right] \\
&\quad +\Big[|\sinh(\lambda y')|^2 - 2\Re\big(\tanh(\lambda)\sinh(\lambda^* y')\cosh(\lambda y')\big) \\
&\quad + |\tanh(\lambda)|^2|\cosh(\lambda y')|^2\Big]\left(\frac{\lambda^*}{\lambda} - \frac{\lambda}{\lambda^*}\right) \\
&\quad +\frac{\lambda^*}{\lambda}\tanh(\lambda)\sinh(\lambda^* y') - \frac{\lambda}{\lambda^*}\tanh(\lambda^*)\sinh(\lambda y') \\
&\quad - |\tanh(\lambda)|^2\left(\frac{\lambda_1^*}{\lambda}\cosh(\lambda^* y') - \frac{\lambda}{\lambda^*}\cosh(\lambda y')\right)\Big\} \\
&= -i\gamma^2 k_0\frac{|A|^2}{4\sinh^2 q}2i\Im\Big\{F_1(y') + F_2(y') + F_3(y')\Big\} \\
&= 2\gamma^2 k_0\frac{|A|^2}{4\sinh^2 q}\Im\Big\{F_1(y') + F_2(y') + F_3(y')\Big\}
\end{aligned}$$

Where the functions $F_1(y')$, $F_2(y')$ and $F_3(y')$ were introduced to simplify the notations. They are defined as follows

$$F_1(y') = \lambda y'\big[\sinh(\lambda y') - \tanh(\lambda)\cosh(\lambda y')\big] \tag{2.4.41}$$

$$F_2(y') = \frac{\lambda^*}{\lambda}\left(\tanh(\lambda)\sinh(\hat{\lambda}^* y') - |\tanh(\lambda)|^2\cosh(\lambda^* y')\right) \tag{2.4.42}$$

$$F_3(y') = \frac{\lambda^*}{\lambda}\Big[|\sinh(\lambda y')|^2 - 2\Re\big[\tanh(\lambda)\sinh(\lambda^* y')\cosh(\lambda y')\big] + |\tanh(\lambda)|^2\,|\cosh(\lambda y')|^2\Big] \tag{2.4.43}$$

Now the horizontal momentum equation (2.4.32) can be written in terms of functions $F_1(y')$, $F_2(y')$ and $F_3(y')$:

$$X_{10,y'y'} = \hat{B}_{10}\Im\Big\{F_1(y') + F_2(y') + F_3(y')\Big\}$$

where the constant $\hat{B}_{10}$ was defined as

$$\hat{B}_{10} = \frac{\gamma^2 k_0}{2}\frac{|A|^2}{\sinh^2 q}\frac{Re}{b_0}\frac{d}{a} \tag{2.4.44}$$

In order to integrate the last equation let us compute the first integrals of the functions $F_1(y')$, $F_2(y')$ and $F_3(y')$. They are

$$\int F_1(y')dy' = \lambda\Big[\int y'\sinh(\lambda y')dy' - \tanh(\lambda)\int y'\cosh(\lambda y')dy'\Big] \tag{2.4.45}$$

$$\int F_2(y')dy' = \frac{\lambda^*}{\lambda}\left(\tanh(\lambda)\int \sinh(\lambda^* y')dy' - |\tanh(\lambda)|^2\int \cosh(\lambda^* y')dy'\right) \tag{2.4.46}$$

$$\int F_3(y')dy' = \frac{\lambda^*}{\lambda}\Big[\int |\sinh(\lambda y')|^2\,dy' - 2\Re\big[\tanh(\lambda)dy'\int \sinh(\lambda^* y')\cosh(\lambda y')dy'\big] + |\tanh(\lambda)|^2\int |\cosh(\lambda y')|^2\,dy'\Big] \tag{2.4.47}$$

The following relationships will be used to calculate the integrals of $F_1(y')$, $F_2(y')$ and

$F_3(y')$:

$$\begin{aligned}\int y' \sinh(\lambda y') dy' &= \frac{1}{\lambda}\left(y' \cosh(\lambda y') - \frac{\sinh(\lambda y')}{\lambda}\right) + const \\ \int y' \cosh(\lambda y') dy' &= \frac{1}{\lambda}\left(y' \sinh(\lambda y') - \frac{\cosh(\lambda y')}{\lambda}\right) + const\end{aligned}$$

In the following the integration constants will be omitted while computing the integrals, and only one global constant of integration will be added in the end. The products and sums of the used hyperbolic functions are related by the following equations

$$\begin{aligned}\sinh(a)\sinh(b) &= \frac{1}{2}\big[\cosh(a+b) - \cosh(a-b)\big] \\ \cosh(a)\cosh(b) &= \frac{1}{2}\big[\cosh(a+b) + \cosh(a-b)\big] \\ \sinh(a)\cosh(b) &= \frac{1}{2}\big[\sinh(a+b) + \sinh(a-b)\big]\end{aligned}$$

The primitives of the products of the hyperbolic functions apearing in the expression of $F_3(y')$ are

$$\begin{aligned}\int |\sinh(\lambda y')|^2 dy' &= \int \sinh(\lambda y')\sinh(\lambda^* y') dy' \\ &= \frac{1}{2}\int \big[\cosh(\lambda+\lambda^*)y' - \cosh(\lambda-\lambda^*)y'\big] dy' \\ &= \frac{1}{2}\left(\frac{\sinh(\lambda+\lambda^*)y'}{\lambda+\lambda^*} - \frac{\sinh(\lambda-\lambda^*)y'}{\lambda-\lambda^*}\right)\end{aligned} \tag{2.4.48}$$

$$\begin{aligned}\int \cosh(\lambda y')\cosh(\lambda^* y') dy' &= \frac{1}{2}\int \big[\cosh(\lambda+\lambda^*)y' + \cosh(\lambda-\lambda^*)y'\big] dy' \\ &= \frac{1}{2}\left(\frac{\sinh(\lambda+\lambda^*)y'}{\lambda+\lambda^*} + \frac{\sinh(\lambda-\lambda^*)y'}{\lambda-\lambda^*}\right)\end{aligned}$$

$$\begin{aligned}\int \sinh(\lambda^* y')\cosh(\lambda y')dy' &= \frac{1}{2}\int\left[\sinh(\lambda^*+\lambda)y' + \sinh(\lambda^*-\lambda)y'\right]dy' \\ &= \frac{1}{2}\left(\frac{\cosh(\lambda+\lambda^*)y'}{\lambda+\lambda*} - \frac{\cosh(\lambda-\lambda^*)y'}{\lambda-\lambda^*}\right)\end{aligned}$$

The primitives of the functions $F_1(y')$, $F_2(y')$ and $F_3(y')$ can now be evaluated:

$$\begin{aligned}\int F_1(y')dy' &= y'\cosh(\lambda y') - \frac{\sinh(\lambda y')}{\lambda} - \tanh(\lambda)\left[y'\sinh(\lambda y') - \frac{\cosh(\lambda y')}{\lambda}\right] \\ &= y'\left[\cosh(\lambda y') - \tanh(\lambda)\sinh(\lambda y')\right] + \frac{1}{\lambda}\left[\tanh(\lambda)\cosh(\lambda y') - \sinh(\lambda y')\right] \\ \int F_2(y')dy' &= \frac{\tanh(\lambda)}{\lambda}\cosh(\lambda^* y') - \frac{|\tanh(\lambda)|^2}{\lambda}\sinh(\lambda^* y') \\ \int F_3(y')dy' &= \frac{1}{2}\frac{\lambda^*}{\lambda}\left\{\left(\frac{\sinh(\lambda+\lambda^*)y'}{\lambda+\lambda^*} - \frac{\sinh(\lambda-\lambda^*)y'}{\lambda-\lambda^*}\right)\right. \\ &\quad + |\tanh(\lambda)|^2\left(\frac{\sinh(\lambda+\lambda^*)y'}{\lambda+\lambda^*} + \frac{\sinh(\lambda-\lambda^*)y'}{\lambda-\lambda^*}\right) \\ &\quad \left. -2\Re\left[\tanh(\lambda)\left(\frac{\cosh(\lambda+\lambda^*)y'}{\lambda+\lambda^*} - \frac{\cosh(\lambda-\lambda^*)y'}{\lambda-\lambda^*}\right)\right]\right\}\end{aligned}$$

Finally the once integrated horizontal momentum conservation equation becomes

$$\begin{aligned}X_{10,y'} = \hat{B}_{10}\Im\Big\{ & y'\left[\cosh(\lambda y') - \tanh(\lambda)\sinh(\lambda y')\right] \\ & + \frac{1}{\lambda}\left[\tanh(\lambda)\cosh(\lambda y') - \sinh(\lambda y')\right] \\ & + \frac{\tanh(\lambda)}{\lambda}\cosh(\lambda^* y') - \frac{|\tanh(\lambda)|^2}{\lambda}\sinh(\lambda^* y') \\ & + \frac{1}{2}\frac{\lambda^*}{\lambda}\left\{\left(\frac{\sinh(\lambda+\lambda^*)y'}{\lambda+\lambda^*} - \frac{\sinh(\lambda-\lambda^*)y'}{\lambda-\lambda^*}\right)\right. \\ & + |\tanh(\lambda)|^2\left(\frac{\sinh(\lambda+\lambda^*)y'}{\lambda+\lambda^*} + \frac{\sinh(\lambda-\lambda^*)y'}{\lambda-\lambda^*}\right) \\ & \left. - 2\Re\left[\tanh(\lambda)\left(\frac{\cosh(\lambda+\lambda^*)y'}{\lambda+\lambda^*} - \frac{\cosh(\lambda-\lambda^*)y'}{\lambda-\lambda^*}\right)\right]\right\}\Big\} + Z_0\end{aligned}$$

Integrating again we find the expression of the mean horizontal displacement X_{10} as

function of the variable y':

$$
\begin{aligned}
X_{10} &= \hat{B}_{10}\Im\Bigg\{\frac{1}{\lambda}\Big[y'\sinh(\lambda y') - \frac{\cosh(\lambda y')}{\lambda}\Big] - \frac{\tanh(\lambda)}{\lambda}\Big[y'\cosh(\lambda y') - \frac{\sinh(\lambda y')}{\lambda}\Big] \\
&\quad + \frac{1}{\lambda^2}\big[\tanh(\lambda)\sinh(\lambda y') - \cosh(\lambda y')\big] \\
&\quad + \frac{\tanh(\lambda)}{|\lambda|^2}\sinh(\lambda^* y') - \left|\frac{\tanh(\lambda)}{\lambda}\right|^2\cosh(\lambda^* y') \\
&\quad + \frac{1}{2}\frac{\lambda^*}{\lambda}\Bigg\{\left(\frac{\cosh(\lambda+\lambda^*)y'}{(\lambda+\lambda^*)^2} - \frac{\cosh(\lambda-\lambda^*)y'}{(\lambda-\lambda^*)^2}\right) \\
&\quad + |\tanh(\lambda)|^2\left(\frac{\cosh(\lambda+\lambda^*)y'}{(\lambda+\lambda^*)^2} + \frac{\cosh(\lambda-\lambda^*)y'}{(\lambda-\lambda^*)^2}\right) \\
&\quad - 2\Re\left[\tanh(\lambda)\left(\frac{\sinh(\lambda+\lambda^*)y'}{(\lambda+\lambda^*)^2} - \frac{\sinh(\lambda-\lambda^*)y'}{(\lambda-\lambda^*)^2}\right)\right]\Bigg\}\Bigg\} + Z_0 y' + Z_1 \\
&= \hat{B}_{10}\Im\Bigg\{\frac{y'}{\lambda}\big[\sinh(\lambda y') - \tanh(\lambda)\cosh(\lambda y')\big] - \frac{1}{\lambda^2}\big[\cosh(\lambda y') - \tanh(\lambda)\sinh(\lambda y')\big] \\
&\quad + \frac{1}{\lambda^2}\big[\tanh(\lambda)\sinh(\lambda y') - \cosh(\lambda y')\big] \\
&\quad + \frac{\tanh(\lambda)}{|\lambda|^2}\sinh(\lambda^* y') - \left|\frac{\tanh(\lambda)}{\lambda}\right|^2\cosh(\lambda^* y') \\
&\quad + \frac{1}{8}\frac{\lambda^*}{\lambda}\Bigg\{\left(\frac{\cosh(2\lambda^r y')}{(\lambda^r)^2} + \frac{\cos(2\lambda^i y')}{(\lambda^i)^2}\right) + |\tanh(\lambda)|^2\left(\frac{\cosh(2\lambda^r y')}{(\lambda^r)^2} - \frac{\cos(2\lambda^i y')}{(\lambda^i)^2}\right) \\
&\quad - 2\Re\left[\tanh(\lambda)\left(\frac{\sinh(2\lambda^r y')}{(\lambda^r)^2} + i\frac{\sin(2\lambda^i y')}{(\lambda^i)^2}\right)\right]\Bigg\}\Bigg\} + Z_0 y' + Z_1 \\
&= \hat{B}_{10}\Im\Bigg\{\frac{y'}{\lambda}\big[\sinh(\lambda y') - \tanh(\lambda)\cosh(\lambda y')\big] - \frac{2}{\lambda^2}\big[\cosh(\lambda y') - \tanh(\lambda)\sinh(\lambda y')\big] \\
&\quad + \frac{\tanh(\lambda)}{|\lambda|^2}\sinh(\lambda^* y') - \left|\frac{\tanh(\lambda)}{\lambda}\right|^2\cosh(\lambda^* y') \\
&\quad + \frac{1}{8}\frac{\lambda^*}{\lambda}\Bigg\{\left(\frac{\cosh(2\lambda^r y')}{(\lambda^r)^2} + \frac{\cos(2\lambda^i y')}{(\lambda^i)^2}\right) + |\tanh(\lambda)|^2\left(\frac{\cosh(2\lambda^r y')}{(\lambda^r)^2} - \frac{\cos(2\lambda^i y')}{(\lambda^i)^2}\right) \\
&\quad - 2\Re\left[\tanh(\lambda)\left(\frac{\sinh(2\lambda^r y')}{(\lambda^r)^2} + i\frac{\sin(2\lambda^i y')}{(\lambda^i)^2}\right)\right]\Bigg\}\Bigg\} + Z_0 y' + Z_1
\end{aligned}
$$

where Z_0 and Z_1 are the constants that will be determined using the boundary conditions. Let us now apply the boundary conditions.

The no slip boundary condition (2.4.40) gives

$$0 = X_{10}|_0 = \hat{B}_{10}\Im\Big\{ -\frac{2}{\lambda^2} - \Big|\frac{\tanh(\lambda)}{\lambda}\Big|^2 + \frac{1}{8}\frac{\lambda^*}{\lambda}\Big[\Big(\frac{1}{(\lambda^r)^2} + \frac{1}{(\lambda^i)^2}\Big) + |\tanh(\lambda)|^2\Big(\frac{1}{(\lambda^r)^2} - \frac{1}{(\lambda^i)^2}\Big)\Big]\Big\} + Z_1$$

This gives the expression of Z_1:

$$\begin{aligned} Z_1 &= \hat{B}_{10}\Im\Big\{\frac{2}{\lambda^2} - \frac{1}{8}\frac{\lambda^*}{\lambda}\Big[\Big(\frac{1}{(\lambda^r)^2} + \frac{1}{(\lambda^i)^2}\Big) + |\tanh(\lambda)|^2\Big(\frac{1}{(\lambda^r)^2} - \frac{1}{(\lambda^i)^2}\Big)\Big]\Big\} \\ &= \hat{B}_{10}\Im\Big\{\frac{2}{\lambda^2}\Big\}\Big\{1 - \frac{1}{8}|\lambda|^2\Big[\Big(\frac{1}{(\lambda^r)^2} + \frac{1}{(\lambda^i)^2}\Big) + |\tanh(\lambda)|^2\Big(\frac{1}{(\lambda^r)^2} - \frac{1}{(\lambda^i)^2}\Big)\Big]\Big\} \end{aligned}$$

The nonlinear term appearing in the boundary condition (2.4.39) is:

$$\begin{aligned} \zeta_{01}^*\,(u_{01,y'y'})|_{y'=1} &= \gamma^2 k_0 \frac{A^2}{4\sinh q}\Big(1 - \frac{\tanh\lambda^*}{\lambda^*}\Big)\lambda^2\big[-\cosh(\lambda y') + \tanh(\lambda)\sinh(\lambda y')\big]|_{y'=1} \\ &= \gamma^2 \frac{A^2}{4\sinh q} k_0 \Big(1 - \frac{\tanh\lambda^*}{\lambda_1^*}\Big)\lambda^2\Big[-\cosh(\lambda) + \frac{\sinh^2(\lambda)}{\cosh(\lambda)}\Big] \\ &= -\gamma^2 \frac{A^2}{4\sinh q} k_0 \Big(1 - \frac{\tanh\lambda^*}{\lambda^*}\Big)\frac{\lambda^2}{\cosh(\lambda)} \end{aligned}$$

The right-hand side of the boundary condition (2.4.39) can now be rewritten as

$$\begin{aligned} X_{10,y'}|_{y'=1} &= 2\frac{\gamma^2 k_0}{b_0}\frac{a}{d}\frac{A^2}{4\sinh q}\Re\Big[\mu\frac{\lambda^2}{\cosh(\lambda)}\Big(1 - \frac{\tanh\lambda^*}{\lambda^*}\Big)\Big] \\ &= 2Re\frac{\gamma^2 k_0}{b_0}\frac{A^2}{4\sinh q}\Re\Big[\frac{\mu}{|\mu|}\frac{e^{-(\theta+\frac{\pi}{2})}}{\cosh(\lambda)}\Big(1 - \frac{\tanh\lambda^*}{\lambda^*}\Big)\Big] \\ &= 2Re\frac{\gamma^2 k_0}{b_0}\frac{A^2}{4\sinh q}\Re\Big[\frac{-i}{\cosh(\lambda)}\Big(1 - \frac{\tanh\lambda^*}{\lambda^*}\Big)\Big] \\ &= 2Re\frac{\gamma^2 k_0}{b_0}\frac{A^2}{4\sinh q}\Im\Big[\frac{1}{\cosh(\lambda)}\Big(1 - \frac{\tanh\lambda^*}{\lambda^*}\Big)\Big] \\ &= \hat{B}_{10}\Im\Big[\frac{1}{\cosh(\lambda)}\Big(1 - \frac{\tanh\lambda^*}{\lambda^*}\Big)\Big] \end{aligned}$$

Where the fact was used that

$$\lambda^2 \equiv Re\frac{d}{a}\frac{1}{|\mu|}e^{-i(\theta+\frac{\pi}{2})}$$

The boundary condition (2.4.39) becomes

$$
\begin{aligned}
X_{10,y'}|_{y'=1} &= \hat{B}_{10}\Im\Big\{\big[\cosh(\lambda)-\tanh(\lambda)\sinh(\lambda)\big]+\frac{2}{\lambda}\big[\sinh(\lambda)-\tanh(\lambda)\cosh(\lambda)\big] \\
&\quad +\frac{\lambda}{\lambda^2}\big[\tanh(\lambda)\cosh(\lambda)-\sinh(\lambda)\big] \\
&\quad +\frac{\tanh(\lambda)}{\lambda}\cosh(\lambda^*)-\frac{|\tanh(\lambda)|^2}{\lambda}\sinh(\lambda^* y') \\
&\quad +\frac{2}{8}\frac{\lambda^*}{\lambda}\Big\{\left(\frac{\sinh(2\lambda^r)}{\lambda^r}-\frac{\sin(2\lambda^i)}{\lambda^i}\right)+|\tanh(\lambda)|^2\left(\frac{\sinh(2\lambda^r)}{\lambda^r}+\frac{\sin(2\lambda^i)}{\lambda^i}\right) \\
&\quad -2\Re\left[\tanh(\lambda)\left(\frac{\cosh(2\lambda^r)}{\lambda^r}+i\frac{\cos(2\lambda^i)}{\lambda^i}\right)\right]\Big\}\Big\}+Z_0 \\
&= \hat{B}_{10}\Im\Big\{\frac{1}{\cosh(\lambda)}+\frac{\tanh(\lambda)}{\lambda}\frac{1}{\cosh(\lambda^*)} \\
&\quad +\frac{1}{4}\frac{\lambda^*}{\lambda}\Big\{\left(\frac{\sinh(2\lambda^r)}{\lambda^r}-\frac{\sin(2\lambda^i)}{\lambda^i}\right)+|\tanh(\lambda)|^2\left(\frac{\sinh(2\lambda^r)}{\lambda^r}+\frac{\sin(2\lambda^i)}{\lambda^i}\right) \\
&\quad -2\Re\left[\tanh(\lambda)\left(\frac{\cosh(2\lambda^r)}{\lambda^r}+i\frac{\cos(2\lambda^i)}{\lambda^i}\right)\right]\Big\}\Big\}+Z_0 \\
&= \hat{B}_{10}\Im\left[\frac{1}{\cosh(\lambda)}\left(1-\frac{\tanh\lambda^*}{\lambda^*}\right)\right]
\end{aligned}
$$

The last equation determines the value of Z_0:

$$
\begin{aligned}
Z_0 &= \hat{B}_{10}\Im\Big\{\frac{1}{\cosh(\lambda)}\left(1-\frac{\tanh\lambda^*}{\lambda^*}\right)-\frac{1}{\cosh(\lambda)}-\frac{\tanh(\lambda)}{\lambda}\cosh(\lambda^*) \\
&\quad -\frac{1}{4}\frac{\lambda^*}{\lambda}\Big\{\left(\frac{\sinh(2\lambda^r)}{\lambda^r}-\frac{\sin(2\lambda^i)}{\lambda^i}\right)+|\tanh(\lambda)|^2\left(\frac{\sinh(2\lambda^r)}{\lambda^r}+\frac{\sin(2\lambda^i)}{\lambda^i}\right) \\
&\quad -2\Re\left[\tanh(\lambda)\left(\frac{\cosh(2\lambda^r)}{\lambda^r}+i\frac{\cos(2\lambda^i)}{\lambda^i}\right)\right]\Big\}\Big\} \\
&= \hat{B}_{10}\Im\Big\{-\frac{1}{4}\frac{\lambda^*}{\lambda}\Big\{\left(\frac{\sinh(2\lambda^r)}{\lambda^r}-\frac{\sin(2\lambda^i)}{\lambda^i}\right)+|\tanh(\lambda)|^2\left(\frac{\sinh(2\lambda^r)}{\lambda^r}+\frac{\sin(2\lambda^i)}{\lambda^i}\right) \\
&\quad -2\Re\left[\tanh(\lambda)\left(\frac{\cosh(2\lambda^r)}{\lambda^r}+i\frac{\cos(2\lambda^i)}{\lambda^i}\right)\right]\Big\}\Big\} \\
&= -\frac{\hat{B}_{10}}{4}\Im\left\{\frac{\lambda^*}{\lambda}\right\}\Big\{\left(\frac{\sinh(2\lambda^r)}{\lambda^r}-\frac{\sin(2\lambda^i)}{\lambda^i}\right)+|\tanh(\lambda)|^2\left(\frac{\sinh(2\lambda^r)}{\lambda^r}+\frac{\sin(2\lambda^i)}{\lambda^i}\right) \\
&\quad -2\Re\left[\tanh(\lambda)\left(\frac{\cosh(2\lambda^r)}{\lambda^r}+i\frac{\cos(2\lambda^i)}{\lambda^i}\right)\right]\Big\}
\end{aligned}
$$

Putting all the information found together we can write the final expression for the

mean displacement of the mud layer X_{10}:

$$
\begin{aligned}
X_{10} \;=\; & \hat{B}_{10}\Im\Big\{\frac{y'}{\lambda}\big[\sinh(\lambda y')-\tanh(\lambda)\cosh(\lambda y')\big] \\
& +\frac{2}{\lambda^2}\big[\tanh(\lambda)\sinh(\lambda y')-\cosh(\lambda y')\big] \\
& +\frac{\tanh(\lambda)}{|\lambda|^2}\sinh(\lambda^* y')-\left|\frac{\tanh(\lambda)}{\lambda}\right|^2\cosh(\lambda^* y') \\
& +\frac{1}{8}\frac{\lambda^*}{\lambda}\Big\{\left(\frac{\cosh(2\lambda^r y')}{(\lambda^r)^2}+\frac{\cos(2\lambda^i y')}{(\lambda^i)^2}\right)+|\tanh(\lambda)|^2\left(\frac{\cosh(2\lambda^r y')}{(\lambda^r)^2}-\frac{\cos(2\lambda^i y')}{(\lambda^i)^2}\right) \\
& -2\Re\left[\tanh(\lambda)\left(\frac{\sinh(2\lambda^r y')}{(\lambda^r)^2}+i\frac{\sin(2\lambda^i y')}{(\lambda^i)^2}\right)\right]\Big\}\Big\}+Z_0 y'+Z_1
\end{aligned}
\tag{2.4.49}
$$

With the constants Z_0 and Z_1 given by:

$$
\begin{aligned}
Z_0 \;=\; & -\frac{\hat{B}_{10}}{4}\Im\left\{\frac{\lambda^*}{\lambda}\right\}\Big\{\left(\frac{\sinh(2\lambda^r)}{\lambda^r}-\frac{\sin(2\lambda^i)}{\lambda^i}\right)+|\tanh(\lambda)|^2\left(\frac{\sinh(2\lambda^r)}{\lambda^r}+\frac{\sin(2\lambda^i)}{\lambda^i}\right) \\
& -2\Re\left[\tanh(\lambda)\left(\frac{\cosh(2\lambda^r)}{\lambda^r}+i\frac{\cos(2\lambda^i)}{\lambda^i}\right)\right]\Big\}
\end{aligned}
\tag{2.4.50}
$$

$$
Z_1 \;=\; \hat{B}_{10}\Im\left\{\frac{1}{\lambda^2}\right\}\left\{2-\frac{1}{8}|\lambda|^2\left[\left(\frac{1}{(\lambda^r)^2}+\frac{1}{(\lambda^i)^2}\right)+|\tanh(\lambda)|^2\left(\frac{1}{(\lambda^r)^2}-\frac{1}{(\lambda^i)^2}\right)\right]\right\}
\tag{2.4.51}
$$

The equations (2.4.49) to (2.4.51) give the explicit expression of the mean horizontal displacement X_{10} inside the mud layer. The profiles of the mean displacement were studied by Zhang and Ng [6], who considered a similar problem of a thin viscoelastic mud layer under a non-decaying progressive wave modeled by a harmonic pressure applied uniformly on the surface of the mud layer. Our approach is different in two ways. First, Zhang and Ng modeled mud as a Voigt body with only two coefficients, but according to the experimental data available to us these coefficients strongly depend on the frequency of the forcing. In our approach for each mud sample we found the dimensional coefficients $\bar{a}_n$ and $\bar{b}_n$ that are frequency independent and represent the mud properties in the entire range of experimentally available frequencies ($0.1Hz < \omega < 20Hz$). The second difference is the wave decay for which Zhang and

Ng did not account in their article. In fact the wave damping is considerable even at the leading order and t he mud movement will change when the waves are damped. In particular for large values of x_1 after the waves are damped there should not be any mud movement. This is taken into account by our approach as the mean horizontal displacement inside the mud layer is proportional to the square of the decaying wave amplitude:

$$X_{10} \propto |A(x_1, t_1)|^2 \propto e^{-2k_1^i x_1} \tag{2.4.52}$$

Zhang and Ng did not provide an explicit expression of the mean displacement and solved the averaged governing equation numerically. We compared our computed mean displacement X_{10} to their numerical results plotted in the article [6] for the same values of the dimensionless parameters introduced by the authors: the elasticity parameter $\widehat{\lambda}_{Ng} = \sqrt{\frac{\rho^{(m)}\omega^2 d^2}{b_0}}$ and the viscosity parameter $\widehat{\delta}_{Ng} = \sqrt{\frac{2\mu^r}{\rho^{(m)}\omega d^2}}$. The results are plotted in figure (2-2) for three values of $\widehat{\delta}_{Ng} = 0.1,\ 0.3,\ 0.5$ and three values of $\widehat{\lambda}_{Ng} = 1,\ 3,\ 10$. The difference in the values of the mean displacement amplitude is due to the difference in the normalization. Otherwise the profiles have the same properties: the reversal at large values of $\widehat{\lambda}_{Ng}$ and for $\widehat{\delta}_{Ng} = 0.1$, the growing values of the amplitude with the elastic parameter λ_{Ng} and even the shapes are the same. Still an important difference is present between the results of Zhang and Ng and figure (2-2). The slope at the edge of the mud layer is finite in the present work but is equal to zero in the work of Zhang and Ng, who considered that the shear stress at the top of the mud layer is zero at both leading and second orders. The shear stress is indeed equal to zero at the leading order but at the second order the interface movement should not be neglected and the shear stress is no more equal to zero. This condition is expressed mathematically by the equation (2.3.42).

It was also checked that in case of a purely elastic mud (all the coefficients $a_{n\geq 1}$ and $b_{n\geq 1}$ equal to zero and b_0 finite) the mean horizontal mud displacement is identically zero. In fact, as it was pointed out by Zhang and Ng, elasticity enables the mud to recover from any applied deformation, while the viscosity makes such a restoring capacity impossible. Therefore it is natural to have no mean deformation of the mud

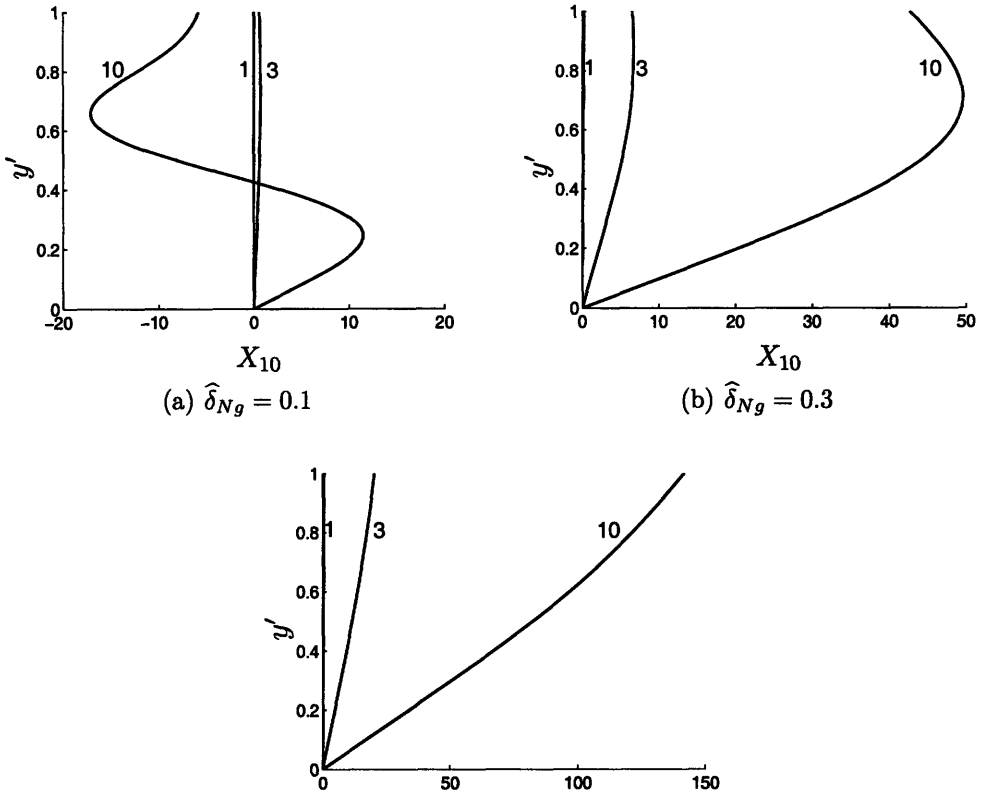

(a) $\widehat{\delta}_{Ng} = 0.1$ (b) $\widehat{\delta}_{Ng} = 0.3$

(c) $\widehat{\delta}_{Ng} = 0.5$

Figure 2-2: Profiles of the mean horizontal displacement X_{10} for three values of $\widehat{\lambda}_{Ng} = 1,\ 3,\ 10$

layer for the purely elastic case. The study of the properties of the mean displacement will be done in section (2.5) for different mud samples.

2.4.5 Long wave equation

Note that till this point the long wave potential $\Phi_{00} = \Phi_{00}(x_1, t_1, t_2, \dots)$ is undetermined. The equation governing it is given by the solvability condition (2.3.141) for $n = 2$. That is:

$$\int_{-H}^{0} F_{20} dy = G_{20} - L_{20} \tag{2.4.53}$$

with the constants G_{20} and L_{20} given by the equations (2.3.116) and (2.3.123):

$$\begin{aligned}
F_{20} &= -\Phi_{00,x_1x_1} \\
G_{20} &= -\Big\{ \Re\left[A^*\left(\Phi_{11,yy}-\Phi_{11,y}\right)|_0\right] + \Re\left[2\eta_{11}^*\left(\Phi_{01,yy}-\Phi_{01,y}\right)|_0\right] + \Re\left[2iA\left(\Phi_{01,yt_1}^*\right)|_0\right] \\
&\qquad + \Phi_{00,t_1t_1} + 2k_0^2\left(\left[|\Phi_{01}|^2\right]_{t_1}\right)\Big|_0 + 2\left(\left[|\Phi_{01,y}|^2\right]_{t_1}\right)\Big|_0 \Big\} \\
L_{20} &= \zeta_{00,t_1} = 0
\end{aligned}$$

Both constants G_{20} and L_{20} will now be computed in terms of the previously found expressions for the first two orders solutions.

To compute G_{20} we first evaluate each term one by one. The first term of the right-hand side becomes:

$$\begin{aligned}
\left(\Phi_{11,y}\right)|_0 &= -\left(\frac{\sinh q}{2\cosh q}+\frac{q}{2}\right)A_{x_1} + ik_1AC_g\cosh^2 q \\
\left(\Phi_{11,yy}\right)|_0 &= -\left(k_0+\frac{qk_0\sinh q}{2\cosh q}\right)A_{x_1} + ik_1AC_g\cosh^2 q \\
\left(\Phi_{11,yy}-\Phi_{11,y}\right)|_0 &= \left(\frac{1}{2k_0}-k_0\right)A_{x_1} \\
\Re\left\{A^*\left(\Phi_{11,yy}-\Phi_{11,y}\right)|_0\right\} &= \left(\frac{1}{2k_0}-k_0\right)\frac{(A^*A)_{x_1}}{2}
\end{aligned}$$

The second term is:

$$\begin{aligned}
\left(\Phi_{01,y}\right)|_0 &= -\frac{i}{2}A \\
\left(\Phi_{01,yy}\right)|_0 &= -\frac{i}{2}Ak_0^2 \\
\left(\Phi_{01,yy}-\Phi_{01,y}\right)|_0 &= -\frac{i}{2}A(k_0^2-1) \\
\Re\left\{2\eta_{11}^*\left(\Phi_{01,yy}-\Phi_{01,y}\right)|_0\right\} &= 2(k_0^2-1)\Re\left\{\left(-\frac{i}{2}A\right)\left(-\frac{i}{2}A_{t_1}^*-k_1^*C_gA^*\sinh^2 q+i\frac{q\sinh q}{2k_0\cosh q}A_{x_1}^*\right)\right\} \\
&= \frac{1}{2}(k_0^2-1)\Re\left\{-A^*A_{t_1}+2ik_1^*C_gA^*A\sinh^2 q+\frac{q\sinh q}{k_0\cosh q}A^*A_{x_1}\right\} \\
&= \frac{1}{4\sinh^2 q}\left[\frac{q\sinh q}{k_0\cosh q}(A^*A)_{x_1}-(A^*A)_{t_1}+4k_1^iC_g\sinh^2 q(A^*A)\right] \\
&= \frac{1}{4\sinh^2 q}\left[\frac{q\sinh q}{k_0\cosh q}(A^*A)_{x_1}-(A^*A)_{t_1}\right]+k_1^iC_g(A^*A)
\end{aligned}$$

The third term is:

$$\Re\left[2iA\left(\Phi^*_{01,yt_1}\right)\big|_0\right] = \Re\left[2iA\left(\frac{i}{2}A^*_{t_1}\right)\right] = -\frac{(A^*A)_{t_1}}{2}$$

The last two terms give:

$$\begin{aligned} 2k_0^2\left(\left[|\Phi_{01}|^2\right]_{t_1}\right)\Big|_0 + 2\left(\left[|\Phi_{01,y}|^2\right]_{t_1}\right)\Big|_0 &= 2k_0^2\left(\frac{(A^*A)_{t_1}}{4}\right) + 2\left(\frac{(A^*A)_{t_1}}{4}\right) \\ &= \frac{1}{2}(k_0^2+1)(A^*A)_{t_1} \end{aligned}$$

So that the constant G_{20} becomes:

$$\begin{aligned} G_{20} &= -\left(\frac{1}{2k_0} - k_0\right)\frac{(A^*A)_{x_1}}{2} - \frac{1}{4\sinh^2 q}\left[\frac{q\sinh q}{k_0\cosh q}(A^*A)_{x_1} - (A^*A)_{t_1}\right] - k_1^i C_g(A^*A) - \Phi_{00,t_1t_1} \\ &\quad + \frac{(A^*A)_{t_1}}{2} - \frac{1}{2}(k_0^2+1)(A^*A)_{t_1} - \Phi_{00,t_1t_1} \\ &= -\frac{1}{2}\left[\frac{1}{2k_0}\left(1+\frac{2q}{\sinh 2q}\right) - k_0\right](A^*A)_{x_1} + \frac{1}{2}\left(\frac{1}{2\sinh^2 q} - k_0^2\right)(A^*A)_{t_1} - \Phi_{00,t_1t_1} - k_1^i C_g(A^*A) \\ &= -\frac{1}{2}\left[C_g - k_0\right](A^*A)_{x_1} + \frac{1}{2}\left(-\frac{1}{2\sinh^2 q} + \frac{1-\cosh^2 q}{\sinh^2 q}\right)(A^*A)_{t_1} - \Phi_{00,t_1t_1} - k_1^i C_g(A^*A) \\ &= -\frac{1}{2}\left[(A^*A)_{t_1} + C_g(A^*A)_{x_1}\right] + \frac{k_0}{2}(A^*A)_{x_1} - \frac{1}{4\sinh^2 q}(A^*A)_{t_1} - \Phi_{00,t_1t_1} - k_1^i C_g(A^*A) \\ &= \frac{k_0}{2}(A^*A)_{x_1} - \frac{1}{4\sinh^2 q}(A^*A)_{t_1} - \Phi_{00,t_1t_1} \end{aligned}$$

Where the use was made of the equation governing the slow evolution of the wave amplitude found previously from the solvability condition for Φ_{11}:

$$A_{t_1} + C_g A_{x_1} = ik_1 C_g A$$

which implies

$$(A^*A)_{t_1} + C_g(A^*A)_{x_1} = -2k_1^i C_g(A^*A)$$

Finally the long wave equation can be fully written:

$$\Phi_{00,t_1t_1} - H\Phi_{00,x_1x_1} = \frac{k_0}{2}(A^*A)_{x_1} - \frac{1}{4\sinh^2 q}(A^*A)_{t_1} \qquad (2.4.54)$$

This is exactly the same equation as the one governing the long waves in the absence of mud layer (see Mei, 1989 [9]). We conclude that the mud layer does not affect the generation of the long waves.

2.5 Physical deductions

This section is dedicated to the analysis of the physical properties and experimental values of previously obtained solutions.

2.5.1 Interface displacement

We now study how the interface displacement is affected by the free surface waves. For that we will study the properties of the ratio R_{amp} of the interface displacement to the surface displacement, both in dimentional terms:

$$R_{amp} \equiv \frac{\bar{\zeta}_{01}}{\bar{\eta}_{01}} = \frac{\epsilon a \zeta_{01}}{aA} = \frac{\epsilon \zeta_{01}}{A} \tag{2.5.1}$$

The interface displacement ζ_{01} was found previously (eq. 2.4.17) and its product with $\epsilon = \frac{a\omega^2}{g}$ is:

$$\epsilon\zeta_{01} = \gamma \frac{A}{2} \frac{q}{\sinh q} \frac{d}{h} \left(1 - \frac{\tanh \lambda}{\lambda}\right)$$

The ratio of interest is finally:

$$R_{amp} \equiv \gamma \frac{d}{h} \frac{q}{\sinh q} \left(1 - \frac{\tanh \lambda}{\lambda}\right) \tag{2.5.2}$$

where $q = k_0 H = \bar{k}_0 h$.

The ratio R_{amp} goes to zero in deep water when the waves are short ($\bar{k}_0 h >> 1$) and do not reach the bottom.

Also the ratio R_{amp} decreases when the ratio $\frac{d}{h}$ of mud layer depth to the water layer depth decreases. Physically this means that the shallower the mud layer is compared to the water depth and the wavelegth the less it will be able to move and dissipate wave energy.

To get an idea of how the factor $1 - \frac{\tanh\lambda}{\lambda}$ influences the ratio R_{amp} let us express it in terms of the parameter θ and the ratio $d_s = \frac{d}{\delta_s}$ explicitly. The parameter θ characterizes elasticity. An entirely viscous material will have $\theta = 0$ and a material which is entirely elastic will have $\theta = \frac{\pi}{2}$. A material which combines both the viscous and elastic properties, as in case of the mud, will be characterized by values of θ between 0 and $\frac{\pi}{2}$. The ratio $\frac{d}{\delta_s}$ determines how much of the mud layer depth will be affected by the motion of the waves. In particular if the ratio $d_s = \frac{d}{\delta_s} \approx 1$ one can expect that the entire mud layer will be in motion. To determine how the two parameters θ and $d_s = \frac{d}{\delta_s}$ affect the amplitudes ratio R_{amp} its expression will now be rewritten explicitly in terms of the two parameters. Note that up to now the effects of elastic properties of mud were implicitly hidden into the parameter $\lambda = d_s\sqrt{2}e^{-i\left(\frac{\theta}{2}+\frac{\pi}{4}\right)}$. To simplify the notations let us introduce two real parameters α and β

$$\alpha \equiv \sqrt{2}\sin\left(\frac{\theta}{2}+\frac{\pi}{4}\right) \tag{2.5.3}$$

$$\beta \equiv \sqrt{2}\cos\left(\frac{\theta}{2}+\frac{\pi}{4}\right) \tag{2.5.4}$$

Note that both parameters are known as long as the value of θ, characterizing the elasticity of the mud, is given. Also note that the values of the parameters α and β are not independent, but linked by the relationship $\alpha^2 + \beta^2 = 2$. The parameter λ can be rewritten in terms of α and β

$$\lambda = (\beta - i\alpha)d_s \tag{2.5.5}$$

Now let us evaluate $\tanh(\lambda)$ in terms of α, β and d_s.

$$\begin{aligned}
\tanh(\lambda) &= \frac{e^{\lambda}-e^{-\lambda}}{e^{\lambda}+e^{-\lambda}} = \frac{e^{\beta d_s}e^{-i\alpha d_s}-e^{-\beta d_s}e^{-i\alpha d_s}}{e^{\beta d_s}e^{-i\alpha d_s}+e^{-\beta d_s}e^{-i\alpha d_s}} \\
&= \frac{e^{\beta d_s}\big(\cos(\alpha d_s)-i\sin(\alpha d_s)\big)-e^{-\beta d_s}\big(\cos(\alpha d_s)+i\sin(\alpha d_s)\big)}{e^{\beta d_s}\big(\cos(\alpha d_s)-i\sin(\alpha d_s)\big)+e^{-\beta d_s}\big(\cos(\alpha d_s)+i\sin(\alpha d_s)\big)} \\
&= \frac{\cos(\alpha d_s)\sinh(\beta d_s)-i\sin(\alpha d_s)\cosh(\beta d_s)}{\cos(\alpha d_s)\cosh(\beta d_s)-i\sin(\alpha d_s)\sinh(\beta d_s)} \\
&= \frac{[\cos(\alpha d_s)\sinh(\beta d_s)-i\sin(\alpha d_s)\cosh(\beta d_s)]\,[\cos(\alpha d_s)\cosh(\beta d_s)+i\sin(\alpha d_s)\sinh(\beta d_s)]}{\cos^2(\alpha d_s)\cosh^2(\beta d_s)+\sin^2(\alpha d_s)\sinh^2(\beta d_s)} \\
&= \frac{\sinh(\beta d_s)\cosh(\beta d_s)-i\sin(\alpha d_s)\cos(\alpha d_s)}{\cos^2(\alpha d_s)\cosh^2(\beta d_s)+\sin^2(\alpha d_s)\sinh^2(\beta d_s)} \qquad (2.5.6)
\end{aligned}$$

The ratio $\frac{\tanh(\lambda)}{\lambda}$ can be computed

$$\frac{\tanh(\lambda)}{\lambda} = \frac{1}{d_s}\frac{\beta+i\alpha}{\alpha^2+\beta^2}\tanh(\lambda) = \frac{\beta+i\alpha}{2d_s}\tanh(\lambda) \qquad (2.5.7)$$

The real and imaginary parts of $1-\frac{\tanh(\lambda)}{\lambda}$ are

$$\begin{aligned}
\Re\left(1-\frac{\tanh\lambda}{\lambda}\right) &= 1-\frac{1}{2d_s}\big[-\alpha\Im\big(\tanh\lambda\big)+\beta\Re\big(\tanh\lambda\big)\big] \\
&= 1-\frac{1}{2d_s}\left(\frac{\alpha\sin(\alpha d_s)\cos(\alpha d_s)+\beta\sinh(\beta d_s)\cosh(\beta d_s)}{\cos^2(\alpha d_s)\cosh^2(\beta d_s)+\sin^2(\alpha d_s)\sinh^2(\beta d_s)}\right) \qquad (2.5.8)
\end{aligned}$$

$$\begin{aligned}
\Im\left(1-\frac{\tanh\lambda}{\lambda}\right) &= -\frac{1}{2d_s}\big[\alpha\Re\big(\tanh\lambda\big)+\beta\Im\big(\tanh\lambda\big)\big] \\
&= -\frac{1}{2d_s}\left(\frac{\alpha\sinh(\beta d_s)\cosh(\beta d_s)-\beta\sin(\alpha d_s)\cos(\alpha d_s)}{\cos^2(\alpha d_s)\cosh^2(\beta d_s)+\sin^2(\alpha d_s)\sinh^2(\beta d_s)}\right) \qquad (2.5.9)
\end{aligned}$$

To simplify the labeling on future figures let us introduce two new functions

$$f_1(k_0H) = \frac{k_0H}{\sinh(k_0H)} \qquad (2.5.10)$$

$$g(\theta,d_s) = 1-\frac{\tanh\lambda}{\lambda} \qquad (2.5.11)$$

The parameter R_{amp} given by the equation (2.5.2) is then rewritten as

$$R_{amp} = \gamma \frac{d}{h} f_1(k_0 H) g(\theta, d_s) \tag{2.5.12}$$

In the limit of a thin Stokes' boundary layer $d_s \to \infty$ we have $g(\theta, d_s) \to 1$ and

$$R_{amp} \quad \to \quad \gamma \frac{d}{h} \frac{k_0 H}{\sinh(k_0 H)}$$

and if we consider only long waves in shallow water ($k_0 H << 1$) then the approximate expression of the amplitude ratio becomes:

$$R_{amp} \to \gamma \frac{d}{h}$$

On the other hand when mud layer is shallow compared to its Stokes boundary layer thickness we have $d_s \to 0$ and

$$\begin{aligned} \Re\left(1 - \frac{\tanh(\lambda)}{\lambda}\right) &\to 1 - \frac{1}{2d_s}\left(\alpha^2 d_s + \beta^2 d_s\right) = 0 \\ \Im\left(1 - \frac{\tanh(\lambda)}{\lambda}\right) &\to -\frac{1}{2d_s}\left(\alpha\beta d_s - \beta\alpha d_s\right) = 0 \\ g(\theta, d_s) &\to 0 \end{aligned}$$

and independently of the fact if waves are short or long the interface displacement is negligible compared to the one of the free surface:

$$R_{amp} \to 0$$

In the general case we need to consider the full formula (2.5.12) for the expression of R_{amp}. The function $f_1(\bar{k}_0 h)$ decreases exponentially for large water depth, as it can be seen in figure (2-3). From the equation (2.5.6) the denominator of the function $g(\theta, d_s)$ is

$$\cos^2(\alpha d_s)\cosh^2(\beta d_s) + \sin^2(\alpha d_s)\sinh^2(\beta d_s)$$

It may become zero, causing a resonant behavior of the amplitude of the interface displacement ζ_{01}. Let us study in which cases that can happen.

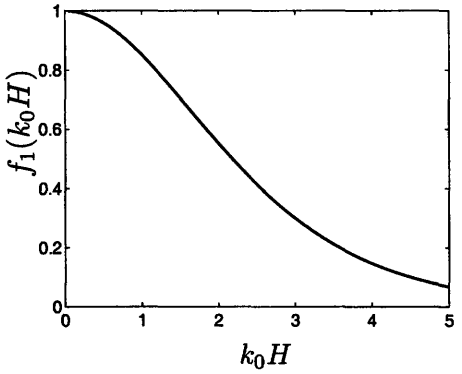

Figure 2-3: Behavior of the function $f_1(q) = f_1(k_0H) = f_1(\bar{k}_0h)$

In order for the denominator of the function $g(\theta, d_s)$ to be equal to zero two conditions should be satisfied simultaneously

$$\begin{aligned} \cos(\alpha d_s)\cosh(\beta d_s) &= 0 \\ \sin(\alpha d_s)\sinh(\beta d_s) &= 0 \end{aligned}$$

As the hyperbolic cosine is always different from zero, and as sine is different from zero when cosine is equal to zero the previous condition becomes:

$$\begin{aligned} \cos(\alpha d_s) &= 0 \\ \sinh(\beta d_s) &= 0 \end{aligned}$$

or

$$\begin{aligned} \alpha d_s &= \left(\frac{1}{2} + m\right)\pi \\ \beta d_s &= 0 \end{aligned}$$

Note that $d_s = 0$ does not satisfy both conditions and therefore does not cancel the

denominator. Using the identity $\alpha^2 + \beta^2 = 2$ the condition of resonance become

$$\begin{aligned} \beta &= 0 \\ d_s &= \left(\frac{1}{2} + m\right)\frac{\pi}{\sqrt{2}} \end{aligned}$$

By definition $\beta \equiv \sqrt{2}\cos\left(\frac{\theta}{2} + \frac{\pi}{4}\right)$ and the condition for resonance in terms of θ and d_s is

$$\theta = \frac{\pi}{2} \tag{2.5.13}$$

$$d_s = \left(\frac{1}{2} + m\right)\frac{\pi}{\sqrt{2}} \tag{2.5.14}$$

with m being an integer. Therefore for the resonance to take place the material

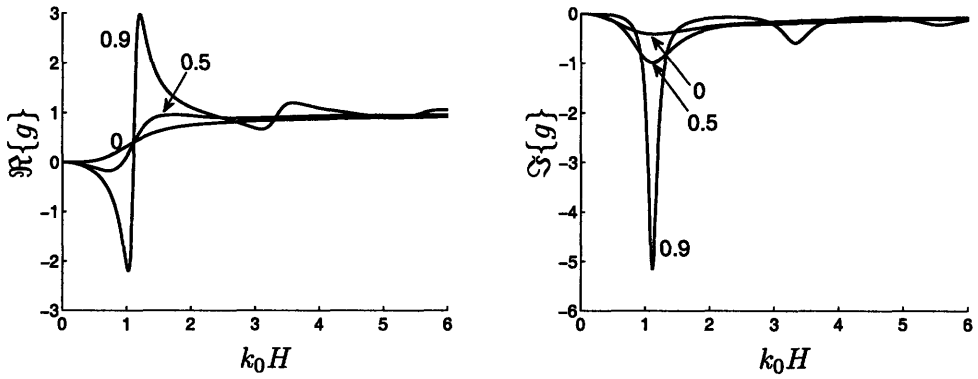

(a) Real part of $g(d_s, \theta)$ (b) Imaginary part of $g(d_s, \theta)$

Figure 2-4: Real and imaginary parts of $g(d_s, \theta)$

should be entirely elastic ($\theta = \frac{\pi}{2}$) and have a particular ratio of the mud layer depth to its Stokes' boundary layer thickness given by (2.5.14). In particular it is clear that no resonance can be observed for an entirely viscous fluid.

From the experimental results available it can be seen that neither of the mud samples has an entirely elastic behavior. However as the material exhibits behavior close to elastic the resonance peaks should become visible. To demonstrate this the dependence of the real and imaginary parts of $g(\theta, d_s)$ on d_s was plotted in figure (2-4) and the dependence of the modulus and phase of $g(\theta, d_s)$ on d_s was plotted in fig-

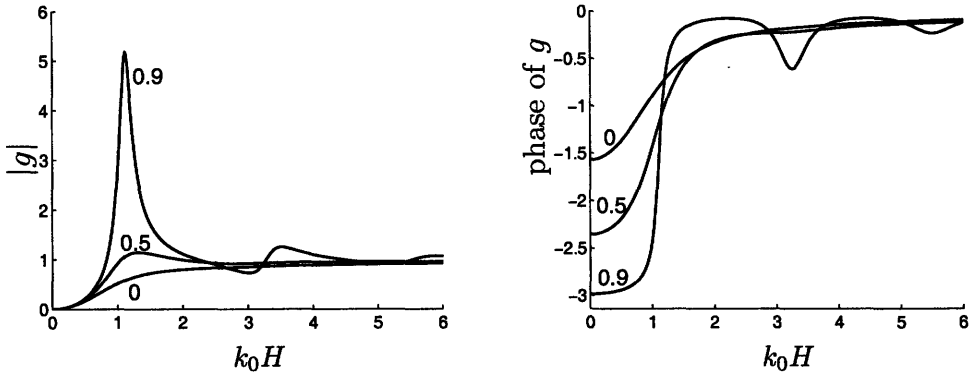

(a) Modulus of $g(d_s, \theta)$ (b) Phase of $g(d_s, \theta)$

Figure 2-5: Modulus and phase of $g(d_s, \theta)$

ure (2-5). In both figures three values of the elasticity parameter θ were considered: $(0, 0.5, 0.9) \times \frac{\pi}{2}$, representing respectively purely viscous, viscoelastic and almost entirely elastic materials. One can see that there is no resonant peak for a purely viscous fluid ($\theta = 0$ case studied by Ng [7]), however when the material becomes more elastic the resonant peak can be seen clearly. At $\theta = 0.5 \times \frac{\pi}{2}$ the resonant peak exists but is not as important as the one corresponding to $\theta = 0.9 \times \frac{\pi}{2}$. The mud samples provided by Huhe & Huang posses average values of θ of approximately 0.3 for all mud samples and thus one should expect to see a small tendency to resonate. For the mud samples provided by Jiang & Mehta the elastic behavior is much more pronounced with the experimental values of θ close to $\frac{\pi}{2}$. Therefore one should expect to observe resonant behavior for values of d_s satisfying the condition of the resonance (2.5.14). The first values of d_s corresponding to the resonant behavior are 1.11 and 3.33 which can clearly be seen in figure (2-5). The expression of both real and imaginary pars of $g(\theta, d_s)$ have a factor $\frac{1}{d_s}$ appearing, the maximum values of the peaks are reduced hyperbolically when d_s increases.

It is interesting to note that the real part of $g(\theta, d_s)$ takes the same value of approximately 0.4 independently of θ at the first resonance (when $d_s = \frac{1}{2}\frac{\pi}{\sqrt{2}}$). As a consequence when the material is highly elastic the imaginary part of $g(\theta, d_s)$ is much larger than the real part at the first resonance, and the phase of $g(\theta, d_s)$ is very close to $\frac{\pi}{2}$ when $d_s = \frac{1}{2}\frac{\pi}{\sqrt{2}}$.

The modulus and phase of the ratio R_{amp} of the interface displacement to the free surface displacement given by the equation (2.5.12) is plotted in figure (2-6) for one sample from Jiang & Mehta's experiments (MB, $\phi = 0.11$). One can clearly see a res-

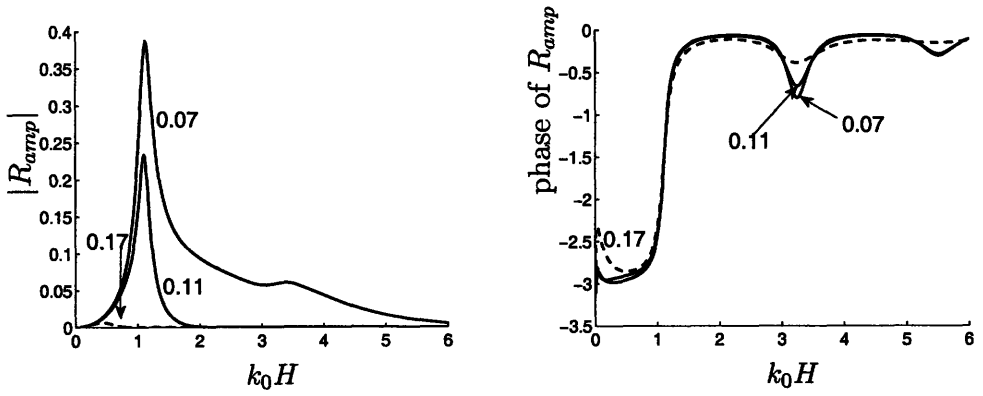

(a) Modulus of R_{amp} (b) Phase of R_{amp}

Figure 2-6: Modulus and phase of R_{amp} for samples by Jiang & Mehta, MB $\phi =$ 0.07, 0.11 0.17

onant behavior for the values of $d_s = 1.11$ as predicted by the equation (2.5.14) with $m = 0$. The resonant peaks at higher values of $d_s = \left(\frac{1}{2} + m\right)\frac{\pi}{\sqrt{2}}$ for $(m = 1, 2, \ldots)$ are not as pronounced. Let us explain why it happens.

In fact it can be seen that the terms creating the resonance of the function $g(d_s, \theta)$ are inversely proportional to d_s. Therefore the amplitude at the resonance decreases when d_s increases. In other words we expect to have a larger amplitude at the first resonant peak of $g(d_s, \theta)$ than at other resonant peaks. The first resonant peak of $g(d_s, \theta)$ is given by the equation (2.5.14) and corresponds to $m = 0$:

$$d_s = \frac{d}{\delta_S} = \frac{\pi}{2\sqrt{2}} \approx 1.11 \tag{2.5.15}$$

The phase of the ratio R_{amp} is plotted in the right part of the figure (2-6). When the mud layer is shallow compared to its Stokes' boundary layer thickness, the interface displacement is almost in antiphase with the free surface (phase shift is approximately equal to $-\pi$). On the other had when d_s is large the interface and the free surface

are almost in phase (phase shift is approximately equal to 0). The small peaks at $d_s = 3\frac{\pi}{2\sqrt{2}} \approx 3.33$, $d_s = 5\frac{\pi}{2\sqrt{2}} \approx 5.55$ etc. correspond to the resonant peaks and can be seen because the elastic parameter θ is very close to $\frac{\pi}{2}$.

Another sample is presented in figure (2-7) where the modulus and the phase of the ratio R_{amp} were plotted for the case of the data set A with solid volume fraction $\phi = 0.08$. One can see that the shorter are the water waves the more in phase are the interface and the free surface. As the elasticity parameter for this sample is only about $0.5 \times \frac{\pi}{2}$ the resonance is much less pronounced compared to the case of Jiang & Mehta. The peak value of R_{amp} is 7 times smaller.

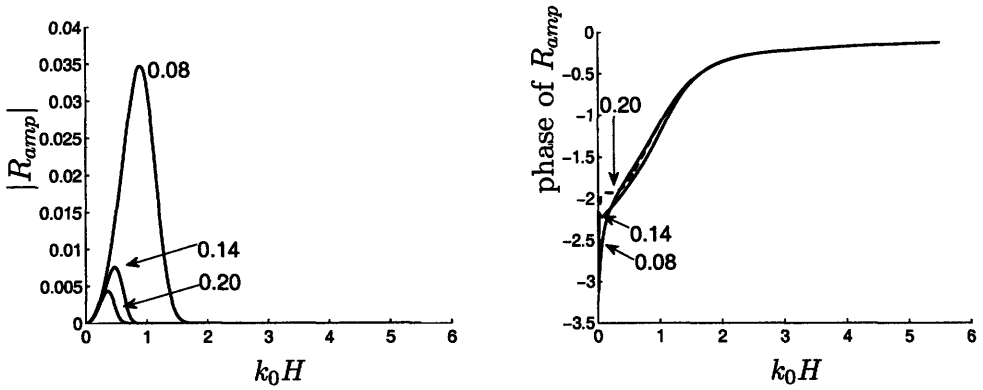

(a) Modulus of R_{amp}

(b) Phase of $g(d_s, \theta)$

Figure 2-7: Modulus and phase of R_{amp} for samples by Huhe & Huang, data set A $\phi = 0.08,\ 0.14\ 0.20$

2.5.2 Analytical study of damping rate and wave number shift

Definitions

The second order correction k_1 to the leading order wavenumber was obtained previously (2.4.23). This expression is complex, and its real part represent the wavenumber shift and the imaginary one - the damping. We will now study both the damping as well as the wavenumber shift. Of particular interest to us is the following dimension-

less ratio:

$$\frac{\epsilon k_1}{k_0} = -\gamma \frac{d}{h}\left(\frac{2q}{2q+\sinh(2q)}\right)\left(1-\frac{\tanh\lambda}{\lambda}\right) \tag{2.5.16}$$

The damping and the induced wavenumber shift can be computed respectively from the real and the imaginary parts of the last expression (2.5.16)

$$D_0 = \Im\left(\frac{\epsilon k_1}{k_0}\right) = -\gamma \frac{d}{h} f_2(q)\Im\{g(\theta, d_s)\} \tag{2.5.17}$$

$$\Delta k = \Re\left(\frac{\epsilon k_1}{k_0}\right) = -\gamma \frac{d}{h} f_2(q)\Re\{g(\theta, d_s)\} \tag{2.5.18}$$

where the function $f_2(q)$ was defined as:

$$f_2(q) = \frac{2q}{2q+\sinh(2q)} \tag{2.5.19}$$

Note that as the imaginary part of $g(\theta, d_s)$ is always negative, hence the damping rate D_0 is always positive.

The behavior of the function $f_2(q) = f_2(\bar{k}_0 h) = f_2(k_0 H)$ is relatively simple and is plotted in figure (2-8). The function $f(\bar{k}_0 h)$, and therefore the damping, decreases exponentially with the increasing depth. As higher frequencies mean shorter waves and larger wavenumbers, we conclude that the high frequency waves are not damped. Physically this happens because the waves do not reach the bottom.

Limiting cases for different mud layer depths

As the mud layer becomes shallower $\frac{d}{h} << 1$ the complex wave number correction vanishes:

$$\frac{\epsilon \bar{k}_1}{\bar{k}_0} \to 0$$

When the mud layer is thick compared to its boundary layer thickness $d >> \delta_s$ ($d_s >> 1$) then the elastic properties lose their influence on the complex wavenumber

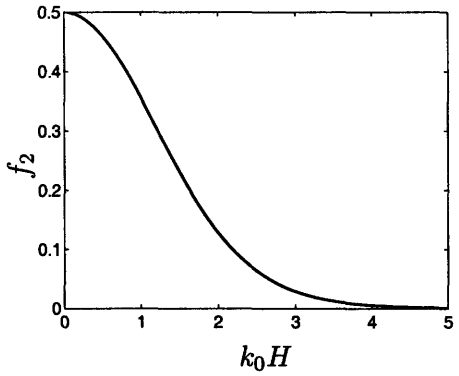

Figure 2-8: $f_2(k_0H)$

correction k_1. In fact for large d_s we have $\frac{\tanh\lambda}{\lambda} \propto \frac{1}{d_s} \approx 0$ and

$$\frac{\epsilon\bar{k}_1}{\bar{k}_0} \approx -\gamma\frac{d}{h}\frac{2q}{2q+\sinh 2q}$$

which is real and negative. In other words for a large values of d_s the damping is small and the waves become longer. Also the damping becomes independent of the viscoelastic properties of the mud layer.

The influence of the water layer depth is the following. For very short waves or deep water, $\bar{k}_0 h \gg 1$, the complex wave number correction vanishes:

$$\frac{\epsilon\bar{k}_1}{\bar{k}_0} \approx 0$$

and for long waves in shallow water the complex wave number correction takes the following form

$$\frac{\epsilon\bar{k}_1}{\bar{k}_0} \approx -\frac{\gamma}{2}\frac{d}{h}$$

Limiting case of a Newtonian fluid

The obtained complex wave number correction should be valid in the case when the mud is modeled as a purely viscous fluid. In that case the expressions of the damping and the wavenumber shift should reduce to the known corresponding expressions for a purely viscous fluid.

In fact in the limiting case of a purely viscous fluid the imaginary part of the viscosity and the parameter θ vanish and we get

$$\begin{aligned}
\theta &\rightarrow 0 \\
\alpha &\rightarrow 1 \\
\beta &\rightarrow 1 \\
\Im\{g(\theta, d_s)\} &\rightarrow -\frac{1}{2d_s}\frac{\sinh d_s \cosh d_s - \sin d_s \cos d_s}{\cos^2 d_s \cosh^2 d_s + \sin^2 d_s \sinh^2 d_s} \\
\Re\{g(\theta, d_s)\} &\rightarrow 1 + \frac{1}{2d_s}\frac{\sin d_s \cos d_s + \sinh d_s \cosh d_s}{\cos^2 d_s \cosh^2 d_s + \sin^2 d_s \sinh^2 d_s}
\end{aligned}$$

The corresponding damping rate and wavenumber shift tend to

$$D_0 \rightarrow \gamma\frac{\delta_s}{h}\left(\frac{q}{2q+\sinh(2q)}\right)\left(\frac{\sinh d_s \cosh d_s - \sin d_s \cos d_s}{\cos^2 d_s \cosh^2 d_s + \sin^2 d_s \sinh^2 d_s}\right) \tag{2.5.20}$$

$$\Delta k \rightarrow -\gamma\frac{d}{h}\left(\frac{2q}{2q+\sinh(2q)}\right)\left(1 + \frac{1}{2d_s}\frac{\sin d_s \cos d_s + \sinh d_s \cosh d_s}{\cos^2 d_s \cosh^2 d_s + \sin^2 d_s \sinh^2 d_s}\right) \tag{2.5.21}$$

The last expression of the damping rate D_0 is exactly the expression obtained by Ng (2000) [7] in case of the inviscid water limit.

2.5.3 Damping rate and wavenumber shift for muds in two experiments

The damping rate and the wavenumber shift were computed using all available experimental data provided by Huhe & Huang (1994) and by Jiang & Mehta (1995). The samples exhibiting the most elastic behavior are from Jiang & Mehta's data and we expect the largest resonant amplitude from these samples.As it will be seen the resonance corresponding to the samples of Jiang & Mehta is about 7 times stronger than the one corresponding to the samples by Huhe & Huang.

The case of a purely viscous material was studied by Ng (2000). Ng did not pre-

dict resonant behavior as the material needs to be at least partly elastic to tend to resonate. The present work differentiates itself by using the viscoelastic model to represent the behavior of the mud and, therefore, by introducing the possibility of the resonant response of the mud layer. The resonance occurs for particular values of dimensionless mud layer depth d_s and the largest resonant amplitude is expected to occur for d_s given by equation (2.5.15). By dispersion relation one can deduce the corresponding values of k_0H, as function of which the damping D_0 and the wavenumbershift Δk are plotted. At resonance the water wave energy dissipates significantly.

Damping rate

The damping rate corresponding to the mud samples MB $\phi = 0.07,\ 0.11,\ 0.17$ provided by Jiang & Mehta is plotted in figure (2-9) for three depth ratios $\frac{d}{h} = 0.1,\ 0.15,\ 0.2$. It clearly possesses a peak that is due to the resonance inside the mud viscoelastic mud layer which increases with the depth ratio $\frac{d}{h}$. Small peaks of damping are observed for some samples close to the predicted values of $d_s = 3\frac{\pi}{2\sqrt{2}} \approx 3.33$ and $d_s = 5\frac{\pi}{2\sqrt{2}} \approx 5.55$. These peaks are not pronounced as they are canceled by the factors $\frac{1}{d_s}\ f_2(k_0H)$ decreasing exponentially with increasing frequency. The damping rate for mud samples OK $\phi = 0.11$, KI $\phi = 0.12$ and AK $\phi = 0.12$ is plotted in figure (2-10) for three depth ratios $\frac{d}{h} = 0.1,\ 0.15,\ 0.2$. Note a difference in the scales. The damping rate corresponding to the samples KI $\phi = 0.12$ and AK $\phi = 0.12$ are one order of magnitude smaller than the one corresponding to MB $\phi = 0.07$ or OK $\phi = 0.11$.

The damping rate corresponding to the data provided by Huhe & Huang is plotted in figures (2-11) and (2-12) for the data set A and in figures (2-13) and (2-14) for the data set B. As the elasticity parameter θ is only about 0.3, the maximum value of the resonant peaks are not as important as in the case of Jiang & Mehta samples (note the difference in the scales of the plots). Moreover, there are two opposite phenomena present: the resonant behavior tending to increase the values of the damping rate D_0 when d_s increases to its first resonant value $\frac{\pi}{2\sqrt{2}} \approx 1.11$ and the factor $f_2(\bar{k}_0h)$

tending to decrease the value of D_0 when d_s , and thus ω increases. As in the case of Huhe & Huang's data the elasticity parameter is small, resonance is moderate and the factor $f_2(\bar{k}_0 h)$ wins and cancels the resonance before the peak at $d_s = \frac{\pi}{2\sqrt{2}} \approx 1.11$ is achieved.

Another interesting phenomenon is that the value of the damping rate decreases consistently when the the solid volume fraction increases. This is due to the fact that an increase of solid volume fraction makes mud heavier and therefore more difficult to move. This can be seen in figure (2-15) where the amplitudes of the interface are plotted for a mud samples of the same chemical composition but for three different solid volume fractions $\phi = 0.08,\ 0.14,\ 0.24$. It is clear that the amplitude of the interface displacement decreases when the solid volume fraction ϕ increases.

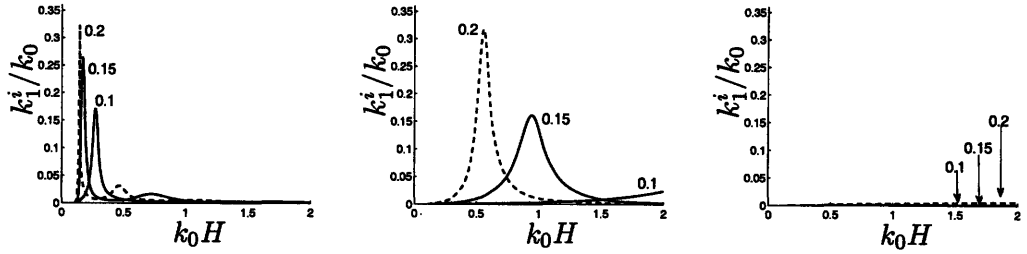

(a) MB $\phi = 0.07$ (b) MB $\phi = 0.11$ (c) MB $\phi = 0.17$

Figure 2-9: Damping coefficient $D_0 = \frac{k_1^i}{k_0}$ for three depth ratios $\frac{d}{h} = 0.1,\ 0.15,\ 0.2$. Samples by Jiang & Mehta, MB $\phi = 0.07,\ 0.11\ 0.17$

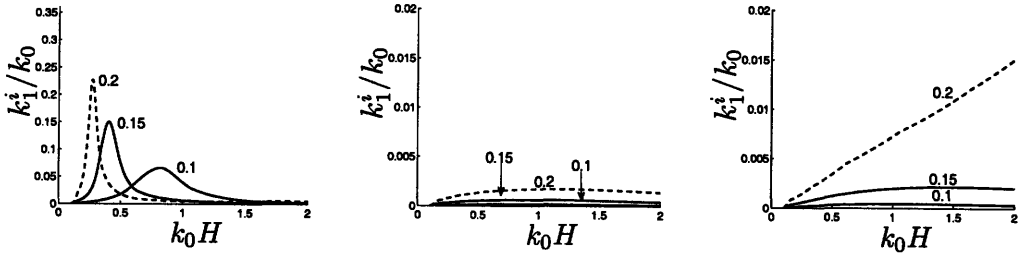

(a) OK $\phi = 0.11$ (b) KI $\phi = 0.12$ (c) AK $\phi = 0.12$

Figure 2-10: Damping coefficient $D_0 = \frac{k_1^i}{k_0}$ for three depth ratios $\frac{d}{h} = 0.1,\ 0.15,\ 0.2$. Samples by Jiang & Mehta, OK $\phi = 0.11$, KI $\phi = 0.12$ and AK $\phi = 0.12$

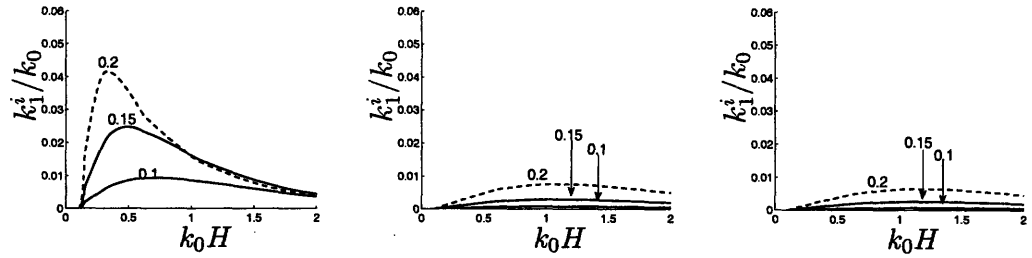

(a) Data set A $\phi = 0.08$ (b) Data set A $\phi = 0.14$ (c) Data set A $\phi = 0.17$

Figure 2-11: Damping coefficient $D_0 = \frac{k_1^i}{k_0}$ for three depth ratios $\frac{d}{h} = 0.1,\ 0.15,\ 0.2$. Samples by Huhe & Huang, data set A, $\phi = 0.08,\ 0.14,\ 0.17$

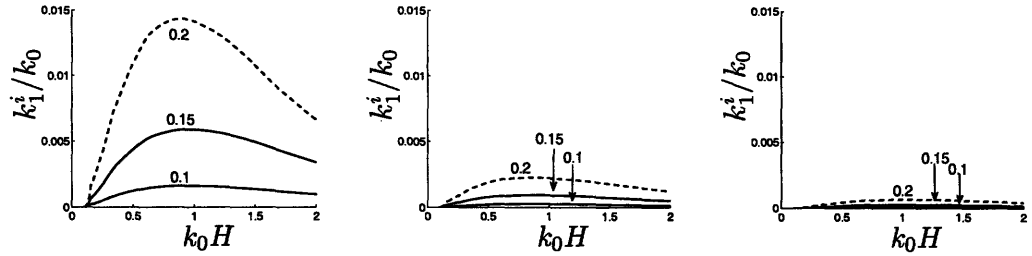

(a) Data set A $\phi = 0.20$ (b) Data set A $\phi = 0.24$ (c) Data set A $\phi = 0.34$

Figure 2-12: Damping coefficient $D_0 = \frac{k_1^i}{k_0}$ for three depth ratios $\frac{d}{h} = 0.1,\ 0.15,\ 0.2$. Samples by Huhe & Huang, data set A, $\phi = 0.20,\ 0.24,\ 0.34$

Wavenumber shift

The wavenumber shift corresponding to the mud samples MB $\phi = 0.07,\ 0.11,\ 0.17$ provided by Jiang & Mehta is plotted in figure (2-16) for three depth ratios $\frac{d}{h} = 0.1,\ 0.15,\ 0.2$. As in case of the damping coefficient, it clearly possesses a peak that is due to the resonance inside the mud viscoelastic mud layer which increases with the depth ratio $\frac{d}{h}$. The wavenumber shift for mud samples OK $\phi = 0.11$, KI $\phi = 0.12$ and AK $\phi = 0.12$ is plotted in figure (2-17) for three depth ratios $\frac{d}{h} = 0.1,\ 0.15,\ 0.2$. Note the difference in the scales. The wavenumber shift corresponding to the samples KI $\phi = 0.12$ and AK $\phi = 0.12$ are one order of magnitude smaller than the one corresponding to MB $\phi = 0.07$ or OK $\phi = 0.11$.

The wavenumber shift corresponding to the data provided by Huhe & Huang is plotted in figures (2-18) and (2-19) for the data set A and in figures (2-20) and (2-21) for the

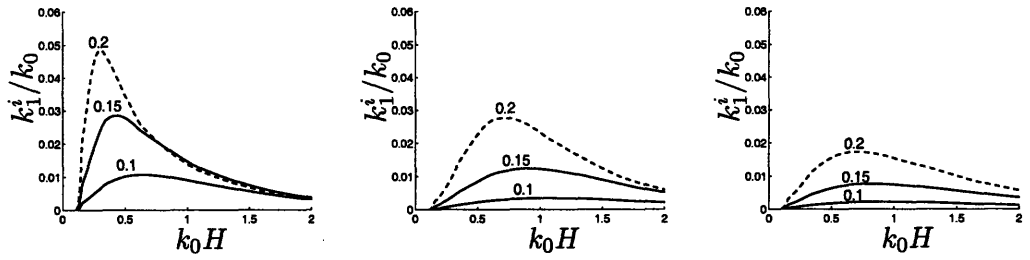

(a) Data set B $\phi = 0.08$ (b) Data set B $\phi = 0.14$ (c) Data set B $\phi = 0.17$

Figure 2-13: Damping coefficient $D_0 = \frac{k_1^i}{k_0}$ for three depth ratios $\frac{d}{h} = 0.1,\ 0.15,\ 0.2$. Samples by Huhe & Huang, data set B, $\phi = 0.08,\ 0.14,\ 0.17$

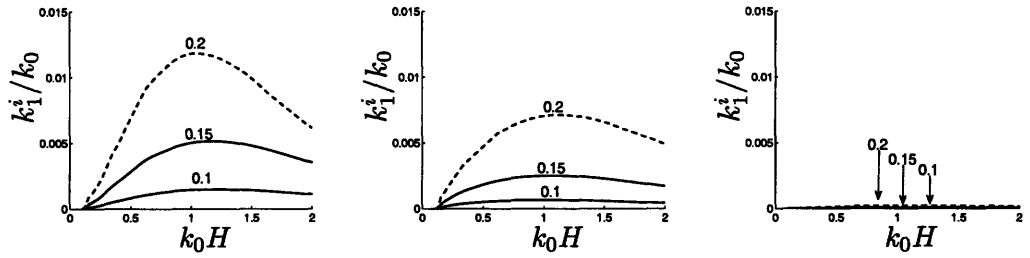

(a) Data set B $\phi = 0.20$ (b) Data set B $\phi = 0.23$ (c) Data set B $\phi = 0.37$

Figure 2-14: Damping coefficient $D_0 = \frac{k_1^i}{k_0}$ for three depth ratios $\frac{d}{h} = 0.1,\ 0.15,\ 0.2$. Samples by Huhe & Huang, data set B, $\phi = 0.20,\ 0.23,\ 0.37$

data set B.

To determine whether the waves become shorter or longer due to the interaction with the mud layer, one needs to determine the sign of Δk. The sign of the wavenumber shift Δk is determined by the sign of the real part of $g(\theta, d_s)$ plotted in the left part of the figure (2-4). One can immediately infer that for a purely viscous fluid $g(\theta = 0, d_s) \geq 0$ is positive for all values of d_s, and therefore the wavenumber shift is negative for the entire range of frequencies. If the mud is purely viscous (no elasticity) then the water waves become longer due to the interaction with mud layer.

When the elasticity becomes more important the behavior of the function $g(\theta, d_s)$ and therefore Δk changes. When the parameter k_0H is lower than the the one at which the mud layer resonates (let us call it $(k_0H)_{res}$), $\left(\frac{k_0H}{(k_0H)_{res}} < 1\right)$ the wavenumber shift is positive $\Delta k > 0$, meaning shorter waves. For larger frequencies $\left(\frac{k_0H}{(k_0H)_{res}} > 1\right)$ the

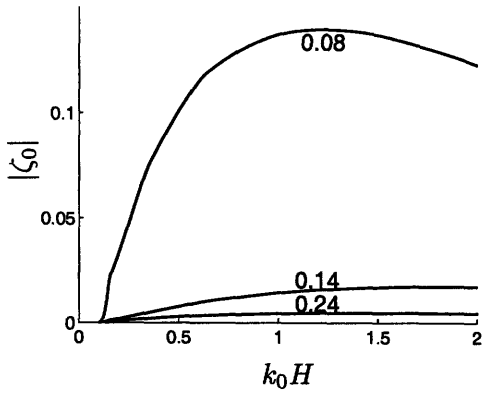

Figure 2-15: Amplitude of the interface displacement $|\zeta_0|$ for different values of solid volume fraction ϕ. Data by Huhe & Huang (1994), data set A, $\phi = 0.08,\ 0.14,\ 0.24$

wavenumber shift is negative $\Delta k < 0$ (longer waves).

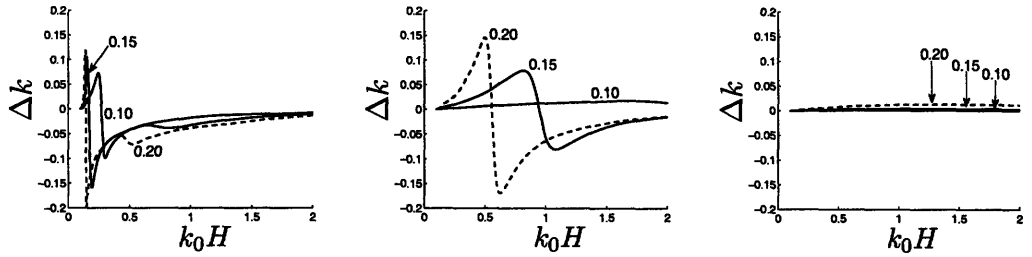

(a) MB $\phi = 0.07$ (b) MB $\phi = 0.11$ (c) MB $\phi = 0.17$

Figure 2-16: Wavenumber shift Δk for three depth ratios $\frac{d}{h} = 0.1,\ 0.15,\ 0.2$. Samples by Jiang & Mehta, MB $\phi = 0.07,\ 0.11\ 0.17$

2.5.4 Mean horizontal displacement X_{10} inside the mud layer

The analytical expression for the mean displacement $X_{10}(y')$ inside the mud layer was computed previously in this chapter and is given by equations (2.4.49)-(2.4.51). In the present section we will study graphically its behavior and use the experimental data to compute the predicted values of X_{10} for different mud samples.

First let us note that the shape of the profile of the mean horizontal displacement is entirely determined by only two parameters: the dimensionless mud layer depth $d_s = \frac{d}{\delta_s}$ and the phase θ of the complex viscosity μ representing the proportions of

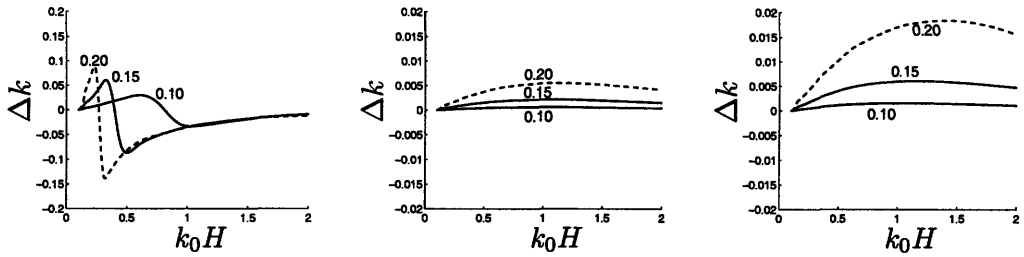

(a) OK $\phi = 0.11$ (b) KI $\phi = 0.12$ (c) AK $\phi = 0.12$

Figure 2-17: Wavenumber shift Δk for three depth ratios $\frac{d}{h} = 0.1,\ 0.15,\ 0.2$. Samples by Jiang & Mehta, OK $\phi = 0.11$, KI $\phi = 0.12$ and AK $\phi = 0.12$

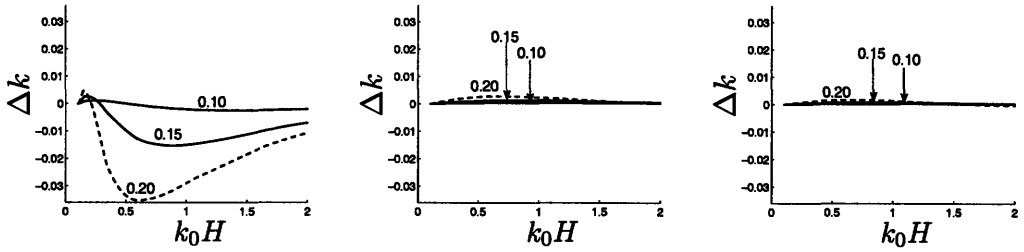

(a) Data set A $\phi = 0.08$ (b) Data set A $\phi = 0.14$ (c) Data set A $\phi = 0.17$

Figure 2-18: Wavenumber shift Δk for three depth ratios $\frac{d}{h} = 0.1,\ 0.15,\ 0.2$. Samples by Huhe & Huang, data set A, $\phi = 0.08,\ 0.14,\ 0.17$

elasticity compared to viscosity (for a purely viscous mud $\theta = 0$ and for a purely elastic mud $\theta = \frac{\pi}{2}$). The amplitude of the mean horizontal displacement is proportional to the constant $\widehat{B}_{10}$ given by the equation (2.4.44).

From the experimental data (see figure (1-3(b))) the value of the parameter θ is approximately $\theta \approx 0.3 \times \frac{\pi}{2}$ for the mud samples provided by Huhe and Huang and $\theta \approx 0.9 \times \frac{\pi}{2}$ for the mud samples provided by Jiang and Mehta (see figure (1-8(b))). These two cases represent a moderately elastic mud and a highly elastic mud respectively. The profiles of the mean horizontal displacement X_{10} are plotted in figure (2-22(a)) for the case of a moderately elastic mud $\theta = 0.3 \times \frac{\pi}{2}$ and in figure (2-22(b)) for a highly elastic case $\theta = 0.9 \times \frac{\pi}{2}$ for three values of the dimensionless mud layer depth $d_s = 0.1,\ 2,\ 5$. For simplicity in both cases the value of the parameter $\widehat{B}_{10}$ was taken to be unity $\widehat{B}_{10} = 1$.

In figure (2-22(c)) are plotted the profiles of the mean horizontal displacement for

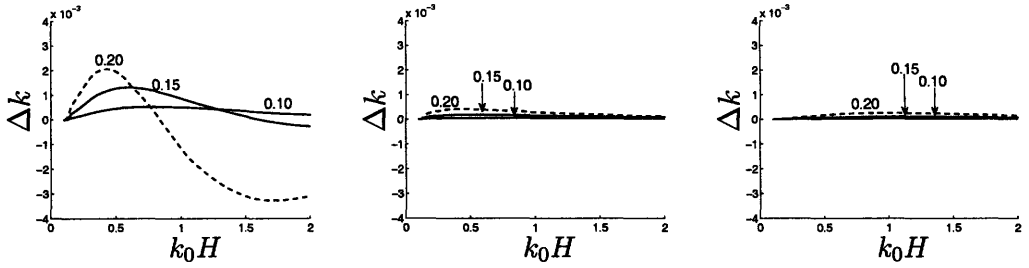

(a) Data set A $\phi = 0.20$ (b) Data set A $\phi = 0.24$ (c) Data set A $\phi = 0.34$

Figure 2-19: Wavenumber shift Δk for three depth ratios $\frac{d}{h} = 0.1,\ 0.15,\ 0.2$. Samples by Huhe & Huang, data set A, $\phi = 0.20,\ 0.24,\ 0.34$

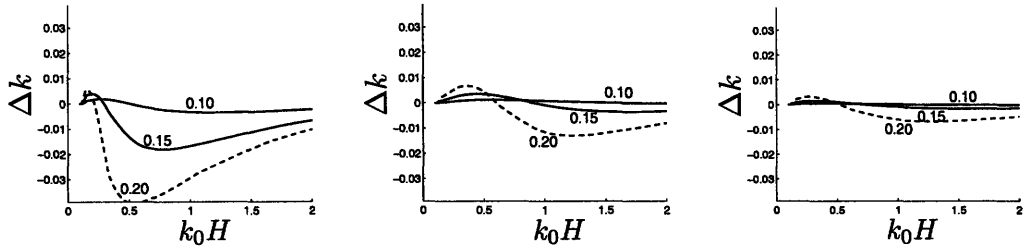

(a) Data set B $\phi = 0.08$ (b) Data set B $\phi = 0.14$ (c) Data set B $\phi = 0.17$

Figure 2-20: Wavenumber shift for three depth ratios $\frac{d}{h} = 0.1,\ 0.15,\ 0.2$. Samples by Huhe & Huang, data set B, $\phi = 0.08,\ 0.14,\ 0.17$

$\theta = 0.3$ and for values of d_s smaller than 1.5. From this figure it can clearly be inferred that when the mud layer is shallow or comparable to the Stokes boundary layer thickness $d_s = \frac{d}{\delta_s} < 1.5$ the profile is close to linear. It was checked that the same linear profile with a different amplitude is observed for other values of the parameter θ. The amplitude of the mean horizontal displacement for the linear profiles defined as $X_{10}|_{y'=1}$ is plotted as function of dimensionless mud depth d_s for three values of the elasticity parameter $\theta = 0.1,\ 0.3,\ 0.9$ in figure (2-22(d)). In summary the profile of the mean horizontal displacement inside the mud layer is linear while $d_s < 1.5$ and only its amplitude depends on the value of θ. It only starts to have a nonlinear shape when the dimensionless mud layer depth becomes larger than $d_s \approx 1.5$.

When the mud layer is deep compared to its Stokes boundary layer thickness, the profile becomes highly nonlinear and can reverse as it can be seen in figure (2-22(b)) for the case $d_s = 5$. The extreme case of a deep mud layer of low viscosity $d_s = 15 >>$

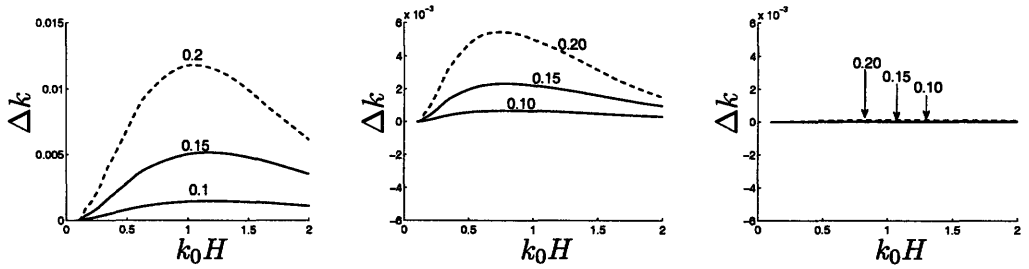

(a) Data set B $\phi = 0.20$ (b) Data set B $\phi = 0.23$ (c) Data set B $\phi = 0.37$

Figure 2-21: Wavenumber shift Δk for three depth ratios $\frac{d}{h} = 0.1,\ 0.15,\ 0.2$. Samples by Huhe & Huang, data set B, $\phi = 0.20,\ 0.23,\ 0.37$

1 is plotted in figure (2-22(e)) where one can see a strongly nonlinear profile.

Let us now obtain the values of the mean horizontal displacement inside the mud layer using the experimental data available. We will not present the results for each of the mud samples available but only for selected ones. From the data of Jiang and Mehta, 1995 we selected the three MB mud samples corresponding to the solid volume fractions $\phi = 0.07$, 0.11 and 0.17. These mud samples have the same chemical composition but different solid volume fractions.

As it was pointed out the two parameters that govern the shape of the profile of the mean horizontal displacement are θ and $d_s = \frac{d}{\delta_S}$. Given the experimental data (see fig (1-8(b))) the parameter θ is approximately constant $\theta \approx 0.9 \times \frac{\pi}{2}$ on the entire range of experimental frequencies. However the dimensionless depth $d_s = \frac{d}{\delta_S}$ depends strongly on the frequency through the Stokes boundary layer thickness $\delta_S = \sqrt{\frac{2|\bar{\mu}|}{\rho^{(m)}\omega}}$. As it was inferred from figures (2-22), the profile of the mean horizontal displacement is linear while the dimensionless depth is smaller than $d_s < 1.5$, therefore it is important to know the order of magnitude of the experimental Stokes boundary layer thickness. The experimental data for the viscosity fixes the values of the Stokes boundary layer thickness δ_S that is plotted in figure (2-23(a)) for the MB mud samples. In the case of the solid volume fraction $\phi = 0.17$ and $\phi = 0.11$ the mud layer depth should be larger than $3m$ in order to get a non linear profile of the mean horizontal displacement ($d_s < 1.5$). In reality the mud layer depth is no more than $d = 1m$ with a usual depth of $d = 10cm$, hence the profile of the mean horizontal displacement will be linear for

the entire range of experimental frequencies for the samples corresponding to $\phi = 0.11$ and $\phi = 0.17$. The mud sample corresponding to $\phi = 0.07$ can potentially have a nonlinear profile if the mud layer depth is sufficiently large.

From the data by Huhe & Huang three samples from the data set A that have a solid volume fraction equal to $\phi = 0.08$, $\phi = 0.14$ and $\phi = 0.24$ where selected and the corresponding Stokes boundary layer thicknesses plotted in figure (2-23(b)). From this figure it is clear that for all three samples considered the Stokes boundary layer thickness is larger than $2m$. Therefore for any mud layer that is thinner than approximately $3m$ the profile of the mean displacement will be linear.

We notice that in the paper [6] Zhang and Ng obtained numerically nonlinear profiles of the mean horizontal displacement X_{10} using certain values of the dimensionless parameters. In fact by translating these values into the dimensional quantities we find that the mud layer depth d should be of order $10m$, the same as the water layer hight h. Under these conditions we naturally expect a nonlinear profile of X_{10} and our results are not contradicting the work of Zhang and Ng [6].

The mean horizontal displacement is proportional to the constant $\widehat{B}_{10}$ given by the equation (2.4.44):

$$\widehat{B}_{10} = \frac{\gamma^2 k_0}{2} \frac{|A|^2}{\sinh^2 q} \frac{Re}{b_0} \frac{d}{a} = \left(\frac{|A|}{2\cosh q} \right)^2 2\gamma^2 k_0^3 \frac{\rho^{(m)} \omega^2 d^2}{\bar{b}_0} \tag{2.5.22}$$

The parameters governing the constant $\widehat{B}_{10}$ are clear. The first factor $\left(\frac{|A|}{2\cosh q}\right)^2$ is simply the square of the value of the dimensionless pressure on top of the mud layer. The factors $\gamma = \frac{\rho^{(w)}}{\rho^{(m)}}$ and $\frac{1}{b_0}$ are fixed for a given mud sample. The factors k_0^3 and ω^2 depend on the frequency and the water layer depth only. Finally the depth of the mud layer d appears explicitly in the expression of $\widehat{B}_{10}$.

Finally the experimental profiles of the mean horizontal displacement are plotted in figure (2-24(a)) for the Jiang & Mehta's data (MB $\phi = 0.17$, $\phi = 0.11$, $\phi = 0.07$) and in figure (2-24(b)) for the Huhe & Huang data (data set A $\phi = 0.24$, $\phi = 0.14$, $\phi = 0.08$). In all the cases the mud layer depth was taken to be equal to $d = 1m$ and the dimensionless water layer depth to $k_0 H = 0.7$. These plots confirm that all the

profiles of the mean horizontal displacement X_{10} are very close to linear except the lightest mud from the data by Jiang & Mehta (MB, $\phi = 0.07$) that start to have a nonlinear shape as d_s approaches the value of 2.

2.5.5 The mean horizontal velocity u_{10} inside the mud layer

The mean horizontal velocity u_{10} was computed previously in this chapter and is given by the equation (2.4.37) and rewritten here for convenience:

$$\begin{aligned} u_{10} \;=\; & -\widehat{u}_{10}\Re\Big\{1-\cosh(\lambda^* y')-\lambda^* y'\sinh(\lambda^* y')+\tanh(\lambda^*)\sinh(\lambda^* y') \\ & +\tanh(\lambda^*)(\lambda^* y')\cosh(\lambda^* y')-\cosh(\lambda y')+|\cosh(\lambda^* y')|^2+\frac{\lambda^*}{\lambda}|\sinh(\lambda^* y')|^2 \\ & -2\frac{\tanh(\lambda^*)}{\lambda}\Re\{\lambda\cosh(\lambda y')\sinh(\lambda^* y')\}+\tanh(\lambda)\sinh(\lambda y') \\ & -2\frac{\tanh(\lambda)}{\lambda}\Re\{\lambda\sinh(\lambda y')\cosh(\lambda^* y')\}+\frac{\lambda^*}{\lambda}\tanh(\lambda)\sinh(\lambda^* y') \\ & +|\tanh(\lambda)|^2|\sinh(\lambda y')|^2+\frac{\lambda^*}{\lambda}|\tanh(\lambda)|^2|\cosh(\lambda^* y')|^2 \\ & -\frac{\lambda^*}{\lambda}|\tanh(\lambda)|^2\cosh(\lambda^* y')\Big\} \end{aligned} \tag{2.5.23}$$

Were the constant $\widehat{u}_{10}$ is the amplitude of the mean horizontal velocity u_{10}:

$$\widehat{u}_{10} = \gamma^2 k_0 \frac{|A|^2}{2\sinh^2 q} \tag{2.5.24}$$

As in the case of the mean horizontal displacement X_{10}, the profile of the mean horizontal velocity u_{10} depends only on two parameters: the dimensionless mud depth $d_s = \frac{d}{\delta_S}$ and the phase θ of the complex viscosity μ indicating how strong the elastic properties of the mud are compared to its viscous properties (for a purely viscous mud $\theta = 0$ and for a purely elastic mud $\theta = \frac{\pi}{2}$). The profiles of the mean horizontal velocity are plotted for three different dimensionless mud layer depths $d_s = 0.5,\ 1,\ 2,\ 5$ in figure (2-25(a)) for $\theta = 0.3 \times \frac{\pi}{2}$ and in figure (2-25(b)) for $\theta = 0.9 \times \frac{\pi}{2}$. For these plots the value of $\widehat{u}_{10}$ was taken to be one: $\widehat{u}_{10} = 1$. It is clear that the profile of the mean horizontal velocity becomes more and more nonlinear at when the dimensionless mud

layer depth increases. In particular we observe a highly nonlinear profile for $d_s = 5$ in both $\theta = 0.3 \times \frac{\pi}{2}$ and $\theta = 0.9 \times \frac{\pi}{2}$ cases. The amplitude of the mean horizontal velocity is much larger for the case of a highly elastic mud $\theta = 0.9 \times \frac{\pi}{2}$ than for a moderately elastic mud $\theta = 0.3 \times \frac{\pi}{2}$. This is something we could expect from the leading order results. In fact we saw that the amplitude of the leading order interface movement is getting stronger when the mud layer becomes more elastic $\theta \to \frac{\pi}{2}$.

The experimental values of the mean horizontal velocity were plotted for two samples from the data provided by Jiang & Mehta (MB, $\phi = 0.07$ and $\phi = 0.11$) in figure (2-26(a)) and for two samples provided by Huhe & Huang (data set A, $\phi = 0.08$ and $\phi = 0.14$) in figure (2-26(b)). Because of a large difference in the magnitudes of u_{10} the scales in the figures (2-26(a)) and (2-26(b)) are different by a factor 15. Both for the data from Jiang & Mehta and from the data from Huhe & Huang the magnitude of the mean horizontal velocity is larger for lighter muds. The magnitude is significantly (more than 10 times) larger for the sample MB $\phi = 0.07$ than for data set A, $\phi = 0.08$, because the MB 0.07 sample is highly elastic $\left(\theta = 0.9 \times \frac{\pi}{2}\right)$, whereas the data set A, $\phi = 0.08$ sample is only moderately elastic $\left(\theta = 0.3 \times \frac{\pi}{2}\right)$.

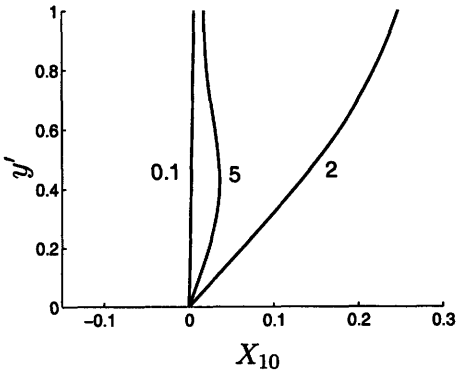

(a) $\theta = 0.3 \times \frac{\pi}{2}$ $d_s = 0.1,\ 2,\ 5$

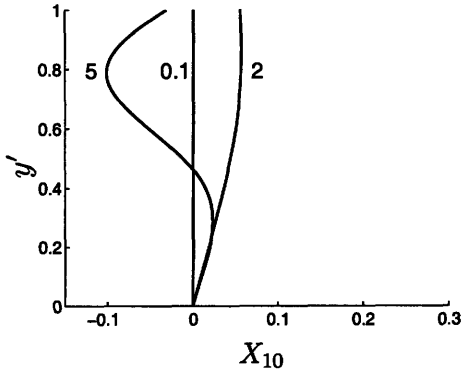

(b) $\theta = 0.9 \times \frac{\pi}{2}$ $d_s = 0.1,\ 2,\ 5$

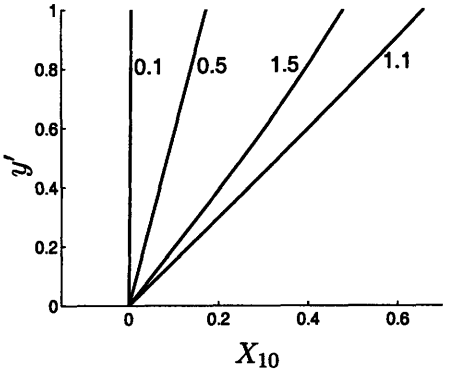

(c) $\theta = 0.9 \times \frac{\pi}{2}$ $d_s = 0.1,\ 0.5,\ 1.1,\ 1.5$

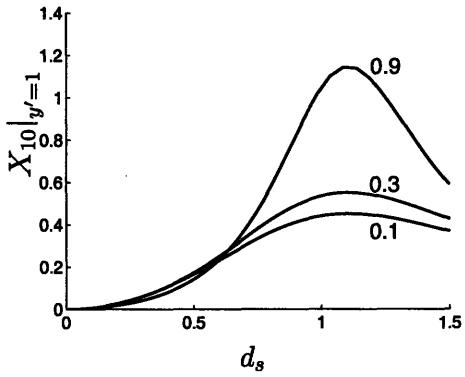

(d) $X_{10}|_{y'=1}$ $\theta = (0.1,\ 0.3,\ 0.9) \times \frac{\pi}{2}$

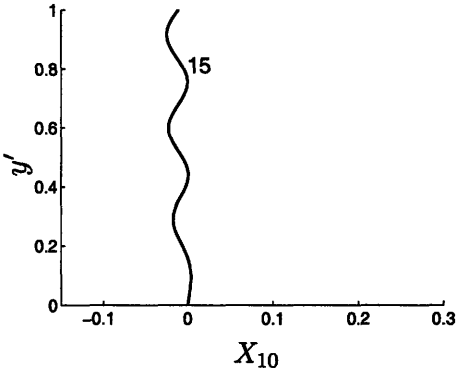

(e) $\theta = 0.3 \times \frac{\pi}{2}$ $d_s = 15$

Figure 2-22: The profiles of the mean horizontal displacement X_{10}

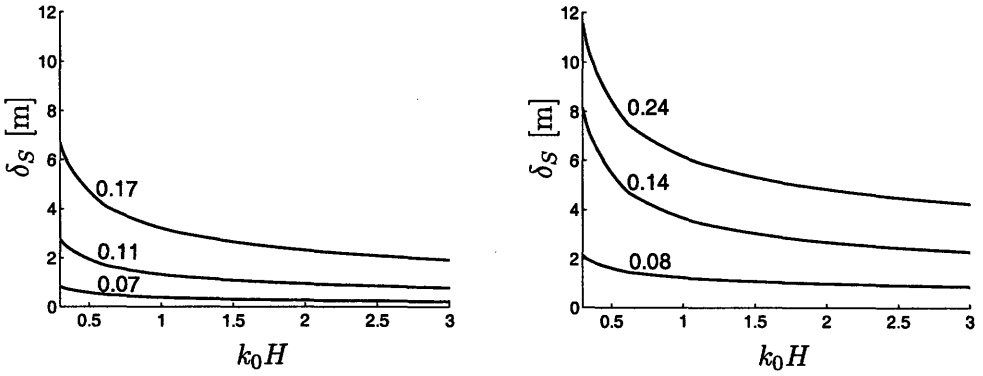

(a) Samples by Jiang & Mehta, MB, ϕ = 0.17, 0.11, 0.07

(b) Samples by Huhe & Huang, data set A $\phi = 0.24,\ 0.14,\ 0.08$

Figure 2-23: Experimental Stokes boundary layer thickness

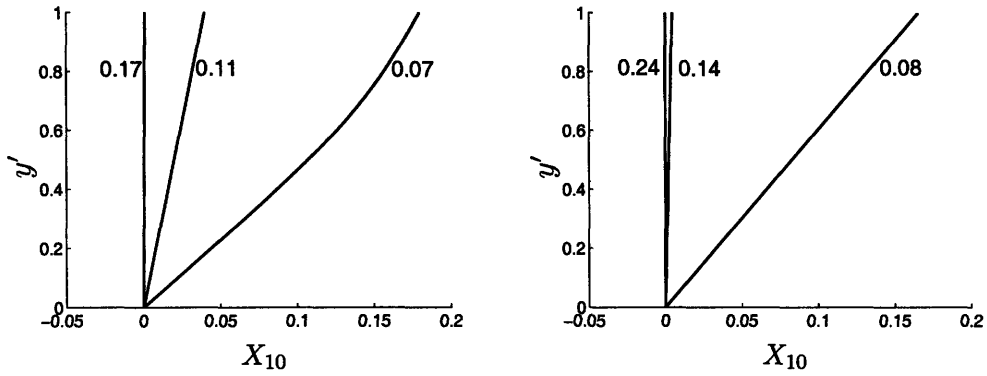

(a) Samples by Jiang & Mehta, MB, ϕ = 0.17, 0.11, 0.07

(b) Samples by Huhe & Huang, data set A $\phi = 0.24,\ 0.14,\ 0.08$

Figure 2-24: The profiles of the mean horizontal displacement X_{10} for $d = 1m$ and $k_0H = 0.7$

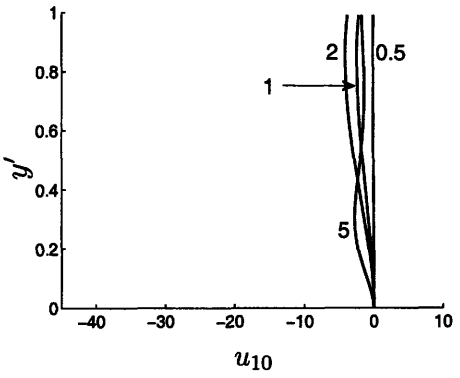

(a) $\theta = 0.3 \times \frac{\pi}{2}$, $d_s = 0.5,\ 1,\ 2,\ 5$

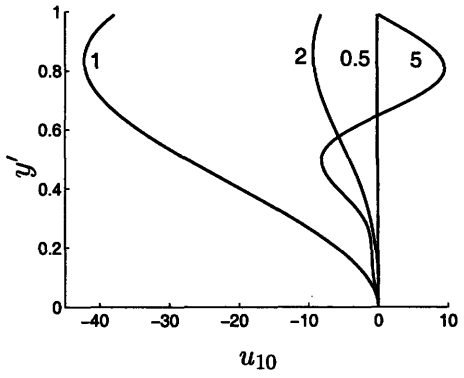

(b) $\theta = 0.9 \times \frac{\pi}{2}$, $d_s = 0.5,\ 1,\ 2,\ 5$

Figure 2-25: The profiles of the mean horizontal velocity u_{10} with $\widehat{u}_{10} = 1$

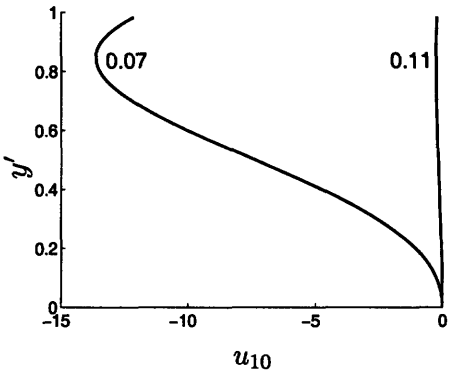

(a) Samples from Jiang & Mehta, MB, ϕ = 0.07, 0.11

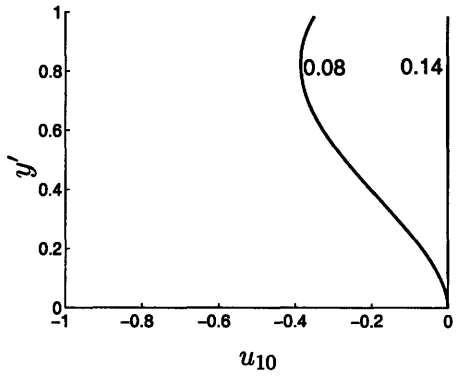

(b) Samples from Huhe and Huang, data set A, $\phi = 0.08,\ 0.14$

Figure 2-26: The profiles of the mean horizontal velocity u_{10} for selected mud samples. Different scales are used for the two plots.

Chapter 3

Narrow-banded waves propagating on top of a shallow semi-infinite mud layer

In the present chapter we will apply previously obtained results to study the propagation of narrow-banded water waves on top of a shallow mud layer. First the case of a semi-infinite mud layer will be considered, then the water waves interaction with a mud layer of a finite length will be studied.

In the case of a semi-infinite mud layer the problem can be decomposed into two domains: the '-' region where there is no mud and the '+' region where a shallow layer of mud is present (see figure 3-1). The problem can then be solved separately for each of the two regions. The two solutions will then be coupled by the boundary conditions at the edge of the mud layer, which are the pressure and the horizontal flux continuity. All the quantities in the '-' region will be indexed with a sign '-' and the quantities in the '+' region will be indexed with a sign '+' respectively.
Before we are able to solve the long wave equation (2.4.54), we need to obtain an explicit expression for the slowly varying amplitude of the water waves.

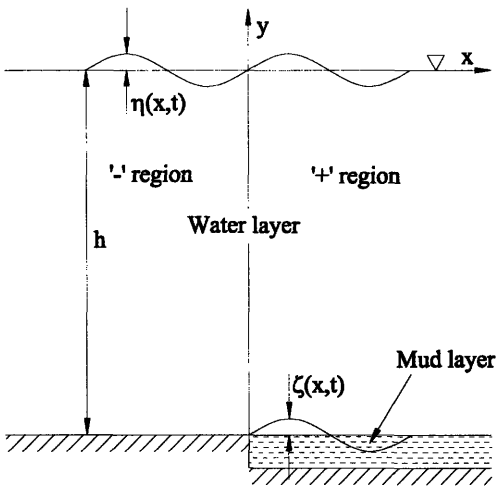

Figure 3-1: Narrow-banded waves on top of a thin semi-infinite mud layer

3.1 Leading order solution

As it was shown in chapter 2 only the amplitude of the leading order wave problem is affected by the presence of a thin mud layer. In particular at the leading order there is no reflected wave generated at the edge of the mud layer and the incoming wave from the '-' region continues its propagation in the '+' region. Thus the velocity potentials Φ_{01}^{-} and Φ_{01}^{+} in both '-' and '+' regions are both given by equation (2.4.2):

$$\begin{aligned}\Phi_{01}^{-}(x,t,x_1,t_1) &= -i\frac{\cosh Q}{2\cosh q}A^{-}(x_1,t_1)\\ \Phi_{01}^{+}(x,t,x_1,t_1) &= -i\frac{\cosh Q}{2\cosh q}A^{+}(x_1,t_1)\end{aligned}$$

the velocity potential is continuous at the boundary $(x,x_1)=(0,0)$.

$$\left(\Phi_{01}^{-}\right)\big|_0 = \left(\Phi_{01}^{+}\right)\big|_0$$

which implies the continuity of the amplitudes at the edge of the mud layer

$$A^{-}(x_1,t_1)\big|_0 = A^{+}(x_1,t_1)\big|_0 \tag{3.1.1}$$

3.2 Slow evolution of the short waves' amplitude $A(x_1, t_1)$

3.2.1 '-' region

In the '-' region where the mud layer is absent we consider the propagation from left to right of the narrow-banded waves, which are modeled by the superposition of waves having very close frequencies. We consider two waves of the same amplitude with dimensionless frequencies $1-\epsilon\Omega$ and $1+\epsilon\Omega$ with $\Omega << 1$. The corresponding dimensionless wavenumbers are respectively $k_0 - \epsilon K$ and $k_0 + \epsilon K$ so that the free surface displacement η^- in the '-' region is written as:

$$\begin{aligned}
\eta_0^- &= \frac{1}{2}\left[\frac{A_0}{2}e^{i[(k_0-\epsilon K)x-(1-\epsilon\Omega)t]} + \frac{A_0}{2}e^{i[(k_0+\epsilon K)x-(1+\epsilon\Omega)t]}\right] + c.c. \\
&= \frac{A_0}{2}e^{i(k_0x-t)}\frac{1}{2}\left[e^{i[-\epsilon Kx+\epsilon\Omega t]} + e^{i[\epsilon Kx-\epsilon\Omega t]}\right] + c.c. \\
&= \frac{A_0}{2}e^{i(k_0x-t)}\cos(\epsilon Kx - \epsilon\Omega t) + c.c. \\
&= \frac{A_0}{2}\cos(Kx_1 - \Omega t_1)e^{i(k_0x-t)} + c.c.
\end{aligned}$$

Finally defining the slowly varying amplitude $A^-(x_1, t_1)$ of the short waves

$$\eta^- = A^-(x_1, t_1)e^{i(k_0x-t)} + c.c \tag{3.2.1}$$

$$A^-(x_1, t_1) = A_0\cos(Kx_1 - \Omega t_1) \tag{3.2.2}$$

In the '-' region the solvability condition (2.4.22) in the absence of the mud layer ($k_1 = 0$) is simply:

$$A^-_{t_1} + C_gA^-_{x_1} = 0 \tag{3.2.3}$$

and provides a relationship between K and Ω:

$$\Omega = C_gK \tag{3.2.4}$$

3.2.2 '+' region

Let us now deduce the explicit expression of the slowly varying free surface wave amplitude in the '+' region where a thin layer of mud is present. First note that the mud layer does not introduce any inhomogeneity in time and we expect the amplitude $A^+(x_1, t_1)$ to be of the form:

$$A^+(x_1, t_1) = \frac{1}{2}\left[B_1^+(x_1)e^{i\Omega t_1} + B_2^+(x_1)e^{-i\Omega t_1}\right] \tag{3.2.5}$$

This amplitude should satisfy the solvability condition (2.4.22), this time with a non zero value of k_1

$$A_{t_1}^+ + C_g A_{x_1}^+ = ik_1 C_g A^+ \tag{3.2.6}$$

This gives:

$$\left[i\Omega B_1^+ + C_g B_{1,x_1}^+\right] e^{i\Omega t_1} + \left[-i\Omega B_2^+ + C_g B_{2,x_1}^+\right] e^{-i\Omega t_1} = ik_1 C_g \left[B_1^+ e^{i\Omega t_1} + B_2^+ e^{-i\Omega t_1}\right]$$

This gives the governing equations of the variables B_1^+ and B_2^+:

$$\begin{aligned} B_{1,x_1}^+ &= \left(\frac{ik_1 C_g - i\Omega}{C_g}\right) B_1^+ = i(k_1 - K)B_1^+, \\ B_{2,x_1}^+ &= \left(\frac{ik_1 C_g + i\Omega}{C_g}\right) B_2^+ = i(k_1 + K)B_2^+, \end{aligned}$$

The solutions are straightforward:

$$\begin{aligned} B_1^+ &= \widehat{B}_1^+ e^{i(k_1 - K)x_1}, \\ B_2^+ &= \widehat{B}_2^+ e^{i(k_1 + K)x_1}, \end{aligned}$$

with $\widehat{B}_1^+$ and $\widehat{B}_2^+$ being constants. The expression of the free surface wave amplitude in the '+' region is then

$$A^+(x_1, t_1) = \frac{1}{2} e^{ik_1 x_1}\left[\widehat{B}_1^+ e^{i(-Kx_1 + \Omega t_1)} + \widehat{B}_2^+ e^{i(Kx_1 - \Omega t_1)}\right] \tag{3.2.7}$$

The constants $\widehat{B}_1^+$ and $\widehat{B}_2^+$ are determined by the boundary condition (3.1.1). In fact the boundary condition (3.1.1) is rewritten as:

$$\begin{aligned}\frac{A_0}{2}\left[e^{i\Omega t_1}+e^{-i\Omega t_1}\right] &= \frac{1}{2}\left[B_1^+(0)e^{i\Omega t_1}+B_2^+(0)e^{-i\Omega t_1}\right] \\ &= \frac{1}{2}\left[\widehat{B}_1^+e^{i\Omega t_1}+\widehat{B}_2^+e^{-i\Omega t_1}\right]\end{aligned}$$

the constants $\widehat{B}_1^+$ and $\widehat{B}_2^+$ are then

$$\begin{aligned}\widehat{B}_1^+ &= A_0 \\ \widehat{B}_2^+ &= A_0\end{aligned}$$

Finally we can write the expression of the free surface wave amplitude in the '+' region:

$$A^+(x_1,t_1)=A_0e^{ik_1x_1}\cos(Kx_1-\Omega t_1) \tag{3.2.8}$$

3.3 Long-wave equation

Now that the explicit dependence of the slowly varying free surface wave amplitudes on x_1 and t_1 is found, the long wave equation (2.4.54) can be solved analytically. It is rewritten here for easier reference:

$$\Phi_{00,t_1t_1}-H\Phi_{00,x_1x_1}=\frac{k_0}{2}(A^*A)_{x_1}-\frac{1}{4\sinh^2 q}(A^*A)_{t_1} \tag{3.3.1}$$

We will need to solve separately the long wave equation in the '-' and '+' regions and then couple the solutions using the second order boundary conditions.

3.3.1 Solution to the long wave equation in the '-' region

First let us evaluate the right-hand side of the long wave equation. To simplify the notations we introduce a new variable

$$\Psi = \Psi(x_1, t_1) \equiv Kx_1 - \Omega t_1 \tag{3.3.2}$$

then we have

$$\begin{aligned}
A^- &= A_0 \cos\Psi = \frac{A_0}{2}\left(e^{i\Psi} + e^{-i\Psi}\right) \\
A^{-*}A^- &= \frac{A_0^2}{4}\left(2 + e^{2i\Psi} + e^{-2i\Psi}\right) \\
(A^{-*}A^-)_{x_1} &= \frac{A_0^2}{4}\left(2iKe^{2i\Psi} - 2iKe^{-2i\Psi}\right) = \frac{iK}{2}A_0^2\left(e^{2i\Psi} - e^{-2i\Psi}\right) \\
(A^{-*}A^-)_{t_1} &= \frac{A_0^2}{4}\left(-2i\Omega e^{2i\Psi} + 2i\Omega e^{-2i\Psi}\right) = -C_g\frac{iK}{2}A_0^2\left(e^{2i\Psi} - e^{-2i\Psi}\right)
\end{aligned}$$

The right-hand side of the long wave equation (3.3.1) is then

$$\begin{aligned}
RHS^- &= \frac{iK}{2}A_0^2\left[\frac{k_0}{2}\left(e^{2i\Psi} - e^{-2i\Psi}\right) + \frac{k_0 C_g}{2\sinh(2q)}\left(e^{2i\Psi} - e^{-2i\Psi}\right)\right] \\
&= \frac{ik_0K}{4}A_0^2\left(1 + \frac{C_g}{\sinh(2q)}\right)\left(e^{2i\Psi} - e^{-2i\Psi}\right) \\
&= i\alpha_0\left(e^{2i\Psi} - e^{-2i\Psi}\right)
\end{aligned}$$

$$RHS^- = i\alpha_0\left(e^{2i\Psi} - e^{-2i\Psi}\right) \tag{3.3.3}$$

where the real constant α_0 is defined as:

$$\alpha_0 = \frac{k_0K}{4}A_0^2\left(1 + \frac{C_g}{\sinh(2q)}\right) \tag{3.3.4}$$

The right-hand side dictates the form of the particular solution P_{00}^- to the long wave equation in the '-' region:

$$P_{00}^-(x_1, t_1) = \widehat{C}_1^-\left(e^{2i\Psi} - e^{-2i\Psi}\right)$$

The value of the constant $\widehat{C}_1^-$ is determined by substituting the expression of P_{00}^- into the long wave equation (3.3.1). This gives

$$(-4\Omega^2 + 4HK^2)\widehat{C}_1^- = i\alpha_0$$

the constant $\widehat{C}_1^-$ is finally equal to

$$\widehat{C}_1^- = \frac{i\alpha_0}{4K^2(H - C_g^2)} \tag{3.3.5}$$

Note that the constant $\widehat{C}_1^-$ is purely imaginary and therefore the particular solution is real and equal to:

$$P_{00}^-(x_1, t_1) = \widehat{C}_1^- e^{2i\Psi} + c.c. \tag{3.3.6}$$

Physically the particular solution is the bound wave generated by the slow amplitude variation and propagating at the group velocity.

Now that a particular solution was found let us find the solution to the homogeneous equation. The homogeneous equation satisfied by the velocity potential Φ_{00}^- (physically the free wave) is simply the wave equation:

$$\Phi_{00,t_1t_1}^- - H\Phi_{00,x_1x_1}^- = 0$$

The most general solution is a superposition of two waves traveling with velocity $\sqrt{H}$ to the left and to the right. The radiation condition eliminates the existence of the right-going wave in the '-' region, as the wave can only be generated at the edge of the mud layer and propagate to the left, as opposed to being generated at $-\infty$ and propagate to the right. Therefore the oscillatory part of the homogeneous solution $G_{00}(x_1, t_1)$ depends only on one variable $x_1 + \sqrt{H}t_1$.

As the presence of the mud layer does not introduce any inhomogeneity in time, the solution can only be of the form

$$G_{00}^- = x_1\widehat{G}_0^- + \widehat{G}_1^- e^{2iK\frac{C_g}{\sqrt{H}}(x_1+\sqrt{H}t_1)} + \widehat{G}_2^- e^{-2iK\frac{C_g}{\sqrt{H}}(x_1+\sqrt{H}t_1)} \tag{3.3.7}$$

where the term $x_1\widehat{G}_0^-$ was introduced in order to allow the existence of a current in the left region that will match the boundary condition at the edge of the mud layer. Note that any constant would also be a solution of the homogeneous long wave equation, but a modification of the velocity potential by a constant does not affect any related physical quantity, since they are obtained by differentiation.
The values of $P_{00}^-(x_1,t_1)$ are real and as the velocity potential $\Phi_{00}^-(x_1,t_1) = P_{00}^-(x_1,t_1)+ G_{00}^-(x_1,t_1)$ is also real, hence the values of the $G_{00}^-(x_1,t_1)$ have to be real as well. Therefore

$$\widehat{G}_2^- = \left(\widehat{G}_1^-\right)^* \tag{3.3.8}$$

The total solution Φ_{00}^- is the superposition of the particular solution and the solution to the particular equation:

$$\Phi_{00}^-(x_1,t_1) = P_{00}^-(x_1,t_1) + G_{00}^-(x_1,t_1)$$

and its final expression is:

$$\Phi_{00}^-(x_1,t_1) = x_1\widehat{G}_0^- + \left[\widehat{G}_1^- e^{2iK\frac{C_g}{\sqrt{H}}(x_1+\sqrt{H}t_1)} + \widehat{C}_1^- e^{2i\Psi} + c.c\right] \tag{3.3.9}$$

3.3.2 Solution to the long wave equation in the '+' region

Let us now compute the right-hand side of the long wave equation in the '+' region:

$$\begin{aligned}
A^+ &= A_0 e^{ik_1x_1}\cos\Psi = \frac{A_0}{2}\left(e^{i[(K+k_1)x_1-\Omega t_1]} + e^{-[(K-k_1)x_1-\Omega t_1]}\right)\\
A^{+*}A^+ &= \frac{A_0^2}{4}\left(2e^{-2k_1^ix_1} + e^{2i[(K+ik_1^i)x_1-\Omega t_1]} + e^{-2i[(K-ik_1^i)x_1-\Omega t_1]}\right)\\
(A^{+*}A^+)_{x_1} &= \frac{A_0^2}{4}\left(-4k_1^ie^{-2k_1^ix_1} + 2i(K+ik_1^i)e^{2i[(K+ik_1^i)x_1-\Omega t_1]} - 2i(K-ik_1^i)e^{-2i[(K-ik_1^i)x_1-\Omega t_1]}\right)\\
&= \frac{iK}{2}A_0^2\left[2i\frac{k_1^i}{K}e^{-2k_1^ix_1} + \left(1+i\frac{k_1^i}{K}\right)e^{2i[(K+ik_1^i)x_1-\Omega t_1]} - \left(1-i\frac{k_1^i}{K}\right)e^{-2i[(K-ik_1^i)x_1-\Omega t_1]}\right]\\
(A^{+*}A^+)_{t_1} &= \frac{A_0^2}{4}\left(-2i\Omega e^{2i[(K+ik_1^i)x_1-\Omega t_1]} + 2i\Omega e^{-2i[(K-ik_1^i)x_1-\Omega t_1]}\right)\\
&= C_g\frac{iK}{2}A_0^2\left[-e^{2i[(K+ik_1^i)x_1-\Omega t_1]} + e^{-2i[(K-ik_1^i)x_1-\Omega t_1]}\right]
\end{aligned}$$

The right-hand side of the equation is then

$$\begin{aligned} RHS^{+} &= \frac{ik_0K}{4}A_0^2\Bigg\{2i\frac{k_1^i}{K}e^{-2k_1^ix_1} + \left[1+i\frac{k_1^i}{K}+\frac{C_g}{\sinh(2q)}\right]e^{2i[(K+ik_1^i)x_1-\Omega t_1]} \\ &\qquad - \left[1-i\frac{k_1^i}{K}+\frac{C_g}{\sinh(2q)}\right]e^{-2i[(K-ik_1^i)x_1-\Omega t_1]}\Bigg\} \\ &= i\alpha_0\Big\{2i\beta_0 e^{-2k_1^ix_1} + [1+i\beta_0]\,e^{2i[(K+ik_1^i)x_1-\Omega t_1]} - [1-i\beta_0]\,e^{-2i[(K-ik_1^i)x_1-\Omega t_1]}\Big\} \end{aligned}$$

with the real constant β_0 defined as

$$\beta_0 = \frac{k_1^i}{K}\left(\frac{1}{1+\frac{C_g}{\sinh(2q)}}\right) \tag{3.3.10}$$

By linearity the particular solution P_{00}^{+} can be obtained by linear superposition of

$$P_0^{+}(x_1,t_1) = \widehat{C}_0^{+}e^{-2k_1^ix_1} \tag{3.3.11}$$

$$P_1^{+}(x_1,t_1) = \widehat{C}_1^{+}e^{-2i[(K-ik_1^i)x_1-\Omega t_1]} \tag{3.3.12}$$

$$P_2^{+}(x_1,t_1) = \widehat{C}_2^{+}e^{2i[(K+ik_1^i)x_1-\Omega t_1]} \tag{3.3.13}$$

The constants $\widehat{C}_0^{+}$, $\widehat{C}_1^{+}$ and $\widehat{C}_2^{+}$ can be determined by substituting the expressions of $P_0^{+}(x_1,t_1)$, $P_1^{+}(x_1,t_1)$ and $P_2^{+}(x_1,t_1)$ into the long wave equation (3.3.1).
For the constant $\widehat{C}_0^{+}$ we get:

$$\begin{aligned} P_{0,t_1t_1}^{+} &= 0 \\ P_{0,x_1x_1}^{+} &= 4(k_1^i)^2\widehat{C}_0^{+}e^{-2k_1^ix_1} \end{aligned}$$

The partial long wave equation gives:

$$-H\times 4(k_1^i)^2\widehat{C}_0^{+}e^{-2k_1^ix_1} = -2\alpha_0\beta_0e^{-2k_1^ix_1}$$

therefore

$$\widehat{C}_0^{+} = \frac{\alpha_0\beta_0}{2H(k_1^i)^2} \tag{3.3.14}$$

For the constant $\widehat{C}_1^+$ we get:

$$\begin{aligned} P^+_{1,t_1t_1} &= -4\Omega^2\widehat{C}_1^+ e^{-2i[(K-ik_1^i)x_1-\Omega t_1]} \\ P^+_{1,x_1x_1} &= -4K^2\left(1-i\frac{k_1^i}{K}\right)\widehat{C}_1^+ e^{-2i[(K-ik_1^i)x_1-\Omega t_1]} \end{aligned}$$

The partial long wave equation gives:

$$\left[-4\Omega^2+4HK^2\left(1-i\frac{k_1^i}{K}\right)^2\right]\widehat{C}_1^+ = -(1-i\beta_0)i\alpha_0$$

therefore

$$\begin{aligned} \widehat{C}_1^+ &= -\frac{(1-i\beta_0)i\alpha_0}{4K^2\left[H\left(1-i\frac{k_1^i}{K}\right)^2-C_g^2\right]} = -\frac{i\alpha_0}{4K^2(H-C_g^2)}\left(\frac{1-i\beta_0}{1-2i\frac{H}{H-C_g^2}\frac{k_1^i}{K}-\frac{H}{H-C_g}\left(\frac{k_1^i}{K}\right)^2}\right) \\ &= -\gamma_0\widehat{C}_1^- \end{aligned}$$

where the complex constant γ_0 was defined as

$$\gamma_0 = \frac{1-i\beta_0}{1-2i\frac{H}{H-C_g^2}\frac{k_1^i}{K}-\frac{H}{H-C_g}\left(\frac{k_1^i}{K}\right)^2} \tag{3.3.15}$$

Note that when there is no mud to the right, k_1^i is equal to zero and $\gamma_0 = 1$.

For the constant $\widehat{C}_2^+$ we get:

$$\begin{aligned} P^+_{2,t_1t_1} &= -4\Omega^2\widehat{C}_2^+ e^{-2i[(K+ik_1^i)x_1-\Omega t_1]} \\ P^+_{2,x_1x_1} &= -4K^2\left(1+i\frac{k_1^i}{K}\right)\widehat{C}_2^+ e^{-2i[(K+ik_1^i)x_1-\Omega t_1]} \end{aligned}$$

The partial long wave equation gives:

$$\left[-4\Omega^2+4HK^2\left(1+i\frac{k_1^i}{K}\right)^2\right]\widehat{C}_2^+ = (1+i\beta_0)i\alpha_0$$

it is clear that

$$\widehat{C}_2^+ = \left(\widehat{C}_1^+\right)^* = -\gamma_0^* \left(\widehat{C}_1^-\right)^* = \gamma_0 \widehat{C}_1^- \tag{3.3.16}$$

Finally the particular solution is real and has the following expression:

$$P_{00}^+(x_1,t_1) = e^{-2k_1^i x_1}\left[\frac{\alpha_0\beta_0}{2H(k_1^i)^2} + \left(\gamma_0^* \widehat{C}_1^- e^{2i\Psi} + c.c.\right)\right] \tag{3.3.17}$$

The homogeneous solution is again the solution of the wave equation:

$$\Phi_{00,t_1t_1}^+ - H\Phi_{00,x_1x_1}^+ = 0$$

The radiation condition says that there is no wave generated in the infinity and therefore the free wave can only propagate to the right in the '+' region.

$$G_{00}^+ = \widehat{G}_1^+ e^{-2iK\frac{C_g}{\sqrt{H}}(x_1-\sqrt{H}t_1)} + \widehat{G}_2^+ e^{2iK\frac{C_g}{\sqrt{H}}(x_1-\sqrt{H}t_1)} \tag{3.3.18}$$

As opposed to the '-' region where short waves exist and propagate, the short waves are sooner or later damped in the '+' region. Therefore we cannot physically accept the mathematically acceptable steady current in the '+' region, which was accepted in the '-' region.

As the values of $P_{00}^+(x_1,t_1)$ are real and as the velocity potential $\Phi_{00}^+(x_1,t_1)$ is real the values of the $G_{00}^+(x_1,t_1)$ have to be real. Therefore

$$\widehat{G}_2^+ = \left(\widehat{G}_1^+\right)^* \tag{3.3.19}$$

Finally the velocity potential on the '+' region is the sum of a particular solution and the solution to the homogeneous equation:

$$\Phi_{00}^+(x_1,t_1) = G_{00}^+(x_1,t_1) + P_{00}^+(x_1,t_1)$$

and its final expression is:

$$\Phi_{00}^{+}(x_1,t_1)=\widehat{C}_0^{+}e^{-2k_1^i x_1}+\left[\widehat{G}_1^{+}e^{-2iK\frac{C_g}{\sqrt{H}}(x_1-\sqrt{H}t_1)}+\gamma_0^{*}\widehat{C}_1^{-}e^{-2k_1^i x_1}e^{2i\Psi}+c.c.\right] \quad (3.3.20)$$

The constants appearing in the expressions of Φ_{00}^{-} and Φ_{00}^{+} will be determined using the second order boundary conditions.

3.3.3 Second order boundary conditions at the edge of the mud layer

The boundary conditions at the edge of the mud layer $(x,x_1)=(0,0)$ are the pressure and horizontal flux continuity. They are at the second order:

$$\begin{aligned}\left(p_1^{(w)-}\right)\Big|_0 &= \left(p_1^{(w)+}\right)\Big|_0\\ \left(\Phi_{0,x_1}^{-}+\Phi_{1,x}^{-}\right)\Big|_0 &= \left(\Phi_{0,x_1}^{+}+\Phi_{1,x}^{+}\right)\Big|_0\end{aligned}$$

We are interested in the zeroth harmonic only and the corresponding boundary conditions are:

$$\begin{aligned}\left(p_{10}^{(w)-}\right)\Big|_0 &= \left(p_{10}^{(w)+}\right)\Big|_0\\ \left(\Phi_{00,x_1}^{-}\right)\Big|_0 &= \left(\Phi_{00,x_1}^{+}\right)\Big|_0\end{aligned}$$

The expression of the zeroth harmonic of the second order pressure was found in previous chapter and is

$$p_{10}^{(w)}=-\Phi_{00,t_1}-\frac{|A|^2}{4\sinh^2 q}\cosh(2Q)$$

As the amplitude of the free surface waves is continuous through the interface we obtain:

$$\left(\Phi^{-}_{00,t_1}\right)\Big|_0 = \left(\Phi^{+}_{00,t_1}\right)\Big|_0 \tag{3.3.21}$$

$$\left(\Phi^{-}_{00,x_1}\right)\Big|_0 = \left(\Phi^{+}_{00,x_1}\right)\Big|_0 \tag{3.3.22}$$

3.3.4 Constants in the expressions of the velocity potentials

To get the final expression of the velocity potentials we need to determine the values of the three constants $\widehat{G}^{-}_0$, $\widehat{G}^{-}_1$ and $\widehat{G}^{-}_2$ appearing in the expression of the the homogeneous solutions $G^{-}_{00}(x_1,t_1)$ and the two constants $\widehat{G}^{+}_1$ and $\widehat{G}^{+}_2$ appearing in the expression $G^{+}_{00}(x_1,t_1)$.

Let us apply the boundary conditions by starting by the continuity of the pressure at the edge of the mud layer (eq. 3.3.21). In the '-' region we have

$$\begin{aligned}
\Phi^{-}_{00,t_1}(x_1,t_1) &= P^{-}_{00,t_1}(x_1,t_1) + G^{-}_{00,t_1}(x_1,t_1) \\
P^{-}_{00,t_1}(x_1,t_1) &= 2i\Omega(-\widehat{C}^{-}_1)e^{-2i\Psi} + c.c. \\
G^{-}_{00,t_1}(x_1,t_1) &= 2i\Omega\widehat{G}^{-}_1 e^{2iK\frac{C_g}{\sqrt{H}}(x_1+\sqrt{H}t_1)} + c.c.
\end{aligned}$$

Thus

$$\Phi^{-}_{00,t_1}(x_1,t_1) = 2i\Omega(-\widehat{C}^{-}_1)e^{-2i\Psi} + 2i\Omega\widehat{G}^{-}_1 e^{2iK\frac{C_g}{\sqrt{H}}(x_1+\sqrt{H}t_1)} + c.c. \tag{3.3.23}$$

and at the edge of the mud layer $x_1 = 0$

$$\begin{aligned}
\left(\Phi^{-}_{00,t_1}\right)\Big|_0 &= \left[2i\Omega\widehat{G}^{-}_1 e^{2i\Omega t_1} - 2i\Omega\widehat{C}^{-}_1 e^{2i\Omega t_1} + c.c.\right] \\
&= \left[2i\Omega\left(\widehat{G}^{-}_1 - \widehat{C}^{-}_1\right)e^{2i\Omega t_1} + c.c.\right]
\end{aligned} \tag{3.3.24}$$

In the '+' region we have

$$\begin{aligned}
\Phi^{+}_{00,t_1}(x_1,t_1) &= P^{+}_{00,t_1}(x_1,t_1) + G^{+}_{00,t_1}(x_1,t_1) \\
P^{+}_{00,t_1}(x_1,t_1) &= e^{-2k_1^i x_1}\left[2i\Omega\gamma_0(-\widehat{C}_1^{-})e^{-2i\Psi} + c.c.\right] \\
G^{+}_{00,t_1}(x_1,t_1) &= 2i\Omega\widehat{G}_1^{+}e^{-2iK\frac{C_g}{\sqrt{H}}(x_1-\sqrt{H}t_1)} + c.c.
\end{aligned}$$

Thus

$$\Phi^{+}_{00,t_1}(x_1,t_1) = 2i\Omega\gamma_0(-\widehat{C}_1^{-})e^{-2k_1^i x_1}e^{-2i\Psi} + 2i\Omega\widehat{G}_1^{+}e^{-2iK\frac{C_g}{\sqrt{H}}(x_1-\sqrt{H}t_1)} + c.c. \quad (3.3.25)$$

and

$$\begin{aligned}
\left(\Phi^{+}_{00,t_1}\right)\Big|_0 &= \left[2i\Omega\widehat{G}_1^{+}e^{2i\Omega} - 2i\Omega\gamma_0\widehat{C}_1^{-}e^{2i\Omega} + c.c.\right] \\
&= 2i\Omega\left(\widehat{G}_1^{+} - \gamma_0\widehat{C}_1^{-}\right)e^{2i\Omega} + c.c. \qquad (3.3.26)
\end{aligned}$$

Equating the expressions of $\left(\Phi^{-}_{00,t_1}\right)\Big|_0$ and $\left(\Phi^{+}_{00,t_1}\right)\Big|_0$ (equations (3.3.24) and (3.3.26)) harmonic by harmonic we get:

$$\widehat{G}_1^{-} - \widehat{C}_1^{-} = \widehat{G}_1^{+} - \gamma_0\widehat{C}_1^{-} \qquad (3.3.27)$$

Now let us apply the flux continuity boundary condition (3.3.22) at the edge of the mud layer. In the '-' region we have:

$$\begin{aligned}
\Phi^{-}_{00,x_1}(x_1,t_1) &= P^{-}_{00,x_1}(x_1,t_1) + G^{-}_{00,x_1}(x_1,t_1) \\
P^{-}_{00,x_1}(x_1,t_1) &= -2iK(-\widehat{C}_1^{-})e^{-2i\Psi} + c.c. \\
G^{-}_{00,x_1}(x_1,t_1) &= \widehat{G}_0^{-} + \left[2iK\frac{C_g}{\sqrt{H}}\widehat{G}_1^{-}e^{2iK\frac{C_g}{\sqrt{H}}(x_1+\sqrt{H}t_1)} + c.c.\right]
\end{aligned}$$

Thus

$$\Phi^{-}_{00,x_1}(x_1,t_1) = \widehat{G}_0^{-} + \left[2iK\frac{C_g}{\sqrt{H}}\widehat{G}_1^{-}e^{2iK\frac{C_g}{\sqrt{H}}(x_1+\sqrt{H}t_1)} + 2iK\widehat{C}_1^{-}e^{-2i\Psi} + G^{-}_{00,x_1}(x_1,t_1) + c.c.\right] \quad (3.3.28)$$

and

$$\begin{aligned}\left(\Phi^-_{00,x_1}\right)\Big|_0 &= \widehat{G}^-_0 + \left[2iK\frac{C_g}{\sqrt{H}}\widehat{G}^-_1 e^{2i\Omega t_1} + 2iK\widehat{C}^-_1 e^{2i\Omega t_1} + c.c.\right] \\ &= \widehat{G}^-_0 + \left[2iK\frac{C_g}{\sqrt{H}}\left(\widehat{G}^-_1 + \frac{\sqrt{H}}{C_g}\widehat{C}^-_1\right)e^{2i\Omega t_1} + c.c.\right]\end{aligned}$$

In the '+' region we have

$$\begin{aligned}\Phi^+_{00,x_1}(x_1,t_1) &= P^+_{00,x_1}(x_1,t_1) + G^+_{00,x_1}(x_1,t_1) \\ P^+_{00,x_1}(x_1,t_1) &= e^{-2k^i_1 x_1}\left[-2k^i_1\widehat{C}^+_0 - 2i(K-ik^i_1)\gamma_0(-\widehat{C}^-_1)e^{-2i\Psi} + c.c.\right] \\ G^+_{00,x_1}(x_1,t_1) &= -2iK\frac{C_g}{\sqrt{H}}\widehat{G}^+_1 e^{-2iK\frac{C_g}{\sqrt{H}}(x_1-\sqrt{H}t_1)} + c.c.\end{aligned}$$

Thus

$$\begin{aligned}\Phi^+_{00,x_1}(x_1,t_1) &= e^{-2k^i_1 x_1}\left[-2k^i_1\widehat{C}^+_0 - 2i(K-ik^i_1)\gamma_0(-\widehat{C}^-_1)e^{-2i\Psi} + c.c\right] \\ &\quad -2iK\frac{C_g}{\sqrt{H}}\widehat{G}^+_1 e^{-2iK\frac{C_g}{\sqrt{H}}(x_1-\sqrt{H}t_1)} + c.c. \qquad (3.3.29)\end{aligned}$$

and

$$\left(\Phi^+_{00,x_1}\right)\Big|_0 = -2k^i_1\widehat{C}^+_0 + \left\{2iK\frac{C_g}{\sqrt{H}}\left[-\widehat{G}^+_1 + \frac{\sqrt{H}}{C_g}\left(1 - i\frac{k^i_1}{K}\right)\gamma_0\widehat{C}^-_1\right]e^{2i\Omega t_1} + c.c.\right\}$$

Equating the expressions of $\left(\Phi^-_{00,x_1}\right)\Big|_0$ and $\left(\Phi^+_{00,x_1}\right)\Big|_0$ harmonic by harmonic we get:

$$\widehat{G}^-_0 = -2k^i_1\widehat{C}^+_0 \qquad (3.3.30)$$

$$\widehat{G}^-_1 + \frac{\sqrt{H}}{C_g}\widehat{C}^-_1 = -\widehat{G}^+_1 + \frac{\sqrt{H}}{C_g}\left(1 - i\frac{k^i_1}{K}\right)\gamma_0\widehat{C}^-_1 \qquad (3.3.31)$$

This, together with the pressure continuity boundary condition, gives us a system of three equations for three unknown constants $\widehat{G}^-_0$, $\widehat{G}^-_1$, $\widehat{G}^+_0$ and $\widehat{G}^+_1$.
The expression of $\widehat{G}^-_0$ is clearly

$$\widehat{G}^-_0 = -2k^i_1\widehat{C}^+_0 \qquad (3.3.32)$$

To determine the expressions of the constants $\widehat{G}_1^-$ and $\widehat{G}_1^+$ we need to solve the following system:

$$\begin{aligned}\widehat{G}_1^- - \widehat{C}_1^- &= \widehat{G}_1^+ - \gamma_0 \widehat{C}_1^- \\ \widehat{G}_1^- + \frac{\sqrt{H}}{C_g}\widehat{C}_1^- &= -\widehat{G}_1^+ + \frac{\sqrt{H}}{C_g}\left(1 - i\frac{k_1^i}{K}\right)\gamma_0 \widehat{C}_1^-\end{aligned}$$

The sum of the last two equations gives:

$$2\widehat{G}_1^- + \frac{\sqrt{H}}{C_g}\widehat{C}_1^- - \widehat{C}_1^- = -\gamma_0 \widehat{C}_1^- + \frac{\sqrt{H}}{C_g}\left(1 - i\frac{k_1^i}{K}\right)\gamma_0 \widehat{C}_1^-$$

and the expression of $\widehat{G}_1^-$ is

$$\widehat{G}_1^- = \frac{1}{2}\widehat{C}_1^- \left\{1 - \gamma_0 - \frac{\sqrt{H}}{C_g}\left[1 - \gamma_0\left(1 - i\frac{k_1^i}{K}\right)\right]\right\} \tag{3.3.33}$$

The difference of the same two equations gives:

$$-\widehat{C}_1^- - \frac{\sqrt{H}}{C_g}\widehat{C}_1^- = 2\widehat{G}_1^+ - \gamma_0 \widehat{C}_1^- - \frac{\sqrt{H}}{C_g}\left(1 - i\frac{k_1^i}{K}\right)\gamma_0 \widehat{C}_1^-$$

and the expression of $\widehat{G}_1^+$ is

$$\widehat{G}_1^+ = \frac{1}{2}\widehat{C}_1^- \left\{-(1 - \gamma_0) - \frac{\sqrt{H}}{C_g}\left[1 - \gamma_0\left(1 - i\frac{k_1^i}{K}\right)\right]\right\} \tag{3.3.34}$$

3.3.5 Final expression of the velocity potentials

Let us now summarize the final expressions of the velocity potentials in the '-' and in the '+' region.

In the '-' region we have:

$$\Phi_{00}^-(x_1, t_1) = x_1 \widehat{G}_0^- + \left(\widehat{C}_1^- e^{2i\Psi} + \widehat{G}_1^- e^{2iK\frac{C_g}{\sqrt{H}}(x_1 + \sqrt{H}t_1)} + c.c.\right) \tag{3.3.35}$$

with constants $\widehat{G}_0^-$, $\widehat{C}_0^+$, $\widehat{C}_1^-$ and $\widehat{G}_1^-$ being defined as

$$\widehat{G}_0^- = -2k_1^i \widehat{C}_0^+ \tag{3.3.36}$$

$$\widehat{C}_0^+ = \frac{\alpha_0\beta_0}{2H(k_1^i)^2} = \frac{k_0 A_0^2}{8Hk_1^i} \tag{3.3.37}$$

$$\widehat{C}_1^- = \frac{i\alpha_0}{4K^2(H-C_g^2)} = \left(1+\frac{C_g}{\sinh(2q)}\right)\frac{ik_0A_0^2}{16K(H-C_g^2)} \tag{3.3.38}$$

$$\begin{aligned}\widehat{G}_1^- &= \frac{1}{2}\widehat{C}_1^-\left\{1-\gamma_0-\frac{\sqrt{H}}{C_g}\left[1-\gamma_0\left(1-i\frac{k_1^i}{K}\right)\right]\right\} \\ &= i\frac{k_0A_0^2\left(1+\frac{C_g}{\sinh(2q)}\right)}{32K(H-C_g^2)}\left\{1-\gamma_0-\frac{\sqrt{H}}{C_g}\left[1-\gamma_0\left(1-i\frac{k_1^i}{K}\right)\right]\right\}\end{aligned} \tag{3.3.39}$$

In the '+' region we have:

$$\begin{aligned}\Phi_{00}^+(x_1,t_1) &= \widehat{C}_0^+ e^{-2k_1^i x_1} \\ &\quad + \left[\gamma_0^*\widehat{C}_1^- e^{-2k_1^i x_1}e^{2i\Psi} + \widehat{G}_1^+ e^{-2iK\frac{C_g}{\sqrt{H}}(x_1-\sqrt{H}t_1)} + c.c.\right]\end{aligned} \tag{3.3.40}$$

with constants γ_0, β_0 and $\widehat{G}_1^+$ being defined as

$$\gamma_0 = \frac{1-i\beta_0}{1-2i\frac{H}{H-C_g^2}\frac{k_1^i}{K}-\frac{H}{H-C_g}\left(\frac{k_1^i}{K}\right)^2} \tag{3.3.41}$$

$$\beta_0 = \frac{k_1^i}{K}\left(\frac{1}{1+\frac{C_g}{\sinh(2q)}}\right) \tag{3.3.42}$$

$$\alpha_0 = \frac{k_0K}{4}A_0^2\left(1+\frac{C_g}{\sinh(2q)}\right) \tag{3.3.43}$$

$$\begin{aligned}\widehat{G}_1^+ &= \frac{1}{2}\widehat{C}_1^-\left\{-(1-\gamma_0)-\frac{\sqrt{H}}{C_g}\left[1-\gamma_0\left(1-i\frac{k_1^i}{K}\right)\right]\right\} \\ &= \frac{ik_0A_0^2\left(1+\frac{C_g}{\sinh(2q)}\right)}{32K(H-C_g^2)}\left\{-(1-\gamma_0)-\frac{\sqrt{H}}{C_g}\left[1-\gamma_0\left(1-i\frac{k_1^i}{K}\right)\right]\right\}\end{aligned} \tag{3.3.44}$$

3.4 The second order mean horizontal velocity

The second order mean horizontal velocity is $\mathcal{U} = \Phi_{00,x_1} + \Phi_{10,x} = \Phi_{00,x_1}$, where the fact that the potential Φ_{10} is independent of the fast scale x was used. The expressions of Φ^-_{00,x_1} and Φ^+_{00,x_1} were computed previously in both '-' and '+' regions and are given by equations (3.3.28) and (3.3.29).

In the '-' region we have:

$$\Phi^-_{00,x_1}(x_1,t_1) = \widehat{G}^-_0 + \left[2iK\frac{C_g}{\sqrt{H}}\widehat{G}^-_1 e^{2iK\frac{C_g}{\sqrt{H}}(x_1+\sqrt{H}t_1)} + 2iK\widehat{C}^-_1 e^{2i\Psi} + c.c.\right]$$

This expression of the velocity has three distinct parts: the mean current, the free wave and the bound wave. Let us study each of the components separately. First we introduce the new notations:

$$\Phi^-_{00,x_1}(x_1,t_1) = \mathcal{U}^-(x_1,t_1) = \langle\mathcal{U}^-\rangle + \widetilde{\mathcal{U}}^-_{\mathcal{F}} + \widetilde{\mathcal{U}}^-_{\mathcal{B}} \tag{3.4.1}$$

Where $\mathcal{U}^-$ is the total mean velocity in the '-' region, $\langle\mathcal{U}^-\rangle$ is the mean current, $\widetilde{\mathcal{U}}^-_{\mathcal{F}}$ is the velocity of the free wave and $\widetilde{\mathcal{U}}^-_{\mathcal{B}}$ is the velocity of the bound wave.

The mean current $\langle\mathcal{U}^-\rangle$ in the '-' region is:

$$\langle\mathcal{U}^-\rangle = \widehat{G}^-_0 = -\frac{k_0A_0^2}{4H} = -U^-_M \tag{3.4.2}$$

Where the constant U^-_M represents the amplitude of the mean current at the edge of the mud layer and is given by:

$$U^-_M = \frac{k_0A_0^2}{4H}$$

Even though the mean current is constant in the '-' region, it will decay exponentially in the '+' region. This is the reason why we introduce the new notation U^-_M.

The steady current is always negative and is generated at the edge of the mud layer. As long as the mud layer exists in the '+' region, there will be steady flux to the left in the '-' region. As will be seen later, this is due to the fact that the t_1 averaged pressure $\langle p^{(w)}_{10}\rangle$ is increasing with x_1 in the '+' region and is pushing the fluid to the

left, creating a negative current in both '-' and '+' regions.

The free wave velocity $\widetilde{\mathcal{U}}_{\mathcal{F}}^{-}$ in the '-' region is:

$$\begin{aligned}
\widetilde{\mathcal{U}}_{\mathcal{F}}^{-} &= 2iK\frac{C_g}{\sqrt{H}}\widehat{G}_1^{-}e^{2iK\frac{C_g}{\sqrt{H}}(x_1+\sqrt{H}t_1)} + c.c. \\
&= 4K\frac{C_g}{\sqrt{H}}\Re\left\{i\widehat{G}_1^{-}e^{2iK\frac{C_g}{\sqrt{H}}(x_1+\sqrt{H}t_1)}\right\} \\
&= -\frac{k_0A_0^2\frac{C_g}{\sqrt{H}}\left(1+\frac{C_g}{\sinh(2q)}\right)}{8(H-C_g^2)}\Re\left\{\left\{1-\gamma_0-\frac{\sqrt{H}}{C_g}\left[1-\gamma_0\left(1-i\frac{k_1^i}{K}\right)\right]\right\}e^{2iK\frac{C_g}{\sqrt{H}}(x_1+\sqrt{H}t_1)}\right\} \\
&= \frac{k_0A_0^2\frac{C_g}{\sqrt{H}}\left(1+\frac{C_g}{\sinh(2q)}\right)}{8(H-C_g^2)}\times \\
&\quad\times\left|1-\gamma_0-\frac{\sqrt{H}}{C_g}\left[1-\gamma_0\left(1-i\frac{k_1^i}{K}\right)\right]\right|\cos\left[2K\frac{C_g}{\sqrt{H}}(x_1+\sqrt{H}t_1+\phi_F^{-}+\pi)\right]
\end{aligned}$$

Where ϕ_F^{-} is the phase of the complex parameter $1-\gamma_0-\frac{\sqrt{H}}{C_g}\left[1-\gamma_0\left(1-i\frac{k_1^i}{K}\right)\right]$.

Finally the free wave velocity in the '-' region $\widetilde{\mathcal{U}}_{\mathcal{F}}^{-}$ is

$$\widetilde{\mathcal{U}}_{\mathcal{F}}^{-} = U_F^{-}\cos\left[2K\frac{C_g}{\sqrt{H}}(x_1+\sqrt{H}t_1)+\phi_F^{-}+\pi\right] \tag{3.4.3}$$

with the amplitude U_F^{-} given by:

$$U_F^{-} = \frac{k_0A_0^2\frac{C_g}{\sqrt{H}}\left(1+\frac{C_g}{\sinh(2q)}\right)}{8(H-C_g^2)}\left|1-\gamma_0-\frac{\sqrt{H}}{C_g}\left[1-\gamma_0\left(1-i\frac{k_1^i}{K}\right)\right]\right| \tag{3.4.4}$$

The velocity $\widetilde{\mathcal{U}}_{\mathcal{B}}^{-}$ of the bound wave is:

$$\begin{aligned}
\widetilde{\mathcal{U}}_{\mathcal{B}}^{-} &= 2iK\widehat{C}_1^{-}e^{2i\Psi} + c.c. = 4K\Re\left\{i\widehat{C}_1^{-}e^{2i\Psi}\right\} \\
&= -\left(1+\frac{C_g}{\sinh(2q)}\right)\frac{k_0A_0^2}{4(H-C_g^2)}\cos(2\Psi)
\end{aligned}$$

Or, written in a more compact form:

$$\widetilde{\mathcal{U}}_{\mathcal{B}}^{-} = U_B^{-}\cos 2\left(Kx_1-\Omega t_1+\frac{\pi}{2}\right) \tag{3.4.5}$$

with the amplitude U_B^-

$$U_B^- = \left(1 + \frac{C_g}{\sinh(2q)}\right) \frac{k_0 A_0^2}{4(H - C_g^2)} \tag{3.4.6}$$

In the '+' region the total mean velocity $\Phi^+_{00,x_1}(x_1,t_1)$ is given by the equation (eq. 3.3.29) and is rewritten for easier reference below:

$$\begin{aligned}\Phi^+_{00,x_1}(x_1,t_1) &= -2k_1^i \widehat{C}_0^+ e^{-2k_1^i x_1} \\ &+ \left[-2iK\frac{C_g}{\sqrt{H}}\widehat{G}_1^+ e^{-2iK\frac{C_g}{\sqrt{H}}(x_1-\sqrt{H}t_1)} + 2iK\left(1 - i\frac{k_1^i}{K}\right)\gamma_0 \widehat{C}_1^- e^{-2k_1^i x_1} e^{2i\Psi} + c.c.\right]\end{aligned}$$

As in the case of the '-' region the expression of the mean velocity $\Phi^+_{00,x_1}(x_1,t_1)$ has three distinct parts: the mean current, the free wave and the bound wave. Let us study each of the components separately. First we introduce the new notations:

$$\Phi^+_{00,x_1}(x_1,t_1) = \mathcal{U}^+(x_1,t_1) = \langle \mathcal{U}^+ \rangle + \widetilde{\mathcal{U}}_{\mathcal{F}}^+ + \widetilde{\mathcal{U}}_{\mathcal{B}}^+ \tag{3.4.7}$$

Where U^+ is the total mean velocity in the '+' region, $\langle U^+ \rangle$ is the mean current, $\widetilde{U}_F^+$ is the velocity of the free wave and $\widetilde{U}_B^+$ is the velocity of the bound wave.
The mean current $\langle U^+ \rangle$ in the '+' region is:

$$\langle \mathcal{U}^+ \rangle = -2k_1^i \widehat{C}_0^+ e^{-2k_1^i x_1} = -\frac{k_0 A_0^2}{4H} e^{-2k_1^i x_1} = -U_M^+ e^{-2k_1^i x_1}$$

Where the parameter U_M^+ represents the amplitude of the mean current at the edge of the mud layer and its expression is given by:

$$U_M^+ = \frac{k_0 A_0^2}{4H} \tag{3.4.8}$$

The last expression shows that the mean current is also negative in the '+' region and decreases exponentially with $k_1^i x_1$. Naturally at $+\infty$ when the short waves are totally damped the t_1 averaged mean current $\langle \mathcal{U}^+ \rangle$ vanishes.

The free wave velocity $\widetilde{\mathcal{U}}_{\mathcal{F}}^{+}$ in the '+' region is:

$$\begin{aligned}
\widetilde{\mathcal{U}}_{\mathcal{F}}^{+} &= -2iK\frac{C_g}{\sqrt{H}}\widehat{G}_1^{+}e^{-2iK\frac{C_g}{\sqrt{H}}(x_1-\sqrt{H}t_1)} + c.c \\
&= -4K\frac{C_g}{\sqrt{H}}\Re\left\{i\widehat{G}_1^{+}e^{-2iK\frac{C_g}{\sqrt{H}}(x_1-\sqrt{H}t_1)}\right\} \\
&= -\frac{k_0A_0^2\frac{C_g}{\sqrt{H}}\left(1+\frac{C_g}{\sinh(2q)}\right)}{8(H-C_g^2)}\Re\left\{\left\{(1-\gamma_0)+\frac{\sqrt{H}}{C_g}\left[1-\gamma_0\left(1-i\frac{k_1^i}{K}\right)\right]\right\}e^{-2iK\frac{C_g}{\sqrt{H}}(x_1-\sqrt{H}t_1)}\right\} \\
&= \frac{k_0A_0^2\frac{C_g}{\sqrt{H}}\left(1+\frac{C_g}{\sinh(2q)}\right)}{8(H-C_g^2)}\times \\
&\quad\times\left|(1-\gamma_0)+\frac{\sqrt{H}}{C_g}\left[1-\gamma_0\left(1-i\frac{k_1^i}{K}\right)\right]\right|\cos\left[2K\frac{C_g}{\sqrt{H}}(x_1-\sqrt{H}t_1)-\phi_F^{+}+\pi\right]
\end{aligned}$$

Or, in a more compact form the free wave velocity $\widetilde{\mathcal{U}}_{\mathcal{F}}^{+}$ in the plus region is:

$$\widetilde{\mathcal{U}}_{\mathcal{F}}^{+} = U_F^{+}\cos\left[2K\frac{C_g}{\sqrt{H}}(x_1-\sqrt{H}t_1)-\phi_F^{+}+\pi\right] \tag{3.4.9}$$

with the amplitude U_F^{+} of the free wave given by:

$$U_F^{+} = \frac{k_0A_0^2\frac{C_g}{\sqrt{H}}\left(1+\frac{C_g}{\sinh(2q)}\right)}{8(H-C_g^2)}\times\left|(1-\gamma_0)+\frac{\sqrt{H}}{C_g}\left[1-\gamma_0\left(1-i\frac{k_1^i}{K}\right)\right]\right| \tag{3.4.10}$$

The velocity $\widetilde{\mathcal{U}}_{\mathcal{B}}^{+}$ of the bound wave in the '+' region is:

$$\begin{aligned}
\widetilde{\mathcal{U}}_{\mathcal{B}}^{+} &= 2iK\left(1-i\frac{k_1^i}{K}\right)\gamma_0\widehat{C}_1^{-}e^{-2k_1^ix_1}e^{2i\Psi} + c.c. \\
&= 4K\Re\left\{i\left(1-i\frac{k_1^i}{K}\right)\gamma_0\widehat{C}_1^{-}e^{-2k_1^ix_1}e^{2i\Psi}\right\} \\
&= -\left(1+\frac{C_g}{\sinh(2q)}\right)\frac{k_0A_0^2}{4(H-C_g^2)}e^{-2k_1^ix_1}\Re\left\{\left(1-i\frac{k_1^i}{K}\right)\gamma_0e^{2i\Psi}\right\} \\
&= -\frac{k_0A_0^2\left(1+\frac{C_g}{\sinh(2q)}\right)}{4(H-C_g^2)}\left|\gamma_0\left(1-i\frac{k_1^i}{K}\right)\right|e^{-2k_1^ix_1}\cos 2\Psi
\end{aligned}$$

A more compact expression is

$$\widetilde{\mathcal{U}}_{\mathcal{B}}^{+} = U_B^{+} e^{-2k_1^i x_1} \cos 2\left(Kx_1 - \Omega t_1 + \frac{\pi}{2}\right) \tag{3.4.11}$$

with the amplitude U_B^+ defined as:

$$U_B^{+} = \frac{k_0 A_0^2 \left(1 + \frac{C_g}{\sinh(2q)}\right)}{4(H - C_g^2)} \left|\gamma_0 \left(1 - i\frac{k_1^i}{K}\right)\right| \tag{3.4.12}$$

Note that the factor $\frac{k_0 A_0^2}{4H}$ is common to all six constants U_M^-, U_M^+, U_F^-, U_F^+, U_B^- and U_B^+ can be rewritten using the dispersion relation (2.4.5) in terms of $k_0 H$ only:

$$\frac{k_0 A_0^2}{4H} = \frac{k_0^2 A_0^2}{4k_0 H} = \frac{A_0^2}{4k_0 H \tanh^2(k_0 H)} \tag{3.4.13}$$

Let us summarize the results for the mean velocity.

In the '-' region we have:

$$\mathcal{U}^-(x_1, t_1) = \langle \mathcal{U}^- \rangle + \widetilde{\mathcal{U}}_{\mathcal{F}}^- + \widetilde{\mathcal{U}}_{\mathcal{B}}^- \tag{3.4.14}$$

$$\langle \mathcal{U}^- \rangle = -U_M^- \tag{3.4.15}$$

$$\widetilde{\mathcal{U}}_{\mathcal{F}}^- = U_F^- \cos\left[2K\frac{C_g}{\sqrt{H}}(x_1 + \sqrt{H}t_1) + \phi_F^- + \pi\right] \tag{3.4.16}$$

$$\widetilde{\mathcal{U}}_{\mathcal{B}}^- = U_B^- \cos 2(Kx_1 - \Omega t_1 + \frac{\pi}{2}) \tag{3.4.17}$$

With the constants U_M^-, U_F^- and U_B^- defined as

$$U_M^- = \frac{k_0 A_0^2}{4H} \tag{3.4.18}$$

$$U_F^- = \frac{k_0 A_0^2}{4H} \frac{\frac{C_g}{\sqrt{H}}\left(1 + \frac{C_g}{\sinh(2q)}\right)}{2(1 - \frac{C_g^2}{H})} \left|1 - \gamma_0 - \frac{\sqrt{H}}{C_g}\left[1 - \gamma_0\left(1 - i\frac{k_1^i}{K}\right)\right]\right| \tag{3.4.19}$$

$$U_B^- = \frac{k_0 A_0^2}{4H} \frac{\left(1 + \frac{C_g}{\sinh(2q)}\right)}{(1 - \frac{C_g^2}{H})} \tag{3.4.20}$$

In the '+' region we have:

$$\mathcal{U}^+(x_1,t_1) = \langle \mathcal{U}^+ \rangle + \widetilde{\mathcal{U}}_{\mathcal{F}}^+ + \widetilde{\mathcal{U}}_{\mathcal{B}}^+ \tag{3.4.21}$$

$$\langle \mathcal{U}^+ \rangle = -U_M^+ e^{-2k_1^i x_1} \tag{3.4.22}$$

$$\widetilde{\mathcal{U}}_{\mathcal{F}}^+ = U_F^+ \cos\left[2K\frac{C_g}{\sqrt{H}}(x_1 - \sqrt{H}t_1) - \phi_F^+ + \pi\right] \tag{3.4.23}$$

$$\widetilde{\mathcal{U}}_{\mathcal{B}}^+ = U_B^+ e^{-2k_1^i x_1}\cos\left[2(Kx_1 - \Omega t_1) + \pi\right] \tag{3.4.24}$$

With the constants U_M^-, U_F^- and U_B^- defined as

$$U_M^+ = \frac{k_0 A_0^2}{4H} \tag{3.4.25}$$

$$U_F^+ = \frac{k_0 A_0^2}{4H}\frac{\frac{C_g}{\sqrt{H}}\left(1+\frac{C_g}{\sinh(2q)}\right)}{2\left(1-\frac{C_g^2}{H}\right)}\left|1-\gamma_0+\frac{\sqrt{H}}{C_g}\left[1-\gamma_0\left(1-i\frac{k_1^i}{K}\right)\right]\right| \tag{3.4.26}$$

$$U_B^+ = \frac{k_0 A_0^2}{4H}\frac{\left(1+\frac{C_g}{\sinh(2q)}\right)}{\left(1-\frac{C_g^2}{H}\right)}\left|\gamma_0\left(1-i\frac{k_1^i}{K}\right)\right| \tag{3.4.27}$$

Note that all the amplitudes depend only on two parameters: the dimensionless depth $k_0 H$ and the fraction $\frac{k_1^i}{K}$ representing the ratio of the characteristic length of modulation to the characteristic length of damping. The constant mean current $\langle \Phi_{00,x_1} \rangle$ is the same in both '-' and '+' regions, depends only on the dimensionless depth $k_0 H$ and is equal to

$$\langle \Phi_{00,x_1} \rangle = -\frac{k_0 A_0^2}{4H} = -\frac{A_0^2}{4k_0 H \tan(k_0 H)} \tag{3.4.28}$$

The amplitude of the mean current $|\langle \Phi_{00,x_1} \rangle|$ is plotted in figure (3-2). From this figure it can be seen that the value of the current is singular for $k_0 H = 0$ and the theory is invalid for too shallow water, as the theory was developed for a water layer of intermediate depth $k_0 H = O(1)$. The current is weak in deep water and increases in intensity in shallow water.

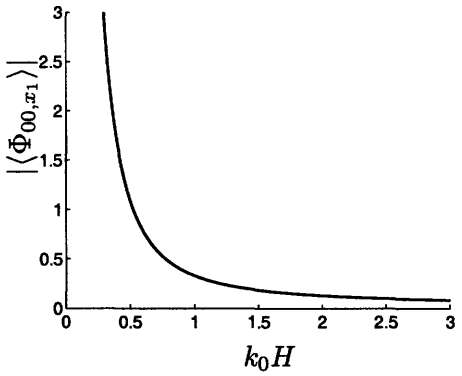

Figure 3-2: Amplitude of the mean current $\langle\Phi_{00,x_1}\rangle = U_M^- = U_M^+$

3.5 Second order mean pressure

As it was shown in chapter 2 (eq. 2.4.19) the second order mean pressure has the following expression

$$p_{10}^{(w)} = -\Phi_{00,t_1} - \frac{|A|^2}{4\sinh^2 q}\cosh(2Q)$$

The last term on the right-hand side can easily be evaluated in both '-' and '+' regions.

In the '- region we have:

$$|A^-|^2 \;=\; A_0^2\cos^2\Psi = \frac{A_0^2}{4}\left[2 + \left(e^{2i\Psi} + c.c.\right)\right]$$

The first term of the right-hand side of the second order mean pressure has been computed previously and is given by the equation (3.3.23):

$$\Phi^-_{00,t_1}(x_1,t_1) \;=\; \left[2i\Omega\widehat{G}_1^- e^{2iK\frac{C_g}{\sqrt{H}}(x_1+\sqrt{H}t_1)} - 2i\Omega\widehat{C}_1^- e^{2i\Psi} + c.c.\right]$$

The second order mean pressure in the '-' region becomes:

$$p_{10}^{(w)-} = -\frac{\cosh(2Q)}{8\sinh^2 q}A_0^2 - \left[2i\Omega\widehat{G}_1^- e^{2iK\frac{C_g}{\sqrt{H}}(x_1+\sqrt{H}t_1)} - \left(2i\Omega\widehat{C}_1^- - \frac{\cosh(2Q)}{16\sinh^2 q}A_0^2\right)e^{2i\Psi} + c.c.\right] \tag{3.5.1}$$

The averaged in t_1 slowly varying pressure is

$$\langle p_{10}^{(w)-} \rangle = -\frac{\cosh(2Q)}{8\sinh^2 q} A_0^2 = -\frac{k_0 A_0^2}{4} \frac{\cosh(2Q)}{\sinh 2q}$$

In the '+' region we have:

$$|A^+|^2 = A_0^2 e^{-2k_1^i x_1} \cos^2 \Psi = \frac{A_0^2}{4} e^{-2k_1^i x_1} \left[2 + \left(e^{2i\Psi} + c.c.\right)\right]$$

The first term of the right-hand side of the second order mean pressure has been computed previously and is given by the equation (3.3.25):

$$\Phi^+_{00,t_1}(x_1, t_1) = \left[2i\Omega \widehat{G}_1^+ e^{-2iK\frac{C_g}{\sqrt{H}}(x_1 - \sqrt{H}t_1)} - 2i\Omega\gamma_0^* \widehat{C}_1^- e^{-2k_1^i x_1} e^{2i\Psi} + c.c.\right]$$

The second order mean pressure in the '+' region becomes:

$$\begin{aligned} p_{10}^{(w)+} = & -\frac{\cosh(2Q)}{8\sinh^2 q} A_0^2 e^{-2k_1^i x_1} \\ & - \left[2i\Omega \widehat{G}_1^+ e^{-2iK\frac{C_g}{\sqrt{H}}(x_1 - \sqrt{H}t_1)} - \left(2i\Omega\gamma_0^* \widehat{C}_1^- - \frac{\cosh(2Q)}{16\sinh^2 q} A_0^2\right) e^{-2k_1^i x_1} e^{2i\Psi} + c.c.\right] \end{aligned} \tag{3.5.2}$$

The averaged in t_1 slowly varying pressure is

$$\langle p_{10}^{(w)+} \rangle = -\frac{\cosh(2Q)}{8\sinh^2 q} A_0^2 e^{-2k_1^i x_1} = -\frac{k_0 A_0^2}{4} \frac{\cosh(2Q)}{\sinh 2q} e^{-2k_1^i x_1}$$

Note that at large values of x_1 the averaged pressure vanishes

$$\langle p_{10}^{(w)+} \rangle \to 0$$

and this term is due exclusively to the free wave generated by the presence of the mud layer and traveling with the velocity $\sqrt{H}$.

In particular we see that the averaged in t_1 pressure increases with x_1. Therefore we expect to have a mean current independent of t_1 and going to the left.

3.6 Second order mean free surface displacement

As it was shown in chapter 2 (eq. 2.4.20) the second order mean free surface displacement has the following expression

$$\eta_{10} = -\Phi_{00,t_1} - \frac{|A|^2}{4\sinh^2 k_0 H}$$

This expression is in all ways similar to the second order mean pressure expression except for the factor $\cos 2Q$. The expressions for the free-surface displacement can be deduced right away.

In the '-' region we use the equation (3.5.1) and replace $\cos 2Q$ by 1 to get:

$$\eta_{10}^{-} = -\frac{A_0^2}{8\sinh^2 k_0 H} - \left[2i\Omega\widehat{G}_1^{-} e^{2iK\frac{C_g}{\sqrt{H}}(x_1+\sqrt{H}t_1)} - \left(2i\Omega\widehat{C}_1^{-} - \frac{A_0^2}{16\sinh^2 k_0 H}\right)e^{2i\Psi} + c.c.\right]$$

Similarly to the case of the mean long wave velocity, the last equation shows that the mean free surface displacement η_{10}^{-} consists of three distinct terms. The first one represents a constant free surface set down and is due to the short waves modulation, the second is the free wave contribution and the last term is due to the short waves modulation. Let us study each of the terms separately. Let us first introduce short notations for each of the above mentioned terms:

$$\eta_{10}^{-}(x_1,t_1) = \mathcal{N}^{-}(x_1,t_1) = \langle\mathcal{N}^{-}\rangle + \mathcal{N}_{\mathcal{F}}^{-} + \mathcal{N}_{\mathcal{B}}^{-} \tag{3.6.1}$$

where $\langle\mathcal{N}^{-}\rangle$ is the constant free surface set down,$\mathcal{N}_{\mathcal{F}}^{-}$ is the mean free surface displacement due to the free waves generated at the edge of the mud layer and $\mathcal{N}_{\mathcal{B}}^{-}$ is the mean free surface displacement due to the bound waves. Let us now compute the expressions of each of these three terms.

The constant free surface set down in the '-' region is

$$\langle\mathcal{N}^{-}\rangle = -N_M^{-} \tag{3.6.2}$$

with N_M^- being the amplitude of the set down, which expression follows straightforwardly from the equation (3.6.1):

$$N_M^- = \frac{A_0^2}{8\sinh^2 k_0 H} \tag{3.6.3}$$

The mean free surface displacement $\mathcal{N}_{\mathcal{F}}^-$ due to the free wave generated at the edge of the mud layer is:

$$\begin{aligned}
\mathcal{N}_{\mathcal{F}}^- &= 2\Re\left\{-2i\Omega\widehat{G}_1^- e^{2iK\frac{C_g}{\sqrt{H}}(x_1+\sqrt{H}t_1)}\right\} \\
&= -4\Omega\Re\left\{i\widehat{G}_1^- e^{2iK\frac{C_g}{\sqrt{H}}(x_1+\sqrt{H}t_1)}\right\} \\
&= \frac{k_0 A_0^2\left(1+\frac{C_g}{\sinh(2q)}\right)}{8K(H-C_g^2)}\Omega\Re\left\{\left[1-\gamma_0-\frac{\sqrt{H}}{C_g}\left[1-\gamma_0\left(1-i\frac{k_1^i}{K}\right)\right]\right]e^{2iK\frac{C_g}{\sqrt{H}}(x_1+\sqrt{H}t_1)}\right\} \\
&= \frac{k_0 A_0^2}{8H}C_g\left(\frac{1+\frac{C_g}{\sinh(2q)}}{1-\frac{C_g^2}{H}}\right)\left|1-\gamma_0-\frac{\sqrt{H}}{C_g}\left[1-\gamma_0\left(1-i\frac{k_1^i}{K}\right)\right]\right|\times \\
&\qquad \times\cos\left(2K\frac{C_g}{\sqrt{H}}(x_1+\sqrt{H}t_1)+\phi_F^-\right)
\end{aligned} \tag{3.6.4}$$

where the constant $\widehat{G}_1^-$ was replaced by its previously computed expression (3.3.39) and where ϕ_F^- is the phase of the complex parameter $1-\gamma_0-\frac{\sqrt{H}}{C_g}\left[1-\gamma_0\left(1-i\frac{k_1^i}{K}\right)\right]$. The mean free surface displacement $\mathcal{N}_{\mathcal{F}}^-$ due to the free wave can be rewritten as

$$\mathcal{N}_{\mathcal{F}}^- = N_F^-\cos\left(2K\frac{C_g}{\sqrt{H}}(x_1+\sqrt{H}t_1)+\phi_F^-\right) \tag{3.6.5}$$

With the amplitude N_F^- of the mean free surface displacement due to the free wave:

$$N_F^- = \frac{k_0 A_0^2}{8H}C_g\left(\frac{1+\frac{C_g}{\sinh(2q)}}{1-\frac{C_g^2}{H}}\right)\left|1-\gamma_0-\frac{\sqrt{H}}{C_g}\left[1-\gamma_0\left(1-i\frac{k_1^i}{K}\right)\right]\right| \tag{3.6.6}$$

The mean free surface displacement $\mathcal{N}_{\mathcal{B}}^{-}$ due to the bound wave generated by the slow modulations of the short waves envelope is:

$$\begin{aligned}
\mathcal{N}_{\mathcal{B}}^{-} &= 2\Re\left\{\left(2i\Omega\widehat{C}_1^{-} - \frac{A_0^2}{16\sinh^2 k_0 H}\right)e^{2i\Psi}\right\} \\
&= 4\Omega\Re\left\{\left(i\widehat{C}_1^{-} - \frac{1}{\Omega}\frac{A_0^2}{16\sinh^2 k_0 H}\right)e^{2i\Psi}\right\} \\
&= 4\Omega\Re\left\{\left[-\left(1+\frac{C_g}{\sinh(2q)}\right)\frac{k_0 A_0^2}{16K(H-C_g^2)} - \frac{1}{\Omega}\frac{A_0^2}{16\sinh^2 k_0 H}\right]e^{2i\Psi}\right\} \\
&= \frac{k_0 A_0^2}{4HK}\Omega\left[\left(1+\frac{C_g}{\sinh(2q)}\right)\frac{1}{(1-\frac{C_g^2}{H})} + \frac{K}{\Omega}\frac{H}{k_0\sinh^2 k_0 H}\right]\cos\left[2(Kx_1-\Omega t_1)+\pi\right] \\
&= \frac{k_0 A_0^2}{4H}\left[C_g\left(\frac{1+\frac{C_g}{\sinh(2q)}}{(1-\frac{C_g^2}{H})}\right) + \frac{k_0 H}{\cosh^2 k_0 H}\right]\cos\left[2(Kx_1-\Omega t_1)+\pi\right]
\end{aligned} \tag{3.6.7}$$

Where we used the dispersion relation (2.4.5) and the expression (3.3.38) of the constant C_1^{-}. Finally the mean free surface displacement $\mathcal{N}_{\mathcal{B}}^{-}$ due to the bound wave generated by the slow modulations of the short waves envelope is:

$$\mathcal{N}_{\mathcal{B}}^{-} = N_B^{-}\cos\left[2(Kx_1-\Omega t_1)+\pi\right] \tag{3.6.8}$$

with N_B^{-} being the amplitude of the surface wave:

$$N_B^{-} = \frac{k_0 A_0^2}{4H}\left[C_g\left(\frac{1+\frac{C_g}{\sinh(2q)}}{(1-\frac{C_g^2}{H})}\right) + \frac{k_0 H}{\cosh^2 k_0 H}\right] \tag{3.6.9}$$

In the '+' region we use the equation (3.5.2) and replace $\cos 2Q$ by 1 to get:

$$\begin{aligned}
\eta_{10}^{+} &= -\frac{1}{8\sinh^2 q}A_0^2 e^{-2k_1^i x_1} \\
&\quad - \left[2i\Omega\widehat{G}_1^{+}e^{-2iK\frac{C_g}{\sqrt{H}}(x_1-\sqrt{H}t_1)} - \left(2i\Omega\gamma_0^{*}\widehat{C}_1^{-} - \frac{1}{16\sinh^2 q}A_0^2\right)e^{-2k_1^i x_1}e^{2i\Psi} + c.c.\right]
\end{aligned} \tag{3.6.10}$$

As in the case of the '-' region, the last equation shows that the mean free surface displacement η_{10}^{+} consists of three distinct terms. The first one represents a constant free surface set down and is due to the short waves modulation, the second is the free wave contribution and the last term is due to the short waves modulation. Let us study each of the terms separately. Let us first introduce short notations for each of the above mentioned terms:

$$\eta_{10}^{+}(x_1,t_1) = \mathcal{N}^{+}(x_1,t_1) = \langle \mathcal{N}^{+} \rangle + \mathcal{N}_{\mathcal{F}}^{+} + \mathcal{N}_{\mathcal{B}}^{+} \tag{3.6.11}$$

The constant free surface set down in the '+' region is

$$\langle \mathcal{N}^{+} \rangle = -N_M^{+} e^{-2k_1^{i} x_1} \tag{3.6.12}$$

with N_M^{+} being the amplitude of the set down, which expression follows straightforwardly from the equation (3.6.10):

$$N_M^{+} = \frac{A_0^2}{8 \sinh^2 k_0 H} = N_M^{-} \tag{3.6.13}$$

The mean free surface displacement $\mathcal{N}_{\mathcal{F}}^{+}$ due to the free wave generated at the edge of the mud layer is:

$$\begin{aligned}
\mathcal{N}_{\mathcal{F}}^{+} &= 2\Re\left\{-2i\Omega\widehat{G}_1^{+}e^{-2iK\frac{C_g}{\sqrt{H}}(x_1-\sqrt{H}t_1)}\right\} \\
&= 4\Omega\Re\left\{\frac{k_0A_0^2\left(1+\frac{C_g}{\sinh(2q)}\right)}{32K(H-C_g^2)}\left\{-(1-\gamma_0)-\frac{\sqrt{H}}{C_g}\left[1-\gamma_0\left(1-i\frac{k_1^i}{K}\right)\right]\right\}e^{-2iK\frac{C_g}{\sqrt{H}}(x_1-\sqrt{H}t_1)}\right\} \\
&= \frac{k_0A_0^2\left(1+\frac{C_g}{\sinh(2q)}\right)}{8K(H-C_g^2)}\Omega\Re\left\{\left[-(1-\gamma_0)-\frac{\sqrt{H}}{C_g}\left[1-\gamma_0\left(1-i\frac{k_1^i}{K}\right)\right]\right]e^{-2iK\frac{C_g}{\sqrt{H}}(x_1-\sqrt{H}t_1)}\right\} \\
&= \frac{k_0A_0^2}{8H}C_g\left(\frac{1+\frac{C_g}{\sinh(2q)}}{1-\frac{C_g^2}{H}}\right)\Re\left\{\left[(1-\gamma_0)+\frac{\sqrt{H}}{C_g}\left[1-\gamma_0\left(1-i\frac{k_1^i}{K}\right)\right]\right]e^{i\pi-2iK\frac{C_g}{\sqrt{H}}(x_1-\sqrt{H}t_1)}\right\} \\
&= \frac{k_0A_0^2}{8H}C_g\left(\frac{1+\frac{C_g}{\sinh(2q)}}{1-\frac{C_g^2}{H}}\right)\left|(1-\gamma_0)+\frac{\sqrt{H}}{C_g}\left[1-\gamma_0\left(1-i\frac{k_1^i}{K}\right)\right]\right|\times \\
&\qquad\times\cos\left(2K\frac{C_g}{\sqrt{H}}(x_1-\sqrt{H}t_1)+\pi-\phi_F^{+}\right)
\end{aligned} \tag{3.6.14}$$

where the constant $\widehat{G}_1^{+}$ was replaced by its previously computed expression (3.3.44) and Where ϕ_F^{+} is the phase of the complex parameter $(1-\gamma_0)+\frac{\sqrt{H}}{C_g}\left[1-\gamma_0\left(1-i\frac{k_1^i}{K}\right)\right]$. So that the mean free surface displacement $\mathcal{N}_{\mathcal{F}}^{+}$ due to the free wave is:

$$\mathcal{N}_{\mathcal{F}}^{+}=N_F^{+}\cos\left(2K\frac{C_g}{\sqrt{H}}(x_1-\sqrt{H}t_1)+\pi-\phi_F^{+}\right) \tag{3.6.15}$$

With N_F^{+} being the amplitude of the mean free surface displacement $\mathcal{N}_{\mathcal{F}}^{+}$ due to the free wave:

$$N_F^{+}=\frac{k_0A_0^2}{8H}C_g\left(\frac{1+\frac{C_g}{\sinh(2q)}}{1-\frac{C_g^2}{H}}\right)\left|(1-\gamma_0)+\frac{\sqrt{H}}{C_g}\left[1-\gamma_0\left(1-i\frac{k_1^i}{K}\right)\right]\right| \tag{3.6.16}$$

The mean free surface displacement $\mathcal{N}_{\mathcal{B}}^{+}$ due to the bound wave generated by the slow modulations of the short waves envelope is:

$$\mathcal{N}_{\mathcal{B}}^{+} = 2\Re\left\{\left(2i\Omega\gamma_0^{*}\widehat{C}_1^{-}-\frac{A_0^2}{16\sinh^2 q}\right)e^{-2k_1^ix_1}e^{2i\Psi}\right\} \tag{3.6.17}$$

$$
\begin{aligned}
\mathcal{N}_B^+ &= 2\Re\left\{\left(2i\Omega\gamma_0^*\widehat{C}_1^- - \frac{A_0^2}{16\sinh^2 k_0H}\right)e^{-2k_1^i x_1}e^{2i\Psi}\right\} \\
&= 4\Omega e^{-2k_1^i x_1}\Re\left\{\left(i\gamma_0^*\widehat{C}_1^- - \frac{1}{\Omega}\frac{A_0^2}{16\sinh^2 k_0H}\right)e^{2i\Psi}\right\} \\
&= 4\Omega e^{-2k_1^i x_1}\Re\left\{\left[-\gamma_0^*\left(1+\frac{C_g}{\sinh(2q)}\right)\frac{k_0A_0^2}{16KH(1-\frac{C_g^2}{H})} - \frac{k_0^2H}{H\Omega}\frac{A_0^2}{16\cosh^2 k_0H}\right]e^{2i\Psi}\right\} \\
&= \frac{k_0A_0^2}{4H}e^{-2k_1^i x_1}\Re\left\{\left[-\gamma_0^*C_g\left(\frac{1+\frac{C_g}{\sinh(2q)}}{(1-\frac{C_g^2}{H})}\right) - \frac{k_0H}{\cosh^2 k_0H}\right]e^{2i\Psi}\right\} \\
&= \frac{k_0A_0^2}{4H}e^{-2k_1^i x_1}\left|\gamma_0^*C_g\left(\frac{1+\frac{C_g}{\sinh(2q)}}{(1-\frac{C_g^2}{H})}\right) + \frac{k_0H}{\cosh^2 k_0H}\right|\cos\left[2(Kx_1-\Omega t_1)+\pi+\phi_B^+\right]
\end{aligned}
\tag{3.6.18}
$$

where ϕ_B^+ is the phase of the complex parameter $\left[\gamma_0^*C_g\left(\frac{1+\frac{C_g}{\sinh(2q)}}{(1-\frac{C_g^2}{H})}\right) + \frac{k_0H}{\cosh^2 k_0H}\right]$.
Finally the mean free surface displacement $\mathcal{N}_B^+$ due to the bound wave generated by the slow modulations of the short waves envelope is:

$$
\mathcal{N}_B^+ = N_B^+ e^{-2k_1^i x_1}\cos\left[2(Kx_1-\Omega t_1)+\pi+\phi_B^+\right] \tag{3.6.19}
$$

with N_B^+ being the amplitude of the free surface displacement $\mathcal{N}_B^+$ due to the bound wave:

$$
N_B^+ = \frac{k_0A_0^2}{4H}\left|\gamma_0^*C_g\left(\frac{1+\frac{C_g}{\sinh(2q)}}{(1-\frac{C_g^2}{H})}\right) + \frac{k_0H}{\cosh^2 k_0H}\right| \tag{3.6.20}
$$

Let us finally summarize the results for the mean free surface displacement in both '-' and '+' region.

In the '-' (no mud) region we have:

$$
\eta_{10}^-(x_1,t_1) = \mathcal{N}^-(x_1,t_1) = \langle\mathcal{N}^-\rangle + \mathcal{N}_{\mathcal{F}}^- + \mathcal{N}_B^- \tag{3.6.21}
$$

$$
\langle\mathcal{N}^-\rangle = -N_M^- \tag{3.6.22}
$$

$$
\mathcal{N}_{\mathcal{F}}^- = N_F^-\cos\left(2K\frac{C_g}{\sqrt{H}}(x_1+\sqrt{H}t_1)+\phi_F^-\right) \tag{3.6.23}
$$

$$
\mathcal{N}_B^- = N_B^-\cos\left[2(Kx_1-\Omega t_1)+\pi\right] \tag{3.6.24}
$$

With N_M^- being the amplitude of the set down, N_F^- being the amplitude of the mean free surface displacement due to the free wave, and N_B^- is the amplitude of the free surface displacement generated by the bound waves. The expressions of the amplitudes are:

$$N_M^- = \frac{A_0^2}{8\sinh^2 k_0 H} \tag{3.6.25}$$

$$N_F^- = \frac{k_0 A_0^2}{4H} C_g \left(\frac{1+\frac{C_g}{\sinh(2q)}}{1-\frac{C_g^2}{H}}\right) \frac{1}{2} \left| 1-\gamma_0 - \frac{\sqrt{H}}{C_g}\left[1-\gamma_0\left(1-i\frac{k_1^i}{K}\right)\right]\right| \tag{3.6.26}$$

$$N_B^- = \frac{k_0 A_0^2}{4H} C_g \left(\frac{1+\frac{C_g}{\sinh(2q)}}{1-\frac{C_g^2}{H}}\right) \left[1+\frac{1}{C_g}\left(\frac{1-\frac{C_g^2}{H}}{1+\frac{C_g}{\sinh(2q)}}\right)\frac{k_0 H}{\cosh^2 k_0 H}\right] \tag{3.6.27}$$

In the '+' (mud) region we have:

$$\eta_{10}^+(x_1,t_1) = \mathcal{N}^+(x_1,t_1) = \langle \mathcal{N}^+\rangle + \mathcal{N}_{\mathcal{F}}^+ + \mathcal{N}_{\mathcal{B}}^+ \tag{3.6.28}$$

$$\langle \mathcal{N}^+\rangle = -N_M^+ e^{-2k_1^i x_1} \tag{3.6.29}$$

$$\mathcal{N}_{\mathcal{F}}^+ = N_F^+ \cos\left(2K\frac{C_g}{\sqrt{H}}(x_1-\sqrt{H}t_1)+\pi-\phi_F^+\right) \tag{3.6.30}$$

$$\mathcal{N}_{\mathcal{B}}^+ = N_B^+ e^{-2k_1^i x_1}\cos\left[2(Kx_1-\Omega t_1)+\pi+\phi_B^+\right] \tag{3.6.31}$$

With N_M^+ being the amplitude of the set down, N_F^+ being the amplitude of the mean free surface displacement due to the free wave, and N_B^+ is the amplitude of the free surface displacement generated by the bound waves. The expressions of the amplitudes are:

$$N_M^+ = \frac{A_0^2}{8\sinh^2 k_0 H} \tag{3.6.32}$$

$$N_F^+ = \frac{k_0 A_0^2}{4H} C_g \left(\frac{1+\frac{C_g}{\sinh(2q)}}{1-\frac{C_g^2}{H}}\right) \frac{1}{2} \left| 1-\gamma_0 + \frac{\sqrt{H}}{C_g}\left[1-\gamma_0\left(1-i\frac{k_1^i}{K}\right)\right]\right| \tag{3.6.33}$$

$$N_B^+ = \frac{k_0 A_0^2}{4H} C_g \left(\frac{1+\frac{C_g}{\sinh(2q)}}{1-\frac{C_g^2}{H}}\right) \left|\gamma_0^* + \frac{1}{C_g}\left(\frac{1-\frac{C_g^2}{H}}{1+\frac{C_g}{\sinh(2q)}}\right)\frac{k_0 H}{\cosh^2 k_0 H}\right| \tag{3.6.34}$$

The constant free surface displacement $\langle \mathcal{N}\rangle$ is negative in both '-' and '+ regions , and as one can intuitively expect vanishes for $x_1 \to +\infty$. In fact while the short

waves exist it is a well known fact that the average free surface sets down and this is confirmed by the negative sign of η_{10} in both the '-' and the '+' regions (equations (3.6.22) and (3.6.29)). However when the short waves are damped (at large values of x_1) there is no more reason for the average free surface to set down, and the average value $\langle \mathcal{N}^+ \rangle$ vanishes exponentially together with the amplitude of the short waves. For the plotting purposes let us define the following functions:

$$f_N(k_0H) = \frac{k_0A_0^2}{4H}C_g\left(\frac{1+\frac{C_g}{\sinh(2q)}}{1-\frac{C_g^2}{H}}\right) \tag{3.6.35}$$

$$n_F^-(k_0H,\frac{k_1^i}{K}) = \frac{1}{2}\left|1-\gamma_0-\frac{\sqrt{H}}{C_g}\left[1-\gamma_0\left(1-i\frac{k_1^i}{K}\right)\right]\right| \tag{3.6.36}$$

$$n_F^+(k_0H,\frac{k_1^i}{K}) = \frac{1}{2}\left|1-\gamma_0+\frac{\sqrt{H}}{C_g}\left[1-\gamma_0\left(1-i\frac{k_1^i}{K}\right)\right]\right| \tag{3.6.37}$$

$$n_B^-(k_0H,\frac{k_1^i}{K}) = \left[1+\frac{1}{C_g}\left(\frac{1-\frac{C_g^2}{H}}{1+\frac{C_g}{\sinh(2q)}}\right)\frac{k_0H}{\cosh^2 k_0H}\right] \tag{3.6.38}$$

$$n_B^+(k_0H,\frac{k_1^i}{K}) = \left|\gamma_0^*+\frac{1}{C_g}\left(\frac{1-\frac{C_g^2}{H}}{1+\frac{C_g}{\sinh(2q)}}\right)\frac{k_0H}{\cosh^2 k_0H}\right| \tag{3.6.39}$$

Now the amplitudes N_M^-, N_F^-, N_B^-, N_M^+, N_F^+ and N_B^+ can be rewritten as:

$$N_M^- = \frac{A_0^2}{8\sinh^2 k_0H} \tag{3.6.40}$$

$$N_F^- = f_N(k_0H)n_F^-(k_0H,\frac{k_1^i}{K}) \tag{3.6.41}$$

$$N_B^- = f_N(k_0H)n_B^-(k_0H,\frac{k_1^i}{K}) \tag{3.6.42}$$

$$N_M^+ = \frac{A_0^2}{8\sinh^2 k_0H} \tag{3.6.43}$$

$$N_F^+ = f_N(k_0H)n_F^+(k_0H,\frac{k_1^i}{K}) \tag{3.6.44}$$

$$N_B^+ = f_N(k_0H)n_B^+(k_0H,\frac{k_1^i}{K}) \tag{3.6.45}$$

The t_1-averaged free surface displacement $N_M^- = N_M^+$ is plotted against k_0H in figure (3-3), together with the function $f_N(k_0H)$. The functions n_F^- and n_F^+ are plotted in

figures (3-4(a)) and (3-4(b)), and the functions n_B^- and n_B^+ are plotted in figures (3-4(c)) and (3-4(d)) against the dimensionless water layer depth $k_0 H$ for three values of the parameter $\frac{k_1^i}{K}$. Note that the constant free surface displacement and the amplitude of the bound waves in the '-' region are unaffected by the presence of the mud layer in the '+' region.

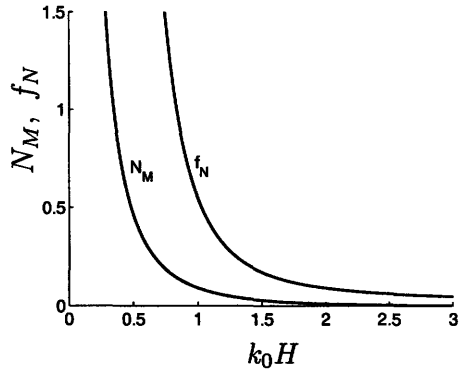

Figure 3-3: Constant free surface displacement N_M and the function f_N

The analytical expression of the damping coefficient k_1^i is given by the imaginary part of the equation (2.4.23) and depends not only on the mud properties but also on the properties of the water waves. Its expression is rewritten below for convenience:

$$k_1^i = -\gamma \frac{d}{a} \left(\frac{2k_0^2}{2q + \sinh 2q} \right) \Im \left\{ 1 - \frac{\tanh \lambda}{\lambda} \right\} \tag{3.6.46}$$

It is interesting to see directly the influence of the dimensionless mud depth d_s and of the phase θ of the complex viscosity μ on the slow evolution of the free surface waves. For simplicity we take $\gamma \frac{d}{a} = 1$ and $K = 1$. In figure (3-5) we plotted for three values of the dimensionless depth $d_s = 0.1,\ 1.1,\ 3$ the functions n_F^-, n_F^+ and n_B^+ for a highly elastic case ($\theta = 0.9 \times \frac{\pi}{2}$). The value $d_s = 1.1$ corresponds to the resonance of the function $\Im \left\{ 1 - \frac{\tanh \lambda}{\lambda} \right\}$ appearing in the expression of k_1^i. The dependence of the functions n_F^-, n_F^+ and n_B^+ on the parameter θ for a fixed value of $d_s = 1.1$ corresponding to the resonance is plotted in figure (3-6).

From the figures (3-5) and (3-6) we infer that the amplitude of the free waves in the '-' (no mud) region is extremely small and is of any significance only when the function

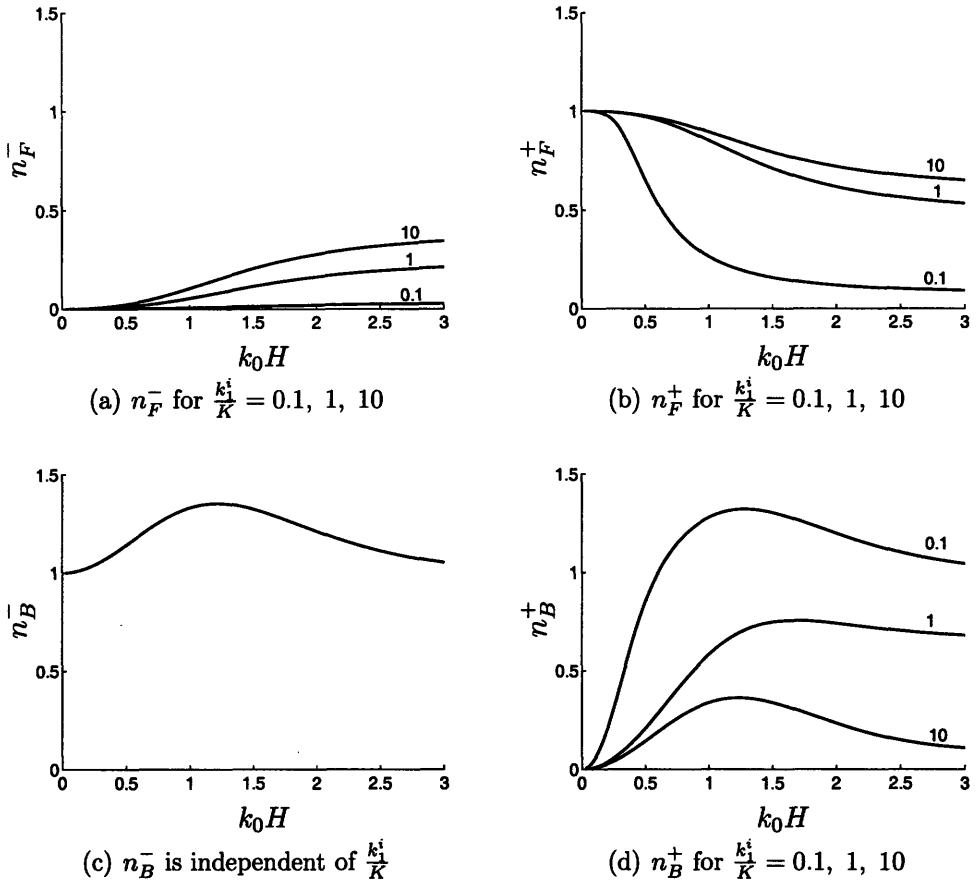

(a) n_F^- for $\frac{k_1^i}{K} = 0.1,\ 1,\ 10$

(b) n_F^+ for $\frac{k_1^i}{K} = 0.1,\ 1,\ 10$

(c) n_B^- is independent of $\frac{k_1^i}{K}$

(d) n_B^+ for $\frac{k_1^i}{K} = 0.1,\ 1,\ 10$

Figure 3-4: Functions n_F^-, n_F^+, n_B^- and n_B^+ against the dimensionless water layer depth k_0H for several values of $\frac{k_1^i}{K} = 0.1,\ 1,\ 10$

$\Im\{g(d_s,\theta)\} = \Im\left\{1 - \frac{\tanh\lambda}{\lambda}\right\}$ is very close to resonance ($d_s = 1.1$ and $\theta \to \frac{\pi}{2}$). The amplitude of the free waves in the '+' (mud) region vanishes slower with increasing k_0H in case when the function $\Im\{g(d_s,\theta)\}$ is close to resonance ($d_s = 1.1$ and $\theta \to \frac{\pi}{2}$). On the other hand the amplitude of the bound waves in the '+' region vanishes faster when the function $\Im\{g(d_s,\theta)\}$ is close to resonance ($d_s = 1.1$ and $\theta \to \frac{\pi}{2}$).

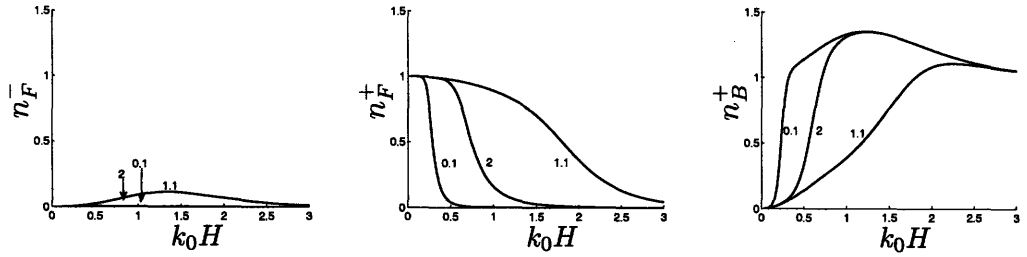

(a) n_F^- (b) n_F^+ (c) n_B^+

Figure 3-5: Functions n_F^-, n_F^+, n_B^- and n_B^+ against the dimensionless water layer depth k_0H for $\theta = 0.9 \times \frac{\pi}{2}$ and $d_s = 0.1,\ 1.1,\ 3$

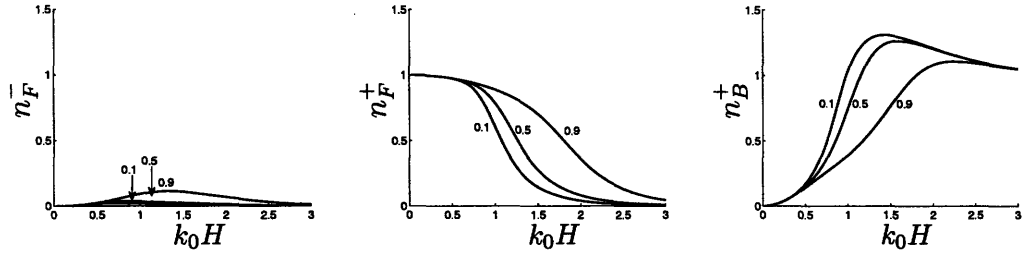

(a) n_F^- (b) n_F^+ (c) n_B^+

Figure 3-6: Functions n_F^-, n_F^+, n_B^- and n_B^+ against the dimensionless water layer depth k_0H for $d_s = 1.1$ and $\theta = (0.1,\ 0.5,\ 0.9) \times \frac{\pi}{2}$

Conclusion

We have introduced a generalized viscoelastic model to fit the existing experimental data so that the constitutive coefficients are just material properties independent of frequency. We showed that the use of 8 coefficients was enough to obtain a good fit of the experimental data in the considered range of frequencies. By applying the perturbation analysis we obtained an analytical solution to the problem of the interaction of a thin viscoelastic mud layer with a sinusoidal wave propagating on top of a water layer of intermediate depth.

At the leading order we found that a strong damping and wave number shift are possible if the waves induced Stokes boundary layer thickness is a certain fraction of the mud depth (see equation (2.5.15)) and if the material has a large proportion of elasticity compared to viscosity (phase θ of the complex viscosity μ close to $\frac{\pi}{2}$). It was further noticed that lighter mud corresponded to a more significant damping. This is due to the fact that lighter muds are easier to move and hence have a larger amplitude of movement at the resonance that in its turn enhances the energy dissipation by viscosity. Therefore a light highly elastic mud will be extremely efficient at the energy dissipation for the values of forcing frequencies such that the induced Stokes boundary layer thickness is approximately equal to the mud layer depth.

At the second order we obtained analytically that a mean horizontal displacement occurs inside the mud layer under sinusoidal waves if the real part of the viscosity is non zero. In fact, as it was mentioned by Zhang and Ng [6] a purely elastic solid will always restore its initial position when the stress is released, meaning that for an elastic mud the displacement will be zero. In case of a general viscoelastic mud the viscous part will be responsible for a non zero mean displacement. We found that the mean displacement inside the mud layer has a linear profile as long as the dimensionless mud layer depth $d_s = \frac{d}{\delta_S}$ is smaller than 1.5. As the Stokes boundary layer thickness δ_S is larger than $2m$ for most of the experimental samples considered

we predict that the profile of the mean horizontal displacement inside the considered mud layers should be linear unless the mud layer depth d is larger than $3m$.

As we studied the water/mud interaction in a fixed frame, we found a non zero mean Eulerian velocity at the second order which is due to convection. For mud layer depth d such that $d_s = \frac{d}{\delta_S} < 3$ the mean horizontal velocity is negative. Its amplitude strongly depends on the phase θ of the complex viscosity μ. As the material becomes more elastic (θ approaches $\frac{\pi}{2}$) the amplitude of the mean horizontal velocity increases together with the leading order quantities.

Finally, we studied the evolution of the narrow-banded waves on top of a thin semi-infinite mud layer. The analytical expressions of the mean second order velocity, free surface displacement and pressure were obtained. It was shown that due to the damping of waves through viscous dissipation inside the mud layer a negative current will be generated in water with an amplitude independent of the mud properties. The amplitude of the steady current depends only on the amplitude of the free surface waves and on the dimensionless water layer depth $k_0 H$. In the mud region the current decays together with the amplitude of the short waves to vanish when the short waves are completely damped by the mud layer.

The next steps will be to study the evolution of the narrow-banded waves on top of a finite mud layer and to extend the perturbation analysis to a slopping bottom.

Appendix A

Experimental data

A.1 Experimental data by Jiang & Mehta, 1998

The physical characteristics of the mud samples used in the experiments by Jiang & Mehta are listed in table A.1.

Type	Size	ϕ	Principal Constituents
KI - Kerala, India mud	2μm	0.12	Montmorillonite, kaolinite, illite, gibbsite, organic matter (5%)
OK - Okeechobee mud	9μm	0.11	Kaolinite, sepiolite, montmorillonite, organic matter (40%)
MB - Mobile Bay mud	15μm	0.07, 0.11, 0.17	Clayey silt of undetermined composition, sand
AK - Attapulgite + kaolinite	1μm	0.12	Attapulgite (50%), kaolinite(50%)

Table A.1: Physical characteristics of mud samples used

For each of the mud samples the values of the parameters ϵ and Δ defining G_1, G_2 and μ_m are listed in the table A.2. The real and imaginary parts of the resulting viscosity are listed in the table A.3.

		G_1 (Pa)		G_2 (Pa)		μ (Pa.s)	
Mud	ϕ	ϵ	Δ	ϵ	Δ	ϵ	Δ
KI	0.12	9.160	0.257	3.843	-0.405	9.292	-0.405
OK	0.11	5.548	0.127	0.318	-0.687	5.290	-0.687
MB	0.07	3.659	-0.030	-1.439	-0.975	3.165	-0.975
MB	0.11	6.352	0.075	2.139	-0.745	6.695	-0.745
MB	0.17	8.274	0.108	-3.864	-0.696	8.374	-0.696
AK	0.12	8.049	0.114	2.604	-0.490	8.222	-0.490

Table A.2: Coefficients of Equation (1.3.2) for KI, OK, MB and AK muds

ω (in s^{-1})		0.13	0.25	0.57	1.26	2.51	5.65	12.6	25.1
KI	$\Re(\mu)$	2.2107	1.1551	5.1640	0.2270	0.1090	0.0463	0.0197	0.0094
$\phi = 0.12$	$\Im(\mu)$	4.3051	2.8111	1.6448	0.9454	0.5769	0.3206	0.1787	0.1072
OK	$\Re(\mu)$	0.0861	0.0438	0.0194	0.0086	0.0042	0.0018	0.0008	0.0004
$\phi = 0.11$	$\Im(\mu)$	0.2072	0.1181	0.0604	0.0309	0.0172	0.0086	0.0043	0.0024
MB	$\Re(\mu)$	0.0193	0.0094	0.0040	0.0017	0.0008	0.0003	0.0001	0.0001
$\phi = 0.07$	$\Im(\mu)$	0.0617	0.0307	0.0135	0.0060	0.0030	0.0013	0.0057	0.0003
MB	$\Re(\mu)$	0.1417	0.0683	0.0285	0.1191	0.0056	0.0023	0.0010	0.0662
$\phi = 0.11$	$\Im(\mu)$	0.6366	0.3420	0.1639	0.0790	0.0419	0.0199	0.0095	0.0050
MB	$\Re(\mu)$	1.1567	0.5557	0.2343	0.0996	0.0473	0.0197	0.0083	0.0004
$\phi = 0.17$	$\Im(\mu)$	3.7310	2.0534	1.0150	0.5048	0.2744	0.1342	0.0662	0.0358
AK	$\Re(\mu)$	1.4015	0.6648	0.2598	0.0986	0.0416	0.0150	0.0054	0.0022
$\phi = 0.12$	$\Im(\mu)$	2.2662	1.3981	0.7495	0.3895	0.2164	0.1073	0.0534	0.0290

Table A.3: Real and imaginary parts of the complex viscosity μ (in N/cm^2), Jiang & Mehta

A.2 Experimental data by Huhe & Huang, 1993

The mud samples used in the experiments of Huhe & Huang differ by the type of flume from which they were obtained and by their solid volume fraction ϕ. For the mud samples from the flume A (respectively from the flume B) the measured parameters G_m and μ_m are listed as functions of frequency and of solid volume volume fraction ϕ in tables A.4 and A.5 (respectively in tables A.6 and A.7). The resulting real and imaginary parts of the complex viscosity are given in table A.8 for the data set A and in table A.9 for the data set B.

ϕ	0.34	0.24	0.20	0.17	0.14	0.08
ω						
0.11	9.00	0.65	0.40	0.31	0.39	0.05
0.19	5.00	0.55	0.37	0.22	0.30	0.05
0.30	3.80	0.42	0.11	0.25	0.32	0.01
0.46	3.50	0.41	0.15	0.29	0.28	0.04
0.74	3.50	0.48	0.17	0.23	0.30	0.03
1.10	3.60	0.75	0.19	0.18	0.31	0.01
2.00	3.70	1.40	0.19	0.20	0.38	0.06
3.00	3.70	1.80	0.19	0.30	0.38	0.07
4.80	4.30	2.30	0.30	0.40	0.38	0.12
7.50	6.50	2.90	0.45	0.80	0.45	0.15
11.00	12.0	3.20	1.10	1.00	0.49	0.28
19.00	21.0	3.60	1.80	1.30	0.65	0.21

Table A.4: Real elastic module G_m (in N/cm^2) - data set A

	ϕ	0.34	0.24	0.20	0.17	0.14	0.08
ω							
0.11		190	17.0	7.00	5.00	5.00	0.40
0.19		75.0	7.00	2.50	2.10	2.50	0.30
0.30		40.0	4.00	1.50	1.10	1.50	0.12
0.46		21.0	2.50	0.80	0.70	0.90	0.21
0.74		12.0	2.00	0.60	0.55	0.70	0.11
1.10		9.00	1.70	0.40	0.40	0.50	0.11
2.00		6.00	1.80	0.28	0.35	0.40	0.08
3.00		4.00	1.50	0.29	0.30	0.22	0.06
4.80		3.30	1.10	0.23	0.25	0.17	0.04
7.50		3.10	0.80	0.23	0.25	0.11	0.03
11.0		2.80	0.50	0.23	0.25	0.08	0.02
19.0		2.60	0.33	0.15	0.09	0.05	0.01

Table A.5: Viscosity μ_m (in $N.s/cm^2$) - data set A

	ϕ	0.37	0.23	0.20	0.17	0.14	0.08
ω							
0.11		20.0	1.00	0.35	0.09	0.30	0.03
0.19		18.0	0.65	0.28	0.12	0.10	0.03
0.30		14.0	0.84	0.17	0.11	0.17	0.04
0.46		13.0	0.74	0.18	0.12	0.14	0.05
0.74		13.0	0.75	0.19	0.13	0.06	0.06
1.10		13.0	0.76	0.20	0.12	0.11	0.05
2.00		13.0	0.80	0.12	0.11	0.09	0.05
3.00		13.0	0.93	0.12	0.15	0.07	0.07
4.80		14.0	1.10	0.14	0.31	0.12	0.08
7.50		15.0	1.80	0.24	0.69	0.22	0.08
11.0		19.0	2.10	0.72	0.90	0.42	0.11
19.0		28.0	2.30	1.90	1.10	0.55	0.18

Table A.6: Real elastic module G_m (in N/cm^2) - data set B

	ϕ	0.37	0.23	0.20	0.17	0.14	0.08
ω							
0.11		600	15.0	6.50	1.70	2.00	0.50
0.19		210	4.50	3.00	1.00	0.70	0.12
0.30		110	2.50	1.50	0.70	0.40	0.50
0.46		70.0	1.60	0.80	0.50	0.36	0.20
0.74		41.0	1.00	0.45	0.35	0.31	0.10
1.10		26.0	0.80	0.30	0.25	0.21	0.09
2.00		15.0	0.60	0.25	0.24	0.15	0.08
3.00		10.0	0.55	0.18	0.21	0.13	0.06
4.80		7.00	0.55	0.15	0.20	0.10	0.04
7.50		5.20	0.45	0.15	0.20	0.09	0.03
11.0		4.50	0.30	0.20	0.12	0.08	0.02
19.0		4.00	0.20	0.19	0.08	0.05	0.01

Table A.7: Viscosity μ_m (in $N.s/cm^2$) - data set B

ω (in s^{-1})		0.11	0.19	0.30	0.46	0.74	1.10	2.00	3.00	4.80	7.50	11.0	19.0
	$\Re(\mu)$	190	75.0	40.0	21.0	12.0	9.00	6.00	4.00	3.30	3.10	2.80	2.60
$\phi = 0.34$	$\Im(\mu)$	81.8	26.3	12.7	7.61	4.73	3.27	1.85	1.23	0.89	0.87	1.09	1.11
	$\Re(\mu)$	17.0	7.00	4.00	2.50	2.00	1.70	1.80	1.50	1.10	0.80	0.50	0.33
$\phi = 0.24$	$\Im(\mu)$	5.91	2.89	1.40	0.89	0.65	0.68	0.70	0.60	0.48	0.39	0.29	0.19
	$\Re(\mu)$	7.00	2.50	1.50	0.80	0.60	0.40	0.28	0.29	0.23	0.23	0.23	0.15
$\phi = 0.20$	$\Im(\mu)$	3.64	1.94	0.36	0.33	0.23	0.17	0.09	0.06	0.06	0.06	0.10	0.09
	$\Re(\mu)$	5.00	2.10	1.10	0.70	0.55	0.40	0.35	0.30	0.25	0.25	0.25	0.09
$\phi = 0.17$	$\Im(\mu)$	2.82	1.16	0.83	0.63	0.31	0.16	0.10	0.10	0.08	0.11	0.09	0.07
	$\Re(\mu)$	5.00	2.50	1.50	0.90	0.70	0.50	0.40	0.22	0.17	0.11	0.08	0.05
$\phi = 0.14$	$\Im(\mu)$	3.55	1.58	1.07	0.61	0.41	0.28	0.19	0.13	0.08	0.06	0.04	0.03
	$\Re(\mu)$	0.40	0.30	0.12	0.21	0.11	0.11	0.08	0.06	0.04	0.03	0.02	0.01
$\phi = 0.07$	$\Im(\mu)$	0.42	0.24	0.03	0.08	0.04	0.01	0.03	0.02	0.03	0.02	0.02	0.01

Table A.8: Real and imaginary parts of the complex viscosity μ (in $N.s/cm^2$), data set A, Huhe & Huang

ω (in s^{-1})		0.11	0.19	0.30	0.46	0.74	1.10	2.00	3.00	4.80	7.50	11.0	19.0
	$\Re(\mu)$	600	210	110	70.0	41.0	26.00	15.00	10.00	7.00	5.20	4.50	4.00
$\phi = 0.37$	$\Im(\mu)$	182	94.7	46.7	28.3	17.6	11.8	6.50	4.33	2.92	2.00	1.73	1.47
	$\Re(\mu)$	15.0	4.50	2.50	1.60	1.00	0.80	0.60	0.55	0.55	0.45	0.30	0.23
$\phi = 0.23$	$\Im(\mu)$	9.09	3.42	2.80	1.61	1.01	0.69	0.40	0.31	0.23	0.24	0.19	0.12
	$\Re(\mu)$	6.50	3.00	1.50	0.80	0.45	0.30	0.25	0.18	0.15	0.15	0.20	0.19
$\phi = 0.20$	$\Im(\mu)$	3.18	1.47	0.57	0.39	0.26	0.18	0.06	0.04	0.03	0.03	0.07	0.10
	$\Re(\mu)$	1.70	1.00	0.70	0.50	0.35	0.25	0.24	0.21	0.20	0.20	0.12	0.08
$\phi = 0.17$	$\Im(\mu)$	0.82	0.63	0.37	0.26	0.18	0.11	0.06	0.05	0.06	0.09	0.08	0.06
	$\Re(\mu)$	2.00	0.70	0.40	0.36	0.31	0.21	0.15	0.13	0.10	0.09	0.08	0.05
$\phi = 0.14$	$\Im(\mu)$	2.72	0.53	0.57	0.30	0.08	0.10	0.05	0.02	0.03	0.3	0.04	0.03
	$\Re(\mu)$	0.50	0.12	0.50	0.20	0.10	0.09	0.08	0.06	0.04	0.03	0.02	0.01
$\phi = 0.08$	$\Im(\mu)$	0.27	0.16	0.13	0.11	0.08	0.05	0.03	0.02	0.02	0.01	0.01	0.01

Table A.9: Real and imaginary parts of the complex viscosity μ (in $N.s/cm^2$), data set B, Huhe & Huang

Bibliography

[1] Huhe, O. D. & Huang, Z. H 1994 An experimental study of fluid mud rheology - mud properties in Hangchow Bay navigation channel. Part II, (in Chinese), Beijing. Institute of Mechanics Report, Chinese Academy of Sciences., pp 34-56

[2] Armstrong, R.A., Bird, R. B., Hassinger, O. and Curtiss, C. F. Dynamics of Polymeric Fluids, McGraw-Hill.

[3] de Wit P.J, and Kranenburg C., 1997 "On the Liquefaction and Erosion of Mud Due to Waves and Current" INTERCOH '94, Cohesive Sediment, ed. Burt N. and al.

[4] Jiang F., Mehta A.J., 1995 Mudbanks of the Southwest Coast of India IV: Mud Viscoelastic Properties. Journal of Coastal Research, 11(3), 918-926

[5] Ng C., Zhang X., 2007 Mass Transport in Water waves over a thin layer of soft viscoelastic mud. Journal of Fluid Mechanics, vol. 573, pp. 105-130

[6] Zhang X., Ng C., 2006, On the oscillatory and mean motions due to waves in a thin viscoelastic layer, Wave Motion Volume 43, Issue 5, May Pages 387-405.

[7] Ng C. 2000 Water waves over a muddy bed: a two-layer Stokes' boundary layer model. Coastal Engineering, vol. 40 Issue , pp. 221-242

[8] Liu K., Mei C., 1989, Effects of water-induced friction on a muddy seabed modeled as a Bingham-plastic Fluid. Journal of Coastal Research, 5, 4, pp. 777-789

[9] Mei, C.C., 1989, The Applied Dynamics of Ocean Surface Waves. World Scientific, Singapore, 740 pp.

[10] Dalrymple R., Liu P., 1978, Waves over Soft Muds: A Two-Layer Fluid Model. Journal of Physical Oceanography, pp. 11211131

[11] J. Wen, P.L.-F. Liu, 1995, Mass transport in water waves over an elastic bed, Proc. R. Soc. Lond. A 450, pp 371-390

[12] T. Yamamoto, H.L. Koning, H. Sellmeigher, E.V. Hijum, 1978, On the response of a poro-elastic bed to water waves, J. Fluid Mech. 87, pp 193-206

[13] H. MacPherson, 1980, The attenuation of water waves over a non-rigid bed, J. Fluid Mech. 97, pp 721-742

[14] J.P.-Y. Maa, A.J. Mehta, 1990, Soft mud response to water waves, J. Waterway Port Coast. Ocean Eng. 116 (5), pp. 634-650